A PALEOETHNOBOTANICAL ANALYSIS OF CULTIVATION AND CLIMATE IN THE EARLY TO MIDDLE BRONZE AGE JORDAN VALLEY

by

Steven Porson

A dissertation submitted to the faculty of
The University of North Carolina at Charlotte
in partial fulfillment of the requirements
for the degree of Doctor of Philosophy in
Geography

Charlotte

2024

Approved by:

_____
Dr. Patricia Fall

_____
Dr. Steven Falconer

_____
Dr. Martha Cary Eppes

_____
Dr. Wenwu Tang

ABSTRACT

STEVEN PORSON. A Paleoethnobotanical Analysis Of Cultivation And Climate In The Early To Middle Bronze Age Jordan Valley (Under the direction of DR. PATRICIA FALL)

This dissertation presents an exploration of agriculture and climate of the Southern Levant (modern day Israel, Palestine, and Jordan) in the Early and Middle Bronze Ages (EB and MB), roughly 4500-3600 BP. Analyses from four archaeological sites (Tell Abu en-Ni'aj, Tell el-Hayyat, Khirbat Iskandar, and Zahrat adh-Dhra' 1) are used to study climate change and agricultural responses surrounding the 4.2 ka BP climate event. Paleoethnobotany, the study of ancient plants and how people used them, is used to assess what early farmers cultivated. Stable isotope analyses of carbonized seeds and archaeological shells offer comparison of climate and culture. Data for the carbonized seed analyses are provided in Supplementary Tables S1-S4. Results help us understand what ancient settlements were producing and how they may have used crops in EB IV and MB I, periods with relatively mobile populations and fewer archaeological remains, and also reveal the timing and extent of climate shifts in the region.

In terms of agriculture, results suggest that settlements in the northern Jordan Valley practiced agriculture more intensively, with farms producing a wider variety of goods and farms likely expanding outwards from sites over time. They managed cereals and fruits most intensively, but also cultivated a variety of pulses and potentially utilized several wild plants. In the south, people made do with a more limited array of cereal and fruit cultigens, perhaps turning to livestock agriculture to sustain themselves. For settlements that did focus on agriculture, they intensively managed crops through manuring and selective crop timing or placement in order to maximize soil nutrient and water availability.

In terms of climate there are notable distinctions between the Early Bronze IV, Middle Bronze I, and Middle Bronze II. Surrounding the 4.2 ka BP event the driest conditions were present in the valley, with gradually rising drought conditions in EB IV and more rapidly ameliorating conditions around the start of MB II. This dissertation's findings agree with a roughly 300-year period of heightened aridity from around 4200 to 3900 BP from the end of EB IV through MB I, with the driest environment noted around MB I-II Zahrat adh-Dhra' 1. Additionally, this study highlights the benefit of using stable isotopes to study crop management rather than climate, with signals revealing changes in water and soil nutrient availability related to farming practices. Early farmers appear to have responded through the intentional sowing of drought-tolerant crops like hulled cereals during drier periods, and drought-intolerant species like wheat received more manure and water application.

This work provides new data from three Jordan Rift sites for future paleoethnobotanical analyses, new stable isotope data for four sites, and provides a robust methodology for more localized comparisons of climate and culture.

ACKNOWLEDGEMENTS

I would like to acknowledge those who helped support this project, with special thanks to my primary advisor Dr. Patricia Fall, and to Dr. Steven Falconer. This project could not have been completed without the time, resources, assistance, and opportunities each has provided me. This dissertation relies heavily on the continued efforts of our team, with assistance from Dr. Suzanne Birch at the University of Georgia, Dr. Elizabeth Ridder from California State University at San Marcos, and Dr. Mary Metzger. I would also like to offer special thanks to Dr. Suzanne Richard of Gannon University for providing carbonized seeds for the analysis of Khirbat Iskandar, and to my other committee members Dr. Missy Eppes and Dr. Wenwu Tang who have graciously provided their time and assistance for this project.

I also want to acknowledge some of the other inspirational professors I have had the fortune to learn from during my time at UNC Charlotte, including Dr. Jack Scheff, Dr. John Diemer, and Dr. Wei-Ning Xiang.

Finally, I would like to thank the Herschel and Cornelia Everett Foundation fellowship program for the financial support to attend graduate school at UNCC. This support made this research possible.

DEDICATION

I dedicate this work *in memoriam* my mother, Judy Porson. You supported me whatever path I chose to follow. You inspired me to continue my education in graduate school even through adversity and hardship during the toughest period of my life. I hope I made you proud.

TABLE OF CONTENTS

LIST OF TABLES

APPENDIX TABLES

SUPPLEMENTARY TABLES

LIST OF FIGURES

APPENDIX FIGURES

CHAPTER 1: INTRODUCTION

Goals and Hypotheses

Plant cultivation and climate change are topics that have fascinated researchers for decades. The practice of domesticating wild plants and cultivating crops evolved quickly and dramatically over the course of the Holocene and was a major defining factor in where our foods come from today (Zohary and Hopf, 1973; Miller, 1992). It also has another benefit, however, in that cultivation practices may respond to changes in climate. While the farmers of today can manage the water availability of their crops through automated irrigation systems, farmers in ancient times would have had to rely on their knowledge of rainfall patterns, more basic irrigation methods, and historical yields in determining what seeds to sow. This dissertation serves to unravel what ancient climate was like in the Bronze Age Near East and how early farmers may have adapted to climate change through an investigation of ancient cultivation.

The roots of modern western agricultural systems stem from the ancient Near East. The practice of sedentary agriculture became a prominent feature of Levantine society in ancient times, with important changes occurring at the dawn of the Bronze Age (Sherratt, 1980; Fall et al., 1998). The Bronze Age marked a period of urbanism in the ancient Southern Levant (the region encompassed by modern Israel, Jordan and the Palestinian territories), when societies began to coalesce in larger sedentary settlements or towns (Gophna, 1984; Gophna and Portugali, 1988; Esse, 1989; Finkelstein, 1989; Falconer, 1994; Falconer and Savage, 1995; Chesson and Philip, 2003). The Early Bronze Age (EBA) and Middle Bronze Age (MBA) (about 3500-1600 Before the Common Era, or BCE) were periods of urbanization, in which agriculture was practiced in the fields surrounding settlements that typically were built on stratified ancient

mounds or *tell*s (Richard, 1987; Gophna and Portugali, 1988; Wilkinson, 2003). However, Early Bronze IV (EB IV), approximately 2500 to 2000 BCE, was a critical turning point during the rise of urbanism, marking a widespread abandonment of many early Levantine cities (Dever, 1980; 1995; Ibrahim, 2009; Paz, 2015). The persistence of sedentary agrarian lifestyle at some EB IV communities demonstrates the resilience of Levantine agriculture and the level to which it had become engrained in the ancient societies that endured through this time period (Fall et al., 1998; Richard and Long, 2008; Schwartz et al., 2012; Prag, 2014).

The abandonment of urban settlements meant a decline in the amount of archaeological information preserved during EB IV, leading to this period being more complicated to decipher archaeologically (Cohen, 2022). The transition away from sedentism in EB IV and its re-establishment in Middle Bronze I-II (MB I and MB II), approximately 2000 to 1700 BCE, may have played a critical role in agricultural practices at urban centers and in the surrounding landscape. Thus, the addition of comprehensive data from the Southern Levant greatly broadens our knowledge of Levantine agricultural practices and anthropogenic landscapes. Furthermore, exploring the agricultural evidence from these periods strengthens our understanding of agrarian responses to social and environmental change that will help to elucidate human responses to climate dynamics.

This investigation provides additional context for a suite of knowledge gaps regarding ancient Bronze Age agricultural dynamics. The goal of this research is to address the two following questions. First, what did cultivation patterns and management look like in the Southern Levant during Early Bronze IV to Middle Bronze II? Second, what did climate look like at this time and how do archaeological remains of cultivated and uncultivated plants indicate responses to climate change in the region during this time? An in-depth analysis of cultivation

from three additional ancient settlements greatly improves our knowledge about ancient agriculture and our ability to respond to both questions. Thus, this research project represents a combination of an exploratory analysis into cultivation trends and a hypothesis-driven analysis of the impacts and extent of paleoclimate change.

For the first question, I explore which plants ancient farmers grew and how they managed them by quantifying plant remains in archaeological contexts. This provides a baseline for our broadened understanding of what cultivation looked like in the Jordan Valley during the Bronze Age. Plant remains also reveal insight into the wild vegetation around a site, painting a more complete picture of the agrarian environment. This investigation is further tied to my second question, in that climate change may have affected which crops were more productive to cultivate. I hoped to find that humans were intentionally growing more drought-tolerant crops where and when the climate was drier (Pokharia et al., 2017). I also expected to find indications of more intensive agricultural management during these times, such as the use of irrigation and soil fertilization.

To address my second question, I look at the composition of plant macrofossil assemblages and isotopically derived climate signals from archaeological seeds and shells to find evidence of responses to a climate shift associated with the 4.2 ka BP climate change event. This event occurred about 4200 years Before Present (BP) and 2200 years Before the Common Era (BCE). This has been proposed as a leading cause of altered agrarian landscapes in the Northern Levant and Upper Mesopotamia during EB IV (Weiss et al., 1993; deMenocal, 2001; Weiss, 2016). Past studies have suggested the 4.2 ka BP Event was a punctuated climate event roughly 300-years long from about 4200-3900 BP, with global effects on precipitation and temperature (Weiss, 2016; Pokharia et al., 2017; Railsback et al, 2018; Xiao et al., 2018; Bini et al., 2019;

Kaniewski et al., 2020) that terminated around the time of the Middle Bronze Age reurbanization (Weiss et al., 1993; Kaniewski et al., 2008; 2018). However, regional climate records do not all agree on the length of this event nor on the intensity of its effects, with subsequent wetter climates emerging in the northwestern Mediterranean and drier climates in the Levant (Kaniewski et al., 2018; Bini et al., 2019).

Furthermore, the start and end of the event at roughly 4200 BP and around 4000 to 3900 BP does not correlate perfectly with the timing of Levantine urban abandonments, particularly the start of the abandonments. Urban abandonments started at the end of EB III, previously around 2300 to 2200 BCE, but new chronological evidence pushes this period back to around 2500 BCE or around 4500 BP, with abandonments having occurred gradually over two to three centuries (Dever, 1995; Wilkinson, 2003; Richard and Long, 2008; de Miroschedji, 2009; Prag, 2014; Bieniada, 2016).

Settlements started to become reoccupied early in the Middle Bronze Age, primarily around 1950 to 1900 BCE or 3950 to 3900 BP (Gerstenblith, 1983 in Falconer, 1994; Gophna, 1984; Gophna and Portugali, 1988; Finkelstein and Langgut, 2014). Some settlements returned earlier in the Middle Bronze, including sites like Pella or Tell el-Hayyat, around 2000 to 1950 BCE. However, many appeared later, gradually arising around the late Middle Bronze I or early Middle Bronze II, closer to 1900 BCE (Falconer, 1987; 1994; Bourke, 2006; 2014). This dissonance, caused by the pushback of start of the EB IV and reconceptualization of the Middle Bronze Age, has led to questions regarding the reason for abandonments, postulating that a longer-term climate shift may have surrounded the 4.2 ka BP event, one that was more gradual in nature (Wilkinson et al., 2014; Marta D'Andrea, 2020).

This analysis of the Jordan Valley Bronze Age paleoclimate tested the hypothesis that settlements may have experienced lower rainfall and drier conditions towards the beginning of EB IV, and may have experience more humid conditions gradually arising around the transition of Middle Bronze I-II.

With the investigation of agricultural practice, I seek to reveal insights into the anthropological study of factors such as cultivation preferences, food processing, fuel use, and site management. The rich assemblage of macrofloral data presented in this dissertation will further fill in growing regional plant macrofossil datasets, strengthening our interpretations of crop management. With the investigation of climate, I hope to better understand the extent of climate change in the ancient Jordan Valley. I explore agricultural practices in Early Bronze IV and the Middle Bronze Age to determine whether the large-scale, regional climate shifts, noted to be nearly ubiquitous throughout the Eastern Mediterranean (Bini et al., 2019), perhaps began earlier in EB IV and had lingering effects into the Middle Bronze Age. Data will help reveal the potential responses that early farmers had to climate change, inferred by assessing the differences in crop management. I also present a methodology applicable for future ethno-ecological analyses, comparing these sites within the wider context of urban agrarian landscapes in the Eastern Mediterranean.

Research Strategy

This dissertation presents a combination of paleoethnobotany and stable isotopic analyses to compare the cultivation strategies of sedentary communities during the early EB IV and early-to-middle Middle Bronze Age. Paleoethnobotany examines ancient plants with specific consideration for how people used them, while stable isotopic analysis examines the chemical

composition of remains. I incorporate temporal trends by comparing differences in carbonized floral assemblages excavated from EB IV and MBA settlements, while a spatial perspective is studied through comparison of sites in the northern Jordan Valley and in the Dead Sea Basin to the south. This spatio-temporal analysis is made feasible thanks to the well-stratified archaeological evidence from four settlements along the Jordan Rift: Tell Abu en-Ni'aj and Tell el-Hayyat in the northern Jordan Valley, and Khirbat Iskandar and Zahrat adh-Dhra' 1 by the Dead Sea.

One focus of this dissertation is to identify the crops grown at each of the ancient villages. I also studied crops with a higher likelihood of being impacted by potential drought stresses for a paleoenvironmental analysis. Drought stress was examined through a two-part investigation of local climate and environmental conditions via stable isotopic investigations of carbon, nitrogen, and oxygen concentrations in carbonized seeds from all four archaeological sites, and from shells collected from the two Jordan Valley sites. By comparing the floral assemblages within and between these sites, I reveal a host of distinctions in ancient cultivation strategies, some of which may be linked to climate impacts.

Research Objectives and Significance

In doing the research for this dissertation, I expanded my knowledge of Near Eastern agriculture in several ways. Regarding paleoethnobotanical floral surveys, this dissertation provides detailed discussion and interpretations of the assemblages from three Southern Levantine sites, one of which was occupied in Early Bronze IV and the other two which were inhabited during the Middle Bronze Age. This work also serves as the most updated compilation of the macrobotanical data from each site and offers a three-way comparison of cultivation dynamics

between these settlements. Further, the paleoethnobotanical investigations from Tell el-Hayyat presented here alter the scope and interpretations of earlier studies of the site (Fall et al., 1998, 2002; Falconer and Fall, 2006; Klinge and Fall, 2010; Fall et al., 2015).

A significant portion of this dissertation is focused on the investigation of paleoenvironmental trends, which offers new insights into the local climate conditions of the Jordan Valley and the Dead Sea Basin in western Jordan. Attaining a two-proxy comparative local climate signal, which I achieved through the incorporation of archaeological shells with carbonized seeds, is an underused methodology that could prove useful for future studies in the Near East. Alongside this, my colleagues and I incorporate a robust dataset of new stable isotopic measurements from a rich variety of cultigens and common wild taxa which seeks to dramatically expand the current regional database. I present data from many relatively understudied plant taxa and significant expansion of sampling from the primary cereal cultigens, allowing interregional comparison of several taxa for which the type of comparative analysis I present may not have been feasible in the past.

This dissertation will help our understanding of recent human adaptation and the ongoing practice of Near Eastern agriculture, the long-term impacts of punctuated climate events like the 4.2 ka BP event on the environment and agricultural practices, and the resilience of ancient human communities in sedentary agrarian settings to climatic disturbance.

Dissertation Structure

The dissertation is organized into thirteen chapters, with eight primary chapters discussing results to address the two hypotheses laid out in the Goals and Hypotheses section. Chapter 2 provides the context for this study, introduces the landscape of the Southern Levant and the time

periods of the Early to Middle Bronze Ages, and discusses each of the four archaeological sites from which proxy data are derived. Chapter 3 provides background for the paleoethnobotanical analysis and describes the key considerations that will be used to interpret the data.

Chapters 4-6 address the plant macrofossil analyses, and the study of the composition of plant remains, from each of the three archaeological sites that contained plant macrofossil remains. Each chapter presents methods, results, and a brief discussion section to summarize the major findings. These chapters present the backbone of this dissertation, with seed quantification providing evidence of agricultural history, site role and function, the natural environment, and change through time. Chapter 7 presents the analysis and discussion of intrasite and intersite comparisons of the spatial patterns of plant macrofossils, in particular at Tell el-Hayyat. This chapter pulls from data presented in Chapters 4-6, expanding on the results from these sections. Spatial analysis of carbonized seed deposition patterns is an invaluable resource for investigating how ancient peoples managed plants goods and waste products. Consideration of spatial aspects of deposition was necessary for interpretation of site use and cultivation strategies, and helped reveal how certain plants played a role in a site.

Chapters 8 and 9 present the methods, results, and discussion of the stable isotopic analyses. Chapter 8 focuses on the stable isotopes of oxygen and carbon from archaeological shells to assess the similarity of climate and environmental conditions during EB IV at Tell Abu en-Ni‘aj and the MBA at Tell el-Hayyat. This analysis serves as a vital secondary proxy to compare paleoclimate interpretations from the seeds, discussed in Chapters 4-6, as shells serve as a good indicator of the regional microclimatic around these settlements. Chapter 9 assesses the climate and cultivation strategy comparisons between the four focal settlements based on stable isotopes of carbon and nitrogen from carbonized seeds. It examines water and soil nutrient

availability trends to discern the influence climate and cultivation strategies may have had on cultivated flora. The chapter provides essential results and discussion of human responses to climate and environmental stress.

Chapters 10 synthesizes the results presented in the previous chapters, further comparing the results between the focal settlements and within the wider framework of the Near East to interpret the paleoenvironment at Southern Levantine sedentary agricultural settlements. I place my focal sites within the regional context of settlements to understand the broader Bronze Age Eastern Mediterranean landscape, and to examine the viability of stable isotopic analysis from carbonized seeds for interpreting climate change and human response. Chapter 11 serves to summarize the broader interpretations of the findings from my earlier chapters. It highlights the major findings from agricultural and crop management changes and from trends in climate change through the Early to Middle Bronze Ages to address the initial two hypotheses presented in this chapter.

CHAPTER 2: STUDY AREA AND FOCAL SITES

Geography of the Near East

The majority of this dissertation will focus on the Southern Levant. The Levant is a region of the fertile crescent sitting between ancient Egypt, Anatolia, and Mesopotamia. The Southern Levant generally encompasses modern day Israel, the Palestinian territories, and Jordan, while the Northern Levant includes Lebanon and western Syria. The Southern Levant is home to several diverse landscapes, such as the Coastal Plain and Central Hills of Israel and Palestine, the highlands along the western edge of the Trans-Jordanian Plateau and southern Syria, and the low-lying floodplains along the Jordan Rift. The focus of this study will be on settlements along the Jordan Rift between approximately the 31st to 33rd north parallels (Figure 2.1). The Jordan Rift formed from the Dead Sea Transform fault, which runs from Lake Hula to the Gulf of Aqaba (Al-Zoubi and Abu-Hamatteh, 2009). The Jordan Rift, a highly active fault zone throughout the Holocene (Garfunkel and Ben-Avraham, 1996; Ferry et al., 2007), marks the divide between Cisjordan (land west of the Jordan River) and Transjordan (land east of the river). The Rift Valley is bound to the east by the escarpment of the Trans-Jordanian Plateau, an upland area with elevations of around 700 m above sea level (a.s.l.) and higher, east of which lie the expansive deserts of the Arabian Peninsula. The Central Hills bound the Rift Valley to the west, with an undulating topography averaging about 500 m a.s.l.

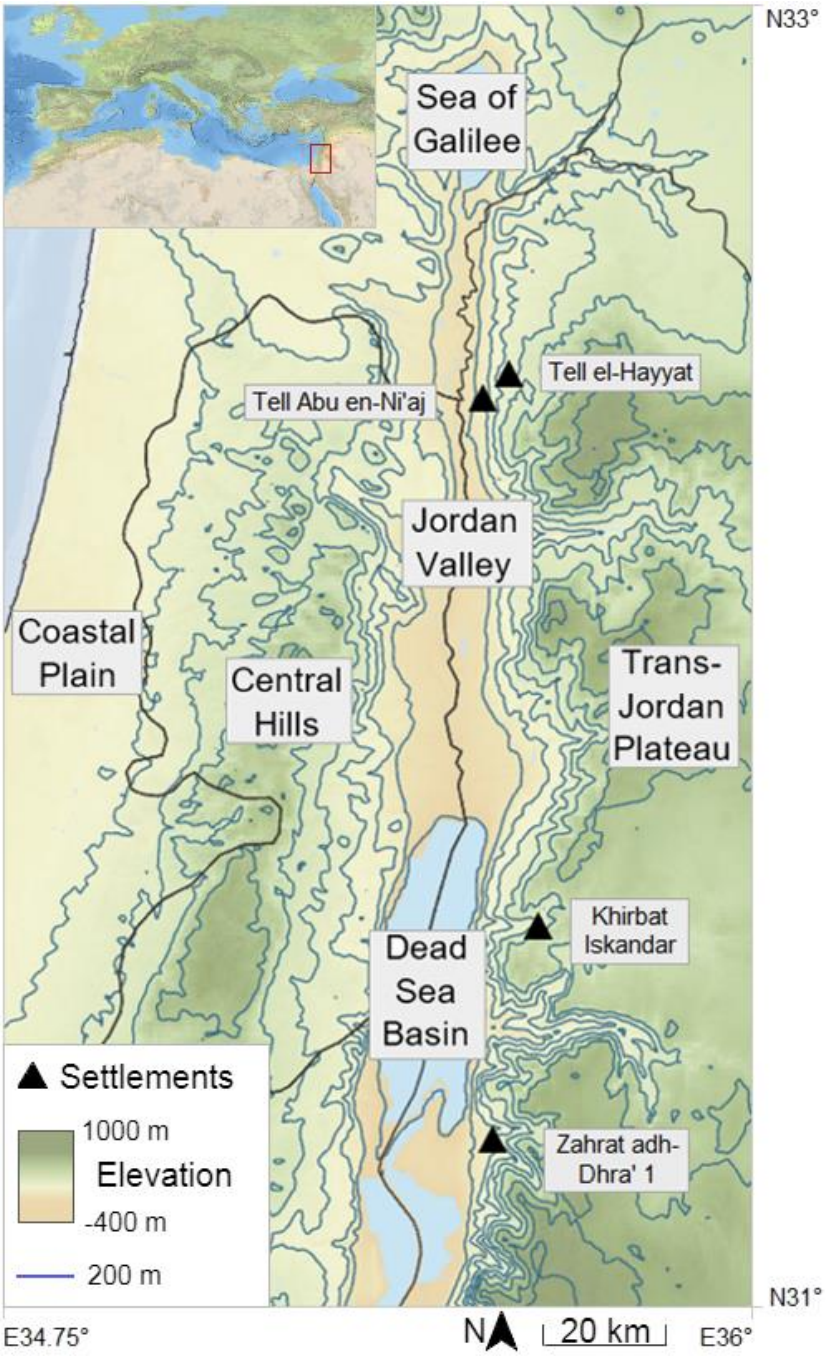

Figure 2.1 Map of southern Levantine geography along the Jordan Rift. Black triangles indicate the four focal sites in this research.

This study compares settlements along the eastern side of the Jordan Valley and Dead Sea Basin. The Jordan Valley is bounded by the Sea of Galilee (Lake Tiberias or Lake Kinneret) to the north and the Dead Sea to the south, which lies at around 420 m below sea level (b.s.l.)

(Gat, 2001). To the north, the Jordan Valley basin sits about 250 m b.s.l. with a series of low Pleistocene lacustrine terraces (known in Arabic as the *ghor*) overlooking the modern Jordan River floodplain (known as the *zor*). The Jordan River is fed from the west by numerous tributaries cut latitudinally through a set of quickly aggraded hills, rising to around 500 m a.s.l. (Al-Zoubi and Abu-Hamatteh, 2009). The Dead Sea Basin encompasses the modern extent of the Dead Sea and the Dead Sea Plain. In the low-lying hills to the immediate east, the landscape exhibits an undulating topography of deeply incised stream beds carved into a series of alluvial terraces, with steep mountainous terrain situated close behind. To the north, mountainous terrain transitions to hilly slopes along the eastern shore of the Dead Sea, with much of the modern agriculture shifting into the tributary valleys and beyond the highest plateaus. To the south, extensive plateaus open into floodplains past the south end of the Dead Sea as the mountainous terrain extends eastward.

The geography of this part of the rift will be referred to as the Jordan Valley, indicating the stretch from the Sea of Galilee to the Dead Sea Basin and including the foothills along the Dead Sea. The terms northern and southern refer to latitudinal gradients, while the terms upper and lower refer to elevational gradients, with the Lower Jordan Valley indicating the low-lying floodplains and foothills along the valley bottom and Upper Jordan Valley indicating the upper terraces and plateau of the Transjordan.

The northern Jordan Valley is a mix of Pleistocene age fluvial sediments underlain by Precambrian to Cambrian aged granite-rich bedrock (Meadows and Jones, 1996; Al-Zoubi and Abu-Hamatteh, 2009) with limestone capped plateaus and Cretaceous sandstone foothills that serve as the source of the many groundwater springs (Meadows and Jones, 1996; Singer, 2007; Al-Zoubi and Abu-Hamatteh, 2009; Ali et al., 2009). The sites in the central portion of the valley

sit at an interchange of soils along both an altitudinal and latitudinal gradient. The moisture regime is considered aridic (arid) to ustic-aridic (semi-arid to arid), and typical soils include dry, nutrient-poor entisols, aridisols, and inceptisols. These are defined as soils with little horizination and the occasional inclusion of an ochric horizon (a pale or white horizon with low organic content) or calcic horizon (denoting calcium-carbonate-rich but organic-carbon-poor conditions) (Al-Bakri, 2008).

The Dead Sea Basin is primarily comprised of sandstone, with sandstone rich bedrock of Cambrian to Ordovician age in the eastern foothills and sequences of sandstone, limestone, and marl from Triassic-Late Cretaceous in the mountains. Quaternary marls and halite formation are present around the Dead Sea shores and upper plateaus respectively, with Pleistocene age alluvium in valley bottoms and Pliocene age basalts occasionally dotting the landscape (Garfunkel and Ben-Avraham, 1996; Akawwi et al., 2009). The moisture regime is hot and dry similar to the northern Jordan Valley, but with a higher presence of calcic soils, denoting the high concentration of soluble salts along the lower valley (Al-Bakri, 2008).

Modern Climate and Vegetation

The Southern Levant has a dry, Mediterranean climate due to its position in the subtropical high-pressure zone, a partial rain-shadow effect, continentality, high evapotranspiration, and high regional salinity (Neumann, et al., 2010). Precipitation is delivered by North Atlantic storm tracks and Eastern Atlantic advection currents, which in the winter months deliver rains primarily from the west and northwest (Lionello et al., 2006; Black et al., 2010; 2011; Brayshaw et al., 2010; Ben Dor et al., 2018). Water in the Jordan River, regenerated partially from snow on the Anti-Lebanon Mountains, is sourced from the Sea of Galilee. The

Jordan River is fed by the Yarmouk and Zarqa rivers and various smaller streams among the foothills, and terminates at the northern end of the Dead Sea.

The Southern Levant receives around 400-800 mm of rainfall annually along the valley ridges to 250-400 mm in the Jordan Valley in the lower valleys (Black et al., 2011; Soto-Berelov et al., 2012). A Mediterranean climate is denoted by long, dry, and hot summers and mild, wet winters, while a semi-arid climate is typified by low precipitation and high rates of evapotranspiration. To the south, around the Dead Sea Basin, there is a transition from a semi-arid climate to an arid climate (Black et al., 2011; Soto-Berelov et al., 2012). This region has relatively low rainfall, which can fall to below 50 mm annually in the southernmost wadis, and its high temperatures average between 20°C to over 40°C in summers (Shehadeh, 1985, as cited in Richard et al., 2010; Black et al., 2011; Fall et al., 2019).

Modern vegetation along the Jordan Rift has been described in detail in previous works, and its vegetation associations have been determined (Zohary, 1950; 1962; 1966; 1972; 1982; Feinbrun-Dothan 1978; 1986; Danin, 1995; Soto-Berelov et al., 2012). Phytogeographical zones are categorized according to plant species composition, with modern vegetation represented by plants in the Mediterranean, Irano-Turanian, Saharo-Arabian, and Sudanean plant geographic zones from north to south and from high to low elevation. The primary phytogeographical zone is Irano-Turanian, denoting vegetation found in Iran or Turkey, which includes shrubs like *Artemisia herba-alba*, *Noaea mucronate*, *Salsola vermiculata* and *Anabasis syriaca*, as well as steppe grassland vegetation. Mediterranean vegetation is more abundant at higher elevations and latitudes and is often intermixed with Irano-Turanian vegetation (Davies and Fall, 2001). Mediterranean vegetation includes dense, woody scrub, with a variety of small trees and bushes capable of withstanding summer droughts. Major species include woody trees such as *Quercus*

ithalburensis and *Q. calliprinos*, *Pinus halepensis*, *Olea europaea* var. *sylvestris*, *Ceratonia siliqua*, *Juniperus phoenica*, *Pistacia lentiscus,* and *P. palaestina.* Farther into valley bottoms and stretching down to the top of the Dead Sea, the vegetation transitions into a shrubby steppe, with species like *Ziziphus lotus* and *Retama raetam* (van Zeist, 1985). Progressing south, the Jordan Valley transitions from steppe to a desert biome, with more prevalent woody species like *Populus euphratica, Tamarix jordanensis*, *Acacia* sp., *Suaeda asphaltica*, *Ziziphus spina-christi*, *Z. lotus*, and *Anabasis articulata*. Many grasses are found in this region, such as *Stipa capensis* and wild relatives of cultivated cereals like *Hordeum murinum* (van Zeist, 1985; Danin, 1995; Davies and Fall, 2001; Soto-Berelov et al., 2012; 2015).

Past Climate and Ancient Vegetation

Over the course of human settlement, the environment of the Southern Levant has been dramatically modified by both human actions and climate change. One of the most important changes in the paleoclimate of the Holocene was the 4.2 ka BP event, a global climate event expressed as a decline in precipitation in the Levant, the timing of which roughly correlated with the abandonment of Early Bronze Age urban centers throughout the ancient Near East (Weiss et al., 1993; Rambeau and Black, 2011; Bieniada, 2016; Weiss, 2016; Kaniewski et al., 2008; 2018). Evidence for this phenomenon was first noted by Harvey Weiss based on his excavations at Tell Leilan, Syria (Weiss et al., 1993). A climate shift has since been noted in a variety of sediment and biological proxies across the Middle East and typically appears as a punctuated, multi-century event (Cullen et al., 2000; Edelman-Furstenberg et al., 2008; Frumkin, 2009; Weiss, 2017). The Jordan Rift contains several biogeographic zones in close proximity (Soto-

Berelov et al., 2012; 2015), such that small variations in precipitation and temperature could have exaggerated impacts in this region (Rambeau, 2010).

Climate models can help to retrodict what climate might have been like during the Early to Middle Bronze Ages. Potential vegetation modeling (Soto-Berelov et al., 2015; Fall et al., 2018) in conjunction with paleoclimate modeling (Bryson and DeWall, 2007) suggests that mean annual precipitation gradually declined over the Bronze Age, while mean annual temperature remained relatively steady with punctuated periods of cooling. This model proposes that the Middle Bronze was slightly cooler and wetter than the preceding EB IV, and the vegetation and climate model puts the wettest period around 4000 BP (Soto-Berelov et al. 2015; Fall et al. 2018). However, while several models seem to pick up the 4.2 ka BP Event (Guiot and Kaniewski, 2015), not all of them agree on the length of the event or the magnitude of regional temperature or precipitation change (Arikan, 2015). There are several proxies that can help assess these paleoclimate models.

Regional paleoclimate proxies include speleothems and lacustrine sediments, which can be used to reconstruct signals of climate over multiple timescales, revealing seasonal to millennium-scale change (Polyak and Denniston, 2012; Bradley, 2015). Multiple regional dripstone records are available for comparative discussion, such as those from Soreq Cave in Israel, Jeita Cave in Lebanon, and multiple smaller caves around the Dead Sea (Bar-Matthews et al., 1997; 1999; Verheyden et al., 2008; Bar-Matthews and Ayalon, 2011). General interpretation of speleothem records indicates multiple cycles of wet and dry periods, often with offsets of a century or longer between regional records, which show a decline in annual rainfall in the continental interior at 4200-3800 BP (U-Th dated; Bar-Matthews and Ayalon, 2011), around the time of the EB IV to MB I transition. Results generally agree on a drier climate around 4200 to

4000 BP, but disagree on the climate from 4000 BP onwards (Verheyden et al., 2008; Bar-Matthews et al., 2019; Burstyn et al., 2019). Records from the central Southern Levant indicate drier conditions, but variation between the Northern and Southern Levant suggests differences in timing and intensity of the event (Cheng et al., 2015; Burstyn et al., 2019), Figure 2.2.

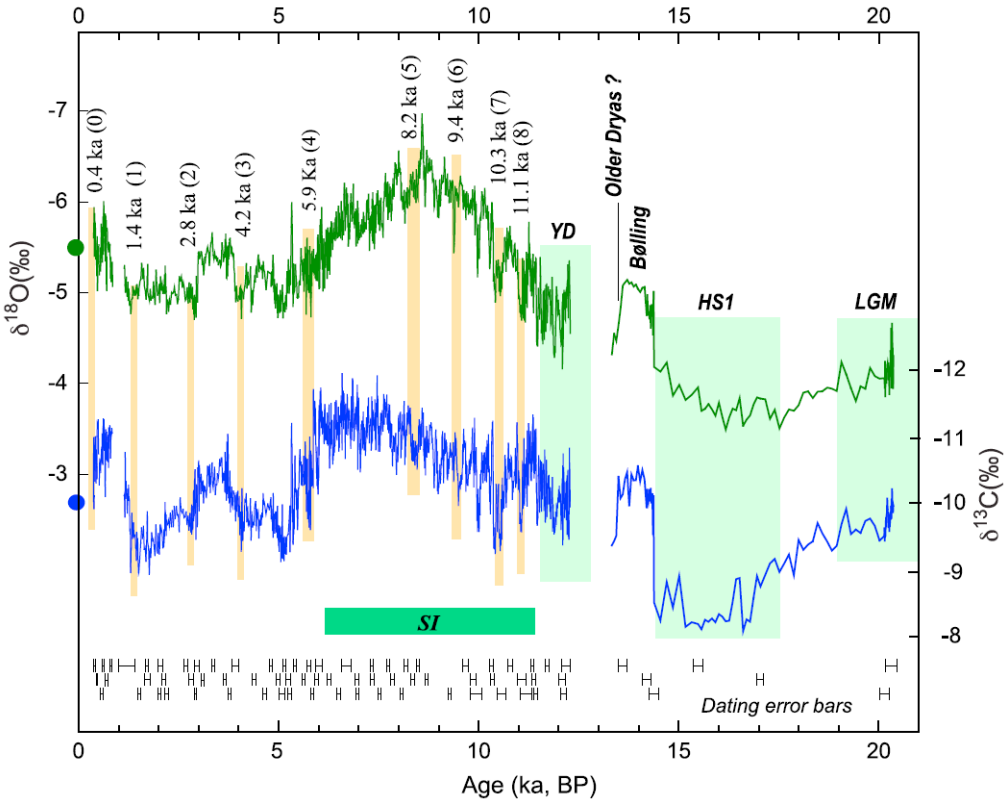

Figure 2.2 Values of $\delta^{18}O$ and $\delta^{13}C$ from a speleothem in Jeita Cave, Lebanon. Data suggest decreased precipitation, reflected as an increase in ^{18}O, during the 4.2 ka BP event. (Image from Cheng et al., 2015: Fig 2).

These findings are reinforced by rainfall modelling and sediment records, including sediment geochemistry. Rainfall and sediment records from the Sea of Galilee and Dead Sea in particular shed light on regional precipitation and evaporation rates over past millennia, indicating a net decline in precipitation in the southern portion of the Jordan Rift around the Dead Sea around the beginning of the Middle Bronze Age, suggesting a much longer period of decline potentially continuing until around 3200 BP (Enzel et al., 2003; Ken-Tor et al., 2004;

Morin et al., 2019). Other datasets, based on older proxies, suggest a drying that began in early to mid EB IV, about 4300 to 4200 BP and running to around 4000 BP (Migowski et al., 2006; Goldsmith et al., 2023). This is further supported by sediments indicating coastline regressions of the Dead Sea starting around 4400 BP and remaining low until around the Late Bronze (Klinger et al., 2003). However, records from the Sea of Galilee suggest a more stable, wet climate in the northern Jordan Valley during this time, supported by evidence of a steady sea level, suggesting variable climates from north to south along the Rift Valley (Vossel et al., 2018). Lake level records also suggest a contrast between the Northern and Southern Levant at the start of EB IV, indicative of an offset in climates (Cheng et al., 2015). These studies suggest regional climate variability with potentially no climatic deterioration in the northern Jordan Valley, but multi-century wet to dry shifts in the southern Jordan Valley, which start again in the mid-second millennium BCE (Migowski et al., 2006; Vossel et al., 2018). The Southern Levant also experienced a sequence of hydrological shifts featuring changes in river incision and sedimentation rates which culminated in increased floodplain alluviation during EB IV (Rosen, 1995, as cited in Rosen, 2007).

Vegetation change can also be a good indication of climate change and environmental shifts. Regional pollen core analyses have been conducted on varved sediments from Birket Ram, Lake Hula, the Sea of Galilee and the Dead Sea, situated along the Jordan Rift Valley from North to South (Baruch, 1986; 1990; Baruch and Bottema 1999, as cited in Weiss, 2017; Hunt, 2004; Schwab et al., 2004; Neumann et al., 2007; 2010; Hajar et al., 2008; Langgut et al., 2013; 2015; Finkelstein and Langgut, 2014; Schiebel and Litt, 2018). Vegetation inferred for the EBA suggests a cooler, wetter climate in the Southern Levant, with more extensive woodland taxa and humid conditions through the end of EB III (Roberts et al., 2011; Langgut et al., 2015). Records

from regional charcoal and tree ring records likewise suggest a decline in precipitation at the end of the Early Bronze Age (Frumkin, 2009; Masi et al., 2012). Woodlands were most extensive in EB I and II, and were dominated Mediterranean maquis forests of oak and pistachio, as well as large concentrations of olive and pine, transitioning to grasslands in EB III (Baruch, 1986; Liphschitz, 1996; Neumann et al., 2007). The most common woodland species were evergreen and deciduous oak (*Quercus calliprinos, Q. ithalburensis*), pine (*Pinus halepensis*), pistachio (*Pistacia lentiscus, P. terebinthus, P. palaestina*) and olive (*Olea europaea*), with tamarisk (*Tamarix aphylla*) in the lower latitudes and elevations (Liphschitz, 1996; Willcox, 1999; Benzaquen et al., 2019). Pollen and charcoal data suggest dry conditions in EB IV and MB I, followed by relatively more humid conditions in MB II and III (Roberts et al., 2011; Langgut et al., 2015; Ehrlich et al., 2022). In MB II-III, vegetation in the northern portions of the Southern Levant returned to Mediterranean forests dominated by oak, pine, and olive taxa (Lev-Yadun et al., 1996; Schwab et al., 2004). Significant amounts of olive pollen are noted in Chalcolithic and EBA sediments, particularly around Hula Valley during EB IV. This evidence has been used to suggest increased aridity in the Jordan Valley (Neef, 1990; van Zeist et al., 2009; Langgut et al., 2015; Sorrel and Mathis, 2016; Benzaquen et al., 2019).

The Southern Levant in EB IV had a mix of Mediterranean woodland vegetation at higher elevations and latitudes, including oak, pine, pistachio, olive, and grape (*Vitis vinifera*), as well as herbaceous plants like plantain (*Plantago* sp.) (Baruch, 1986, Langgut et al., 2015). Oak decreased in abundance during EB IV, accompanied by increasingly abundant drought- or salt-tolerant taxa like *Tamarix*, *Olea*, *Acacia*, *Juniperus*, *Ziziphus,* and various *Poaceae* (grasses) further south, as woodlands continued their transition to scrubland and grassland (Baruch, 1986; Hunt et al., 2007; Finkelstein and Langgut, 2014; Langgut et al., 2015; Schiebel and Litt, 2018).

In the Middle Bronze Age, climate either remained dry or further deteriorated from EB IV conditions (Finkelstein and Langgut, 2014; Langgut et al., 2015), but more humid conditions returned during MB II and early MB III (Migowski et al., 2006; Neumann et al., 2010; Finkelstein and Langgut, 2014; Langgut et al., 2015; Soto-Berelov et al., 2015). Forest species diminished late in the southern Levantine Middle Bronze Age (Fall et al., 2018), due to regional drying which began around 1700-1650 BCE (Roberts et al., 2011).

While these proxies include some conflicting evidence, in combination they reveal a general trend of drier conditions beginning roughly around 4500-4200 BP and lasting until around 4000-3900 BP, with a potentially drier period existing from around 4200-4000 BP. The length and intensity, as well as the start and end dates for this aridification vary across the Southern Levant, reflecting local climate conditions. According to these reconstructions, precipitation trends during Middle Bronze II are thought to have returned to levels similar to those in EB III, which serves as an important factor for interpreting environmental conditions during EB IV and the MBA. Figure 2.3 shows the timeline of Southern Levantine chronology with a summarized graphic of the climate trends inferred from the cumulative results of paleoenvironmental models and proxies compared to ages of the focal sites to be used in this study, described in the following sections.

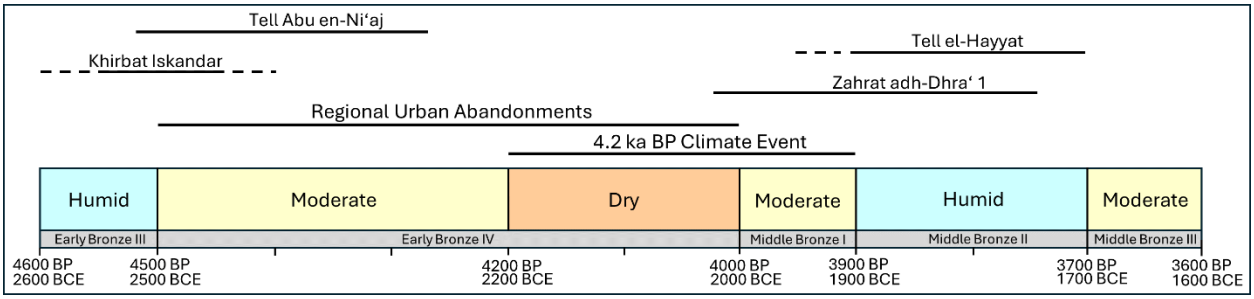

Figure 2.3 Southern Levantine chronology showing the radiocarbon dated ranges from each of the four focal sites used in this study. Dashed lines indicate potential occupation outside a radiocarbon-dated range. Determination of humid, moderate, and dry periods comes from interpretations of the models and proxies from previous studies, which are presented in Chapter 2.

Regional Chronology

This study focuses on the third to second millennia BCE, specifically the Early and Middle Bronze Ages of the Southern Levant. Age ranges have been previously defined by ceramic types that are regionally variable and have traditionally been determined by changes in ceramic vessel forms and styles (Albright, 1962; Dever, 1995; Tsuneki and Miyake, 1996; Kennedy, 2015; D'Andrea, 2019). These early chronostratigraphic efforts based on ceramic types have now incorporated radiocarbon dating to help revise and pinpoint the timing of major chronological boundaries (Weinstein, 1984; Bronk Ramsey et al., 2002). Bayesian modeling of AMS ages sets forth a revised chronology for the Southern Levant (e.g., Regev et al. 2012) that holds important implications for our interpretation of Levantine settlement and society during Early Bronze IV and Middle Bronze Ages (Bronk Ramsey, 2009).

For the sake of consistency, archaeological dates are referred to in the standard BCE format, while paleoclimate dates are typically referred to using BP. These can be informally considered to be around 2000 years apart, though for the sake of calibration the year 1950 AD is the base year for BP calculations.

The temporal ranges for each cultural age discussed in this work are noted in Table 2.1. The Early to Middle Bronze Ages span around 3500-1600 BCE in the Levant. The EBA is divided into four periods, denoted by Roman numerals as Early Bronze I, II, III and IV. I use EB IV to signify the period from 2500 to roughly 2200 BCE (although the period runs until 2000 BCE) denoting the timeframe from which data are available from the four archaeological focal sites used in this dissertation. Radiocarbon dating has pushed the timing of the transition from EB III to EB IV much earlier than estimated traditionally to around 2500 cal BCE, significantly lengthening the EB IV period from 200 to 500 years (Regev et al., 2012; Höflmayer et al., 2014;

Falconer and Fall, 2016; 2017, Fall et al., 2021; Fall et al., 2023). The Middle Bronze Age is divided into three periods, previously labeled MB II A-C, now known as Middle Bronze I, II, and III, roughly 2000-1600 BCE (Höflmayer et al., 2016; Falconer and Fall, 2017; Höflmayer, 2017; Fall et al., 2021; 2022; 2023). While only EB IV and MB I-II are directly investigated in this dissertation, these higher chronologies for each period are used for regional intersite comparisons.

Table 2.1 Chronology for the Early and Middle Bronze Ages in the Southern Levant, indicating occupation dates by phase (Ph) for the four focal archaeological sites featured in this study. Ages based on radiocarbon studies and ceramic chronology from Bourke et al., 2009; Regev et al., 2012; Richard, 2014; Höflmayer et al., 2014; 2016; Falconer and Fall, 2016; Fall et al., 2019; 2020; 2023. No Data is used to signify that no archaeological remains were recovered from the four focal sites for this time range. Slashes between two ages signify that the transition happened roughly between the listed ages. BP dates in this table are presented informally, offset 2000 years from OxCal calibrated BCE dates.

Southern Levantine Periods	**Age (cal BCE)**	**Age (cal BP)**	**Site Occupation**
Middle Bronze III (MB III)	1700-1600	3700-3600	Tell el-Hayyat (Ph 1)
Middle Bronze II (MB II)	1850/1800-1700	3850/3800-3700	Tell el-Hayyat (Ph 5-2) Zahrat adh-Dhra‘ 1 (Ph 3-2)
Middle Bronze I (MB I)	2000/1950-1850/1800	4000/3950-3850/3800	Tell el-Hayyat (Ph 6-5) Zahrat adh-Dhra‘ 1 (Ph 4-3)
Early Bronze IV (EB IV)	2200-2000/1950	4200-4000/3950	*No Data*
Early Bronze IV (EB IV)	2500-2200	4500-4200	Tell Abu en-Ni‘aj (Ph 7-1) Khirbat Iskandar (Ph 3-1)
Early Bronze III (EB III)	2900-2500	4900-4500	Khirbat Iskandar (Pre-Ph 1)
Early Bronze II (EB II)	3000-2900	5000-4900	*No Data*
Early Bronze I (EB I)	3500-3000	5500-5000	*No Data*

Focal Archaeological Sites

Introduction

Four ancient villages were selected for analysis, providing carbonized seeds for paleoethnobotanical, spatial, and stable isotopic investigations. These include Tell Abu en-Ni‘aj, Tell el-Hayyat, Khirbat Iskandar, and Zahrat adh-Dhra‘ 1. Khirbat Iskandar provides limited

seed content and is used only for stable isotopic analysis in this study. Tell Abu en-Ni‘aj and Tell el-Hayyat also provide ancient shells for stable isotopic analysis.

Tell Abu en-Ni‘aj (Ni‘aj)

Tell Abu en-Ni‘aj (Figure 2.4) was a settlement in the northern Jordan Valley occupied in the EB IV period (Falconer and Fall, 2019; Fall et al., 2021). It was a ~2.5 ha sedentary agricultural village located above the floodplain of the Jordan River, 250 m b.s.l. near the Wadi el-Yabis, a minor tributary of the Jordan River. Ni‘aj was excavated in three seasons in 1985, 1996/7 and 2000, revealing seven stratigraphic habitation phases (Falconer, 1987; Falconer et al., 1998; 2001; Falconer and Fall, 2019). The site is comprised of a network of mudbrick houses with numerous adjoining rooms, courtyards, and passageways separated by sherd-paved streets. Ni‘aj may have housed around 500-600 people, yet there is no surrounding wall typical of settlements from the Early Bronze Age (Falconer and Fall, 2019). The radiocarbon chronology for Tell Abu en-Ni‘aj comes from AMS analyses of archaeological seeds and shows that the village was occupied about 2500-2200 cal BCE (Fall et al., 2021).

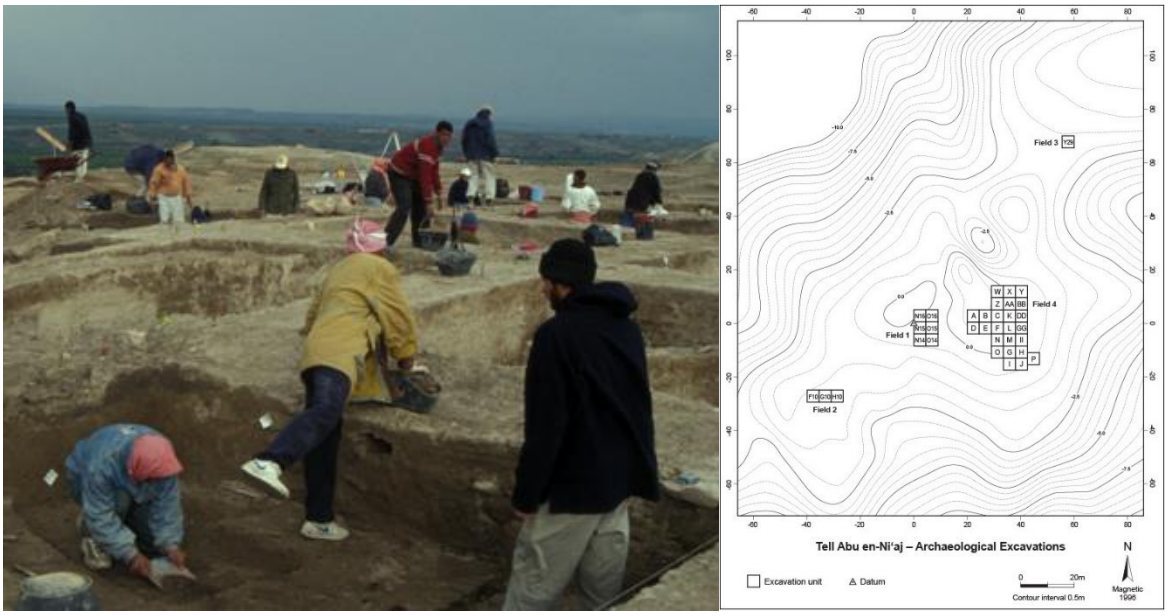

Figure 2.4 Left: Excavation at Tell Abu en-Ni'aj, Jordan in 2000, facing northwest across the northern Jordan Valley. Right: Excavation areas at Tell Abu en-Ni'aj. (Falconer and Fall, 2019: fig 1.1, photo; fig. 2.1, map).

Tell el-Hayyat (Hayyat)

Tell el-Hayyat (Figure 2.5) was a small agricultural village occupied during the latest EB IV and through MB I-III (Falconer and Fall, 2006; Fall et al., 2021). The radiocarbon chronology for Tell el-Hayyat comes from AMS analyses of archaeological seeds and shows that the village was occupied from about 1900-1650 cal BCE (Fall et al. 2020; 2023), placing the occupation of Hayyat primarily within the Middle Bronze Age. The distinctive ceramics of Phase 6 indicate that occupation began in EB IV (Falconer and Fall, 2017). Hayyat is a small settlement (~0.5 ha) sitting atop a lacustrine terrace 240 m b.s.l. in the Jordan Valley, about 1.5 km northeast of Ni'aj. The site was excavated in 1982, 1983 and 1985, revealing six occupation phases (Falconer et al., 1984; Magness-Gardiner and Falconer, 1991; Falconer and Fall, 2006). Streets, courtyards, mudbrick houses, and four stratified Canaanite temples were found at Hayyat, and the settlement probably had no more than 150 inhabitants (Magness-Gardiner and Falconer, 1991; Falconer, 1995; Falconer and Fall, 2006; 2017; 2022).

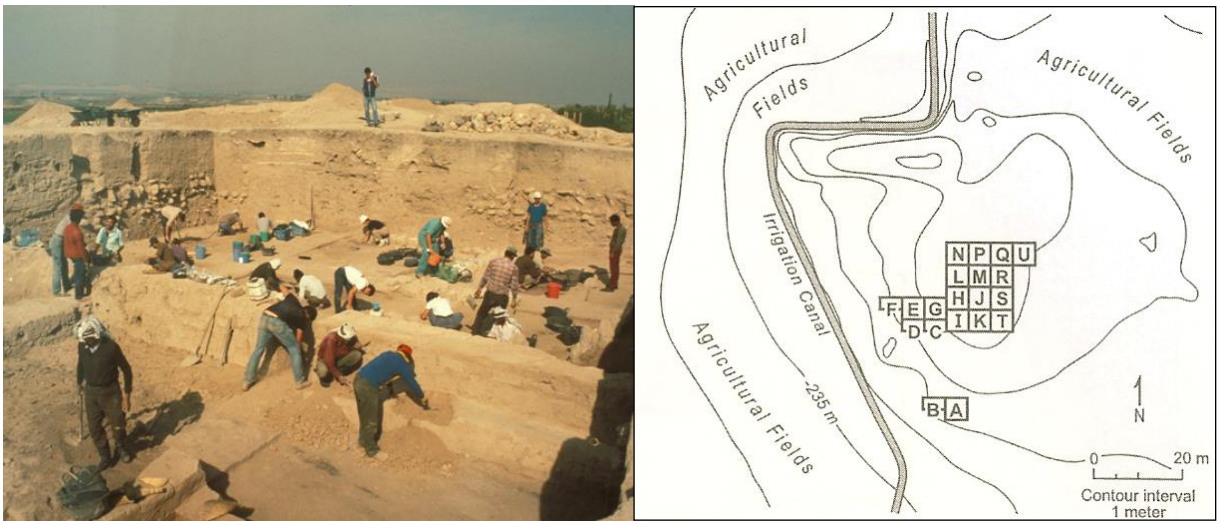

Figure 2.5 Left: Excavation at Tell el-Hayyat, Jordan in 1985, facing northwest. The Jordan River flows at the foot of the cut bank to the left in the distance. Right: Excavation areas at Tell el-Hayyat (Falconer and Fall, 2006: fig. 2.16, photo; fig. 2.3, map).

Khirbat Iskandar (Iskandar)

Khirbat Iskandar (Figure 2.6) was a moderately-sized 3 ha agricultural settlement on a northern terrace of the Wadi Wala, an eastern tributary of the Dead Sea, to the northeast of ZAD 1. Evidence for menhirs to the south and further cultural remains to the east suggest Iskandar may have stretched to around 12 ha or larger (Richard et al., 2010). Iskandar was occupied in EB III and IV, and possibly as early as EB II (Richard, 2014). The settlement sits approximately 500 m a.s.l., lying to the west of an escarpment above the Dead Sea Basin. It sits upon an alluvial terrace bounded by Cretaceous limestones and sandstones (Richard et al., 2010). Khirbat Iskandar was excavated by a team directed by Dr. Suzanne Richard of Gannon University. Excavations at Iskandar were conducted over multiple seasons starting in the 1950s and is currently being studied by Dr. Suzanne Richard (Parr, 1960, as cited in Richard, 1980; Richard, 1986; 1990; Richard and Long, 2006; Richard et al., 2013; 2018). Iskandar was a settlement of stone-founded mudbrick architecture with signs of EB III/IV fortification, including re-use of an EB III surrounding wall and a possible EB IV gateway (Richard, 1986; Richard et al., 2010).

Three areas, each consisting of multiple excavation units, have been uncovered. Chronological information for samples from Khirbat Iskandar is currently available based on the stratigraphy of Areas B and C indicating at least three phases in EB IV and four phases in EB III (Richard et al., 2010; Fall et al., 2022). Currently, there are twelve published radiocarbon ages from the site (Fall et al., 2022), but stratigraphy has suggested the potential for a wider occupational range. Notably, only material from phases dating to EB IV are used in this dissertation.

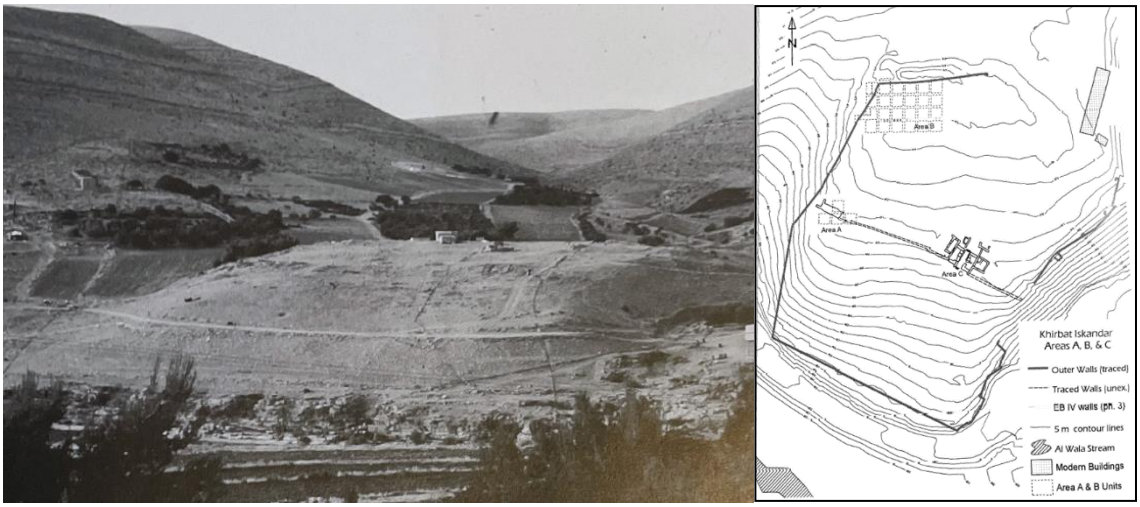

Figure 2.6 Left: Khirbat Iskandar, Jordan and its vicinity, facing north. Right: Topographic map of Khirbat Iskandar showing excavation areas (Richard et al., 2010: fig. 1.3, photo; fig. 1.2 map).

Zahrat adh-Dhra‘ 1 (ZAD 1)

Zahrat adh-Dhra‘ 1 (Figure 2.7) represents an agrarian settlement roughly 6 ha in size, in a marginal agricultural environment. Due to downcutting of adjacent tributary channels, a probable result of declining Dead Sea level over the recent Holocene (Frumkin et al., 1994, as cited in Fall et al., 2019), the full extent of ZAD 1 shows it originally spread across roughly 12 ha (Edwards et al., 2001; Falconer et al., 2001). Based on AMS ages from carbonized seeds, it was occupied during MB I-II, between about 2050 and 1700 cal BCE (Falconer and Fall, 2016; Fall et al., 2019; Fall et al., 2023). The site is situated on a ridge above the Dead Sea Plain between Wadi Dhra‘ and Wadi Wa’ida, two tributaries of the Wadi al-Karak, which flows

westward to the Dead Sea (Fall et al., 2019; 2023). ZAD 1 sits around 180 m b.s.l. over-looking the Lisan Peninsula, which juts into the Dead Sea from the east (Edwards et al., 2001). The site was geographically isolated during the Middle Bronze Age, as part of a larger pattern of sparse settlement in southern Jordan during this age (Bourke, 2014), but integration with other settlements is indicated by ceramic vessels at ZAD 1 that were probably not made locally (Edwards et al. 2001). ZAD 1 was excavated by Falconer and Fall in winter 1999/2000 and reveals three phases of occupation over a period of several centuries (Falconer et al., 2001; Falconer and Fall, 2016; Fall et al. 2023). It is a settlement of dispersed, semi-subterranean, one- and two-room mudbrick houses, some with adjoining enclosure walls (Falconer et al., 2001; Falconer and Fall, 2016; Fall et al., 2019).

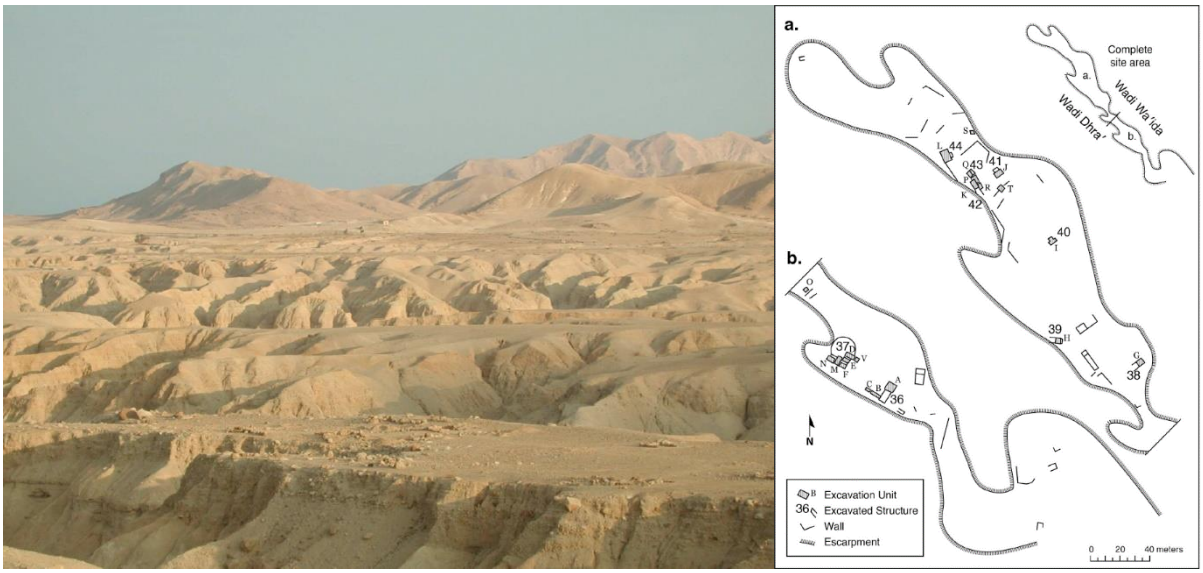

Figure 2.7 Left: Plain of Dhra‘, Jordan showing Structures 40-44, facing north. Right: Excavated structures from Zahrat adh-Dhra‘ 1, Jordan showing the locations of lettered excavation units (Fall et al., 2019: fig. 2, photo; fig. 6, map).

CHAPTER 3: METHODS FOR PALEOETHNOBOTANICAL ANALYSES

Introduction

Paleoethnobotany was pioneered in the Eastern Mediterranean by Hans Helbaek in the 1950s and 1960s (Helbaek, 1958; 1960; 1964), based on the analysis of carbonized plant macro- and micro-remains to interpret local paleoenvironments and ancient human cultivation practices. The methodology involves the recovery, taxonomic identification, and quantification of carbonized macro remains, often seeds and wood, using a combination of descriptive and analytical statistical methods which provide direct context for the analysis of plant evidence. Methodology for tallying and simple statistical analysis in this dissertation follows established procedures (Jones, 1991; Fritz and Nesbitt, 2014). This chapter describes the analytical process used for the recovery, identification, and quantification of the floral assemblages excavated at Tell Abu en-Ni‘aj, Tell el-Hayyat, and Zahrat adh-Dhra‘ 1, while Chapters 4, 5, and 6 describe the assemblages of each site.

Field Methods

The excavations of Ni‘aj, Hayyat, and ZAD 1 were overseen by Dr. Patricia Fall and Dr. Steven Falconer from 1982-2000. Archaeological excavation for each settlement began with mapping of the archaeological site and selection of excavation areas. Ni‘aj was excavated over 35 areas, Hayyat over 21, and ZAD 1 over 24 areas. The term ‘area’ typically indicates a 4 x 4 m square separated from adjacent areas by a 1 m balk (i.e., unexcavated section). At ZAD 1, areas of various sizes and orientation were positioned to best capture architectural features, which are spread out along the 12 km ridge unlike a typical *tell* settlement. Primary excavation areas were

labelled alphabetically A-ZZ while test trenches were given alpha-numeric codes (Falconer and Fall, 2006; 2019; Fall et al., 2019). To provide a unique spatial identifier indicative of archaeological context, sediment samples were collected and labeled according to the letter of their excavation area, locus number (a three-dimensional feature), and a bag number, as indicated in Tables S1-S4. Samples from Khirbat Iskandar add a fourth spatial identifier, a pail number (see Table S4).

Flotation samples containing sediment with carbonized plant remains were collected during excavation from areas where burned organic matter was visible. Flotation sampling prioritized features in which organic matter may be more prevalent and least disturbed, which were ash lenses, pits, earthen surfaces and occupational debris accumulated on surfaces. Sample volume and contextual information were recorded at the time of collection. A total sediment volume of about 1000 L was processed by water flotation at the three sites. An average volume of around three liters per sample was collected at ZAD 1 and Hayyat, and four liters per sample at Ni‘aj (Falconer and Fall, 2006; 2019; Fall et al., 2019).

Samples sorted for this analysis contain carbonized floral remains recovered from sediment via non-mechanized water flotation using metal baskets and mesh screens (Hayyat, ZAD 1, and one season at Ni‘aj), by mechanized water flotation (for samples collected in 1996/97 and 2000 at Ni‘aj) using Flote-Tech technology to separate the sediment (Pearsall, 1989), or hand-picked from the sediment, in the case of large charcoal samples (Falconer and Fall, 2006; 2019; Fall et al., 2019). Organics were skimmed off the surface, sun dried, and bagged.

A total of 87 sediment samples was recovered from ZAD 1. From Hayyat, 235 sediment samples were recovered, with 164 sorted for carbonized seeds. From Ni‘aj, roughly 515 sediment

samples were recovered, though around half of these contained only non-seed charcoal after initial inspection. A total of 156 samples were sorted for Ni‘aj.

Laboratory Methods for Paleoethnobotanical Analysis

Sample Selection and Preparation Methods

Partial paleoethnobotanical analysis was previously conducted for all three sites at Arizona State University as part of preliminary studies on cereals, fruits, and charcoal (Lines 1995; Meegan, 2005; Klinge and Fall, 2010; Fall et al., 2015). This included (1) sorting of 86 sediment samples for cultivated taxa from ZAD 1, (2) sorting of 152 sediment samples from Hayyat, and (3) selective sorting of seeds from Ni‘aj primarily from Area C. Some domesticates were quantified from Hayyat and ZAD 1 in these previous studies, but not separated, so required extraction and resorting for both a paleoethnobotanical and stable isotope analysis. All flotation samples included in this study have thus been sorted or resorted as part of my research.

The selection of sediment samples for analysis primarily focused on excavation contexts where high concentrations of carbonized plant macrofossils were available, but also used a tripart strategy to further explore a mix of different architectural structures, locus types (denoting the type of sediment or archaeological feature), and occupational phases. The goal for selecting new samples was to generate data with both spatial and temporal coverage, which would aid in intra- and inter-site comparisons, as previous studies have suggested that poor coverage of locus types or excavation areas may hinder accurate interpretation of the floral assemblage (Lennstrom and Hastorf, 1995). A non-random sampling strategy ensured that robust floral datasets could be acquired by selecting samples from multiple areas across each site from different archaeological contexts and sampling those same areas across each phase. I tallied roughly 50,000 carbonized

plant fragments from 390 archaeological contexts, with over 34,000 of these contributing to the identified seed and chaff specimens that were used in the analysis in this dissertation.

The results of the paleoethnobotanical analysis of carbonized plant remains are presented in Chapters 4-6 for three sites, Tell Abu en-Ni‘aj, Tell el-Hayyat, and Zahrat adh-Dhra‘ 1, and cover the time period from about 2500 to 1650 BCE. Tables 3.1-3.3 indicate the approximate age range for the occupational phases of each site along with the flotation volumes, counts, and densities of carbonized seeds retrieved. Sample counts from the first and last phase at each site have the lowest number of samples due to erosion of the latest, topmost phase and limited excavation or limited cultural deposition in the earliest phase. A density metric was calculated as the number of macrofossils recovered per liter of floated sediment. Ni‘aj generally has a higher macrofossil recovery rate than Hayyat, while Hayyat maintained a higher recovery rate than ZAD 1 for all phases except for Hayyat Phase 6 (the earliest phase). Macrofossil recovery rates appear generally lowest at ZAD 1, with a maximum of 13 seeds per liter in Phase 2.

For Tell Abu en-Ni‘aj, I sampled roughly 20 samples per phase, bringing the total sample count to 156 samples (Table 3.1). Previous sorting focused on temporal sequences, primarily exploring multiple phases in Areas AA, C, and GG, all of which have samples well distributed throughout the seven occupation phases at Ni‘aj (Porson, 2018). Further sampling for this dissertation targeted Areas K, H, M, and D, with intensive sampling for these units allowing for comparison of temporal trends and spatial comparisons (see Figure 2.4). This most recent sample selection targeted new contexts to fill gaps in the spatial and temporal paleoethnobotanical record of the site. The most recent analysis has broadened site coverage to include samples from 15 of the 27 excavated areas.

Table 3.1 Number of samples, number of identified macrofossils, liters floated, and number of plant macrofossils per liter floated by phase at Tell Abu en-Ni'aj, Jordan. Radiocarbon age ranges are based on modeled phase boundary medians in Fall et al. 2021.

Age Range (cal BCE)	Phase	Flotation Samples	Identified Macrofossils	Liters Floated	Macrofossil Density
2294–2264	1	12	202	55.4	3.6
2331–2294	2	27	2279	138.6	16.4
2375–2331	3	37	3872	189.6	20.4
2418–2375	4	24	3696	111.5	33.1
2456–2418	5	17	2901	66.1	43.9
2487–2456	6	23	4459	66.7	66.9
2524–2487	7	16	3553	49.5	71.7

Sample selection at Tell el-Hayyat included a majority of the excavated portions of the site and included all but a few samples. A maximum of 49 samples and an average of around 20 per phase were analyzed for Hayyat (Table 3.2), with Areas A, K, P, and T most intensively sampled (see Figure 2.5). Of the 151 total samples, 123 represent partial resamples while 28 were previously unsorted. New sampling focused on Areas K and T, which provide additional floral evidence from Hayyat's domestic sectors, Area A which lies just beyond the household units and provides an exterior context, and Area P, which is a central unit with almost no previous sampling that is used for comparison with Areas K and T.

Table 3.2 Number of samples, number of identified macrofossils, liters floated, and number of plant macrofossils per liter floated by phase at Tell el-Hayyat, Jordan. Radiocarbon age ranges are based on modeled phase boundary medians in Fall et al. 2021.

Age Range (cal BCE)	Phase	Flotation Samples	Identified Macrofossils	Liters Floated	Macrofossil Density
1711–1660	1	1	44	3.0	14.7
1779–1711	2	22	3153	132.0	23.9
1798–1779	3	38	5248	220.0	23.9
1834–1798	4	49	5285	271.0	19.5
1887–1834	5	38	6107	216.3	28.2
1921–1887	6	3	294	44.0	6.7

Sampling strategy at Zahrat adh-Dhra‘ 1 focused on the contexts from Areas I, L, and K for comparative analysis (see Figure 2.7). Spatial and temporal analyses are different from those at Ni‘aj and due to ZAD 1’s structures being independent of one another. A total of 85 samples from ZAD 1 are sorted across Phases 4, 3 and 2 (Table 3.3).

Table 3.3 Number of samples, number of identified macrofossils, liters floated, and number of plant macrofossils per liter floated by phase at Zahrat adh-Dhra‘ 1, Jordan. Radiocarbon age ranges are based on modeled phase boundary medians in Fall et al. 2023.

Age Range (cal BCE)	Phase	Flotation Samples	Identified Macrofossils	Liters Floated	Macrofossil Density
1802–1761	2	35	1063	81.7	13.0
1879–1829	3	44	881	150.2	5.9
2029–1950	4	5	117	13.2	8.9

Carbonized remains were analyzed at UNCC in the paleoethnobotany laboratory. Preparation included sieving the flotation remains through nested 2 mm, 1 mm, 0.5 mm, and 0.25 mm sieves. Sieving helps to remove fine dust and sediment. Samples that were particularly small or that did not have much fine dust, which often hindered identification, did not require sieving. Samples are poured into petri dishes for microscopy. No minimum sample size was set, but large samples were split into smaller samples (½ or ¼ of the original size) if more than roughly two petri dishes would be required to fully sort a sample.

A Zeiss Stemi 305 microscope was used at 40x magnification for all sorting and identification. All carbonized seeds and select chaff fragments (rachis internodes and glume bases) were identified to the lowest possible taxonomic classification and quantified. A collection of comparative literature was used for primary seed identification (e.g., Isely, 1947; Delorit 1970; van Zeist, 1970; 1974; 1976; Gunn, 1972; Martin and Barkley, 1973; Zohary, 1966; 1972; Zohary and Hopf, 1973; 1988; Zohary and Spiegel-Roy, 1975; Feinbrun-Dothan, 1978; 1986; van Zeist and Bakker-Heeres, 1982; 1984a; 1984b; Hubbard, 1992; Jacomet, 2006;

Cappers and Bekker, 2013). The tally of each taxon and associated contextual information was recorded in a lab notebook and Microsoft Excel.

Carbonized Plant Macrofossil Quantification Methodology

All taxa from Ni'aj, Hayyat, and ZAD 1 were tallied according to the number of identified specimens (NISP) (O'Connor, 2000: 54). NISP measures the maximum number of specimens by counting every seed or seed fragment as a unique specimen. It is generally useful for whole seeds, but can overrepresent floral taxa that produce abundant seeds or seeds that readily fragment.

The taxa from Hayyat were also tallied according to the minimum number of individuals (MNI) (Jones, 1990; Reitz and Wing, 2008; Antolin and Buxó, 2011), which uses counts of a characteristic morphological feature for each taxon to minimize the effects of overcounting taxa. MNI provides a more cautious estimate and tends to undercount taxa. Both NISP and MNI were provided to give complementary estimates of the relative abundances of plant taxa (Jones, 1990). MNI was calculated on the basis of the following fragmentation quantification strategy developed for this dissertation. For grasses, a fragmented seed was counted if it contained an embryo. If a fragment did not have an embryo, it was tallied only if at least 10% of the seed was present, then this count was divided by 10.

Non-grass seeds were counted if over 90% of the seed was present. If smaller fragments were present, they were tallied only if at least 10% of the seed was present, then this count was divided by 10. This can be summarized by the following method:

$$\mathrm{COUNT}_{\mathrm{MNI}} = \sum \left(\mathrm{COUNT}_{\mathrm{Whole}} + \mathrm{COUNT}_{\mathrm{Embryo}} + \frac{\mathrm{COUNT\ Fragments}}{10}\right) \quad (1)$$

For chaff, all rachis internodes were counted as one, whether conjoined, fragmented, or as part of a full spikelet. Glume bases were found individually or part of a full spikelet. If unbroken, a spikelet was counted as two glume bases.

Three categories of tallied plant remains (cultivated cereal fragments, wild legume fragments, and unknown plant fragments) were removed to aid analysis in this dissertation. Cultivated cereal fragments and wild legume fragments were prominent and counts of unknown plant remains were low at all three focal sites. The original values of each of these categories are recorded in the supplementary tables of macrofossil counts (Tables S1-S4).

Floral Assemblage Quantification

Following tallying of the seeds and plant fragments by taxon, NISP counts were used to calculate density, frequency, and ubiquity to identify patterns in the floral assemblages of all three sites (Fritz and Nesbitt, 2014). Density was measured as the number of seeds per liter of floated sediment; this measure accommodates sediment sample size variation. Frequency was measured as the percentage of one taxon out of the entire assemblage or as the percentages of one taxon to another. Density and frequency are particularly appropriate methods for standardization for comparing taxonomic abundances (Miller, 1988; Kreuz et al., 2005; van der Veen, 2007; Fritz and Nesbitt, 2014). Ubiquity was measured as the percentage of samples in which a taxon is present (Hubbard, 1980). This metric is valuable for comparing species with low cultivation or preservation rates and provides a complementary measure to densities and frequencies (Popper, 1988; Pearsall, 1989).

Each taxon was evaluated at the species level (e.g., bread wheat versus emmer wheat), at the genus level (e.g., wheat versus barley), and at the family-level level (e.g., cultivated cereals

vs cultivated legumes) for both the temporal and spatial analyses. Temporal changes were illustrated using *TILIA* and *TGView* to create diagrams of seed taxa or groups of taxa (Grimm, 2004). Barley to wheat frequency and hierarchical CONISS clustering of the cultivated assemblages were incorporated within *TILIA* diagrams to draw distinctions in the assemblages between phases (Grimm, 1987). Bar charts and scatterplots were then used to highlight the key differences between the floral assemblages.

Background: Common Plant Taxa From Focal Sites and Why They Matter

Cultivated Crops

This section briefly discusses the commonly noted and culturally relevant plant taxa recovered from flotation sampling at Tell Abu en-Ni'aj, Tell el-Hayyat and Zahrat adh-Dhra' 1. Common taxa are determined as those appearing at multiple sites or with high relative macrofossil frequencies per site. Since their domestication, cultivated cereals have been one of the most influential food crops for ancient peoples of the Southern Levant (Weiss and Zohary, 2011). One of the most well-known cereals in ancient societies was *Triticum*, or wheat. *Triticum aestivum* (bread wheat) was particularly notable with its high yield and ability to rise higher when made into bread compared to other cereals (Samuel, 1989).

Triticum aestivum is an early-domesticated, hexaploid, free-threshing variety commonplace throughout the Levant, and has been suggested to have been an important trade commodity in the Early Bronze Age (Fall et al., 1998). Sown in both spring and summer today, *T. aestivum* is known for having strict soil nutrient and water requirements, stricter than *T. dicoccum* (emmer wheat) (Oleinikova, 1976, as cited in Riehl and Bryson, 2007; Konvalina et al., 2011; 2014; Marinova and Valamoti, 2014; Setter et al., 2016). *Triticum durum* (durum

wheat) is a tetraploid form of domesticated *T. dicoccum*. It is the other free-threshing *Triticum* species common in the region. It is most commonly fall-sown and has only slightly higher drought tolerance than *T. aestivum* (Jasny, 1944, as cited in Chernoff, 1988). The other common *Triticum* species in Levantine antiquity are *T. dicoccum* (emmer wheat) and *T. monococcum* (einkorn wheat). *Triticum dicoccum* is a hulled, tetraploid wheat and a domesticated subspecies of *T. dicoccoides* (wild emmer). It is one of the more resilient varieties, able to tolerate semi-arid conditions and poorer soils (Jasny, 1944, as cited in Chernoff, 1988; Riehl, 2010; Konvalina et al., 2011). *Triticum dicoccum* is often a spring-sown crop today, but may have been a winter-sown crop in antiquity due to a higher water requirement than other cereals (Hillman, 1981). Finally, *T. monococcum* is a domesticated, diploid variant of *T. boeoticum* (wild einkorn) and a relative of *T. urartu* (red Urartu wheat) (Willcox, 2005; Fuller, 2006). *Triticum dicoccum* and *T. monococcum*, common taxa found at the focal sites, along with the less frequent *T. spelta* (spelt wheat), are glume wheats or hulled wheats (i.e., wheats with protective hulls). *Triticum monococcum* was typically a winter-sown crop with lower drought tolerance than emmer, despite it being a hulled wheat (Riehl, 2010).

Barley includes *Hordeum vulgare* ssp. *spontaneum* (wild barley), *H. vulgare* ssp. *vulgare* (hulled barley) which includes both *H. vulgare* var. *distichum* (two-row hulled barley) and *H. vulgare* var. *hexastichum* (six-row hulled barley), and naked barley (*H. vulgare* var. *nudum*). For the cultivated barley at our focal sites, there are two common taxa: *Hordeum vulgare distichum* [hereafter *Hordeum vulgare*] and *H. vulgare* var. *nudum*. *Hordeum vulgare* was a common cereal grain in antiquity used for breadmaking, as animal feed, and for brewing beer (Powell, 1984; Zohary and Hopf, 1988: 52; Miller, 2002). This cereal was more prominent in arid regions due to its lower water requirement and increased tolerance of poor soils (Renfrew, 1973; Zohary, 1982;

Hopf, 1983; Zohary and Hopf, 1988; Riehl, 2010). *H. vulgare* var. *nudum* was less frequent in regional macrofloral surveys, but was still a common crop in ancient times. This species is somewhat resilient to climate stress, but more drought intolerant than *H. vulgare* due to its lack of a hull (Djelel et al., 2010; Sturite et al., 2019). Both species of *Hordeum* have a shorter growing season and are more tolerant of drought conditions than the *Triticum* species (Renfrew, 1973, as cited in Rosen, 2007; Riehl, 2010), so spring-sown barleys may be able to avoid summer drought conditions in comparison to spring-sown wheat (Leonard and Martin, 1970, as cited in Chernoff, 1988). Climate stress decreases the yield of drought-intolerant crops like wheat faster than that of drought-tolerant crops (Marinova and Valamoti, 2014). As a result, higher proportions of barley to wheat have been found growing in drier environments and with poorer soil conditions (Fall et al., 1998; 2002; 2019).

Chaff fragments, primarily resulting from cereal processing, are another important part of the carbonized floral record. Chaff refers to the dry seed coating material found at the spike (also called ear or head) of a grass plant (Hillman, 1981; Charles, 1984). The two types of chaff fragments selected for analysis from the flotation material were rachis internodes, which make up the rachis (or the spinal column) of each cereal spike, and glume bases, which form part of the outer leaves of the cereal spikelet (Figure 3.1). A spikelet represents each individual packet of seeds and glumes. Due to fragmentation during cereal processing, carbonization, mastication, or other disturbances, the glume base is often found shattered into two halves in carbonized remains, so the expected ratio of glume bases to rachis fragments if all plant material was collected would 2:1.

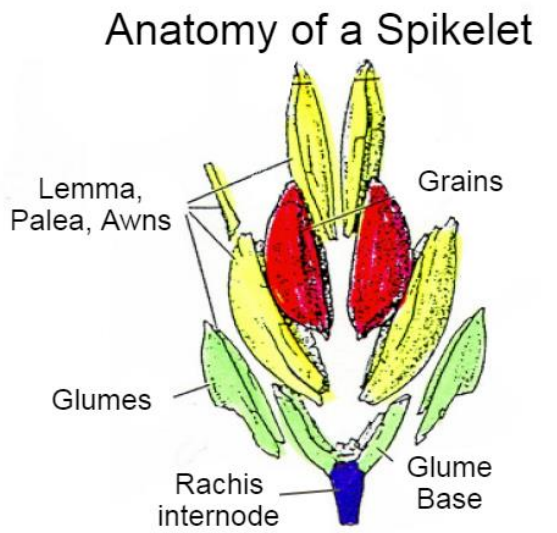

Figure 3.1 The anatomy of a spikelet, or head of a grass showing the glumes (green), seeds (red), rachis (blue) and other light chaff (yellow) (Image from Jacomet, 2006; Original image from Zohary and Hopf, 2000).

As rachises and glumes are closely associated with cereal grains, their presence and quantification can reveal information about crop processing and waste. Cereal spikes come in various configurations with typically anywhere from 1 to 3 seeds per spikelet depending on the taxon (Jones, 1990; Charles, 1984; Jacomet, 2006). Each spikelet contains a series of alternating leaves which protect the seeds. The lower and upper glumes are on the exterior, with the lemma and palea serving as the innermost seed coating.

A variety of pulse and fruit crops were cultivated regionally (Zohary and Hopf, 1973; Waines and Price, 1975-1977; Hopf 2008; Weiss and Zohary, 2011; Ramsay and Mueller, 2016; Caracuta et al., 2017) which helped augment ancient diets due to their high caloric value (Kislev and Bar-Yosef, 1988). Cultivated legume crops are known as pulses. The most frequent pulses at our sites are *Lens culinaris* (lentil), *Pisum sativum* (garden pea), *Lathyrus sativus* (grass pea), *Vicia faba* (broad bean), and *Vicia ervilia* (bitter vetch). Several pulses were fairly drought intolerant (Zohary and Hopf, 1973; Riehl 2009) and many, including *Pisum sativum* and *Lens culinaris*, are cool-season crops, indicative of winter cultivation (Riehl and Bryson, 2007;

Simchoni et al., 2007). The most frequent fruits include *Ficus carica* (fig)*, Vitis vinifera* (grape)*,* and the sole oil crop *Olea europaea* (olive)*.* Fruit crops had a wider range of tolerances, with taxa like *Vitis vinifera* being more drought intolerant (Riehl, 2009) and *Olea europaea* being drought resistant (Galán et al., 2008). *Olea, Vitis,* and *Ficus* are each typically fall-fruiting crops.

Orchards produced both fruit-based foodstuffs and could be used to produce secondary products such as oil, wine, and dried fruits, making them particularly valuable commodities for sedentary societies (Goor, 1966; Lines, 1995; Fall et al., 2002). Secondary products plays a key role in a crop assemblage, as farmers may be more inclined to cultivate crops that produce marketable products if food production goals are being sufficiently met (Goor, 1966; Lines, 1995; Fall et al., 2002). While there is limited evidence for secondary product production at our sites, it has been suggested at other sites in the ancient and modern (Sherratt, 1981, as cited in Levy, 1983; Sherratt, 1983; Zohary and Hopf, 1988; Fall et al., 2002; Genz, 2003). Goods like wine from grapes or oil from olives are secondary products which give these crops a heightened importance over simply serving as a food source. *Olea europaea*, in particular, was not cultivated for human consumption in the Bronze Age, but rather for oil production. However, orchards require maintenance throughout the year, with orchard trees like *O. europaea* taking decades until they reach full maturity (Zinger, 1985, as cited in Langgut et al., 2019). Since this level of land management is unsuitable for mobile communities, the production of orchard crops has been used to suggest long-term investment by settlers (Lines, 1995).

Each of the aforementioned cultigens had been domesticated and cultivated in the Eastern Mediterranean as early as the Epipaleolithic. In the Southern Levant, cultivation of *Hordeum vulgare*, *Triticum dicoccum, T. monococcum, Lens culinaris*, and *Pisum sativum* is noted by at least the Neolithic (Zohary and Hopf, 1973; van Zeist; 1976; Hubbard, 1980; Fuller, 2006; Weiss

and Zohary, 2011; Asouti and Fuller, 2012; 2013; Arranz-Otaegui et al., 2016). Cultivation of *Ficus carica, Vicia faba, Vicia ervilia,* and other cereals, pulses, and fruits came soon after during Chalcolithic to Early Bronze Age (Zohary and Spiegel-Roy, 1975; Ladizinsky, 1979; Kislev and Bar-Yosef, 1988; van Zeist, 1992; Erskine et al., 1994; Garrard, 1999; Lister and Jones, 2012; Miller and Enneking, 2014; Caracuta et al., 2015; 2017).

Other Plants

The composition of wild taxa can be just as informative as that of the major cultigens. Some non-cultivated species were gathered and used by humans (Bogaard et al., 2018b). These potentially utilized taxa, like *Rumex, Medicago, Prosopis farcta* or *Malva parviflora*, to name a few, have been suggested as supplements in both human and animal diets (Felker and Moss, 1996; Baytop, 1984, as cited in Ertug-Yaras, 1997; Charles, 1998). Others like *Beta vulgaris, Bupleurum*, and *Coriandrum sativum* have been reported to be used as medicines, condiments, dyes, or oils in ancient times (Renfrew; 1973; Zohary and Hopf, 1988).

Common wild taxa present in all three sites include several species of small grasses and sedges, a selection of wild leguminous plants, and a wide array of small herbaceous taxa typical of ruderal environments (i.e., with disturbed natural vegetation). Frequent wild grasses include *Avena fatua, Bromus* sp*., Digitaria sanguinalis, Lolium temulentum*, and *Phalaris canariensis*. Notable sedges include *Bolboschoenus maritimus* and *Carex* spp. Wild legumes were particularly common, with *Astragalus* sp., *Trigonella* sp*., Medicago/Onobrychis* spp., and *Melilotus* sp. Finally, particularly prevalent wild herbaceous taxa include *Aizoon hispanicum, Amaranthus graecizans, Bellevalia* sp., *Chenopodium* sp., *Galium aparine, Lysimachia arvensis, Malva parviflora, Plantago* spp., and *Rumex/Polygonum* spp. Identification criteria for each of

the most commonly cultivated and wild plants are provided in Appendix A. See Tables 4.1, 5.1, and 6.1 for common names of wild species.

Wild taxa carry particular value for the interpretation of environmental factors, as these plants, particularly species that do not grow in arable fields, will be better indicators of the natural environment. Interpretations can be drawn from species with a limited bioclimatic range, or distinct habitat. Weeds also reflect the landscape from which the plant remains at a site are produced, with the combination of arable, ruderal, and facultative weeds indicating where livestock grazed and the type of pasture. Arable (or segetal) weeds grow amidst cultivated fields, while ruderal weeds grow further afield in more open and disturbed environments. Facultative weeds are those capable of growth in a variety of landscapes (Willcox, 1974; Baruch, 1986; Langgut et al., 2015; Woodbridge et al., 2018). Some wild taxa implicate specific environmental conditions, for instance *Bolboschoenus maritimus,* which is primarily found in wetland ecosystems. Other plants may hint at economic activities, such as use as foodstuff, a condiment, or as medicine.

Other Considerations for Interpretation

Consideration of Environmental Factors on Crop Selection

The selective cultivation of certain plants by ancient farmers is a reflection of the impacts that farmers are feeling from a variety of stressors, a particular stress being the relationship between climate and crop yield. For this, I consider the benefits of cultivating one crop over another under various precipitation regimes. For cereals in high-precipitation climate regimes, free-threshing wheat harvests may produce grains with a similar or greater yield than that of barley (Cossani et al., 2009). With similar yields, the large size of wheat seeds may allow for

increased bread production. If a region had low precipitation, the yield of wheat may decrease faster than the yield of barley. Under this scenario, drought-tolerant crops like *Hordeum vulgare* or *Vicia ervilia* could produce higher yields than drought-intolerant crops like *Triticum aestivum* or *Hordeum vulgare* var. *nudum* (Djelel et al., 2010; Konvalina et al., 2010; Zhang et al., 2015; Sturite et al., 2018; van Bommel et al., 2021). A farmer would naturally wish to produce crops that provided a high return, so switching which crops they cultivated to accord with climatic conditions may have played an important role.

The paleoenvironment also undoubtedly affected taxonomic presence and frequency of wild crop progenitors in the Southern Levant. Wild cereals (Willcox, 2005; Fuller, 2006; Lister and Jones, 2012) and fruit cultigens like *Olea europaea* or *Vitis vinifera* (Liphschitz et al., 1991; Miller, 2008) were common staples of the region, so their appearance in the record is no surprise, but some crops such as *Cicer arietinum* are not native to this region, so their appearance indicates trade. Some wild taxa can also reveal facets of the paleoenvironment, if they are only found in a narrow range of environmental conditions, as they reveal the presence of these environments nearby the site.

Consideration of Inedible or Unpalatable Taxa in a Floral Assemblage

The appearance of poisonous or unpalatable plants can be a useful indicator of the past. Unpalatable plants can include both cultivated taxa (*Lathyrus sativus*, and *Vicia ervilia*) as well as wild species like ryegrass (*Lolium temulentum*) or pimpernel (*Lysimachia arvensis*) (Freeman, 1903; Hillman, 1984; Grime et al., 1990, as cited in Filipović, 2012; Riehl, 2010). Taxa like *V. ervilia* can be processed by leaching and roasting in order to become edible, but in ancient agrarian societies they were more likely consumed by animal like sheep or goat, to whom they

are not harmful (Lines, 1995; Chernoff and Paley, 1998; Miller and Enneking, 2014). The inclusion of inedible weeds in a floral assemblage might indicate accidental collection during grain harvesting, or subsequent use as fuel, as exemplified by the prevalence of *Phalaris canariensis* amidst cereal fields (Renfrew, 1973). Later stages of processing would be required to weed out inedible taxa from cereal harvests. However, if not poisonous to livestock, the most likely pathway for carbonization of weeds is through animal diet.

Consideration of the Alteration of a Floral Assemblage Pre-Deposition

The primary factors affecting the likelihood of a plant becoming carbonized include the crop processing requirements, crop use, carbonization process, and digestion. Crop processing involves taxonomically-specific multi-step processes of harvesting, cleaning, and storing crops (Dennell, 1972, as cited in Dennell, 1974). These processes are most often considered in regard to cereals, as the processing of cereal grains requires many steps unique to certain grain types. The typical procedure a cereal grain might go through is outlined in Jones 1984 (with similar processes noted in Hillman, 1981; 1984; Reddy, 1997; Anderson, 1998; Fuller and Harvey, 2006; Alonso et al., 2014), and follows a progression of processing stages including harvesting, drying, light to heavy threshing, light to heavy winnowing, raking, coarse sieving, fine sieving, hand sorting, and storing. This procedure may be further expanded for hulled grains, with steps like parching, pounding, grinding, fine-threshing and sieving in order to fully remove the grain from their glumes. Hulled cereals may also be roasted within their glumes in order to sterilize the grain and remove the bracts more easily (Hillman, 1984; Alonso et al., 2014). Roasting may carbonize some grains, potentially increasing the preservation and recovery rates of glume wheats and hulled barley (Alonso et al., 2014). To summarize, crops that require processing with

fire, such as hulled cereals (Hillman, 1984), as well as those whose remains are more likely to be used as fuel, such as olive, are more likely to come into contact with fire and become carbonized.

For cereal chaff, the by-products from each stage are distinguished by the unique proportions of wild and cultivated plant remains. Cereal chaff can be incorporated into a site's record through livestock grazing, foddering, burning of threshing-floor remains, incorporation of cereal by-processing waste into dung cakes, or direct use as kindling. Plant remains from later stages of crop processing have a higher likelihood of preservation and recovery (Jones, 1983).

Another primary factor affecting the pre-deposition assemblage is whether a site uses dung- or wood-burning. Dung burning sites have been found to contain assemblages of floral material most representative of animal diets (Miller, 1984; Miller and Smart, 1984; Valamoti and Charles, 2005; Miller and Marston, 2012). Dung-burning provides a simple pathway to carbonization for wild taxa, incorporating them as seeds packed into dung cakes, which are then burned as fuel. Thus, floral assemblages from these sites should incorporate a variety of wild taxa. Regardless of the method, carbonization limits the incorporation of taxa whose seeds cannot withstand high temperatures (van der Veen, 2007). Certain seeds, like those of hulled cereals, may be more prone to surviving this process and thus may be preserved at higher rates in a floral record (Boardman and Jones, 1990; Braadbaart, 2008; Bonhomme et al., 2017).

Finally, given that my focal sites are dung-burning, a primary consideration is the effect of digestion (Miller, 1984; Charles, 1998). Seeds that are more suited to survive mastication and digestion by ruminants (such as sheep, goat, and cow) may be preserved at higher rates in the floral record (Hastorf and Wright, 1998). Plants with many small seeds with thick, resistant seed coatings are best equipped to survive digestion, while larger taxa, including the cereals, may be less frequently preserved (Poppi et al., 1985; Wallace and Charles, 2013; Spengler, 2019).

Consideration of the Alteration of a Floral Assemblage Post-Deposition

The primary post-depositional effects on the carbonized seed records would come from site disturbance and weathering. This effect is most pronounced in the final phase of each site, which led to a decline in recovery of carbonized remains at all three sites. Thus, the assemblages from these phases are interpreted with increased caution or excluded for later analyses.

CHAPTER 4: PALEOETHNOBOTANICAL RESULTS FROM TELL ABU EN-NI‘AJ

Tell Abu en-Ni‘aj Paleoethnobotanical Results

Quantification of Macrofossil Remains

Approximately 15,000 seeds are identified from Ni‘aj at a family level or lower taxonomic level. In addition, 7,100 chaff fragments are estimated to be from cereal grains, and an additional approximately 11,500 indeterminant cultivated cereal fragments, wild legume fragments, and other indeterminant plant remains are noted in Table S1. Carbonized plant remains are identified from every phase at Tell Abu en-Ni‘aj, with the majority in Phases 7-2. Cereal grains from Ni‘aj are recorded in NISP. NISP per species are reported in Table 4.1 alongside frequencies and ubiquities per taxon across the entire site. Table 4.2 shows density values for each plant category grouped by phases.

The floral assemblage at Tell Abu en-Ni‘aj includes cultigens and wild taxa with a notable abundance of *Hordeum vulgare* and *Triticum dicoccum*. Other common cereals include *H. vulgare* var. *nudum*, *T. aestivum,* and *T. monococcum*. Cereal chaff is common in most samples, represented most frequently as glume base fragments. Other common plants include *Ficus carica* and *Lens culinaris*, with *Pisum sativum*, *Olea europaea*, and *Vitis vinifera* present to a slightly lesser extent. Notably, only small fragments of *O. europaea* are noted in sediments from Ni‘aj.

Table 4.1 NISP, frequency, and ubiquity for plant taxa recovered at Tell Abu en-Ni'aj, Jordan. Counts of indeterminant cultivated cereal fragments, wild legume fragments, and other unknown plant remains were excluded from analysis but can be found in Table S1.

Scientific Name	Common Name	NISP	Frequency	Ubiquity
Cereals				
Cerealia (frags excluded)	Cereals	120	0.78	25.64
Hordeum sp.	Barleys	703	4.56	68.59
Hordeum vulgare	Two-row hulled barley	3589	23.26	87.18
Hordeum vulgare (hexastichum)	Six-row hulled barley	13	0.08	3.85
Hordeum vulgare var. *nudum*	Naked barley	491	3.18	60.26
Triticum sp.	Wheats	318	2.06	46.79
Triticum aestivum	Bread wheat	44	0.29	14.74
Triticum dicoccum	Emmer wheat	586	3.80	62.18
Triticum monococcum	Einkorn wheat	240	1.56	42.95
Panicum miliaceum	Broomcorn millet	9	0.08	5.77
cf. *Secale cereale*	Rye	14	0.09	6.41
Cereal total		6127	39.74	96.15
****Cereal chaff**				
**Glume base fragments		5498	35.63	84.62
**Rachis fragments		1622	10.51	67.31
****Cereal chaff total**		7120	46.15	89.10
Cultivated fruits				
Ficus carica	Fig	1811	11.74	57.69
Vitis vinifera	Grape	67	0.43	23.08
Cultivated fruit total		1878	12.17	63.46
Cultivated legumes				
Cultivated *Fabaceae*	Pulse	12	0.08	5.13
Lathyrus sativus	Grass pea	8	0.05	4.49
Lens culinaris	Lentil	217	1.41	39.74
Pisum sativum	Garden pea	98	0.64	28.21
Vicia sp.	Vetches	3	0.02	1.92
Cultivated legume total		338	2.19	53.85
Oils				
Olea europaea	Olive	46	0.30	7.69
Oil total		46	0.30	7.69

Wild grasses				
Poaceae	Grasses	2010	13.03	88.46
Avena fatua	Wild oat	47	0.30	9.62
Bromus sp.	Bromes	80	0.52	14.74
cf. *Digitaria* spp.	Crabgrasses	21	0.14	9.62
cf. *Echinaria capitata*	-	6	0.04	1.92
cf. *Eremopyrum* sp.	-	2	0.01	1.28
cf. *Festuca* sp.	Fescues	1	0.01	0.64
cf. *Holcus annuus*	Annual fog	3	0.02	1.28
Lolium temulentum	Darnel ryegrass	156	1.01	17.95
Phalaris canariensis	Canary grass	613	3.97	52.56
cf. *Stipa* sp.	-	7	0.05	2.56
Wild grass total		2946	19.09	89.74
Wild sedges				
Bolboschoenus maritimus	Sea clubrush	118	0.76	20.51
Carex spp.	Sedges	35	0.23	12.82
Cyperus sp.	-	2	0.01	1.28
Eleocharis sp.	Spikerush	5	0.03	3.21
Wild sedge total		160	1.04	32.69
Wild legumes				
Fabaceae (frags excluded)	Legumes	325	2.11	46.15
Astragalus sp.	Milkvetches	12	0.08	6.41
Crotalaria sp.	Rattlepods	6	0.04	2.56
cf. *Lotus* sp.	Deervetches	10	0.06	2.56
cf. *Lupinus graecus*	White lupin	1	0.01	0.64
Medicago/Onobrychis spp.	Burclovers/Sainfoins	628	4.07	48.08
Melilotus sp.	Sweet clovers	27	0.17	11.54
Prosopis farcta	Syrian mesquite	1020	6.61	40.38
Trifolium sp.	Clovers	2	0.01	0.64
Vachellia nilotica	Acacia nilotica	3	0.02	0.64
cf. *Vigna* sp.	-	1	0.01	0.64
Wild legume total		2035	13.19	67.95
Wild woody and herbaceous				
cf. *Abutilon theophrasti*	Velvetleaf	6	0.04	2.56
Adonis sp.	Pheasant's eyes	7	0.05	3.85
cf. *Agrostemma githago*	Corncockle	1	0.01	0.64
Aizoon hispanicum	Spanish aizoon	15	0.10	6.41
Amaranthus graecizans	Mediterr. amaranth	51	0.33	12.82

cf. *Amygdaloideae*	-	4	0.03	1.92
cf. *Anthemis cotula*	Chamomile	3	0.02	1.28
cf. *Arabis* sp.	Rockcresses	2	0.01	1.28
Arnebia cf. *decumbens*	-	18	0.12	5.77
cf. *Asteraceae*	Daisies	29	0.19	10.90
Atriplex sp.	Saltbushes	8	0.05	1.92
Bellevalia sp.	-	61	0.40	12.82
cf. *Berberis* sp.	Barberries	3	0.02	0.64
cf. *Berteroa* sp.	-	2	0.01	0.64
Beta vulgaris	Beet	7	0.05	3.21
cf. *Bifora testiculata*	-	49	0.32	0.64
cf. *Boraginaceae*	-	18	0.12	7.05
cf. *Brassica* sp.	-	7	0.05	2.56
Bupleurum sp.	Thorow waxes	123	0.80	23.72
cf. *Capparis* sp.	-	1	0.01	0.64
Centaurea cf. *melitensis*	Maltese starthistle	4	0.03	1.92
Chenopodium sp.	Goosefoots	88	0.57	21.79
cf. *Cleome* sp.	Spider flowers	2	0.01	0.64
cf. *Cocculus pendulus*	-	1	0.01	0.64
cf. *Conium* sp.	-	1	0.01	0.64
cf. *Convolvulus arvensis*	Field bindweed	1	0.01	0.64
Coriandrum sativum	Coriander	64	0.41	14.74
cf. *Corispermum* sp.	-	1	0.01	0.64
cf. *Coronilla* sp.	-	2	0.01	0.64
cf. *Crataegus monogyna*	Hawthorn	2	0.01	1.28
Euphorbiaceae	Spurges	1	0.01	0.64
cf. *Euphorbia esula*	Leafy spurge	8	0.05	3.85
cf. *Fumaria* sp.	Fumitories	5	0.03	3.21
Galium aparine	Cleavers	109	0.71	25.00
cf. *Geranium molle*	Dovesfoot cranesbill	2	0.01	0.64
cf. *Hieracium* sp.	Hawkweeds	5	0.03	1.92
cf. *Lamiaceae*	Mints	1	0.01	0.64
cf. *Lepidium* sp.	Peppergrasses	5	0.03	2.56
cf. *Linaria vulgaris*	Yellow toadflax	1	0.01	0.64
Lithospermum officinale	Common gromwell	2	0.01	1.28
Lysimachia arvensis	Scarlet pimpernel	239	1.55	28.21
Malva parviflora	Cheeseweed	86	0.56	27.56
cf. *Myosotis arvensis*	Field forget-me-not	2	0.01	0.64
cf. *Myrica* sp.	Bayberries	14	0.09	2.56
Ornithogalum sp.	-	6	0.04	1.92
cf. *Oxalis* sp.	-	1	0.01	0.64

cf. *Picris* sp.	-	1	0.01	0.64
Plantago spp.	Fleaworts	166	1.08	28.21
cf. *Potentilla* sp.	Cinquefoils	2	0.01	1.92
cf. *Prunus* sp.	-	1	0.01	0.64
cf. *Rhamnaceae*	Buckthorns	1	0.01	0.64
Rumex/Polygonum spp.	Sorrels/Knotweeds	458	2.97	43.59
cf. *Salsola* sp.	Saltworts	1	0.01	0.64
cf. *Saponaria* sp.	Soapworts	11	0.07	2.56
cf. *Scutellaria* sp.	Scullcaps	1	0.01	0.64
cf. *Sherardia arvensis*	Field madder	1	0.01	0.64
Silene cf. *noctiflora*	-	6	0.04	1.92
cf. *Sonchus arvensis*	Perennial sowthistle	9	0.06	1.28
Spergula arvensis	Corn spurry	21	0.14	8.33
Stellaria cf. *media*	Chickweed	1	0.01	0.64
cf. *Suaeda* sp.	Sea blites	7	0.05	0.64
cf. *Thymelaea* sp.	Sparrow worts	17	0.11	5.77
cf. *Torilis* sp.	-	1	0.01	0.64
Wild woody and herbaceous total		1773	11.49	78.21
Unknowns				
Unknown 1	-	25	0.16	8.33
Unknown 3	-	2	0.01	0.64
Unknown 4	-	2	0.01	1.28
Unknown 5	-	1	0.01	0.64
Unknown 6	-	1	0.01	0.64
Unknown 8	-	1	0.01	0.64
Unknown 9	-	4	0.03	1.92
Unknown 10	-	1	0.01	0.64
Unknown 11	-	1	0.01	0.64
Unknown 12	-	74	0.48	16.67
Unknown 13	-	1	0.01	0.64
Unknown 14	-	2	0.01	1.28
Unknown 15	-	2	0.01	1.28
Unknown 17	-	1	0.01	0.64
Unknown 18	-	3	0.02	1.28
Unknown 19	-	3	0.02	0.64
Unknown total		124	0.80	23.08
Grand Total		22547	100.00	
** chaff not included in seed frequency calculations				

Table 4.2 NISP and densities for plant categories per phase at Tell Abu en-Ni'aj, Jordan.

Phase	**7**	**6**	**5**	**4**	**3**	**2**	**1**	**Total**
Volume	49.5	66.7	66.1	111.5	189.6	138.6	55.4	
Cereals	879	764	718	772	2070	874	50	6127
Cereal chaff	1171	2049	992	1418	1034	384	72	7120
Cultivated fruits	1090	223	247	165	82	60	11	1878
Cultivated legumes	43	79	27	29	82	74	4	338
Oil	0	13	1	15	13	3	1	46
Wild grasses	539	553	413	463	662	294	22	2946
Wild sedges	7	27	14	86	11	14	1	160
Wild legumes	301	303	240	452	272	445	22	2035
Wild woody and herbaceous	477	448	248	294	156	131	19	1773
Total NISP	4507	4459	2900	3694	4382	2279	202	22423
Cereals	17.75	11.46	10.86	6.92	10.92	6.31	0.90	
Cereal chaff	23.65	30.72	15.00	12.72	5.45	2.77	1.30	
Cultivated fruits	22.01	3.34	3.74	1.48	0.43	0.43	0.20	
Cultivated legumes	0.87	1.18	0.41	0.26	0.43	0.53	0.07	
Oil	0	0.19	0.02	0.13	0.07	0.02	0.02	
Wild grasses	10.88	8.29	6.25	4.15	3.49	2.12	0.40	
Wild sedges	0.14	0.40	0.21	0.77	0.06	0.10	0.02	
Wild legumes	6.08	4.54	3.63	4.05	1.43	3.21	0.40	
Wild woody and herbaceous	9.63	6.72	3.75	2.64	0.82	0.95	0.34	
Total Density	91.01	66.86	43.87	33.13	23.11	16.45	3.65	

Frequencies and Ubiquities of Primary Cultigens

Figure 4.1 displays the densities of cultivated taxa per phase. All taxa show a similar trend of declining values through time. *Hordeum vulgare* is the only notable exception, maintaining a similar density until Phase 1. *Ficus carica* appears to show a significant decline, but the high density in Phase 7 is driven by a single outlier sample with over 950 seeds. Without this point, this taxon shows the same trend as all others.

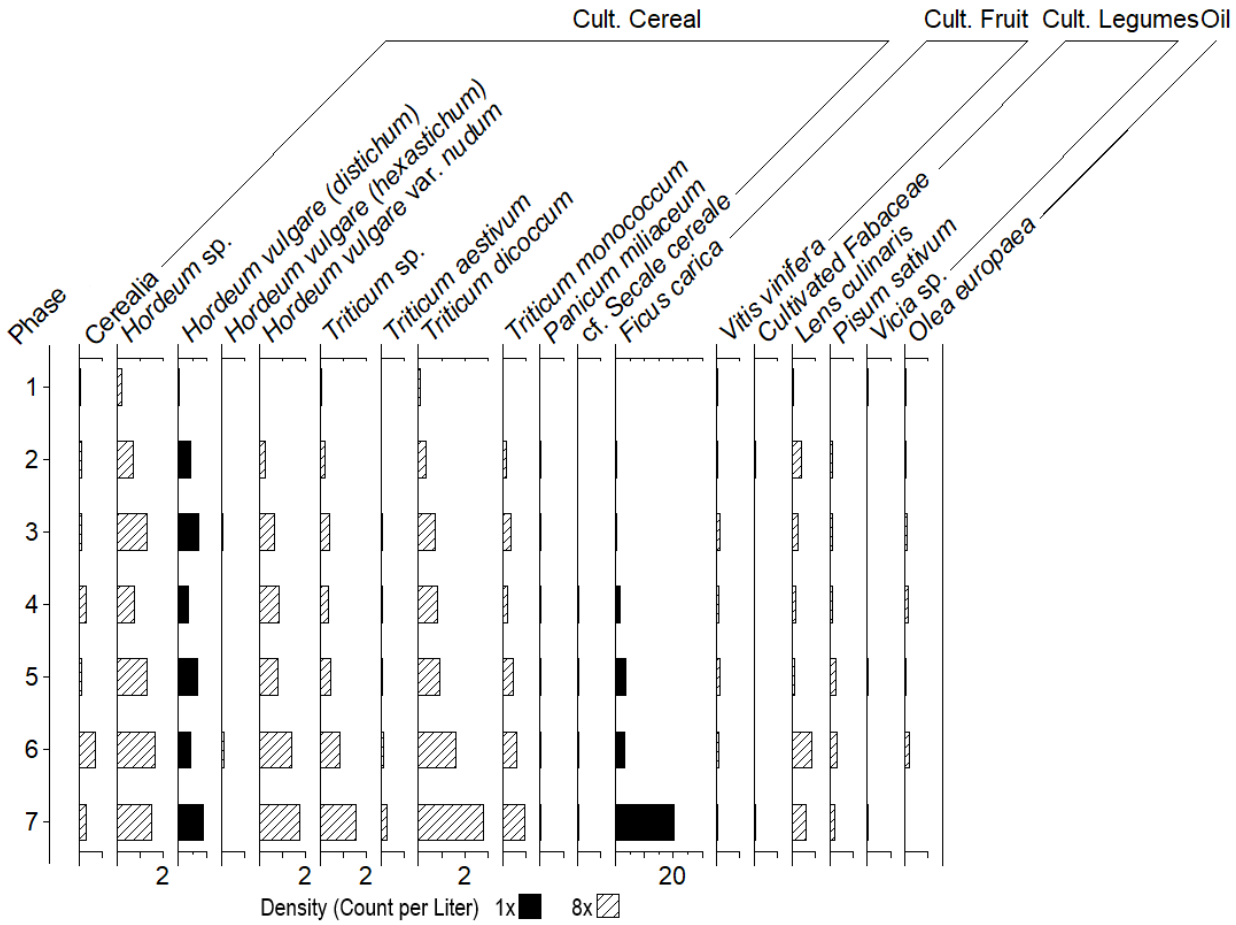

Figure 4.1 Densities, calculated as the NISP per volume of sediment, per phase for all taxa recovered from Tell Abu en-Ni'aj, Jordan. Plant categories are indicated above individual taxa. Striped bars indicate an 8x exaggeration.

Figure 4.2 displays the frequencies of cultigens per phase, with a primary trend being the gradual increase in the proportion of *Hordeum vulgare* relative to all *Triticum* species over time. The highest values of *Triticum dicoccum* and *T. aestivum* are found in Phases 7-6, whereas *Hordeum vulgare* sees its highest frequencies towards the later phases. *Hordeum vulgare* also has the highest ubiquity of any taxon, appearing in roughly 87% of the assemblage. Comparatively, the next most frequent cereals were *T. dicoccum* and *H. vulgare* var. *nudum* at around 60% each. There is an outlier in Phase 3 with a particularly high density of *Hordeum*

vulgare, with over 500 grains in one sample, but the taxa is still the most prominent grain in Phase 3 without this sample.

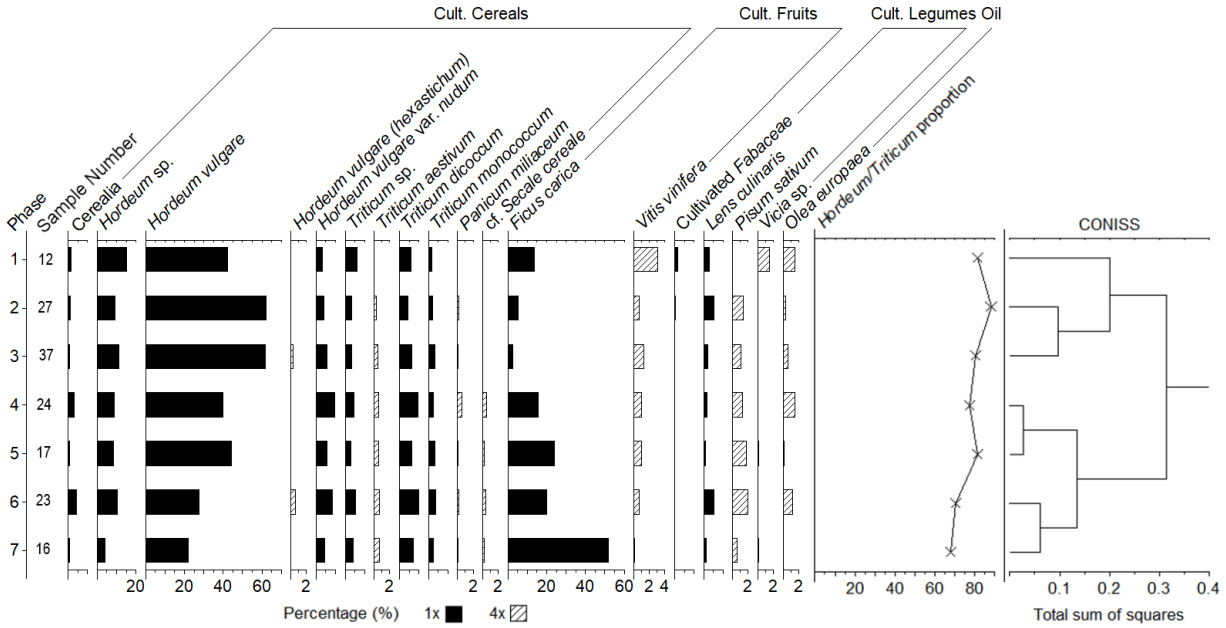

Figure 4.2 Frequencies of cultivated plant taxa per phase from Tell Abu en-Ni'aj, Jordan based on NISP. Plant categories are indicated above individual taxa. Striped bars indicate a 4x exaggeration. The line graph shows the percentage of barley grains from all barley plus wheat grains. The dendrogram shows a CONISS hierarchical cluster analysis indicating the grouping of similar phases, based on all cultivated taxa.

The *Hordeum* to *Triticum* ratio from Figure 4.2 shows an increase from about 68% in Phase 7 to a maximum of 88% in Phase 2, supporting an overall increase in barley over time. The CONISS hierarchical cluster analysis suggests a larger divide between the cultivated assemblages of Phases 4 and 3, suggesting that the overall assemblages of Phases 7-4 and Phases 3-1 are most distinct.

Of the fruits, *Ficus carica* is the most prominent, constituting over 20% of the assemblage in Phase 5. *F. carica* can produce hundreds of seeds per fruit, so this must be considered. Despite its low sample count, *Vitis vinifera* had a relatively high ubiquity of 23%,

suggesting its potential importance. While the oil-producing *Olea europaea* is infrequent, it is sufficiently abundant to be considered an important cultigen.

The most abundant pulse crop was *Lens culinaris*. Like *V. vinifera, L. culinaris* had high ubiquity but low frequency, comprising only 1.6% of the total macrofossil assemblage. Frequencies of some cultigens varied notably, with *Ficus carica* and *Pisum sativum* more prominent during the initial phases and *Vitis vinifera* being most prominent in the later phases.

Frequencies and Ubiquities of Wild Taxa

Figure 4.3 illustrates the frequencies of common wild taxa per phase from Ni'aj. Wild grasses and legumes are prevalent at Ni'aj, including *Bromus, Lolium*, *Medicago/Onobrychis*, *Phalaris*, and *Prosopis farcta* most notably. A wide variety of wild woody and herbaceous taxa were identified, but only a few of these taxa are present in relatively high frequencies, including *Chenopodium* sp*., Galium aparine, Lysimachia arvensis, Malva parviflora, Plantago* sp., and *Rumex/Polygonum* spp. The most notable shifts in wild taxa are the rapid declines in *Phalaris canariensis* and *Rumex/Polygonum* spp., which are replaced in part by grasses, *Prosopis farcta,* and *Medicago/Onobrychis* spp*.* Each of the taxa above had high densities and ubiquities, appearing in at least roughly 20-30% of samples. *Amaranthus graecizans., Asteraceae*, and *Bellevalia* sp. are slightly less frequent and have ubiquities around 10% or greater, but had relatively even frequencies throughout the site's occupation.

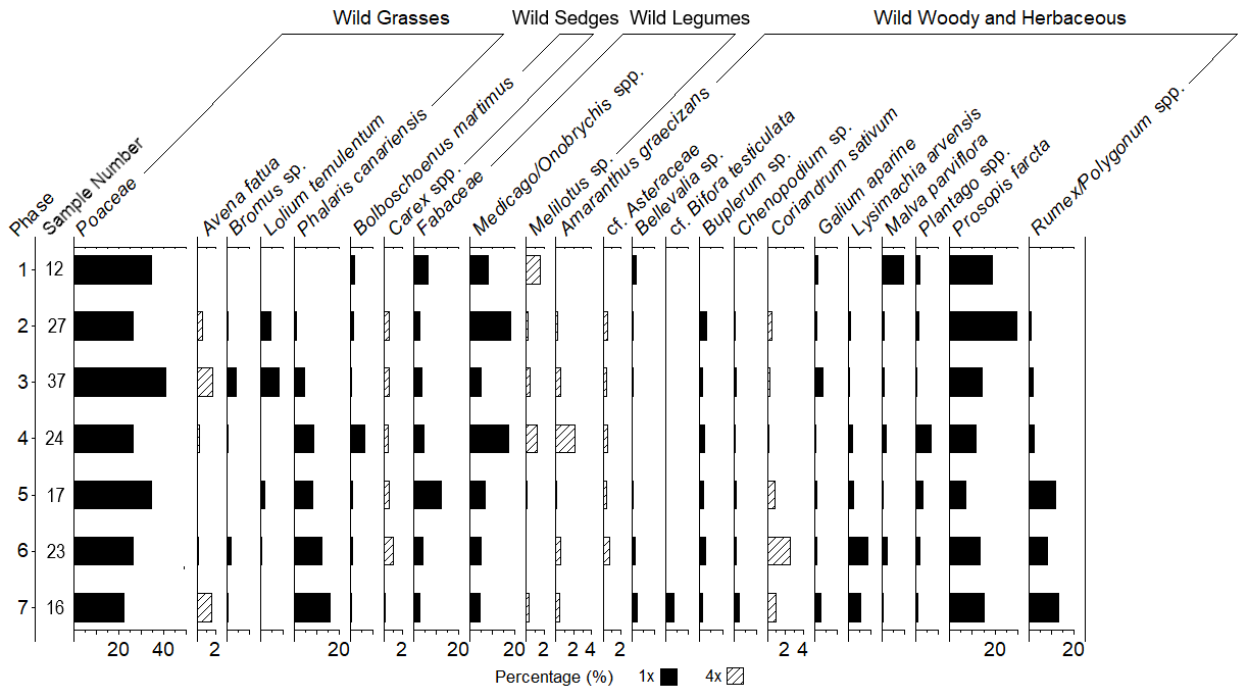

Figure 4.3 Frequencies of common wild plant taxa per phase from Tell Abu en-Ni'aj, Jordan (NISP count ≥ 27). Frequencies are based on all wild taxa. Plant categories are indicated above individual taxa. Striped bars indicate a 4x exaggeration.

Wild *Poaceae* at Ni'aj are dominated by small-seeded grasses, with seeds typically smooth, ovoid, and around 1-2 mm in length. Aside from these, there are high concentrations of *Phalaris canariensis* and *Lolium temulentum*, with *P. canariensis* reaching a ubiquity of over 50%. Of the legumes, *Medicago/Onobrychis* was one of the most frequent wild taxa, constituting over 25% of the Phase 2 assemblage and remaining prominent throughout. This taxon is also present in nearly 50% of all samples, particularly towards the later phases at Ni'aj. *Prosopis farcta*, on the other hand, had an unusually high frequency but low ubiquity compared to other wild taxa. The samples containing this taxa also frequently had large, intact seeds. A final notable trend is the increase in *Malva parviflora* frequency in Phase 1. *Malva parviflora* has a fairly high ubiquity of roughly 28% throughout the site as a whole, despite a relatively low frequency in Phases 7-2.

Discussion of Macrofossil Assemblage Trends

The EB IV settlement Tell Abu en-Ni‘aj is dominated primarily by the cultivated cereal crop *Hordeum vulgare* in both frequency and ubiquity (see Table 4.1), behind only glume fragments in terms of abundance. The glume wheats *Triticum dicoccum* and *T. monococcum,* and the barley crop *H. vulgare* var. *nudum* are also abundant in the assemblage (see Figure 4.2), alongside the arable weeds *Lolium temulentum* and *Phalaris canariensis* (see Figure 4.3). The site is very rich in both wild and cultivated grass taxa, as well as chaff remains, suggesting grain cultivation played a large role in the settlement's subsistence. Chaff is likely being incorporated into the site as a grain-cleaning by-product, potentially used as fuel or supplemental animal feed after grain cleaning is completed. The frequencies of cultivated cereals suggests that most of the remains from Ni‘aj are coming from cultivated fields, likely through livestock grazing in the fields but also through incorporation of cereals and cereal processing by-products in the settlement, while high NISP of chaff and weeds suggest that by-products of cereal harvest are being subsequently utilized.

Hordeum vulgare increases in abundance through time in comparison to all cereal species including *Triticum dicoccum*. The *Hordeum* to *Triticum* ratio is being used as an indication of the human response to climate change, as cultivation choice reflects an understanding of the relationship between aridity and crop yield. At Ni‘aj, the shift towards increased *Hordeum* therefore supports the argument for slightly increasing drought stress towards end of EB IV.

Though limited analysis of chaff is possible, the higher quantity of glume bases over rachis fragments, roughly 3.4:1 (see Table 4.1), indicating that material from later stages of the crop-processing process, in this case processing stages post-threshing, are being preferentially incorporated into the carbonized record. There is no evidence of significant structural burning at

Ni‘aj (Falconer and Fall., 2019), and glumes have a very high ubiquity, so it is unlikely that this ratio is due to accidental burning of a structure dedicated to cereal-processing. Other possible causes for the high ratio of glume to rachis fragments could be the use of dung cake production with winnowing, sieving, or other late-stage processing by-products that are richer in glume remains. This would still support the idea that these processes were conducted nearer the site, as the by-products would be more readily available for dung cake incorporation (Miller and Smart, 1984; Bernard and Kristoferson, 1985, as cited in Charles, 1998; Anderson and Ertug-Yaras, 1998; Ertug, 2000).

Regarding the fruit and oil crops, macrofloral densities and frequencies support the presence of orchards, particularly given the density and ubiquity of *Ficus carica.* This taxon is most abundant in the initial phases but declined during Phases 3 and 2. *Ficus carica* trees can take a few years to reach maturity, but do not represent the same amount of investment as species like *Olea europaea*. The abundance of *O. europaea* seeds is relatively low, possibly suggesting less long-term investment among local farmers; however, *Olea* charcoal densities do suggest that this tree was an important source of fuel wood (Klinge and Fall., 2015). One possibility is that *jift*, the crushed seeds and pomace from olive processing, was simply not being utilized frequently. It may be that enough chaff and wild waste was available for the incorporation into dung cakes that *jift* was not needed.

Also of note was the prominence of a few vine and shrub cultigens, particularly *Vitis vinifera* and *Lens culinaris.* These crops may be sown alongside cereals, as they are often found in higher quantities in samples where cereals are more abundant. Further, the potential importance of either olive or grape, *O. europaea* or *V. vinifera*, is hinted at from an archaeological three-basin feature which could have been used for processing of oil or wine.

Some seeds have higher densities in samples where cereals are infrequent. This suggests a different method of entering the carbonized record. This could occur for many reasons, such as if the plants fruit at different times of the year, if they grow further from the agricultural fields, or, in the case of cultigens, if they were processed in different buildings. *Pisum sativum*, in particular, has high seed densities in samples where cereals were infrequent. In this case, *Pisum* may have served as an off-season food source. Wild taxa like *Medicago/Onobrychis* or *Prosopis farcta*, which also showed this trend, could have served as a winter food source for grazing livestock (Charles, 1998). *Prosopis farcta* today is prevalent around the Dead Sea Plain and grows in riparian areas in the wild, though this species also thrives on dry, rocky, and salty soils near cultivated and especially orchard lands (Zohary, 1982; Abu-Irmaileh, 1982; Felker and Moss, 1996).

The array of wild weeds at Ni‘aj (see Figure 4.3) primarily suggests grazing around cultivated fields amidst a grassland/steppe habitat (Zohary, 1966; 1972; 1982; Feinbrun-Dothan 1978; 1986; Abu-Irmaileh, 1982; Riehl, 2010; Kreuz and Schäfer, 2011). This is supported by relatively more abundant arable weeds than found at Hayyat, with slightly fewer taxa indicative of bare soils. Taxa such as *Lysimachia arvensis, Bifora testiculata*, or *Lolium temulentum* are likely to have been arable weeds, while taxa like *Chenopodium, Plantago, Medicago, Onobrychis, or Malva* may represent ruderal weeds (Zohary, 1966; 1972; 1982; Feinbrun-Dothan 1978; 1986; Abu-Irmaileh, 1982; Riehl, 2010; Kreuz and Schäfer, 2011). Most of the wild taxa at Ni‘aj grow in a temperate to warm climate and can withstand light drought conditions, typical of vegetation in the Irano-Turanian phytogeographic region (Zohary, 1950). Many also have preferred habitats consisting of dry, salty, or sandy soils with a few taxa like *Malva parviflora* or *Chenopodium* sp., present in open, bare, or rocky soil. *Lysimachia arvensis*,

Bolboschoenus maritimus, Plantago sp., and *Prosopis farcta* may be found in saline wetland or riparian environments and suggest livestock grazing in a mesic environment (Zohary, 1966; 1972; 1982; Feinbrun-Dothan 1978; 1986; Abu-Irmaileh, 1982; Riehl, 2010; Kreuz and Schäfer, 2011), which makes sense given the proximity of Ni'aj to Jordan River. The abundance of *Prosopis farcta* at Ni'aj may also suggest that the northern Jordan Valley in EB IV had a slightly drier climate in past, more akin to the semi-arid/arid climate in the modern Dead Sea Basin.

Figure 4.4 illustrates the shift in seed densities through time. The densest concentrations of cereal and chaff material are found in the earlier phases, particularly Phases 7-5, with densities declining through time for most taxa. Phase 1 represents the remains of nearly 55 liters of material floated, compared to the 50 liters from Phase 7, so the incredible shift in macrofossil deposition rate cannot be considered an artifact of under-sampling.

The total macrofossil density declined noticeably from Phases 7 through 1, which can also be seen in the densities of each plant category and seems to be a site-wide trend. The frequency of wild taxa diminished more rapidly than for cultivated taxa, which could suggest that a decline in dung-burning occurred, as dung-burning can result in a higher ratio of wild seeds in a carbonized record (Wallace and Charles, 2013; Spengler, 2019). However, this trend could not explain the rate of decline noted at Ni'aj. There are also no signs of decreasing community activity, as the settlement expanded and architecture became more complex with each phase, indicating the site did not fall into disuse (Fall and Falconer, 2019). However, since density did decline in these later phases, a possible explanation could be a shift in the location of fuel use, with the remains of communal fires recovered less frequently during the excavations of later phases.

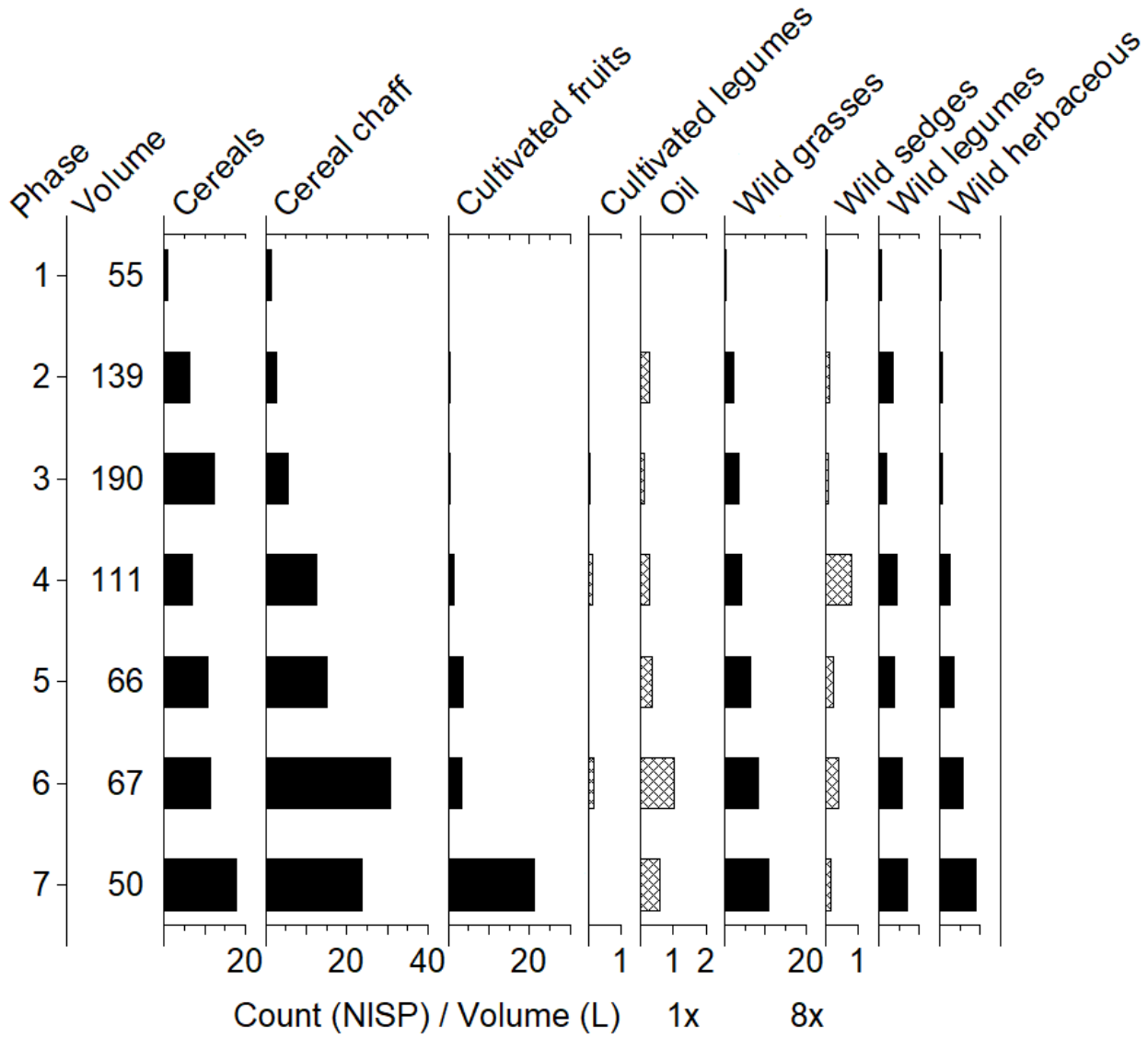

Figure 4.4 Densities (NISP per liter of floated sediment) for categories of cultivated and uncultivated taxa at Tell Abu en-Ni‘aj, Jordan, as expressed in Table 4.2.

A slight shift from dung to wood burning may have occurred at this site, looking at charcoal records. Ni‘aj has notable charcoal deposits from a variety of woody species, implicating some wood burning of fruit trees alongside burning of various shrubby monocots and mixed arid or riparian genera like *Tamarix* sp. (Fall et al., 2015). Densities of charcoal maintain relatively steady values during most of the site’s occupation. The charcoal species at Ni‘aj, rich in fruit tree remains of species like *Olea europaea*, are indicative of a fuel-limited landscape,

with primarily burning of woody shrubs, orchard clippings, and other riparian trees (Klinge and Fall 2010; Fall et al., 2015). This shift in fuel source is not likely suggestive of an ameliorating climate to an EB III state, but the relatively heightened exploitation of wild woody vegetation and increased production and exploitation of woody orchard taxa. However, as stated above, this transition is likely only a small part of the reason for the density decline.

CHAPTER 5: PALEOETHNOBOTANICAL RESULTS FROM TELL EL-HAYYAT

Tell el-Hayyat Paleoethnobotanical Results

Quantification of Macrofossil Remains

Hayyat produced approximately 18,500 identified seeds, 1,500 chaff fragments, and an additional approximately 8,000 indeterminant cultivated cereal fragments, wild legume fragments, and other indeterminant plant remains (Table S2). Carbonized plant remains are identified from every phase at Tell el-Hayyat, the majority from Phases 5-2. Table 5.1 presents the data from Tell el-Hayyat according to NISP, MNI, frequencies and ubiquities per taxon and plant category. Table 5.2 shows density values for each vegetation category by phase.

Plant macrofossils at Tell el-Hayyat include multiple cereal cultigens and a variety of wild weedy taxa. Cultivated cereals make up the primary body of the assemblage. Of the identified cereal species, *Hordeum vulgare* is by far the most abundant, followed by *Triticum dicoccum*. At least 33 grains were able to be concretely labelled as *H. vulgare* var. *hexastichum*.

Table 5.1 NISP, MNI, frequency, and ubiquity for plant taxa recovered at Tell el-Hayyat, Jordan. Counts of indeterminant cultivated cereal fragments, wild legume fragments, and other unknown plant remains were excluded from analysis but can be found in Table S2.

Scientific Name	Common Name	Seeds	Seeds	Frequency	Ubiquity
Cereals					
Cerealia (frags excluded)	Cereals	138	138	0.74	26.49
Hordeum sp.	Barleys	582	403	3.13	60.26
Hordeum vulgare	Two-row hulled barley	2612	2107	14.05	86.75
Hordeum vulgare (hexastichum)	Six-row hulled barley	33	31	0.18	8.61
Hordeum vulgare var. *nudum*	Naked barley	534	473	2.87	58.28
Triticum sp.	Wheats	332	247	1.79	40.40
Triticum aestivum	Bread wheat	234	232	1.26	45.70
Triticum dicoccum	Emmer wheat	1831	1770	9.85	80.79
Triticum monococcum	Einkorn wheat	344	336	1.85	48.34
Triticum cf. *spelta*	Spelt wheat	24	24	0.13	1.32
Panicum miliaceum	Broomcorn millet	19	18	0.10	15.23
Cereal total		6683	5787	35.94	96.69
****Cereal chaff**					
**Glume base fragments		525	525	2.82	43.05
**Rachis fragments		1032	1032	5.55	50.33
****Cereal chaff total**		1557	1557	8.37	64.24
Cultivated fruits					
Ficus carica	Fig	1307	1111	7.03	69.54
cf. *Punica* sp.	Pomegranates	4	1	0.02	0.66
Vitis vinifera	Grape	64	45	0.34	19.87
Cultivated fruit total		1375	1157	7.40	72.19
Cultivated legumes					
Cultivated *Fabaceae*	Pulse	198	70	1.06	34.44
Cicer arietinum	Chickpea	2	2	0.01	0.66
Lathyrus sativus	Grass pea	69	64	0.37	21.19
Lens culinaris	Lentil	223	176	1.20	39.74
Pisum sativum	Garden pea	156	109	0.84	29.80
Vicia sp.	Vetches	1	1	0.01	0.66
Vicia ervilia	Bitter vetch	62	58	0.33	11.92
Vicia faba	Broad bean	29	29	0.16	11.26

Cultivated legume total		740	509	3.98	62.91
Oils					
Olea europaea	Olive	532	115	2.86	25.83
Oil total		532	115	2.86	25.83
Wild grasses					
Poaceae	Grasses	1322	957	7.11	80.79
Avena fatua	Wild oat	14	14	0.08	7.28
Bromus sp.	Bromes	54	51	0.29	11.26
cf. *Digitaria* spp.	Crabgrasses	198	198	1.06	22.52
cf. *Echinaria capitata*	-	2	2	0.01	1.32
cf. *Echinochloa crus-galli*	Barnyardgrass	3	3	0.02	1.99
cf. *Eragrostis* sp.	Lovegrasses	40	40	0.22	8.61
cf. *Holcus annuus*	Annual fog	1	1	0.01	0.66
Lolium temulentum	Darnel ryegrass	195	180	1.05	17.88
Phalaris canariensis	Canary grass	870	829	4.68	64.90
cf. *Stipa* sp.	-	1	1	0.01	0.66
Wild grass total		2700	2276	14.52	92.05
Wild sedges					
Bolboschoenus maritimus	-	157	155	0.84	20.53
Carex spp.	Sedges	19	19	0.10	6.62
cf. *Cyperaceae*	Sedges	4	4	0.02	1.99
Cyperus sp.	-	7	7	0.04	2.65
Eleocharis sp.	Spikerushes	16	16	0.09	7.95
Wild sedge total		203	201	1.09	31.13
Wild legumes					
Fabaceae (frags excluded)	Legumes	588	588	3.16	58.94
Astragalus sp.	Milkvetches	40	40	0.22	12.58
Crotalaria sp.	Rattlepods	8	8	0.04	3.31
cf. *Hippocrepis emerus*	Scorpion senna	12	11	0.06	3.31
Medicago/Onobrychis spp.	Burclovers/Sainfoins	763	739	4.10	62.91
Melilotus sp.	Sweet clovers	116	116	0.62	29.80
Prosopis farcta	Syrian mesquite	539	157	2.90	35.10

Trifolium sp.	Clovers	31	31	0.17	9.27
Vachellia nilotica	Acacia nilotica	6	6	0.03	1.32
Wild legume total		2103	1696	11.31	80.79
Wild woody and herbaceous					
cf. *Abutilon theophrasti*	Velvetleaf	6	6	0.03	2.65
Adonis sp.	Pheasant's eye	29	29	0.16	13.91
Aizoon hispanicum	Spanish aizoon	6	6	0.03	3.31
Amaranthus graecizans	Mediterranean amaranth	236	236	1.27	15.23
cf. *Anemone* sp.	Windflowers	2	2	0.01	0.66
cf. *Anthemis cotula*	Mayweed	35	35	0.19	7.28
cf. *Apiaceae*	Umbellifers	6	6	0.03	1.99
cf. *Arabis* sp.	Rockcresses	7	7	0.04	1.99
Arnebia cf. *decumbens*	-	3	3	0.02	1.32
cf. *Asteraceae*	Daisies	18	18	0.10	7.28
Atriplex sp.	Saltbushes	11	11	0.06	5.30
cf. *Barbarea vulgaris*	Wintercress	7	7	0.04	1.99
Beta vulgaris	Beet	96	65	0.52	17.88
Bellevalia sp.	-	127	117	0.68	35.76
cf. *Bifora testiculata*	-	1	1	0.01	0.66
cf. *Boraginaceae*	-	17	12	0.09	1.99
Bupleurum sp.	Thorow wax	198	188	1.06	38.41
cf. *Calotropis procera*	-	1	1	0.01	0.66
Centaurea cf. *melitensis*	Maltese starthistle	6	6	0.03	3.97
Chenopodium sp.	Goosefoot	476	475	2.56	29.14
cf. *Cirsium arvense*	Creeping thistle	1	1	0.01	0.66
cf. *Convolvulus arvensis*	Field bindweed	2	2	0.01	1.32
Coriandrum sativum	Coriander	12	12	0.06	5.96
cf. *Crataegus monogyna*	Hawthorn	9	9	0.05	3.31
Euphorbiaceae	Spurge	3	2	0.02	1.32
cf. *Euphorbia esula*	Leafy spurge	6	6	0.03	3.97
Galium aparine	Cleavers	149	93	0.80	31.79
cf. *Helianthemum* sp.	Sunroses	2	2	0.01	1.32
cf. *Hieracium* sp.	Hawkweeds	4	4	0.02	0.66
cf. *Ipomoea cairica*	-	17	11	0.09	5.96
cf. *Leucanthemum vulgare*	Oxeye daisy	2	2	0.01	1.32

Lithospermum officinale	Common gromwell	1	1	0.01	0.66
Lysimachia arvensis	Scarlet pimpernel	79	79	0.42	25.83
Malva parviflora	Cheeseweed	1771	1670	9.52	66.89
cf. *Myosotis arvensis*	Field forget-me-not	1	1	0.01	0.66
cf. *Myrica* sp.	Bayberries	7	5	0.04	2.65
Papaver cf. *rhoeas*	Common poppy	1	1	0.01	0.66
Pistacia cf. *terebinthus*	Terebinth	29	20	0.16	9.93
Plantago spp.	Fleaworts	267	267	1.44	27.81
cf. *Portulaca oleracea*	Purslane	1	1	0.01	0.66
cf. *Prunella vulgaris*	Common selfheal	4	4	0.02	0.66
cf. *Prunus* sp.	-	7	4	0.04	2.65
cf. *Rubiaceae*	-	2	2	0.01	0.66
cf. *Rubus* sp.	-	1	1	0.01	0.66
Rumex/Polygonum spp.	Sorrels/Knotweeds	535	532	2.88	56.95
cf. *Salvia officinalis*	Sage	1	1	0.01	0.66
cf. *Sesuvium portulacastrum*	Sea purslane	4	4	0.02	1.32
Silene cf. *noctiflora*	-	3	3	0.02	1.32
cf. *Sonchus arvensis*	Perennial sowthistle	1	1	0.01	0.66
Spergula arvensis	Corn spurry	6	6	0.03	2.65
Stellaria cf. *media*	Chickweed	3	3	0.02	1.32
cf. *Teucrium* sp.	Germanders	6	6	0.03	0.66
cf. *Vaccaria hispanica*	Cowcockle	2	2	0.01	1.32
cf. *Viola* sp.	-	4	4	0.02	1.99
Wild woody and herbaceous total		4231	3993	22.76	89.40
Unknowns					
Unknown 6	-	1	1	0.01	0.66
Unknown 12	-	2	2	0.01	1.32
Unknown 16	-	12	6	0.06	3.97
Unknown 18	-	9	5	0.05	3.31
Unknown 19	-	2	2	0.01	1.32
Unknown Total		26	16	0.14	10.60
Grand Total		20150	15742	100	
** chaff not included in seed frequency calculations					

Table 5.2 NISP and densities of plant categories per phase at Tell el-Hayyat, Jordan.

Phase	**6**	**5**	**4**	**3**	**2**	**1**	**Total**
Volume	44.0	216.3	271.0	220.0	132	3	
Cereals	154	2605	1462	1423	1011	28	6683
Cereal chaff	1	368	618	360	210	0	1557
Cultivated fruits	13	428	160	620	154	0	1375
Cultivated legumes	35	287	155	119	144	0	740
Oil	2	42	320	156	12	0	532
Wild grasses	37	610	739	1024	289	1	2700
Wild sedges	3	27	11	38	124	0	203
Wild legumes	21	688	522	473	387	12	2103
Wild woody and herbaceous	28	1050	1295	1033	822	3	4231
Total NISP	294	6105	5282	5246	3153	44	20124
Cereals	3.50	12.04	5.40	6.47	7.66	9.33	
Cereal chaff	0.02	1.70	2.28	1.64	1.59	0	
Cultivated fruits	0.30	1.98	0.59	2.82	1.17	0	
Cultivated legumes	0.80	1.33	0.57	0.54	1.09	0	
Oil	0.05	0.19	1.18	0.71	0.09	0	
Wild grasses	0.84	2.82	2.73	4.66	2.19	0.33	
Wild sedges	0.07	0.12	0.04	0.17	0.94	0	
Wild legumes	0.48	3.18	1.93	2.15	2.93	4.00	
Wild woody and herbaceous	0.64	4.85	4.78	4.70	6.23	1.00	
Total Density	6.68	28.22	19.49	23.85	23.89	14.67	

Frequencies and Ubiquities of Primary Cultigens

Densities show the highly variable recovery rates of cereals and fruits between phases, with *Hordeum vulgare*, *Triticum dicoccum,* and *Ficus carica* are each prominent through the sequence, Figure 5.1. The major trend from the primary cultigens is a shift in density to increased *Triticum* sp. and *Ficus carica* in later phases.

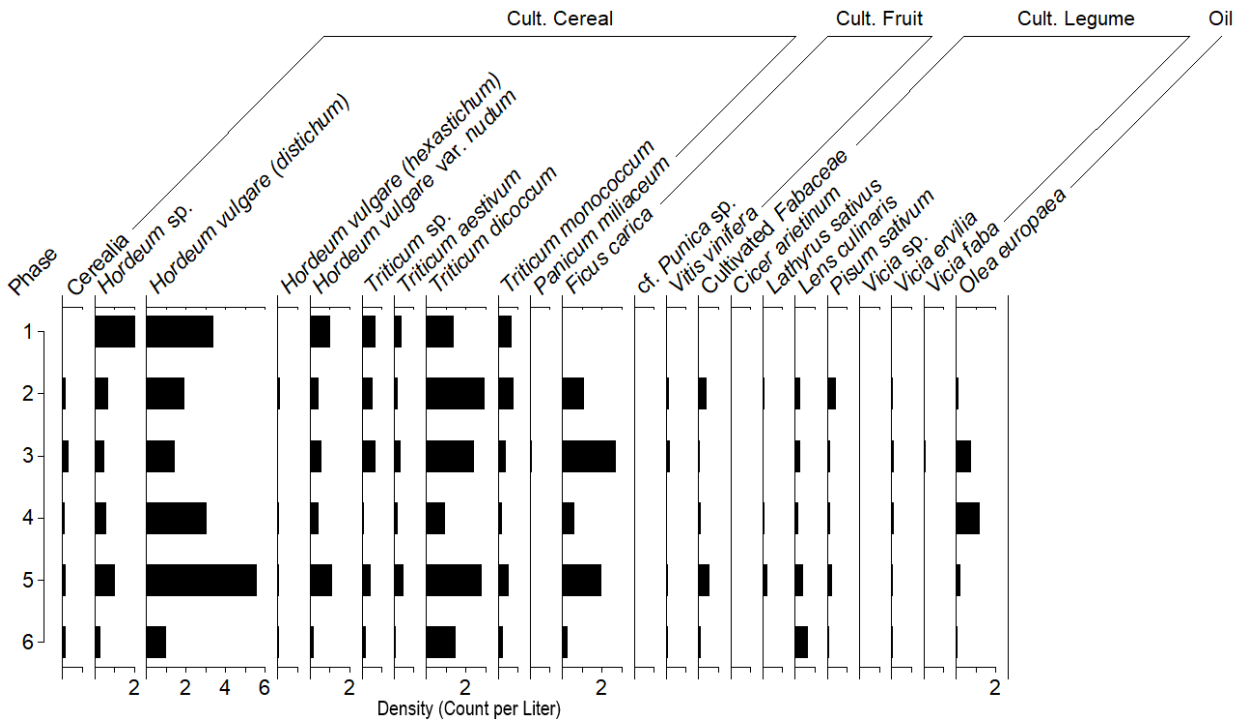

Figure 5.1 Densities, calculated as NISP per liter of sediment, per phase for all taxa from Tell el-Hayyat, Jordan. Plant categories are indicated above individual taxa.

Frequencies for taxa with at least 25 total seeds each are indicated in Figure 5.2. Due to low sample counts for Phases 6 and 1, the best trends were seen in Phases 5-2. *Hordeum vulgare*, *H. vulgare* var. *nudum*, and all three *Triticum* species were recovered in notably high frequencies and ubiquities at Hayyat. Between Phases 5-4 and 3-2 a trend emerges where *Triticum dicoccum* and *Ficus carica* become more prominent while *Hordeum vulgare* becomes scarcer, reinforced by the *Hordeum* to *Triticum* ratio and the break in the CONISS dendrogram between Phase 4 to 3. *Hordeum vulgare* and *H. vulgare* var. *hexastichum* show higher frequencies in the first three phases, while all species of *Triticum* show larger frequencies towards the latter phases. While *Hordeum* was more frequent in early phases, *Triticum dicoccum* do show high densities as early as Phase 5, showing the importance of wheat even early in the site's occupation.

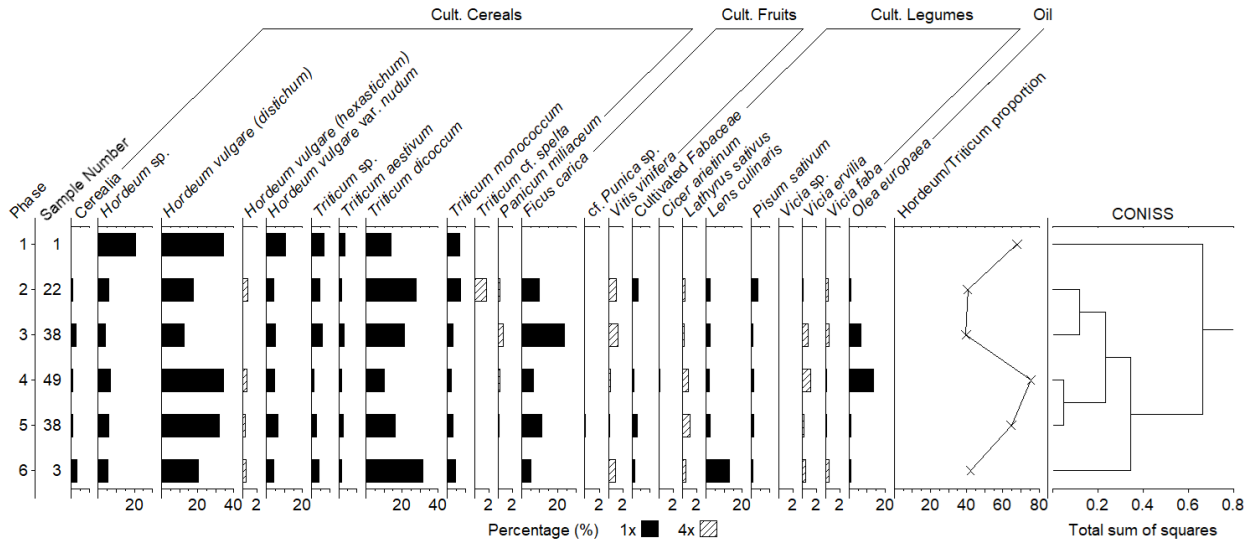

Figure 5.2 Frequencies of all cultivated plant taxa from Tell el-Hayyat, Jordan based on NISP. Plant categories are indicated above individual taxa. Striped bars indicate a 4x exaggeration. The line graph shows the percentage of barley grains from all barley plus wheat grains. The dendrogram shows a CONISS hierarchical cluster analysis indicating the grouping of similar phases, based on all cultivated taxa.

Other common seeds include those from *Ficus carica, Olea europaea, Lens culinaris,* and *Pisum sativum*. *Ficus carica* was frequent primarily due to its numerous seeds per fruit, and a low ubiquity reveals that it was not as prevalent at Hayyat. *Olea europaea* was also likely less frequent, indicated by its lower MNI count indicating high seed fragmentation. *Vitis vinifera* appears in limited quantities but stands out from its relatively higher ubiquity, and may have been comparable in utilization to the other fruits.

Lens culinaris is found throughout Hayyat's occupation and is the most common non-cereal cultigen in Phase 6, suggesting a potential importance for early settlers of the site. Less frequent cultigens at Hayyat include *Cicer arietinum, Lathyrus sativus, Vicia ervilia*, and *Vicia faba*.

Frequencies and Ubiquities of Wild Taxa

Figure 5.3 shows the relative frequencies of the most common wild taxa at Hayyat. Multiple wild grasses and sedges appear in the floral record, the most notable being the arable weed *Phalaris canariensis*. However, the shrub *Malva parviflora*, still found commonly in the vicinity today, is by far the most frequent wild taxon at Hayyat with over 1,700 seeds. *Malva parviflora* has both the highest frequency at around 10% of the total seed count, as well as the highest ubiquity for a wild taxon, being found in almost 67% of samples. *Medicago/Onobrychis* were combined for the sake of identification at all three sites, but both genera are present in high frequencies at Hayyat. The combined *Medicago/Onobrychis* group reached around 60% ubiquity.

There are much clearer temporal shifts in the wild species at Tell el-Hayyat than compared to those from Tell Abu en-Ni'aj. There is a notable, somewhat steady decline in species including *Lysimachia arvensis, Prosopis farcta*, *Poaceae, Plantago* sp., and *Rumex/Polygonum* spp., while several wild legumes, the *Amaranthaceae, Bolboschoenus maritimus*, and even *Pistacia terebinthus* increased from Phases 5-2.

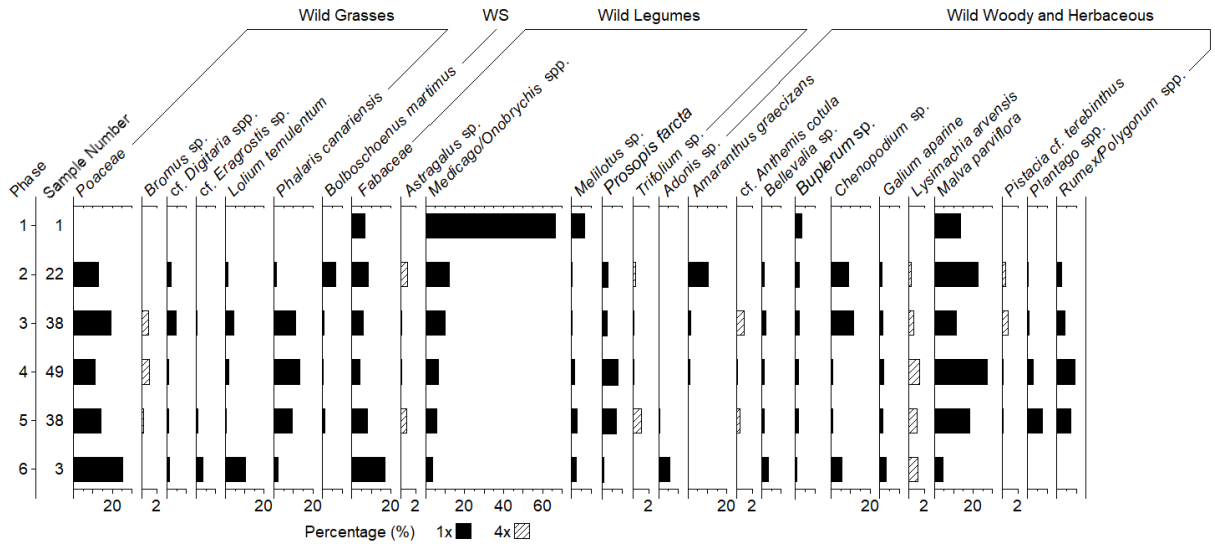

Figure 5.3 Frequencies of wild taxa from Tell el-Hayyat, Jordan (NISP count ≥ 29). Plant categories are indicated above individual taxa (WS – Wild sedge).

Other notable trends for wild taxa include the high ubiquity of 92% for *Poaceae*, indicating its presence in most samples. There is also a large variety of wild plants at Hayyat, including an array of herbaceous genera such as *Amaranthus, Plantago, Rumex/Polygonum*, and *Malva*, and several woody genera like *Pistacia* or *Prosopis*.

Discussion of Macrofossil Assemblage Trends

Looking at changes in frequencies and densities of individual taxa (see Table 5.1), *Hordeum vulgare* has perhaps the clearest shift during Hayyat Phases 5-2. A clear transition happens around the start of Middle Bronze II, between Phases 4 and 3, when its frequency drops roughly 20% (see Figure 5.2). This decline in MB II can be attributed primarily to the rise in cultivation of *Triticum dicoccum*, *Ficus carica,* and to a lesser extent *Vitis vinifera*. The shift from barley to wheat, alongside an increase in fruit production, could support the notion of climatic differences between MB I and MB II, suggesting that MB II became slightly wetter than MB I.

Regarding chaff frequencies, there were relatively more rachis internode fragments than glume base fragments, with low densities and frequencies of overall chaff. This is a stark distinction from Ni‘aj, where glume density was notably more frequent than rachises. Cereal glumes should have a roughly 2:1 ratio to rachis fragments. It seems unlikely that only cereal processing by-products richer in rachis fragments would be collected into dung cakes or for supplemental feed, regardless of the distance from the site that these actions are performed, as glumes are removed in later cereal-processing stages and would likely have been more accessible to humans (Hillman, 1984). This suggests that chaff may not be utilized as fuel to the degree it was at Ni‘aj. The crop processing by-products from later cereal-cleaning stages could have been

utilized for other purposes, such as incorporation into mudbricks for tempering, or strengthening. Alternatively, this could represent more of a grazing signal, with humans allowing animals to feed on remains from the threshing floor, potentially richer in rachis but missing the glumes and seed.

Orchard cultivation is indicated at Hayyat by the presence of the relatively moderate frequencies of *Olea europaea*, *Vitis vinifera,* and *Ficus carica* (see Figure 5.2). An increase in the somewhat drought-intolerant *V. vinifera* (Riehl, 2009) in the latter portion of MB II could support the hypothesis of increased precipitation in MB II, also speculated from the cereal transition. An increase in secondary product reliance might also be supported for MB II by evidence of increased *O. europaea* and *V. vinifera* production. The presence of these fruits in MB II indicates a longer-term mindset for agricultural management. Orchards produce both foodstuffs and secondary products such as oil, wine, and dried foodstuffs, making them valuable commodities for sedentary societies (Goor, 1966; Lines, 1995; Fall et al., 2002), but they require maintenance for multiple years, rather than a single season. Fig trees can take 3-5 years to reach maturity, while olive can take upwards of 50 years (Zinger, 1985, as cited in Langgut et al., 2019). Given the lengthy maturity time needed for olives, the orchards harvested in Phases 4 and 3 may have been planted earlier in Phase 5 or around the start of MB II. The decreased abundance of *O. europaea* in MB II Phase 2 could suggest the taxon became less valuable, but the taxa also has low ubiquity, which could suggest that their disappearance is due to a shift in the storage or processing location in the site, investigated in Chapter 7.

There is a large array of wild grasses, dominated by *Phalaris canariensis*, *Lolium temulentum,* and small *Digitaria*-like grasses (see Figure 5.3). These may be found intermixed in cereal fields (Renfrew, 1973; Riehl, 2010; Fuller and Stevens, 2018) but if not mixed in fields, they are

indicative of an open, steppe environment. Cereal production seems to have played an important role in the site's subsistence, and a mix of accidental harvesting and grazing of these arable weeds could account for their high frequencies.

Other notable changes include the overall shift in wild species over time, including a gradual decline in taxa like *Plantago* or *Rumex/Polygonum*. Many these weedy taxa, both before and after the transition, are fairly commonplace in steppe environments, and are similar to those found at Ni'aj. The climate signal in this period matches that of the Irano-Turanian phytogeographic region given the amount of scrubby, temperate/warm-temperate vegetation (Zohary, 1966; 1972; 1982; Feinbrun-Dothan 1978; 1986; Abu-Irmaileh, 1982; Riehl, 2010; Kreuz and Schäfer, 2011).

Notable distinctions at Hayyat include high frequencies of ruderal species like *A. graecizans* or *Chenopodium* sp. Members of the *Amaranthaceae* appear prominent in open landscapes with dry, bare soils (Bejenaru et al., 2018). Hayyat also maintains a high frequency of *B. maritimus*, a notable wetland taxon (Zohary, 1972) in Phase 2, replacing another potential wetland taxa found in upland regions of the valley in modern, *Prosopis farcta.* This transition possibly denotes the importance of the banks of the nearby Jordan River as a grazing location for livestock. Overall, the transition of wild plants may signify a shift in grazing locations away from cultivated fields and their immediate outskirts to riverbanks and disturbed or open areas further from the site. In this scenario, goats and sheep may have been taken farther from the site to feed over time (Portillo et al., 2019). This would support the idea of agricultural expansion and overuse of the environment in the vicinity of the site that accords with evidence of population expansion, as exhibited by shifts in architecture at Hayyat (Falconer and Fall, 2006).

Although Hayyat is only around 1.5 km apart from Ni‘aj, the habitat is comparable in Early Bronze IV and Middle Bronze. If climate shifted during the occupation of Hayyat, it would likely have been a slight cooling in MB II, indicated by the rise in *Triticum* sp., orchard taxa, and limited remains from weedy species in preference of cooler climates like *Beta vulgaris* (Zohary, 1966; Abu-Irmaileh, 1982). Seed densities at Hayyat are relatively stable through time, though lower than at Ni‘aj. The lower seed to charcoal ratio (Fall et al., 2015) does not appear to be indicative of more wood burning, as Hayyat did not have high charcoal densities (Fall et al., 2002), so is likely a result of the smaller settlement size not producing as much food or burning as much dung.

Figure 5.4 indicates the grouped densities of different plant types based on their macrofossil counts per liter of sediment. By phase, most seed densities slightly increase through Phases 5 to 2, but cereals show their highest density in Phase 5. Most wild taxa, including wild woody and herbaceous plants, increase slightly in density through time, which could indicate increased site activity and burning into MB II. Wild woody and herbaceous plants at Hayyat reach a frequency of almost 25% at their highest and nearly reach the ubiquity of the cultivated cereals in Phase 4, suggesting livestock grazing is playing a key role in the carbonized assemblage from Hayyat. Cereal chaff did not rise in later phases, as might be expected with increased grain production. However, similar to inferenced at Ni‘aj, this trend could suggest that agriculture is expanding further from the site. If cereals are being produced further away, initial crop cleaning stages like threshing may be conducted outside the site’s periphery.

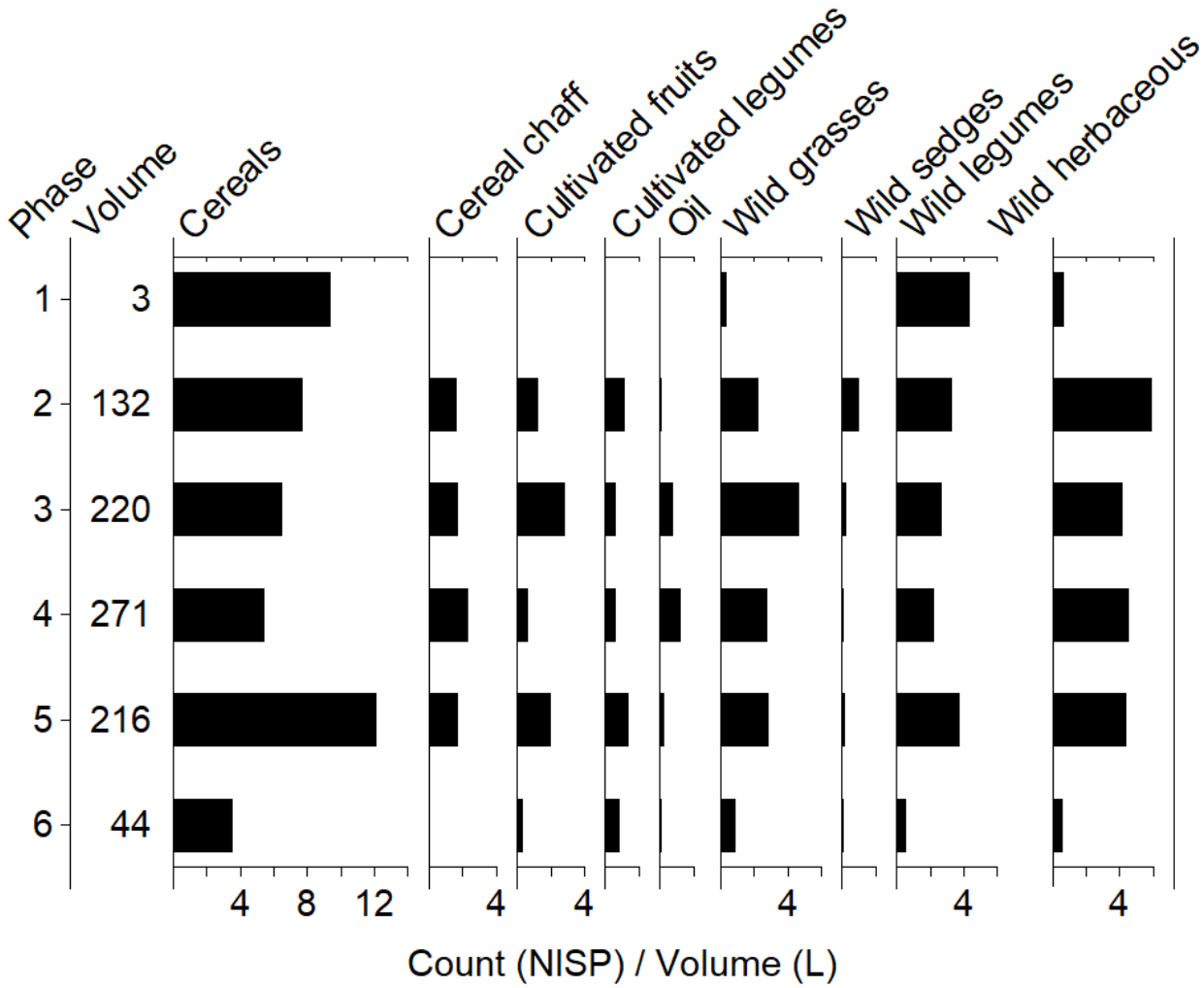

Figure 5.4 Densities (NISP per liter of floated sediment) of plant categories at Tell el-Hayyat, Jordan, as expressed in Table 5.2, with taxa grouped into categories of cultivated and uncultivated taxa.

CHAPTER 6: PALEOETHNOBOTANICAL RESULTS FROM ZAHRAT ADH-DHRA‘ 1

Zahrat adh-Dhra‘ 1 Paleoethnobotanical Results

Quantification of Macrofossil Remains

Zahrat adh-Dhra‘ 1 had approximately 1,800 identified seeds, 150 chaff fragments, and 1,050 indeterminant cultivated cereal fragments, wild legume fragments, and other indeterminant plant remains (Table S3). Carbonized plant remains were identified from Phases 4-2, with the majority originating from Phases 3 and 2. Seeds were recovered from 7 of the 9 structures excavated at ZAD 1 (Structures 36, 37, 39-42, 44). NISP, frequency, and ubiquity are presented in Table 6.1 for all taxa. Table 6.2 shows densities for each of the plant categories.

Table 6.1 NISP, frequency, and ubiquity for plant taxa recovered at Zahrat adh-Dhra‘ 1, Jordan. Counts of indeterminant cultivated cereal fragments, wild legume fragments, and other unknown plant remains were excluded from analysis but can be found in Table S4. No *Fabaceae* fragments were recorded from Zahrat adh-Dhra‘ 1.

Scientific Name	Common Name	Seeds	Frequency	Ubiquity
Cereals				
Cerealia (frags excluded)	Cereals	35	1.8	20.9
Hordeum sp.	Barley	11	0.6	10.5
Hordeum vulgare	Two-row hulled barley	57	2.9	20.9
Hordeum vulgare var. *nudum*	Naked barley	94	4.8	19.8
Triticum sp.	Wheat	2	0.1	2.3
Triticum aestivum/durum	Bread wheat/Durum wheat	33	1.7	14.0
Triticum dicoccum	Emmer wheat	22	1.1	10.5
Triticum monococcum	Einkorn wheat	1	0.1	1.2
Triticum cf. spelta	Spelt wheat	4	0.2	3.5
cf. *Panicum miliaceum*	Broomcorn millet	1	0.1	1.2
Cereal total		260	13.4	52.3
****Cereal chaff**				
**Glume base fragments		8	0.4	3.5
**Rachis fragments		142	7.3	34.9
****Cereal chaff total**		150	7.7	36.0
Cultivated fruits				
Ficus carica	Fig	248	12.8	46.5
Vitis vinifera	Grape	110	5.7	20.9
Cultivated fruit total		358	18.5	57.0
Cultivated legumes				
Cultivated *Fabaceae*	Pulse	60	3.1	7.0
Lathyrus sativus	Grass pea	1	0.1	1.2
Lens culinaris	Lentil	4	0.2	3.5
Pisum sativum	Garden pea	35	1.8	16.3
Vicia ervilia	Bitter vetch	2	0.1	1.2
Vicia faba	Broad bean	9	0.5	4.7
Cultivated legume total		111	5.7	30.2
Wild grasses				
Poaceae	Grasses	33	1.7	12.8
Bromus sp.	Brome	3	0.2	3.5

cf. *Digitaria* sp.	Crabgrasses	1	0.1	1.2
Phalaris canariensis	Canary grass	11	0.6	5.8
Wild grass total		48	2.5	18.6
Wild sedges				
Bolboschoenus maritimus	-	6	0.3	4.7
Carex spp.	Sedges	22	1.1	14.0
Eleocharis sp.	Spikerush	9	0.5	5.8
Wild sedge total		37	1.9	20.9
Wild legumes				
Fabaceae	Legumes	41	2.1	38.4
Astragalus sp.	Milkvetch	2	0.1	2.3
cf. *Trigonella* sp.	Fenugreek	32	1.6	7.0
Medicago sp.	Burclovers	2	0.1	1.2
Melilotus sp.	Sweet clovers	9	0.5	4.7
Wild legume total		86	4.4	43.0
Wild woody and herbaceous				
Adonis sp.	Pheasant's eye	1	0.1	1.2
Aizoon hispanicum	Spanish aizoon	522	26.9	34.9
Amaranthus sp.	Amaranth	61	3.1	9.3
cf. *Asteraceae*	Daisies	2	0.1	2.3
Bellevalia sp.	-	14	0.7	8.1
cf. *Berberis vulgaris*	Barberry	5	0.3	1.2
cf. *Centaurea* sp.	Starthistles	1	0.1	1.2
Chenopodium sp.	Goosefoot	123	6.3	39.5
cf. *Crataegus monogyna*	Hawthorn	1	0.1	1.2
Euphorbiaceae	Spurge	1	0.1	1.2
cf. *Euphorbia esula*	Leafy spurge	42	2.2	2.3
cf. *Fumaria densiflora*	Dense-flowered fumitory	5	0.3	3.5
cf. *Helianthemum* sp.	Sunroses	1	0.1	1.2
Malva parviflora	Cheeseweed	57	2.9	19.8
Ornithogalum sp.	Star-of-Bethlehem	35	1.8	4.7
Pistacia terebinthus	Terebinth	1	0.1	1.2
Plantago spp.	Fleaworts	8	0.4	7.0
cf. *Ranunculus acris*	Tall buttercup	2	0.1	1.2
Rumex/Polygonum spp.	Sorrels/Knotweeds	157	8.1	27.9
Wild woody and herbaceous total		1039	53.6	72.1
Grand Total		2089	100	
** chaff not included in seed frequency calculations				

Table 6.2 NISP and densities of plant categories recovered at Zahrat adh-Dhra‘ 1, Jordan. Samples from Areas B and O (Two samples total; Table S4), lacked phasing and are combined into the ‘Other’ category.

Phase	**4**	**3**	**2**	**Other**	**Total**
Volume	13.2	150.16	81.728	6.33	
Cereals	5	205	50	0	260
Cereal chaff	5	86	59	0	150
Cultivated fruits	44	87	226	1	358
Cultivated legumes	13	53	45	0	111
Wild grasses	0	28	20	0	48
Wild sedges	3	8	26	0	37
Wild legumes	19	35	32	0	86
Wild woody and herbaceous	28	376	605	30	1039
Total NISP	117	878	1063	31	2089
Cereals	0.38	1.37	0.61		
Cereal chaff	0.38	0.57	0.72		
Cultivated fruits	3.33	0.58	2.77		
Cultivated legumes	0.98	0.35	0.55		
Wild grasses	0.00	0.19	0.24		
Wild sedges	0.23	0.05	0.32		
Wild legumes	1.44	0.23	0.39		
Wild woody and herbaceous	2.12	2.50	7.40		
Total Density	8.86	5.88	13.01		

Frequencies and Ubiquities of Primary Cultigens

Several cultivated cereals are found in the assemblage at Zahrat adh-Dhra‘ 1, with *Hordeum* most abundant. *H. vulgare* var. *nudum* is the more common barley species, as opposed to *H. vulgare*, but both taxa had similar ubiquities. *H. vulgare hexastichum* is not found at ZAD 1. The most frequent wheat taxa are *Triticum aestivum/durum*, combined in this analysis to aid identification, and *Triticum dicoccum*. Among other cultigens, *Ficus carica* and *Vitis vinifera* were notably frequent, being more abundant than all cereals. *Pisum sativum*, and *Vicia faba* are also frequent at ZAD 1. Figure 6.1 shows the densities for cultivated crops at Zahrat adh-Dhra‘

1. Lower densities for cultigens were found at ZAD 1 than those for Ni'aj and Hayyat, but the overall trend shows the importance of cultivated fruits and legumes, potentially *Pisum sativum*.

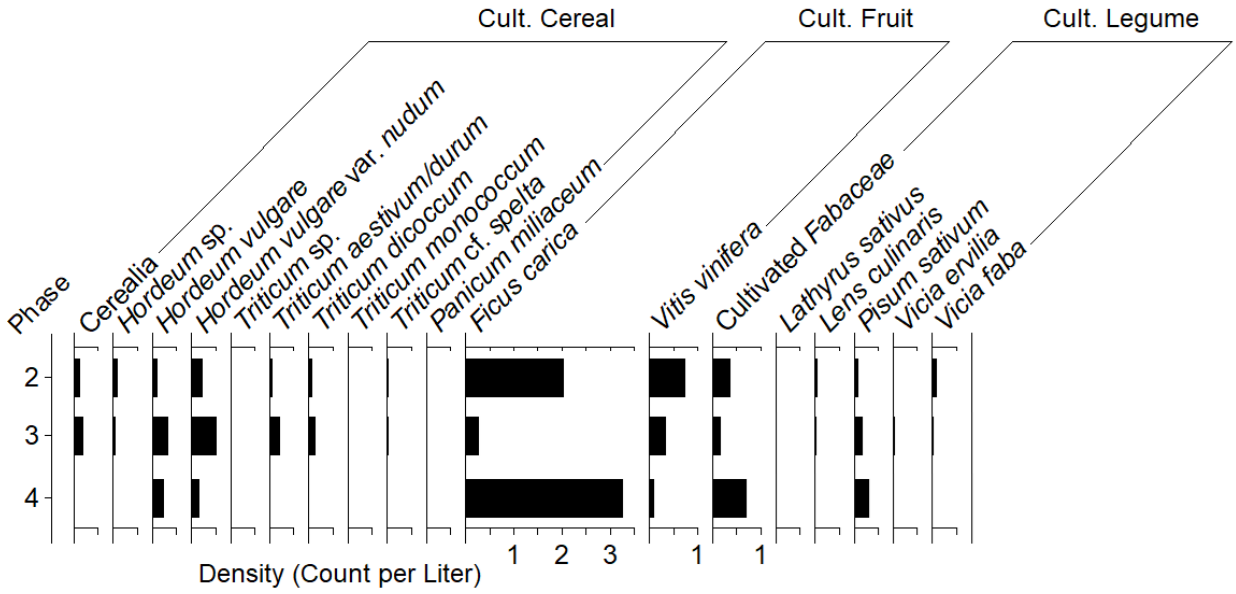

Figure 6.1 Densities, calculated as NISP per liter of sediment, per phase for all taxa from Zahrat adh-Dhra' 1, Jordan. Groups are listed above each individual species.

Frequencies roughly match the trend of density. Figure 6.2 highlights a decline in cultivated cereals alongside a rise in fruit and pulse production from the well-sampled Phases 3 to 2. *Hordeum vulgare* var. *nudum* was more dominant than *H. vulgare* in both phases, suggesting its heightened importance at the site. All cultivated cereals have their highest frequencies and densities in Phase 3.

The *Hordeum* to *Triticum* ratio in Phases 3 and 2 shows that *Hordeum* sp. comprised roughly 70% of the cereal assemblage. Notably, *Triticum* sp. seems to be absent during Phase 4. CONISS clustering expectedly separated Phase 4 as the most distinct.

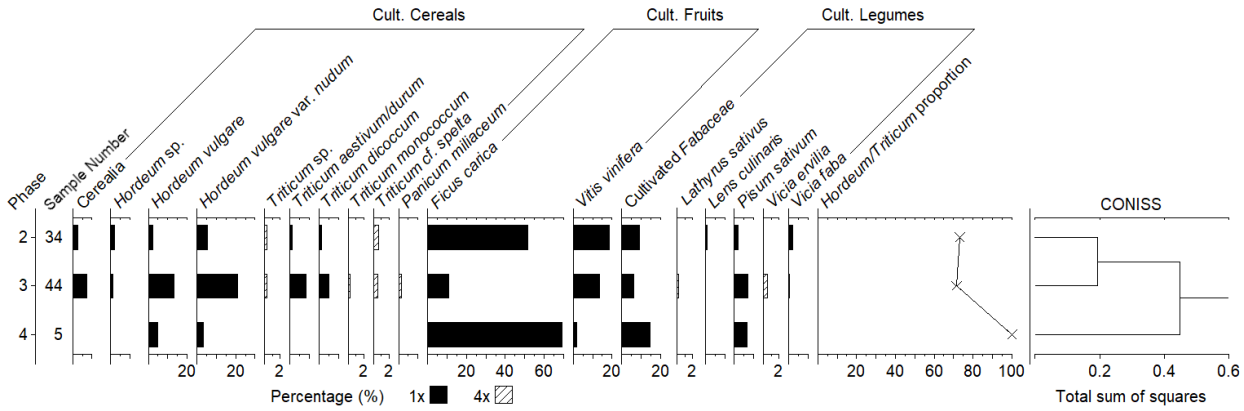

Figure 6.2 Frequencies of cultivated plant taxa from Zahrat adh-Dhra‘ 1, Jordan based on NISP. Plant categories are shown above individual taxa. Striped bars indicate a 4x exaggeration. The line graph shows the percentage of barley grains from all barley plus wheat grains. The dendrogram shows a CONISS hierarchical cluster analysis indicating the grouping of similar phases, based on all cultivated taxa. The two samples from unknown phases were not included.

Frequencies and Ubiquities of Wild Taxa

Wild taxa constitute over half the assemblage from ZAD 1, with most being wild herbaceous species. Common species include *Trigonella* sp., *Aizoon hispanicum, Amaranthaceae*, *Malva parviflora,* and *Rumex/Polygonum* spp. *Aizoon hispanicum* was the most prominent taxa with over 500 seeds spread across the assemblage. Figure 6.3 shows the increase in frequencies of several wild plants, particularly herbaceous taxa, in later phases.

From Phase 4 to Phase 2, taxa such as *Chenopodium* sp.*, Rumex/Polygonum* spp., and *Aizoon hispanicum* replaced taxa including *Bellevalia* sp., *Malva parviflora* and *Trigonella* sp. The overall assemblage shifts from one dominated by wild legumes in Phase 4 to being dominated by various wild herbaceous taxa and the occasional grasses in Phases 3-2.

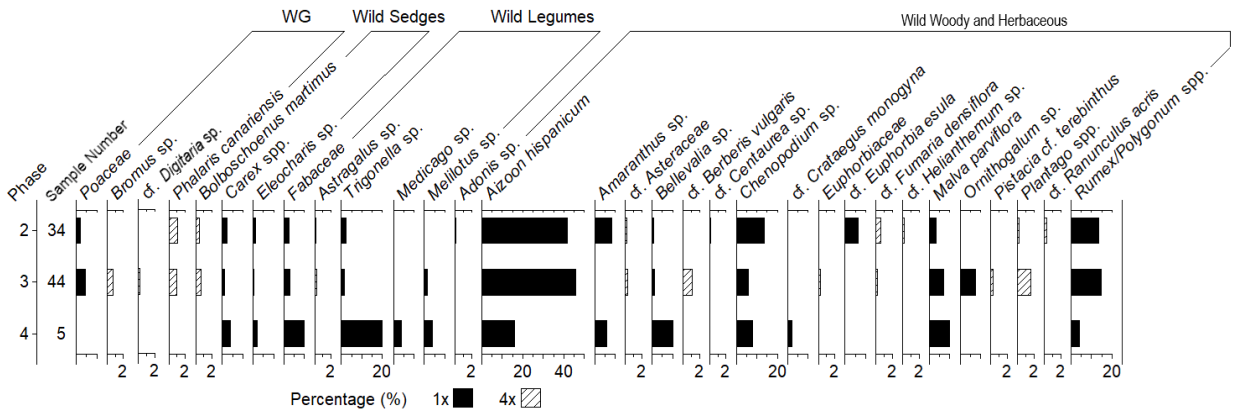

Figure 6.3 Frequencies of wild plant taxa from Zahrat adh-Dhra‘ 1, Jordan with plant categories indicated above individual taxa (WG – Wild grass). Striped bars indicate a 4x exaggeration. The two samples from unknown phases are excluded.

Discussion of Macrofossil Assemblage Trends

The Middle Bronze settlement Zahrat adh-Dhra‘ 1 has limited remains, with a small portion of cereal taxa, several common cultigens, and a small collection of wild taxa (see Table 6.1). The proportion of *Hordeum* to *Triticum* leans heavily toward *Hordeum* dominance. *Hordeum* is dominant throughout all three phases, while cereals in general were most prominent in Phase 3, around the Middle Bronze I to II transition (see Figure 6.2). At ZAD 1, the naked two-row barley variety *H. vulgare* var. *nudum* was nearly twice as frequent as *H. vulgare*, while *Triticum aestivum/durum* surpassed *T. dicoccum* as the most prominent taxon, suggesting a difference in cultivation choice to Ni‘aj and Hayyat. *Hordeum vulgare* var. *nudum* and *Triticum aestivum* are known to be less drought-tolerant hulled cereal varieties (Konvalina et al., 2010; 2011; Konvalina, 2014; Djelel et al., 2020), which indicates that the farmers at ZAD 1 were able to meet these cereal’s higher watering needs to produce satisfactory grain yields.

Despite having few cultivated cereals and fewer wild grasses, a fair amount of chaff was collected. The collection consists of primarily rachis fragments, with almost no glumes. These results suggest a preferential incorporation of early-stage cereal processing by-products. It may

be that material from the threshing process, richer in straw culms and rachises (Peña-Chocarro1 and Rottoli, 2007), was more frequently utilized while material from later stages like winnowing or pounding was unused or was processed and burnt elsewhere in the site. Given the aridity of the modern environment, wood fuel sources were likely scarce outside of taxa like *Tamarix* or *Acacia* (Hunt et al., 2007; Fall et al., 2015), so it may make sense for straw and chaff from threshing to be burnt alongside dung fuel and whatever wood was available (van der Veen, 1999). However, the relatively higher prevalence of hull-less cereals at ZAD 1 suggests glumes would likely be caught in the early threshing and winnowing processes (Dickin et al., 2012). Cultivated fruit is more frequent than cultivated cereals in terms of total seed frequency, behind only wild woody and herbaceous taxa due to the dominance of *Aizoon hispanicum*. *Ficus carica* has a predictably high frequency given its appearance in the assemblage and its tendency to be overrepresented in macrofossil records, but the frequency still suggests a heightened importance at ZAD 1, possibly for dried fruits. *Vitis vinifera* prominence suggests grape consumption and possibly wine making may have occurred at the site. Remains of *V. vinifera* also serve as further evidence of heightened water availability at the site (Riehl, 2009; 2010), particularly in MB II. However, the limited wheat and grape cultivation in MB I may point to this early phase being drier than the subsequent MB II (Fall et al., 1998; Riehl et al., 2009; 2010). The scale of fruit production, indicated by the high frequency and ubiquity of fruit crops, suggests orchard management played a key role at the site (Lines, 1995).

Grouped densities per vegetation category are indicated in Figure 6.4. The figure generally summarizes the shifts noted in Figures 6.2 and 6.3, with the major trends occurring between the relatively well-sampled Phases 3 and 2 for cultivated cereals, fruits, and wild woody and herbaceous taxa.

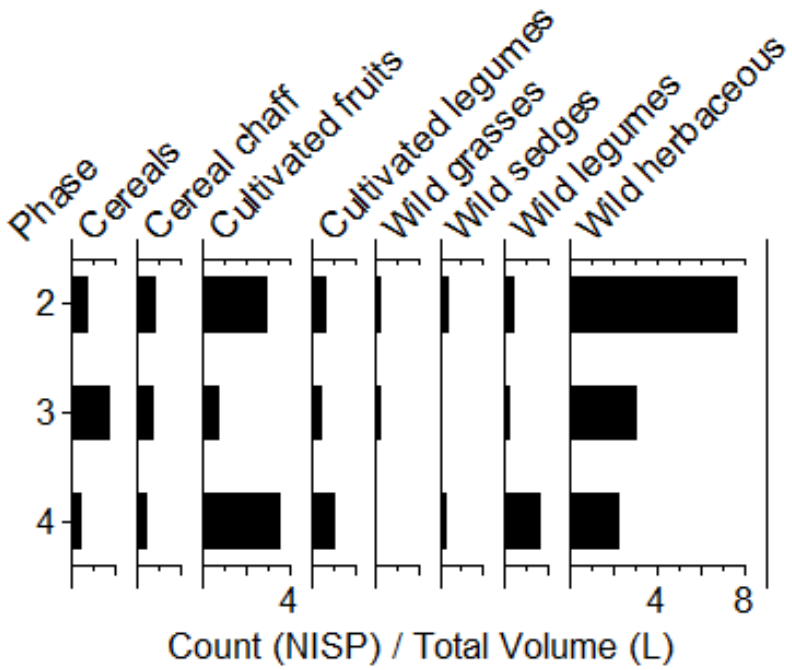

Figure 6.4 Densities (NISP per liter of floated sediment) of plant categories recovered at Zahrat adh-Dhra‘ 1, Jordan, as expressed in Table 6.2, with taxa grouped into categories of cultivated and uncultivated taxa. The two samples from unknown phases are not included.

The density of crops at ZAD 1 remained relatively low over time compared to the other focal sites, with the highest density occurring in Phase 2. This is believed to indicate less activity, and likely less dung burning, explored further in Chapter 8. Regardless, the site is believed to be primarily a dung burning settlement due to the high proportion of seeds to charcoal (Fall et al., 2015).

For the wild taxa, the primary trend is a shift to more remains (see Figure 6.3). This follows a trend similar to the rise at Tell el-Hayyat and potentially suggests the increased utilization of foraging animals at the site. Since densities of other crops did not rise, it is not likely indicating increased dung burning over time, but increased grazing in unmanaged areas.

Of the most frequent weed taxa, few were distinctly arable, whereas *Chenopodium* sp., *M. parviflora, A. graecizans, Euphorbia esula,* and *Trigonella* sp. each may grow as facultative or ruderal weeds. Even with the reduced variety of taxa, the weedy taxa at ZAD 1 indicate the

presence of a number of distinct microenvironments, including cultivated fields for the potentially arable weeds like *Bromus* sp., *Phalaris canariensis* or *Fumaria* sp., wetland environments for *Bolboschoenus maritimus*, and potentially disturbed or open environments for the facultative *Amaranthaceae* (Renfrew, 1973; Hopf, 1983; Miksicek, 1987; Reddy, 1997; Fisher and Holden, 2006; Kruez and Schäfer, 2011; Fuller and Stevens, 2018). The *Aizoon hispanicum* and *Amaranthaceae* are generally suggestive of a drier, open environments, and for *A. hispanicum* may indicate that soils were saline (Zohary, 1966; Gat-Tilman, 1994; Abudullah and Al-Dosari, 2002).

The majority of taxa thus point to a scrubland environment, akin to the Saharo-Arabian or Sudanean phytogeographic regions. There were relatively few grasses or large woody species, with soils that became increasingly dry further from the wadis and increasingly saline over time (Zohary, 1966; 1972; 1982; Feinbrun-Dothan, 1986; Abu-Irmaileh, 1982).

Trigonella was a notably prominent weed at ZAD 1 which did not appear in the northern Jordan Valley. The plant was primarily found in Phase 4, and likely constituted a larger component of animal diet (van Zeist, 1976), later replaced by *Aizoon hispanicum* in Phases 3 and 2. *Trigonella* consists of several species unlikely to be found intermixed in cultivated fields, instead found in disturbed grassland or scrubland environments (Helbaek, 1958; Miller, 1997). Observations of the plant in the modern ecosystem suggest that it resides mainly within more open areas (Zohary, 1972). Given the overlapping habitat range of *Trigonella* and *A. hispanicum*, both fond of dry, open ecosystems, the transition between these taxa may signify a slight shift in grazing location at the end of MB I, towards indicate grazing in or around arable fields, and a slight shift towards more saline soils over time. If the appearance of *Aizoon* signifies a leeching of salts into upper soils this would have large implications for agriculture at the site, as highly

saline soil can make agriculture more difficult (Qadir et al., 2000; Maggio et al., 2011). This could help explain the shift away from agriculture by Phase 2.

Regarding the regional environment, the overall findings from the floral survey taxa portrays the Dead Sea Plain in Middle Bronze I-II as a notably more arid environment. This is further supported by the earlier studies of charcoal, rich in *Acacia* sp. and *Tamarix* sp. remains (Fall et al., 2015) and the lack of *Olea europaea* remains either in this macrofloral survey or in regional pollen records, which has been used to indicate drier conditions (Kaniewski et al., 2018). This interpretation may seem at odds with the evidence of an array of drought-intolerant cereals and fruits cultivated at ZAD 1, which suggests that ancient farmers were able to attain sufficient water for agriculture. However, ZAD 1 in the Middle Bronze would have been sandwiched along the ridge of a narrow strip of land between two wadis and downslope from a nearby spring at ‘Ain Dhra (Edwards et al., 2001; Falconer et al., 2001). In the past, if these wadis were at site level, they may have provided enough water to support the array of water-hungry taxa whose remains were found at ZAD 1. This hypothesis posits that the location of ZAD 1 was uniquely suited to agriculture in this region for its proximity to perennial water sources.

CHAPTER 7: SPATIAL PATTERNS OF SEED DEPOSITION

Introduction

Spatial analysis of paleoethnobotanical evidence from archaeological sites examines the spatial variability of carbonized plant deposits to reveal where and how plants were utilized in each settlement (Weiss et al., 2008; Hald, 2010; Petõ et al., 2015; Snir et al., 2015). Spatial patterns can help support or refute hypotheses of crop cultivation strategies based on quantitative analysis (Murphy et al., 2013; Shin et al., 2021). Attaining a variety of spatial samples ensures a more representative picture of site activity, which augments interpretations developed from the temporal patterns. This chapter studies patterns of carbonized seed deposition at three focal sites to explore sedentary agrarian life during Early Bronze IV and Middle Bronze I-II.

Spatial patterning distinct from the general pattern of wild plants was noted for six taxa: wheat, barley, fig, olive, grape, and lentil. Results revealed important aspects of societies, such as the uses of grape and fig for ritualistic purposes in Hayyat's temple, or the communal storage of olive at Hayyat and the cereal and grape cultigens at ZAD 1.

Methodology of Spatial Investigation

Methods

I used frequencies to assess the distribution of cultigens and wild taxa across contexts at my three primary sites, comparing plant deposition within spatial units. Comparison of NISP is used to verify that the frequency trends highlighted for each site are driven by the plants noted, and not by changes in other taxa. Discussion of spatial patterns according to locus type was used at both Tell Abu en-Ni'aj and Tell el-Hayyat in previous publications (Magness-Gardiner and Falconer,

1994; Falconer, 1995; Falconer and Fall 2006; 2019; Porson et al., 2021b) noting high proportions of fruits, particularly fig pips, in temple contexts and cereal and legume crops in domestic contexts.

Samples at Tell Abu en-Ni‘aj and Tell el-Hayyat were grouped into sectors and loci for spatial analysis (Falconer and Fall 2006; 2019). Figures denoting the distribution of carbonized seeds from plant categories per spatial unit were used to visualize the spatial arrangement of seed deposition within each site. Comparative plant categories followed similar groupings to those used in Chapters 4 through 6, with slight alteration to best highlight the plants that had the most noteworthy spatial trends.

The terms ‘sector classification’ and 'locus category’ are hereafter used to denote groups of sectors and loci. Sector classifications indicate architecturally-defined spaces that defined human activities. Sectors are architecturally bounded spaces, which could describe an alleyway, a single room in a building, or a courtyard, for example. Analysis by sectors give instead of archaeological excavation areas (Kintigh and Ammerman, 1982; Vanderwarker et al., 2014: 206) incorporates architectural information and adds an ethnographic basis for inferring spatial patterns. Sector classifications include the following categories: domestic interior (DI), domestic exterior (DE), temple interior (TI), and temple exterior (TE) (Falconer and Fall, 2006).

Locus categories were denoted for the purpose of this analysis as archaeological features or sediment types of proposed similar depositional types, possibly indicative of anthropogenic use. Loci can include features like a tabun oven, trash pit, the floor of a building, or a burial, for example. The locus categories include anthropogenic surfaces (ANSU), denoting sediment at or just above floor contexts which might contain food remains and other debris; depositional sediments (DEP), denoting fill contexts where trash and other remains may have been

intentionally deposited; fire-associated sediments (FAS), denoting contexts with ash or other burned remains most likely indicative of cooking waste; and structural features (STR), denoting sediments that were at one point incorporated into mudbrick features. Tables 7.1 and 7.2 indicate the sector and locus types that are used in this study, respectively.

At Zahrat adh-Dhra‘ 1, settlement clusters were used to categorize samples, in lieu of archaeological sector or loci data. Multiple methods of spatial categorization are used to analyze spatial variability, with locus categories proving best at Ni‘aj, sector classifications at Hayyat, and settlement clusters at ZAD 1.

Table 7.1 Sector classifications from Tell el-Hayyat, Jordan used for the spatial analysis of the paleoethnobotanical assemblage (after Falconer and Fall 2006).

Sector Classification	Sector	Description
Domestic Interior (DI)	CE	Central Enclosure
	CR	Central Room
	EB	East Building
	EB1	East Building Room 1
	EB2	East Building Room 2
	EB3	East Building Room 3
	WR	West Room
Domestic Exterior (DE)	AB	Exterior Areas A and B
	CA	Central Alley
	CC	Central Courtyard
	EA	East Alley
	EC	East Courtyard
	KL	Kiln-Associated Area (Within Areas A&B)
	OTE	Outer Temple Area
	WE	West Enclosure
Temple Interior (TI)	TI	Temple Interior
Temple Exterior (TE)	TB	Temple Backcourt
	TF	Temple Forecourt
	TFE	Temple Forecourt Exterior
	TS	Temple Sidecourt

Table 7.2 Locus Categories and Locus Types with descriptions at Tell Abu en-Ni‘aj and Tell el-Hayyat, Jordan (after Falconer and Fall 2006; 2019).

Locus Category	Locus Type Code	Description
Anthropogenic-surfaces (ANSU)	DO	Debris, occupational
	S	Surface (earthen)
	SP	Surface, plaster
	SS	Surface, stone
Depositional sediments (DEP)	B	Bin
	BF	Bin fill
	DF	Debris, fill
	H	Posthole
	P	Pit
	PB	Pit, burial
	PS	Pit, stone-lined
Fire-associated sediments (FAS)	A	Ash lens (usually shallow and embedded in a surface)
	K	Kiln
	T	Tabun
	TF	Tabun fill
Structural features (STR)	DM	Debris, mudbrick
	I	Installation (industrial or architectural feature)
	WM	Wall, mudbrick
	WS	Wall, stone

Sector classifications for Ni‘aj were newly defined for this analysis based on architectural plans. Figure 7.1 shows the archeological structures of Ni‘aj Phase 3 as an example of the site’s architecture. The locations of designated domestic interiors and exteriors for Ni‘aj from Phases 7-1 are shown in Appendix D, Figures A8-A14. A network of domestic interior rooms are broken up by a large, paved surface in the northwest and small alleys throughout. Exterior courtyards are noted in the east and a large three-basin feature is shown in the southeast (Falconer and Fall, 2019: 43-68).

Figure 7.1 Archaeological plan of Tell Abu en-Ni'aj Phase 3 showing the architectural layout of the site. Letters are used to designate each excavation unit (after Falconer and Fall 2019: fig 4.20). Colors are used to designate areas representing possible domestic interior sectors (green) and domestic exteriors (yellow) from the areas with carbonized material sampled in this dissertation.

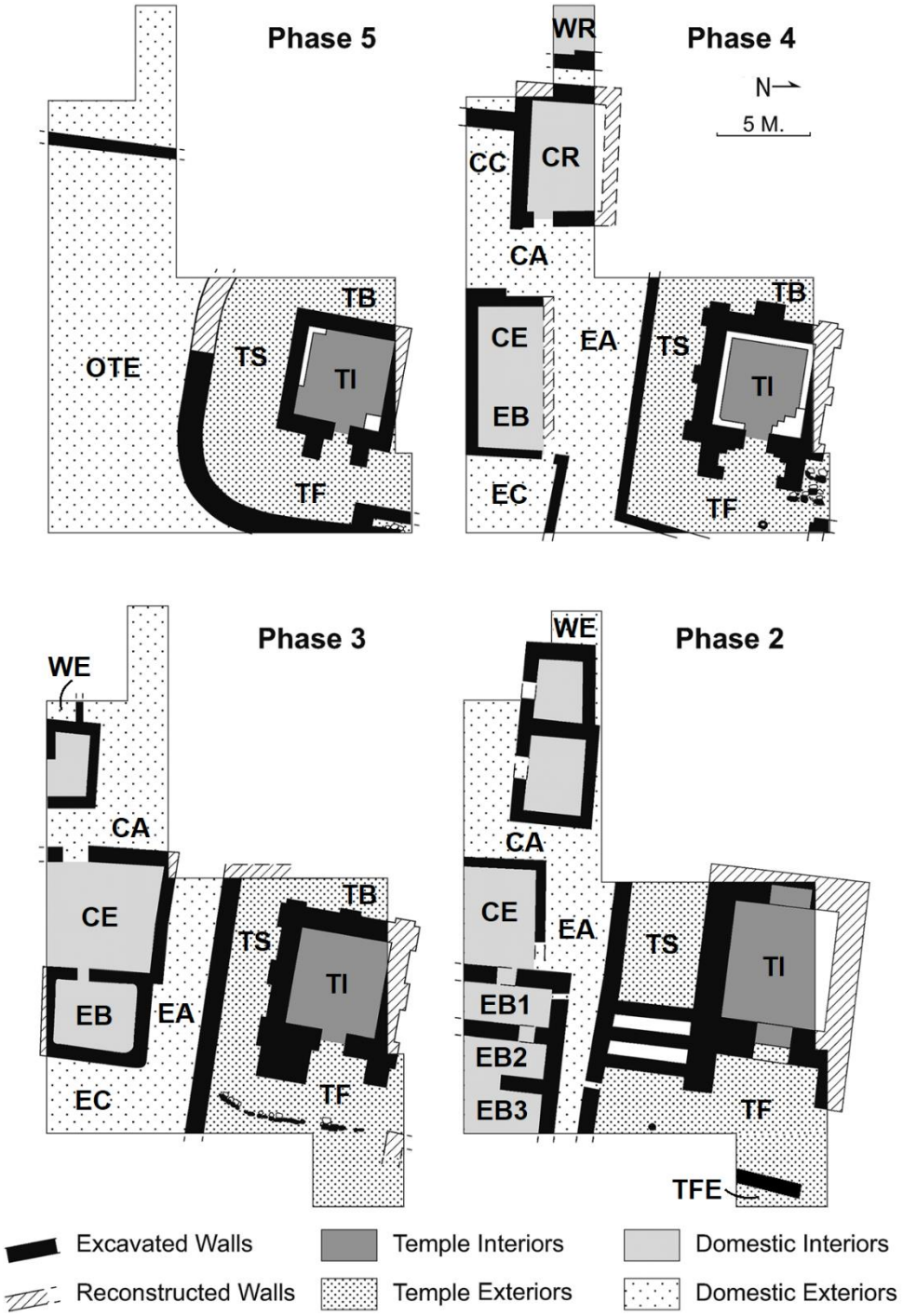

Figure 7.2 Archaeological plans indicating sectors and sector classifications for Tell el-Hayyat, Jordan Phases 5-2 used in spatial analysis of paleoethnobotanical assemblages. Sectors include CE - Central Enclosure, CR - Central Room, EB - East Building, EB1 - East Building Room 1, EB2 - East Building Room 2, EB3 - East Building Room 3, WR - West Room, CA - Central Alley, CC - Central Courtyard, EA - East Alley, EC - East Courtyard, OTE - Outer Temple Area, WE - West Enclosure, TI - Temple Interior, TB - Temple Backcourt, TF - Temple Forecourt, TFE - Temple Forecourt Exterior, TS - Temple Sidecourt (Image modified from Falconer and Fall, 2022: fig. 2; original figure prepared by Barbara Trapido-Lurie).

Sector classifications were determined for contexts at Tell el-Hayyat by Drs. Patricia Fall and Steven Falconer (Fall and Falconer 2006). Spatial analysis was conducted on sectors from Phases 5-2, as these phases had architecturally-defined sectors, whereas Phase 1 has insufficient architectural remains needed to define sectors and Phase 6 lacks architectural remains altogether. Tell el-Hayyat is more completely sampled than either Tell Abu en-Ni‘aj or Zahrat adh-Dhra‘ 1, in that most archaeological sectors per phase have at least one recorded sample. This enables visualization of the spatial patterns, so density data from Hayyat was drawn in ArcGIS Pro for Phases 5-2 for each of the primary, contiguous archaeological areas (Figure 7.2). This included all sectors with the exception of Exterior Areas A and B and the Kiln-Associated Area.

For ZAD 1, patterns of plant deposition in three clusters of structures were used for spatial analysis. These clusters are separated by open space. The clusters are defined as northwest (Structures 41, 42, 44), central (Structures 39 and 40) and southeast (Structures 36 and 37) (Figure 7.3; Image modified from Fall et al., 2023). Radiocarbon dating of this site recently revised the interpretation of this site to suggest three intervals of habitation (Fall et al., 2019; 2023). New radiocarbon dating suggest that the central and southeast clusters were inhabited in Phase 4, structures in all three clusters were occupied in Phase 3, and structures in in the northwest and southeast structures were inhabited in Phase 2 (Fall et al., 2023). On this basis, spatial patterning at ZAD 1 may be compared to Ni‘aj and Hayyat.

For all three sites, samples without locus, sector, or structure designations were removed for the respective analysis. At Hayyat this leaves 147 samples for locus category analysis and 149 samples for sector classification analysis. At Ni‘aj there are 153 samples for locus category analysis and 156 samples for sector classification analysis. Finally, ZAD 1 has 84 samples for structure cluster analysis.

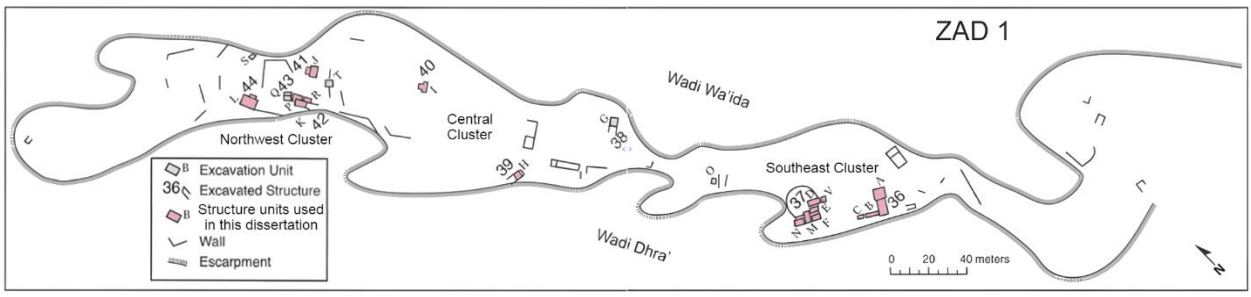

Figure 7.3 Architectural plan indicating building clusters used for spatial analysis at Zahrat adh-Dhra‘ 1, Jordan (Original figure from Fall et al., 2023).

Considerations

The majority of seeds within a site would have been carbonized through incorporation through animal remains, compacted in dung cakes (Miller and Smart, 1984; Miller, 1997; Miller, 2002), but carbonized seeds from unintentional food preparation or intentional fuel use will also play a role in the distribution throughout a site. Food processing involves both the remains of crop processing, where by-products may be subject to unintentional burning such as might occur when a structure collapses, and trash following cooking, breadmaking, or feasting, which may either be left in the location of these activities or moved to designated trash contexts. Dung cake burning and trash deposition was indicated by much higher contributions of seeds, dominated by wild taxa. These samples tended to be in external sectors but were noted all throughout Hayyat, and may be found all throughout a site rather than in defined areas, as also supported by deposition of animal remains (Falconer and Fall., 2006; 2019). Consideration of taxa used for other purposes will look for spatial patterns distinct from this distribution.

Intrasite Spatial Distributions

Tell Abu en-Ni'aj

Spatial analyses reveal two prominent patterns at Ni'aj, first being the high frequency of barley in domestic interior contexts and fire-associated sediments, and the second being the high frequency of chaff in structural features. Figure 7.4 shows the relative frequencies of the various plant groups per sector classification. The spatial pattern is driven by changes in chaff frequency, where chaff constituted much more of domestic exterior than domestic interior samples, offset partially by increased wheat, fruit, and other cultigen taxa in the exteriors. Domestic interiors had higher frequencies of cultivated barley, and wild woody and herbaceous taxa.

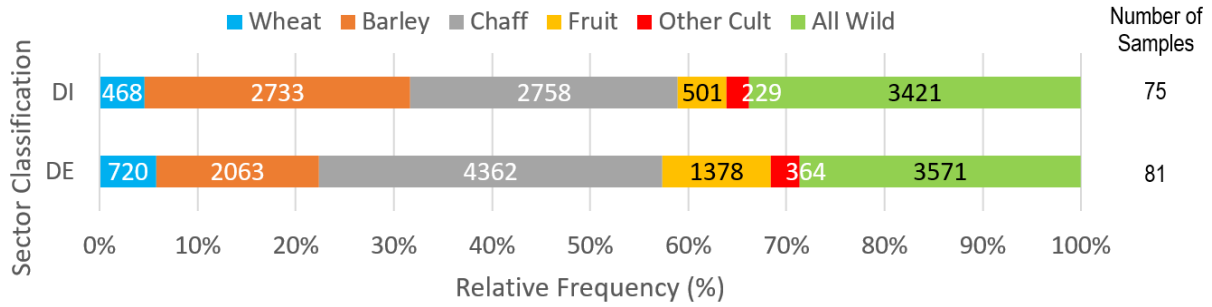

Figure 7.4 Relative frequencies of major cultivated and wild taxa at Tell Abu en-Ni'aj, Jordan in domestic interiors (DI) and domestic exteriors (DE). Frequencies based on NISP are shown by the numbers in the bars. The number of total samples in the DI or DE categories are listed at the right.

The macrofossil assemblage from Ni'aj also varied in its deposition between locus categories. Ash lenses were the only fire-associated sediment features uncovered at this site, and they contained the highest frequencies of cultivated cereals, driven foremost by barley (Figure 7.5). However, the fire-associated sediments had relatively lower NISP compared to the anthropogenic or depositional sediments, with depositional sediments containing higher NISP. Structural features had far more chaff than any other features, constituting over 60% of this category. Depositional features had a higher frequency of cultivated fruits thanks in large part to

a single sample of almost 1000 fig seeds attributed to a domestic exterior pit. All wild plants, including the wild grasses, legumes and woody or herbaceous plants, show similar relative frequencies in the ANSU, DEP, and FAS locus categories, comprising roughly one third of the total macrofossil remains. *Olea europaea* remains, here included in the other cultigens group, were notably absent from fire-associated and structural sediments, but evenly distributed between anthropogenic and depositional sediments.

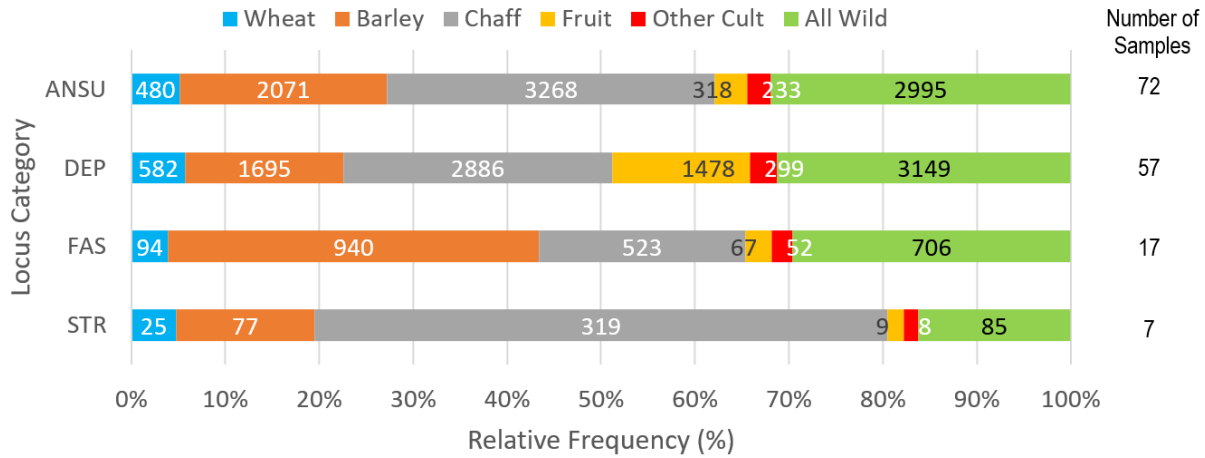

Figure 7.5 Relative frequencies of major cultivated and wild taxa by locus category at Tell Abu en-Ni'aj, Jordan in anthropogenic-surface sediments (ANSU), depositional sediments (DEP), fire-associated sediments (FAS), structural sediments (STR). Frequencies based on NISP are shown by the numbers in the bars. The number of total samples in the ANSU, DEP, FAS, and STR categories are listed at the right.

Tell el-Hayyat Spatial Category Comparisons

From Hayyat, several patterns emerge when considering the spatial distribution of carbonized remains. First is that the greatest deposition of cereals is in domestic contexts. Wheat is especially prominent in domestic interiors and barley in domestic exteriors (Figure 7.6). Chaff is also more prevalent in domestic contexts rather than temple contexts. Finally, fruit and olive deposition shows unique spatial patterning, with olive deposited primarily in domestic interiors, grape in temple interiors, and fig in both temple interiors and exteriors. Though NISP of grape is

low, it makes up roughly 2% of the Temple Interior assemblage, surpassing its frequencies in the other sector types (Table S2).

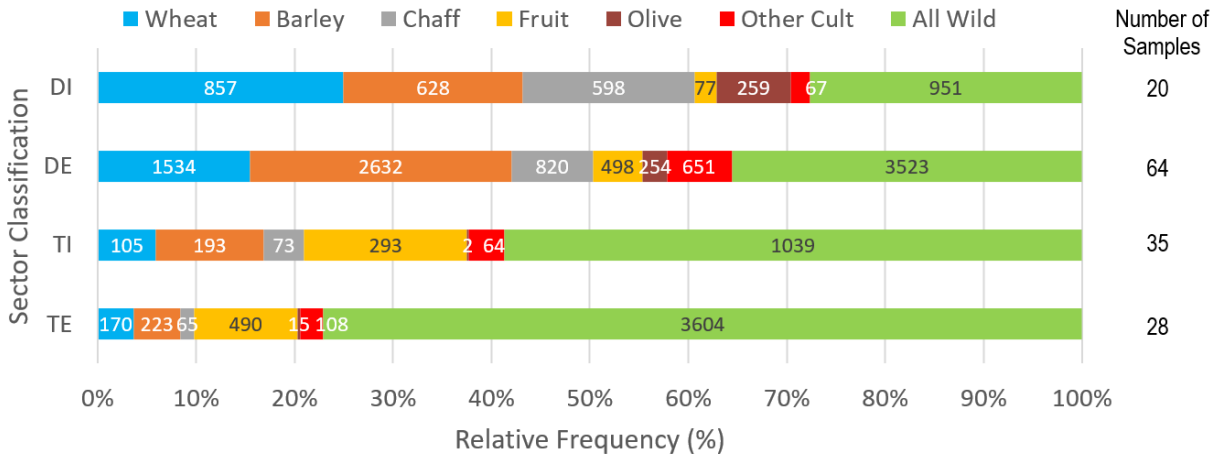

Figure 7.6 Relative frequencies of major cultivated and wild taxa by sector classification at Tell el-Hayyat, Jordan in domestic interiors (DI), domestic exteriors (DE), temple interiors (TI) and temple exteriors (TE). Frequencies based on NISP are shown by the numbers in the bars. The numbers of samples in the DI, DE, TI or TE categories are listed at the right.

Domestic interiors and exteriors are most similar, with cereal frequencies similar between each, but a much higher density in the exteriors. Domestic exteriors have a more mixed array of wild woody and herbaceous taxa, with a notable prevalence of *Prosopis farcta* in this context, likely indicating these are trash from burnt animal dung. Temple contexts are driven by high concentrations of wild legumes and herbaceous weedy species. Temple interior contexts have higher frequencies of cultivated fruit and cereals relative to the exterior. Cultivated cereal, chaff, and olive are relatively infrequent in temple contexts, particularly the exterior. In both domestic and temple sectors, exteriors have far more seeds than interiors and are primarily dominated by wild taxa, particularly in the temple exterior.

The spatial patterning of plant remains also varied according to locus categories, which shows a high frequency of wheat in depositional contexts (Figure 7.7). Cultivated taxa are generally most frequent in depositional sediments, but had highest densities in the anthropogenic and fire-associated features. This is distinct to Ni'aj, as far more fire-associated contexts were excavated

at Hayyat. Hayyat is also unlike Ni'aj is the composition of structural loci, having little chaff and many more wild plant remains. A final notable distinction for Hayyat is the prevalence of remains of olive and garden peas in fire-associated features.

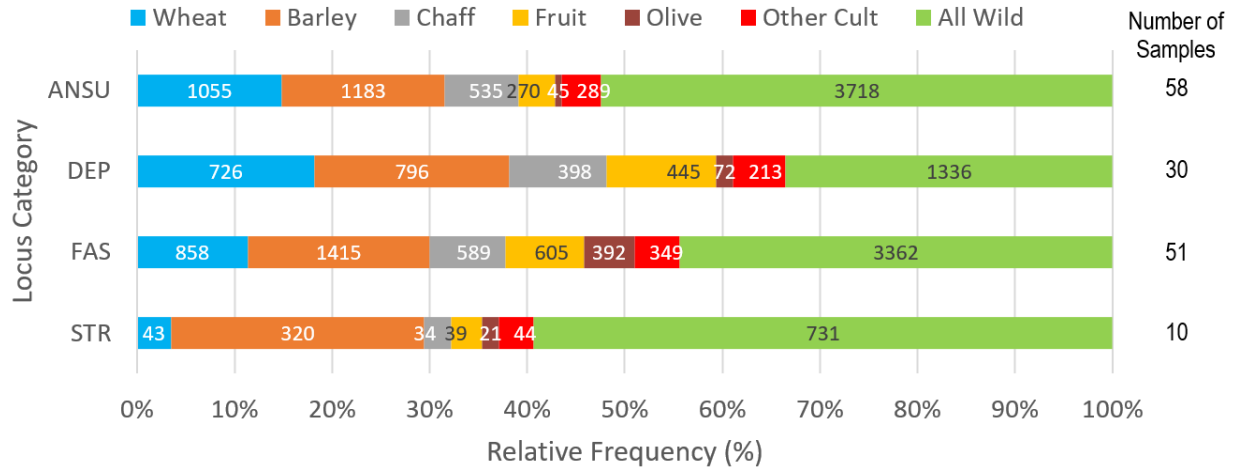

Figure 7.7 Relative frequencies of major cultivated and wild taxa by locus category at Tell el-Hayyat, Jordan in anthropogenic-surface sediments (ANSU), depositional sediments (DEP), fire-associated sediments (FAS), structural sediments (STR). Frequencies based on NISP are shown by the numbers in the bars. The number of total samples in the ANSU, DEP, FAS, and STR categories are listed at the right.

Examining specific locus types, which can be compared in Table S2, shows that almost all cultigens are recovered from either ash lenses, earthen surfaces, pits, or debris. The notable exceptions to this are olive and wild grass taxa, which are found primarily in fire-associated tabun or kiln features.

Tell el-Hayyat Architectural Sector Maps: Barley and Wheat

Spatial-temporal deposition by sector is presented at Hayyat for select cultigens in Phases 5-2 based on seed densities for mixed barleys (*Hordeum* sp.), mixed wheats (*Triticum* sp.), fig (*Ficus carica*), grape (*Vitis vinifera)*, olive (*Olea europaea*), and lentil (*Lens culinaris*) (Figures 7.8-7.13). Taxa were included for discussion here based upon whether they were cultigens and

whether they had a spatial pattern that both varied notably between sectors was from the spatial pattern of wild taxa, which was most prominent in the temple exterior. Densities for each taxon are reported in Table A2. For the figures, density thresholds were subjectively selected that best displayed the range of seed densities per liter of sediment to highlight the distinctions between archaeological sectors.

Figure 7.8 examines the density of the combined barley taxa across Hayyat. In Phase 5, there are no domestic structures, so any seeds recovered outside the curving temple enclosure wall are considered to be in the domestic exterior category. Most barley are found in these domestic exteriors. This trend continues in Phase 4, with the domestic sectors having the largest densities of barley, with remains appearing prominently in all four interior rooms as well as the east alley and courtyard. The density is greatest in the east building, with just over 56 seeds recovered per liter. Barley densities in Phases 3 and 2 are much more even across the site, still appearing in slightly greater densities in interior and exterior domestic sectors. Through Phases 4 to 2 the central enclosure sector has the highest barley densities. In all four phases, the temple sectors saw relatively few barley remains, with some deposition in the temple sidecourt in Phase 5 being the only exception.

Figure 7.8 Barley (*Hordeum* sp.) densities (NISP/liter) at Tell el-Hayyat, Jordan. Gray indicates walls while light-gray indicates large stones or other archaeological features. Higher densities are indicated by more densely gridded patterns and darker blue coloration.

Figure 7.9 examines densities of all combined wheat species. Wheat density patterns show a general similarity to those of barley, but with a key contrast in the location of maximum density. The spatial pattern starts similar to that of barley in Phase 5, with the highest wheat densities in the domestic exterior, though relatively lower in density than barley. In Phase 4, high densities of wheat are only recovered from the east building. Domestic sectors have higher densities than temple sectors.

Figure 7.9 Wheat (*Triticum* sp.) densities (NISP/liter) at Tell el-Hayyat, Jordan. Gray indicates walls while light-gray indicates large stones or other archaeological features. Higher densities are indicated by more densely gridded patterns and darker blue coloration.

By Phase 3, wheat density values exceed those of barley in several sectors, showing that the *Hordeum* to *Triticum* trend noted in Chapter 5 (see Figure 3.5) occurred across the site. Highest density was noted again in the east building, reaching a peak of roughly 16 seeds per liter. By Phase 2, wheat reached moderate densities of at least two seeds per liter throughout much of the site.

Though relatively minimal, wheat also holds a higher density than barley in the temple sectors for Phases 3 and 2. Though the peak of wheat density, with 16 seeds per liter in Phase 3, is much lower than the 56 seeds per liter that barley reached in Phase 4, the location makes a huge difference. In the same east building in Phase 3, barley reaches only one seed per liter. Between barley and wheat, the primary patterns are the high densities in domestic interior

sectors, with different buildings for different taxa, and the notable shift in the abundance over time, shifting from barley to wheat.

Tell el-Hayyat Architectural Sector Maps: Other Cultigens

The fruit cultigens, and lentil to an extent, each have a distinct spatial distribution that suggests different modes of deposition. Fig deposition most closely mirrors the pattern of wild taxa (see Figure 7.6) with its prominence in exterior sectors, particularly the temple exterior. Fig density is highest in the temple exterior contexts (Figure 7.10). In Phase 4, the temple interior and the east building each have high densities of fig. However, Phase 3 is when the taxa becomes most prominent, with a high density of remains recovered in and around the temple entrance. The temple forecourt has the highest density, reaching upwards of fourteen seeds per liter. By Phase 2, fig densities are spread more evenly across the site.

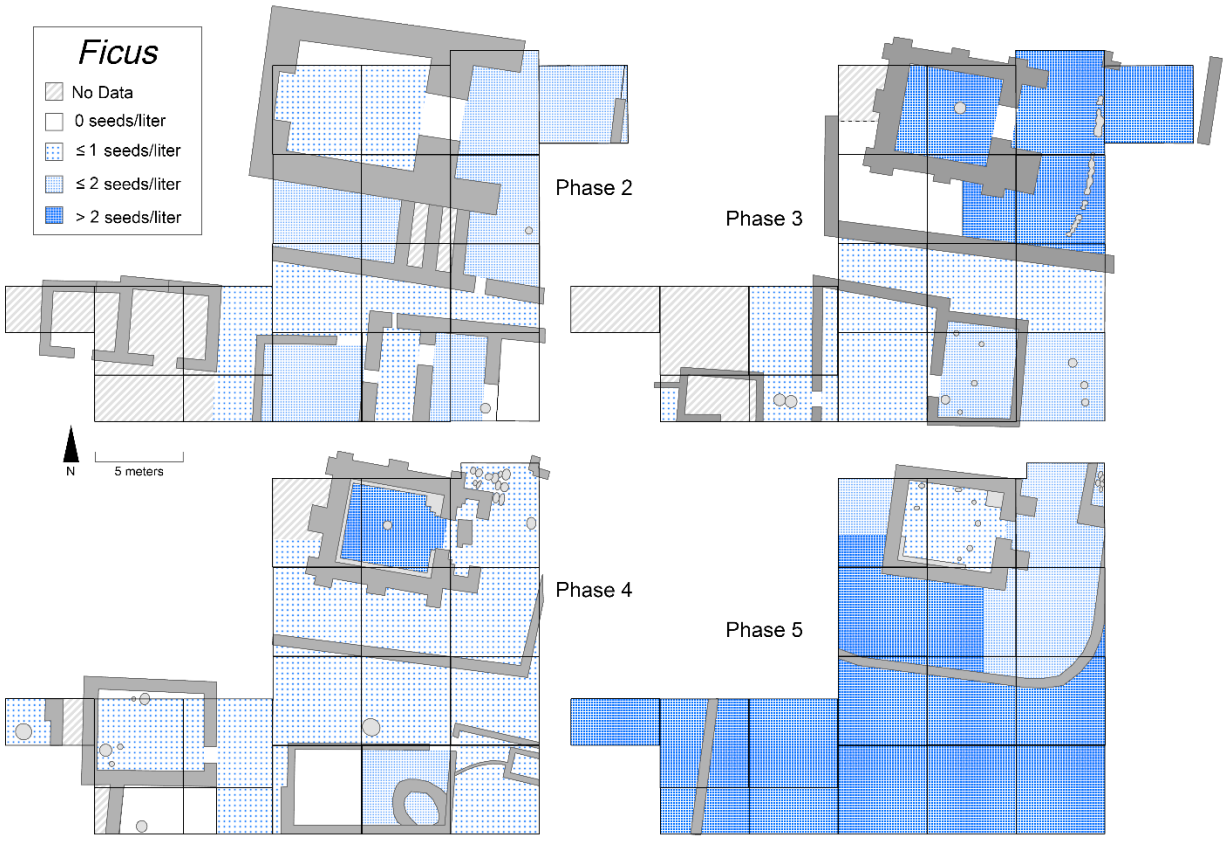

Figure 7.10 Fig (*Ficus carica)* densities (NISP count/liter) at Tell el-Hayyat, Jordan. Gray indicates walls while light-gray indicates large stones or other archaeological features. Higher densities are indicated by more densely gridded patterns and darker blue coloration.

Patterns of grape deposition show minimal appearance of the taxa in the remains from domestic interiors (Figure 7.11). Low, but similar densities of grape were recovered in each phase, with the highest densities recorded from temple interior or exterior contexts. In Phases 5 and 2 the taxa is more prominent in the temple exterior, but in Phases 4 and 3 is notably more common in temple interiors. Grape hits its highest density in Phase 3 in the temple interior, but reaches only a mere 0.6 seeds per liter, suggesting that the fruit was not very common.

Figure 7.11 Grape *(Vitis vinifera)* densities (NISP count/liter) at Tell el-Hayyat, Jordan. Gray indicates walls while light-gray indicates large stones or other archaeological features. Higher densities are indicated by more densely gridded patterns and darker blue coloration.

Olive deposition is similarly low at Hayyat, but distribution suggests a concentrated pattern, with remains being found in high densities in only a few sectors (Figure 7.12). In Phase 4, olive remains are densest in the central room, with the highest density of any taxon occurring here at around 125 seeds per liter. Olive was found in higher densities in a few other domestic sectors in Phases 4 and 3, with the highest densities in exterior sectors. In Phase 3, olive deposition was highest in the central alley, which is situated where the olive-rich central room was located in Phase 4. The density of olive remains is especially low in Phases 5 and 2, with only the domestic exterior alleyways and domestic exterior outer temple area containing olive remains. Temple contexts noticeably lacked olive throughout the occupation of Hayyat.

Figure 7.12 Olive (*Olea europaea)* densities (NISP count/liter) at Tell el-Hayyat, Jordan. Gray indicates walls while light-gray indicates large stones or other archaeological features. Higher densities are indicated by more densely gridded patterns and darker blue coloration.

The final taxa examined was lentil. This taxa was less frequent in the assemblage of carbonized remains from Hayyat. Unlike other pulses though, including the garden pea (*Pisum sativum*), lentil was found more frequently in domestic contexts, including domestic interiors. Lentil was more prominent in Phases 5 and 4 and fairly scarce by Phase 2. The taxa does display a pattern towards appearing in the temple exterior most frequently in Phases 5 and 3, with all temple sectors having high densities in Phase 5. However, in Phase 4 lentil reached its highest densities in two domestic sectors, with a maximum of three seeds per liter in the domestic interior central room sector.

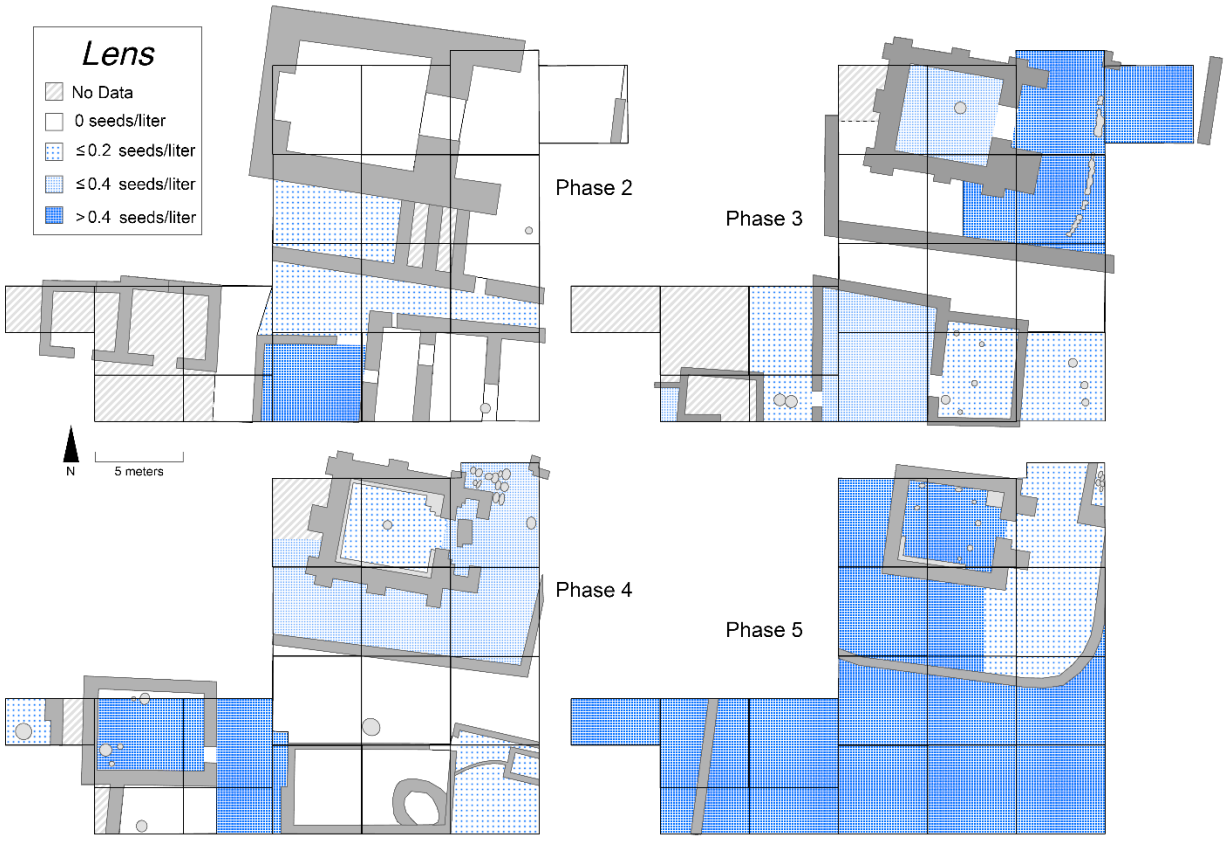

Figure 7.13 Lentil (*Lens culinaris)* densities (NISP count/liter) at Tell el-Hayyat, Jordan. Gray indicates walls while light-gray indicates large stones or other archaeological features. Higher densities are indicated by more densely gridded patterns and darker blue coloration.

Zahrat adh-Dhra‘ 1

Seed deposition frequencies at ZAD 1 show spatial patterns according to each cluster of structures, with the central cluster assemblage being most distinct. In general, ZAD 1 has low frequencies of cereal and chaff, fig, and small pulse cultigens amidst a plethora of wild taxa across the site (Figure 7.14).

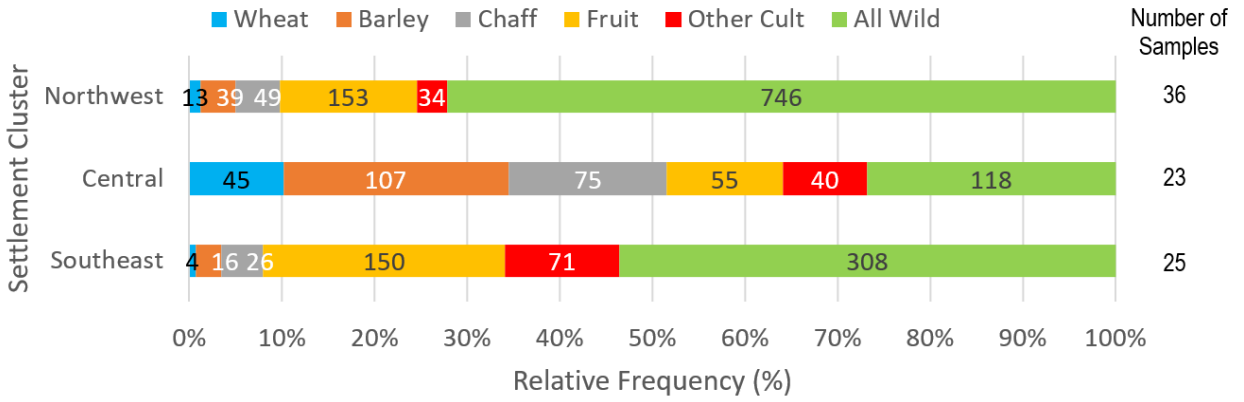

Figure 7.14 Relative frequencies of major cultivated and wild taxa by clusters of structures at Zahrat adh-Dhra‘ 1, Jordan (structure clusters based on Fall et al., 2019). Relative frequencies based on NISP are shown by numbers in the bars. The number of total samples in the Northwest, Central, and Southeast structural clusters are shown at the right.

The northwest cluster has the highest frequency of wild taxa, composed almost entirely of wild woody and herbaceous species, but both the northwest and southeast cluster have a large frequency of wild remains, comprising over 50% of their assemblages. In the central cluster cultivated cereals are most prominent, as is associated chaff. Barley is more abundant than wheat regardless of the location. The frequencies of fruits and other cultigens are fairly steady in all three clusters, but fig and grape do show a distinct pattern, with fig primarily found in the northwest and southeast clusters and grape in the central cluster.

Discussion

Interpretations of Spatial Categories from Tell Abu en-Ni‘aj

While it is likely that incorporation through dung is the primary method that all seeds are entering the site and becoming carbonized, the stark differences in the frequencies of remains by sector and loci type tells us that there is a pattern of where certain plants are more likely to be found. This suggests that processes other than livestock grazing and subsequent dung burning are noticeably impacting the carbonized seed assemblage.

At Tell Abu en-Ni‘aj, the spatial arrangement of cereals suggests that barley, in particular, is more often in domestic, fire-associate contexts, which may suggest a utilization by humans. Barley may be processed in domestic interiors or utilized for breadmaking. Chaff was likely being incorporated in the assemblage in a variety of pathways, including in dung cakes from animal diet, accidental or intentional burning by humans, or through incorporation into fired mudbricks as a binding agent in tempering mudbrick structures (Hillman, 1984).

The other curious pattern was the distribution of olive remains. Their deposition away from fire-associated loci suggests that olive *jift* was not being burned in fire pits, tabuns, or similar contexts as fuel. Olive was not as frequent at Ni‘aj as it was at Hayyat and it was likely consumed to some degree by animal livestock, so its incorporation here may be primarily through animal dung.

Spatial patterns at Ni‘aj were next examined to test various hypotheses of site function. To understand the purpose of a unique three-basin feature in Phase 3, analysis is conducted on carbonized seed deposition in Areas H, I, and J (see Figure 7.1). Results show high wild grass density and a complete absence of olive remains, suggesting this feature was not likely utilized for oil production. The quantity of grass remains around the three-basin feature may point to this area being co-opted for the cleaning of grain. Regarding the basin, the limited presence of grape remains could point to this structure being used for wine production, or it could have been a non-agricultural feature such as a settling basin for clay pottery.

Locus types and sector categories were further examined at Ni‘aj to explore why seed densities declined steadily through time. Sample frequencies suggest that the sampling strategy is not to blame for the density drop, as carbonized-seed-rich loci from early phases are also sampled in later phases. Phase 3 and 2 archaeology reveal a high quantity of pits, clay basins,

and other features that likely served as receptacles for domestic trash (Falconer and Fall, 2019), and many of these were sampled in this study. Since no relationship is found between taxonomic frequencies and locus types that could explain the density declining trend, it cannot be the case that the excavations of later phases did not properly include a variety of trash-prone loci. However, in lieu of other explanations for the decline in density, it is possible that dung and fired dung remains were less frequently deposited within the site in later phases, possibly being used for more intensified manuring of fields.

Interpretations of Spatial Categories from Tell el-Hayyat

The main interpretation of spatial patterns among sectors at Tell el-Hayyat points to the clear importance of cereals and fruits at the site. The discrepancy in cereal and chaff proportions between domestic and temple contexts, with high frequencies in both domestic interiors and exteriors, implicates cereal processing and consumption as a fundamental aspect in the lives of ancient people. Temple contexts at Hayyat show a distinct pattern with both temple interiors and exteriors having far more wild taxa. This was particularly true for temple exteriors, where high concentrations of wild taxa and low concentrations of cereal remains may represent fuel waste perhaps associated with food preparation. In distinction from Ni‘aj, which had higher concentrations of barley than wheat in fire-associated sediments and domestic interiors, Hayyat indicates that wheat remains are just as common in fire-associated contexts and more common than barley in domestic interiors. This suggests a shift in the primary cereal taxa from barleys at Ni‘aj to wheat at Hayyat, generally supporting the interpretations of the paleoethnobotanical analyses in Chapters 3 and 4.

The spatial distributions of olive, grape, and fig point to each taxon having its own potential importance at Hayyat. The heightened presence of olive in fire-associated contexts supports the idea of *jift* incorporation into dung fuel. Olive remains are primarily located in the domestic interiors, suggesting the possibility of household storage. It was likely used in oil production, with burned *jift* remains discarded in the alleyways or courtyards after use.

Grape and fig appear to have been used around the temple, possibly for ritualistic purposes in the temple, specifically for grape but also for fig. If grapes were stored or eaten around the temple, the residue could have been tossed into fires, fed to livestock, or packed into dung cakes for burning at the temple. Figs may have been utilized for communal feasting purposes such as might take place in the temple courtyard. Dry fruit offerings in the temple or accidental burning during feasting activities may be the most viable pathways for carbonization of figs aside from animal consumption. Given the ubiquity of figs, however, animal consumption likely played the largest role.

Spatial patterning may also be notable for the garden pea, *Pisum sativum*, which is found most frequently in fire-associated features and almost exclusively in domestic exteriors. Its presence here, particularly in the fire-associated features, could indicate preparation activities in the domestic exterior courtyards. Garden peas require drying and threshing in a similar manner to cereals (Jones, 1983; Fuller and Harvey, 2006), and the remnant plant fragments, containing some seeds, could have been used as an animal feed supplement or burned as fuel. Lentil and bitter vetch share a similar spatial pattern, but were not found dominantly in the fire-associated loci, so their presence may simply be from animal dung burning.

Of final note is the lack of chaff in structural remains at Hayyat. In Chapter 5, it was hypothesized that the lack of glumes could have been due to a preferentially incorporation of

late-stage crop-processing remains into mudbricks for tempering. However, chaff does not appear to be frequent in these locus types at Hayyat. Therefore, I turn to the secondary hypothesis that the increased frequency of rachis fragments at Hayyat is due to livestock preferentially feeding on threshing/winnowing by-products.

Interpretations Based on Architectural Sectors at Tell el-Hayyat

Tell el-Hayyat has the benefit of architecturally-defined sectors, which permitted visualization and analysis of deposition patterns specific to each architectural structure. Analyses of the grouped barley and wheat taxa show that each appeared frequently at Hayyat, but the genera are typically concentrated in different domestic buildings in each phase. Both occurred in high densities in the east building, which may indicate that this building was a primary location for crop processing, storage, food production, or a mixture of the three, but these practices may have been divided between the central room and east building. Though these sectors lie within the same larger building in some phases, separation of the cereals may make sense given that barley and wheat can require different crop-processing activities (Hillman, 1981; 1984; Jones, 1983; Postgate, 1984; Reddy, 1997). The heightened importance of the east building is supported by the presence of a circular, mudbrick-walled feature within Phase 4 that is hypothesized to be a storage basin (Falconer and Fall, 2019). High cereal frequency in the east courtyards could further support that this part of the settlement conducted cereal processing.

Cereal remains around Hayyat's temple could represent food that was brought for feasting, but likely represents waste incorporated in burnt dung remnants. This is supported by large amounts of cultivated cereal remains in the temple sidecourt in Phases 5 and 2. However, the abundance of wild seed remains in the temple forecourt do suggest that this location was used

for burning dung, so feasting may still have been conducted here. Fig was commonplace throughout the site but more frequent in the temple forecourt than any other sector. Fig deposition patterns may represent the remains of consumption by goats and sheep, but also suggest feasting practices.

The heightened presence of fig and grape in the temple interior may represent their use in ritualistic practices. Fruits and dried fruits could have been consumed or burned in the temple.

Olive was perhaps the most spatially segregated of the cultigens, only noted in a few sectors per phase. Production of oil does not require burning, but *jift* might have been burned in tabuns and tossed into trash pits or nearby alleyways after being burned, which would explain the high proportions of olive remains in domestic sectors and fire-associated features. A single room contained the vast majority of the olive remains from Hayyat, so it is possible that certain locations were treated as storage rooms for pre-processed olives and/or oil, with products distributed throughout the site.

In Phase 4, the concentration of olive was primarily in the central room. The fact that the central room did not exist in either Phase 5 or Phase 3 could explain the lack of olive in these phases, as storage would have had to happen elsewhere in the village and could have been in an unexcavated structure. The importance of olive at Hayyat is further indicated by the burning of the east building in Phase 3, indicated by charring and high quantities of olive wood charcoal (Falconer and Fall, 2006). Olive wood harvesting further indicates the local importance of this taxon.

A conceptual figure of generalized site use patterns for Tell el-Hayyat, as inferred from the combined analyses of spatial categories and architectural sectors is shown in Figure 7.15.

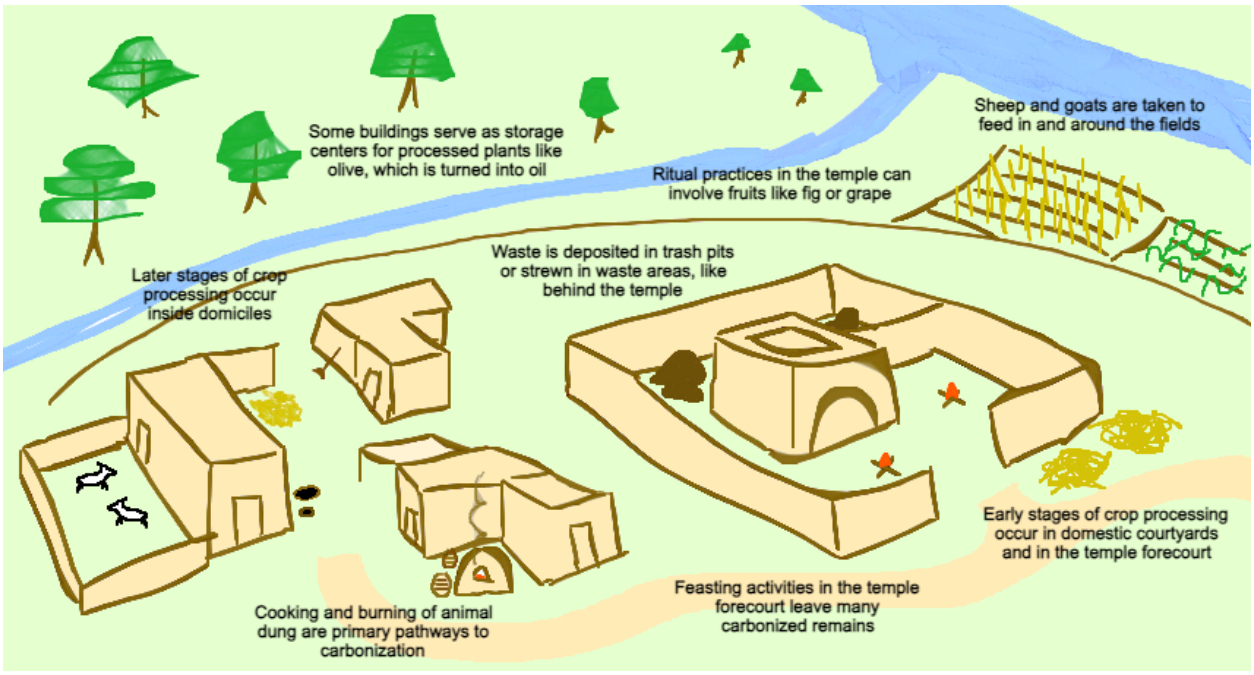

Figure 7.15 A conceptual figure of Tell el-Hayyat showing where plants may have been cultivated, processed, and deposited.

Spatial Interpretations from Zahrat adh-Dhra' 1

Structural clusters reveal spatial distinctions in the floral assemblages of Zahrat adh-Dhra' 1. Structures in the central cluster are the most distinct, having the highest concentrations of cultivated cereal and chaff taxa. In particular, Structure 40 in the central cluster has the highest deposition of cereal remains, giving it a distinct macrofossil assemblage in comparison to the remainder of the site. In the central cluster there are several cultigens that stand out as having a higher frequency here than in the northwestern and southeastern clusters. This could be interpreted as the central cluster of structures being used for agriculturally-focused activities. However, cultivated fig and legume cultigens are found in similar proportions throughout the site, with the highest densities appearing in the southeast cluster.

The central structures, offset from the structure clusters on either end of the site, held the largest amounts of naked cereals and grapes, which require more intense management due to

their water requirements. Considering the location of the site, a strip of land atwix two intermittent wadis, the positioning of the cereal-rich buildings, and the environment of Middle Bronze I-II along the Dead Sea Plain, discussed further in Chapter 7, a possible interpretation is that the structures in the central cluster were acting as a centralized location for crop processing, storage, or cooking. This would indicate that the inhabitants of ZAD 1 may have allocated different structures for distinct purposes as part of community management of agriculture. This also corresponds with indications of faunal remains, which were found predominantly in structures in the northwest and southeast clusters, rather than the central structures (Fall et al., 2019). Together, these patterns suggest aspects of social and agricultural cooperation among the inhabitants of ZAD 1.

Summary

The distinctions in the spatial patterns of certain crops help to highlight which crops were particularly important for ancient farmers. At Tell Abu en-Ni‘aj, Tell el-Hayyat, and Zahrat adh-Dhra‘ 1 the cereals, chaff, fruit, and oil crops each show notable distinctions in their patterning. Spatial distributions from Ni‘aj and Hayyat highlight the relative importance of wheat and barley, *Triticum* and *Hordeum*. The densities and spatial patterns of deposition in domestic interior and exterior contexts associated with burning and other anthropogenic activity suggests the importance of cereals as foodstuffs. Shifting distributions of wheat and barley between both structures and phases points to an organization of food production and storage which evolved through time towards increased wheat cultivation and utilization sitewide at Hayyat. This accords with interpretations from paleoethnobotanical analysis that barley was particularly important for ancient people in EB IV and wheat in MBA.

Spatial patterns at Hayyat reinforce the interpretations from the sector classification results, emphasizing a difference in the use of cultivated cereal, fruit, and oil plants. Distinctions in the location of wheat, barley, and chaff show how certain taxa were more likely to be processed, stored, or consumed in certain rooms or structures. Among the fruits, olive distribution suggests storage and potentially the use of *jift* as fuel; grape suggests use in ritual practices, winemaking, or simply as valuable foodstuff; while fig suggests potential use in ritual practice or feasting and incorporation through animal consumption and dung burning. These patterns reflect the integrated use of internal and external spaces surrounding building units for food production and disposal, and the use of specified locations for further processing, storage, feasting, and other activities. The presence of centralized storage locations is particularly evident with the central room at Hayyat and Structure 40 at ZAD 1. Centralized storage, noted in olive at Hayyat and the cereals and grape at ZAD 1, emphasize the importance of these cultigens and may hint at a higher level of community integration in these two Middle Bronze Age communities.

CHAPTER 8: COMPARATIVE CLIMATE ASSESSMENT FROM ARCHAEOLOGICAL SHELLS

Introduction

This chapter investigates the microclimate in the northern Jordan Valley during the occupations of Tell Abu en-Ni‘aj and Tell el-Hayyat roughly 4500-3700 years ago. Regional climate models have provided temperature and precipitation estimates during this time (Bryson and DeWall, 2007; Arikan, 2015; Soto-Berelov et al., 2015; Guiot and Kaniewski, 2015; Fall et al., 2018; Ön et al, 2023), but a high-resolution, localized paleoclimate record would be invaluable for interpreting temperature and precipitation changes and would allow comparison with the stable isotope analysis of carbonized seeds from my archaeological sites (Chapter 10).

Thus, this chapter presents an important step in the interpretation of the climatic and environmental stresses felt by ancient farmers in the Jordan Rift. My intent was to test the hypothesis that there was a climate shift between the Early and Middle Bronze Ages that accords with vegetation shifts around the end of the fifth millennium BP (Hunt, 2004; Langgut et al., 2013; 2015; Schiebel and Litt, 2018). Around this time, modelled paleoclimate suggests higher precipitation and lower temperatures (Arikan, 2015; Soto-Berelov et al., 2015; Ön et al, 2023). Archaeological shells were used as a secondary proxy of local climate conditions in the northern Jordan Valley to study local climate by examining shifts in paleoprecipitation between EB IV Tell Abu en-Ni‘aj and MB I-II Tell el-Hayyat.

The overall signal shows distinct differences in water availability, suggesting potentially wetter conditions in the middle bronze, particularly Middle Bronze II, over Early Bronze IV. This chapter also presents the data in the modern regional environment, discussing the potential implications of this for interpreting paleoprecipitation.

Background of Shell $\delta^{18}O$

The species studied for this chapter is the freshwater gastropod *Melanopsis buccinoidea.* *Melanopsis* snails typically live for around five years to a decade at most, and their largest whorl results from about a year of growth (Elkarmi and Ismail, 2006; Geary et al., 2012; Zaarur et al., 2016). These organisms acquire isotopes of carbon and oxygen from the water they live in and the algae they consume and use them in the production of calcium carbonate ($CaCO_3$), which is continually secreted along the aperture of their shell. Stable isotopes of oxygen and carbon from freshwater mollusks can be useful proxies for the environment based on the incorporation of calcium carbonate into their shell matrices. The values of $\delta^{18}O$ from a shell matrix generally reflect the $\delta^{18}O$ signature for the water source from which they are collected (McConnaughey and Gillikin, 2008; Scholl-Barna, 2011; Pfister et al., 2019). For riverine species, factors such as the amount and source of precipitation, evaporation, river discharge and salinity may play the largest roles in determining $\delta^{18}O$ (Dansgaard, 1964; Latal et al., 2004; Leng and Lewis, 2016; Sharp, 2017). The fractionation for $\delta^{18}O$ is influenced by evaporation and precipitation, whereby the lighter isotopes of ^{16}O preferentially evaporate from rivers, and the heavier isotopes of ^{18}O preferentially precipitate into them.

In the Transjordan, winter precipitation is relatively enriched in ^{16}O when it arrives and when the groundwater emerges from springs (Gat and Dansgaard, 1972; Gat et al., 2005), with lakes and distal rivers more enriched in ^{18}O (Gat and Dansgaard, 1972; Gat et al., 2005; Hillel et al., 2019). Warmer temperatures in the spring and summer lead to increased evaporation of ^{16}O and increased concentrations of ^{18}O (Marshall et al., 2007: 42; Prendergast and Stevens, 2014; Leng and Lewis, 2016). Winter precipitation, high elevation groundwater springs, and spring snowmelt at higher latitudes recharge ^{16}O. The simple interpretation of this system is that as

precipitation increases in the winter, $\delta^{18}O$ values decrease, becoming more negative, since water molecules with a higher proportion of ^{16}O enter the system. As winter precipitation declines, evaporation increases, river discharge falls in the spring and summer, and values of $\delta^{18}O$, reflective of the changes in precipitation and evaporation, increase.

A typical oxygen profile from freshwater shells may show a sinusoidal annual profile that accords with the expected variation of $\delta^{18}O$ in a freshwater stream of the Jordan Valley. The lowest $\delta^{18}O$ values would occur in months with high rainfall as ^{18}O is recharged in streams, while dry months would have increased evaporation of ^{16}O and thus higher $\delta^{18}O$ values. Shells can also stop producing shells in unfavorable conditions, which in this case could include times of low precipitation and high temperatures during summer. When an organism stops producing shell, there will be a resulting gap in the stable isotopic record from that period of time (Dettman and Lohmann, 1993). The end result of these factors should be a parabolic, rather than sinusoidal pattern for $\delta^{18}O$, with peaks of high $\delta^{18}O$ indicating summer growth cessation and u-shaped trends of $\delta^{18}O$ indicating increased winter precipitation. Figure 8.1 shows an example of what an expected profile might resemble for $\delta^{18}O$ from a freshwater snail in the Jordan Valley.

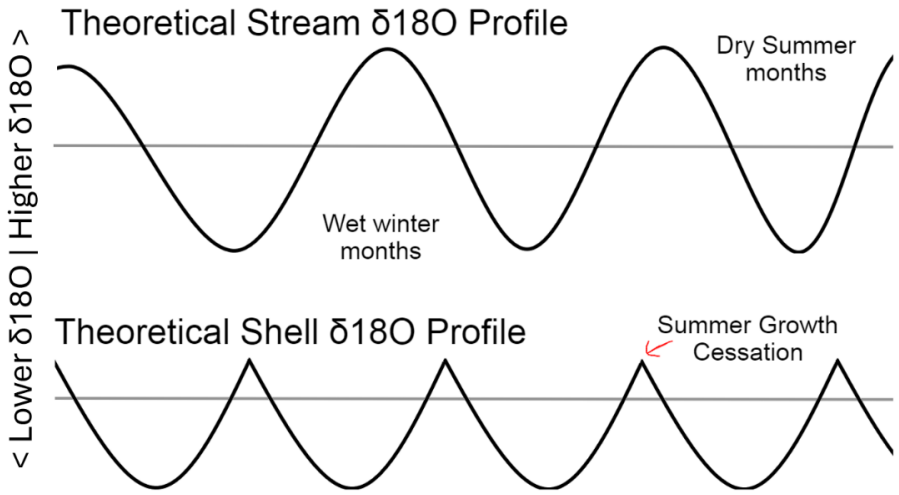

Figure 8.1 Theoretical $\delta^{18}O$ profiles for Jordan Valley stream and *Melanopsis buccinoidea* shell values showing variability between seasons and the effect of cessation in summer growth.

Interpretation of $\delta^{13}C$ is complicated by the potential influences of vital effects, as metabolic processes of freshwater gastropods can alter a shell's $\delta^{13}C$ value. Most variation reflects changes in the $\delta^{13}C$ of dissolved inorganic carbon (DIC) (McConnaughey and Gillikin, 2008; Roach et al., 2016; Zaarur et al., 2016). DIC is impacted by a number of factors, including the $\delta^{13}C$ content from soil and nutrients, local geology and groundwater, and atmospheric CO_2 (Cole and Prairie, 2009). However, values of $\delta^{13}C$ in shells also reflect the hydrological environment, and can be influenced by factors including river discharge, stream order, pCO_2, alkalinity, diet, and plant productivity (Aucour et al., 2003; Roach et al., 2016). Based on these factors, comparative analysis of $\delta^{13}C$ values from terrestrial shells may be used to infer changes in their local environment over time. The use of shell $\delta^{18}O$ and $\delta^{13}C$ in conjunction will be used to provide critical information on the hydrologic environment.

Field and Laboratory Methods

Archaeological Shell Selection and Sampling Methodology

Archaeological shells were recovered from hand-sieved sediments at both Tell Abu en-Ni'aj and Tell el-Hayyat during excavation. Each shells was collected and labelled with its excavation context number, consisting of an area, locus, and bag identification that correlate with the excavation units from Chapter 2. Sorting and taxonomic identification to the genus level was conducted by Dr. David Reese and further identified to species level as part of this dissertation based on a variety of sources (Moshkovitz and Magaritz, 1987; Glaubrecht, 1993; Heller et al., 2005).

Shell analysis focused on stable isotopic sampling of the freshwater gastropod *Melanopsis buccinoidea* in order to assess paleoclimate. Shells of this taxon exhibit indications

of burning, few signs of use for ornamentation, and appear at the sites in higher numbers than other shell taxon, all suggesting potential use as a supplementary foodstuff (Bobrowsky, 1984; Bar-Yosef and Heller, 1987). *Melanopsis* is an aquatic, algae-consuming snail species found in the tributaries of the Jordan River in shallow areas of clear, flowing, freshwater (Glaubrecht, 1993; Heller et al., 2005; Bandel et al., 2007; Lev et al., 2007; Amr et al., 2014; Alhejoj et al., 2017). The environment for these shells in past is assumed to be upper springs feeding the Wadi el-Yabis or along the northern Jordan River, which would have been less saline in past.

I selected a total of seven shells, relatively dated to be from three phases at Ni‘aj and four phases at Hayyat, to provide a temporal sequence (Table 8.1). The shell specimens chosen for analysis contain the highest number of growth bands and bore no signs of charring or human marking. Growth banding refers to dark patterning on the exterior of the shell that potentially correlates with timing of growth cessation in gastropod shells, correlated with environmental stress.

Table 8.1 Phases and excavation contexts for freshwater *Melanopsis buccinoidea* shells analyzed for $\delta^{18}O$ and $\delta^{13}C$ from Tell Abu en-Ni‘aj and Tell el-Hayyat, Jordan.

Archaeological Site	**Phase**	**Context**
Tell el-Hayyat	2	Q.40.103
	3	P.98.132
	4	G.78.280
	5	J.79.315
Tell Abu en-Ni‘aj	2	L.17.118
	3	O.26.92
	4	H.31.186

A preliminary sclerochronological analysis was conducted using visible annual growth bands to determine what segments of the shell may correspond to annual periods of growth (following Deith, 1983; Schöne, 2005). Results indicate good preservation of annual growth banding on all

selected shells along the largest whorls. The only shell with banding covering less than a full year was the sample from Phase 5 at Hayyat, which had a particularly large distance between its last two bands. X-ray diffraction analysis was also conducted on a representative shell from each site to verify preservation of the original shell aragonite, with results indicating no diagenesis (Figure A15).

All *Melanopsis* shells were precleaned in a distilled-water ultrasonicated bath, rinsed with ethanol to remove modern contaminants and any exterior labelling, and desiccated for 24 hours following standard procedures (Hallmann et al., 2009; Burchell et al., 2018). Each shell was sampled along the exterior of the shell coil following exterior, sub-annual banding patterns, visible under microscope, which span roughly 0.15 to 0.25 mm per band. Samples were powderized by hand using a 0.5 mm Dremel, with samples taken every 1 mm following the contours of sub-annual growth bands. Sampling lines were drilled starting at the aperture moving towards the apex in order to capture the latest year(s) of growth (Figure 8.2). Powderized samples of 100 μg or more were collected in aluminum foil and weighed on an analytical balance. Twenty samples were taken per shell to provide information on sub-annual variation in precipitation. Shell powder was then vaporized and processed via GasBench-IRMS to measure shell $\delta^{18}O$ and $\delta^{13}C$. Figure 8.3 illustrates shell terminology and sub-annual band sampling.

Figure 8.2 *Melanopsis buccinoidea* shells from Tell Abu en-Ni‘aj and Tell el-Hayyat, Jordan with Dremel marks (vertical lines on each shell) indicating locations of sampling. Dremel marks are curved to match the curvature of the sub-seasonal growth bands. Shells are arranged chronologically at each site, left to right, from earliest to most recent.

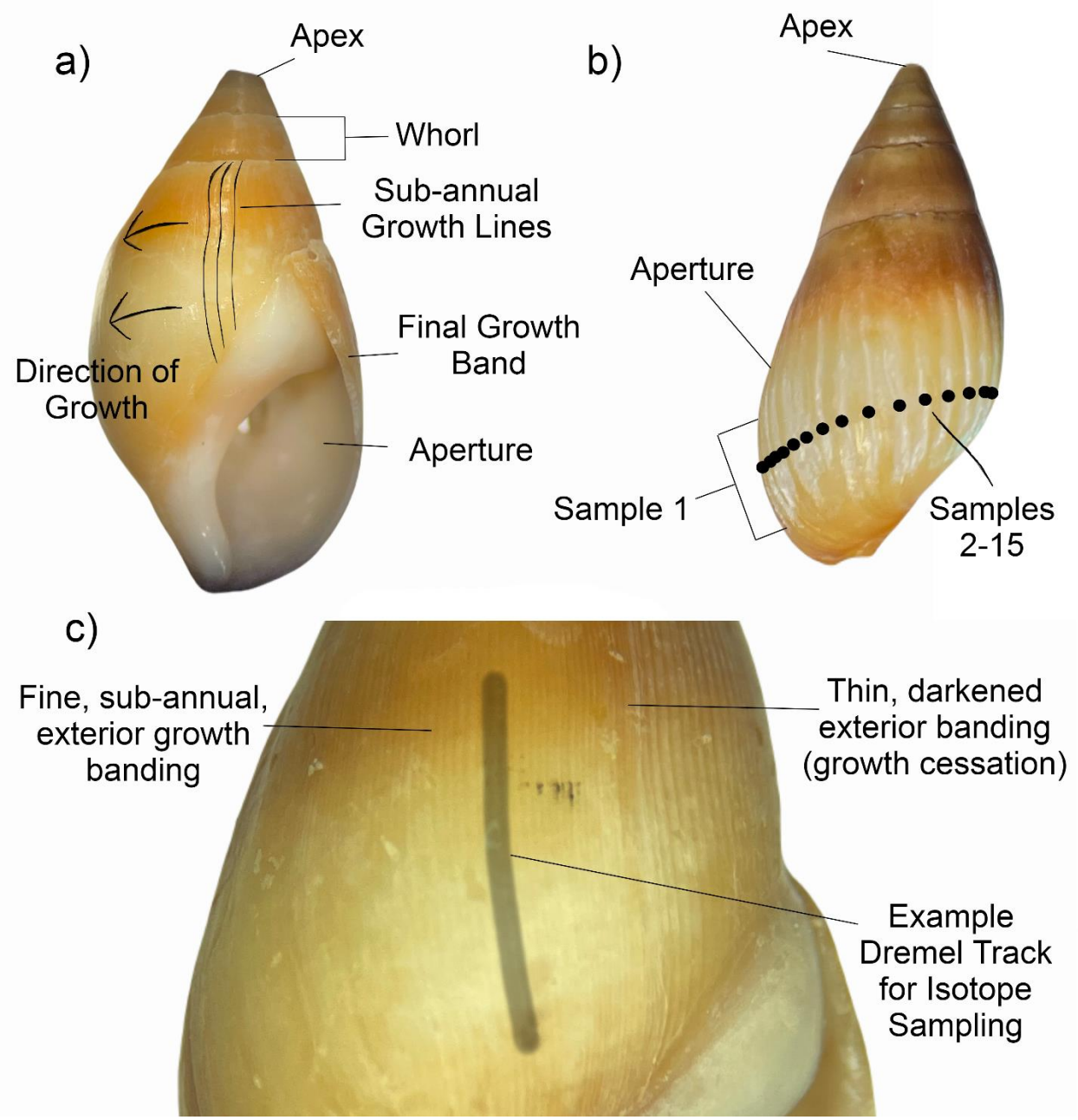

Figure 8.3 *Melanopsis buccinoidea* shells with morphological terminology, showing locations of sampling and the relationship between samples, bands of growth cessation, and exterior sub-annual banding.

Archaeological Shell Stable Isotope Analysis

Several regional studies have illustrated the validity using stable oxygen isotope values to infer paleoclimatic conditions in the Near East (Fastovsky et al., 1993; McConnaughey and

Gillikin, 2008; Spiro et al., 2009; Çakirlar and Şeşen, 2013; Leng and Lewis, 2016; Lewis et al., 2017). The reason is that the biogenic aragonite in shell matrices from many freshwater Mollusca have been demonstrated to fractionate oxygen in equilibrium with oxygen values in water (Grossman and Ku, 1986; Gordillo et al., 2014: 68; Kelemen et al., 2017). Past studies illustrate the potential of *Melanopsis buccinoidea* for paleoclimatic interpretation (Moshkovitz and Margaritz, 1987; Zaarur et al., 2016; Rice, 2023). However, this species may have a slight offset from isotopic equilibrium. Although none else have used this offset yet for fossil *Melanopsis buccinoidea*, Zaarur et al. (2016) studied modern specimens in the Hula Valley and found that this species may have a roughly -1.2‰ offset to $\delta^{18}O$ resulting from vital effects. An adjustment of +1.2‰ was thus applied in accordance with this finding (Zaarur et al., 2016).

Stable oxygen isotope values were measured according to the ratio of ^{18}O:^{16}O relative to the modern reference Vienna Standard Mean Ocean Water (VSMOW) and expressed using the (δ) notation. Carbon isotopes from shells are typically expressed as the ratio of ^{13}C:^{12}C compared to VSMOW. Both ratios are expressed as parts per thousand (‰) (Boutton, 1991b; Ehleringer, 1991). The equations for determining oxygen and carbon stable isotope values are shown below.

$$\delta^{18}O = \left(\frac{18O \text{ sample}/16O \text{ sample}}{18O \text{ standard}/ 16O \text{ standard}} - 1\right) * 1000 + 1.2 \quad (2)$$

$$\delta^{13}C = \left(\frac{13C \text{ sample}/12C \text{ sample}}{13C \text{ standard}/ 12C \text{ standard}} - 1\right) * 1000 \quad (3)$$

Stable oxygen and carbon values were compared along the full, 20-sample profile of each shell, then analyzed in-depth using just the data from its largest annual band, identified using exterior bands and the stable isotope results, to standardize the method of comparison. An annual band is an estimated one-year period of growth between visible shell growth bands. The isotope values were then statistically compared between phases and between sites using simple two-way *t*-tests and one-way ANOVA. Time-series analysis is used to visually interpret $\delta^{18}O$ and $\delta^{13}C$

trends as indicators of temporal change. A biplot and boxplot of site means and medians for oxygen and carbon values is compared to modern regional stream and precipitation values to infer differences between ancient and modern environments and climate regimes.

Modern Water Stable Isotope Sampling

Stable isotopic analysis results for modern samples of *Melanopsis buccinoidea* are not available from the Jordan Valley, so values of modern water were used for comparison. Modern groundwater spring, stream, and precipitation samples were collected along the Jordan Rift and the Transjordanian foothills and highlands in 2017 and in 2023 as part of an ongoing study of Mediterranean stable isotopes under the direction of Drs. Elizabeth Ridder, Suzanne Pilaar Birch, Patricia Fall, and Steven Falconer. At UGA and the University of Utah, modern water samples were filtered for contaminants and sampled using a Picarro Cavity Ring-Down Spectrometer (CRDS) to determine $\delta^{18}O$ values. Comparative point data for stream water isotopes were selected from Farber et al. (2004) and from waterisotopes.org (Waterisotopes Database, 2017). Comparative raster data show $\delta^{18}O$ values from precipitation (Bowen et al., 2005; Waterisotopes Database, 2017).

Results of $\delta^{18}O$ and $\delta^{13}C$ from Archaeological Shells

Tell Abu en-Ni'aj

Three shells were sampled from Tell Abu en-Ni'aj. The values of $\delta^{18}O$ and $\delta^{13}C$ from 20 sequential samples along each shell are plotted in Figure 8.4-8.6 for shells from Phase 4 through 2, respectively (Table A3). Each shell offers a single-year snapshot of riverine $\delta^{18}O$ values. Seasonal variability is noted in the seasonal profiles between shells.

The Phase 4 shell shows the most variation, with a u-shaped trend in $\delta^{18}O$ values that is possibly indicative of winter precipitation (around samples 15-12) followed by summer drying and growth cessation (samples 9-5; Figure 8.4). The curve indicates potential growth cessation at the sample 5-4 boundary. Oxygen values have a range of around 2‰, with a minimum value around -5.5‰. The pattern of $\delta^{13}C$ values is partially consistent with that of $\delta^{18}O$ from roughly samples 10-1.

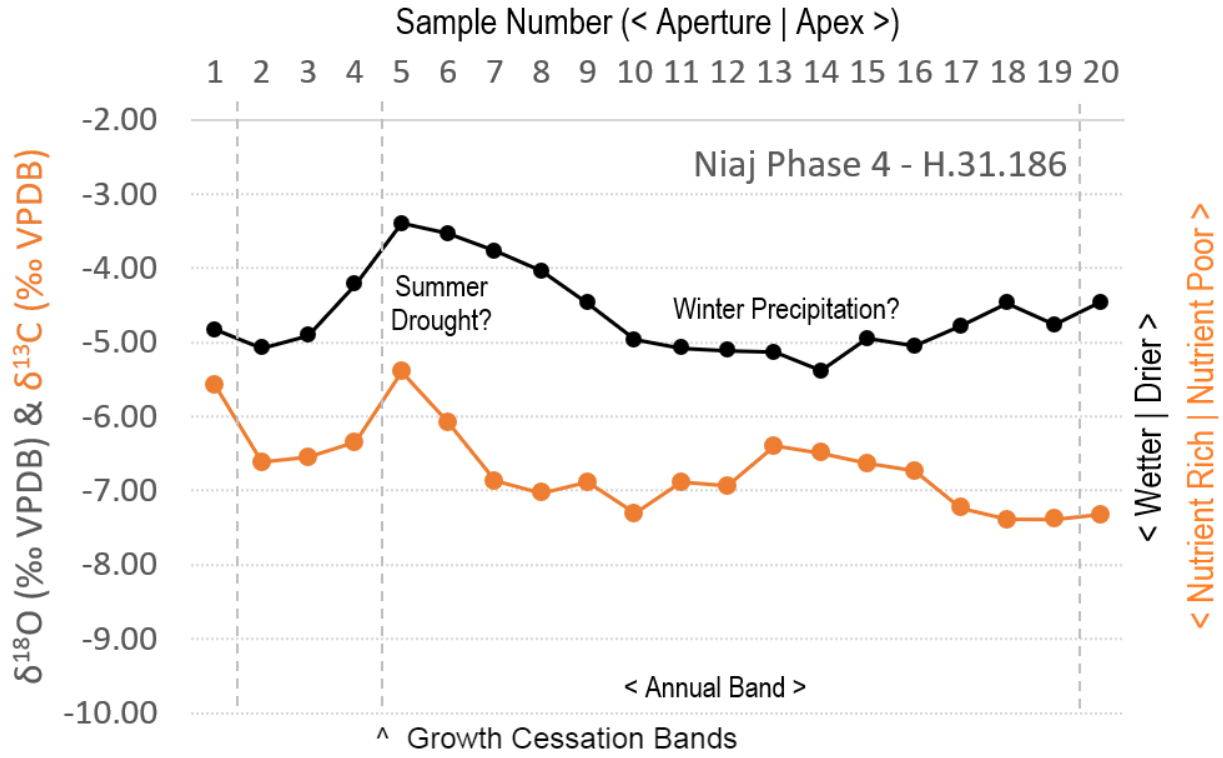

Figure 8.4 Values of $\delta^{18}O$ (black) and $\delta^{13}C$ (orange) from the shell of *Melanopsis buccinoidea* recovered from Tell Abu en-Ni'aj, Jordan Phase 4. Sample numbers are listed at the top with 1 starting at the shell aperture. Time runs from sample 20 to 1, with sample 1 roughly representing the organism's demise. Bands of growth cessation are noted with vertical dashed lines.

The Phase 3 shell shows an interesting trend indicated by the generally flat shape of the annual profile (Figure 8.5). The Phase 3 shell shows no notable variation in $\delta^{18}O$ throughout its annual band, indicated by exterior growth bands between samples 18-17 and samples 4-3. The

$\delta^{13}C$ value mimics this pattern, with both carbon and oxygen suggesting little change occurred during this yearly interval.

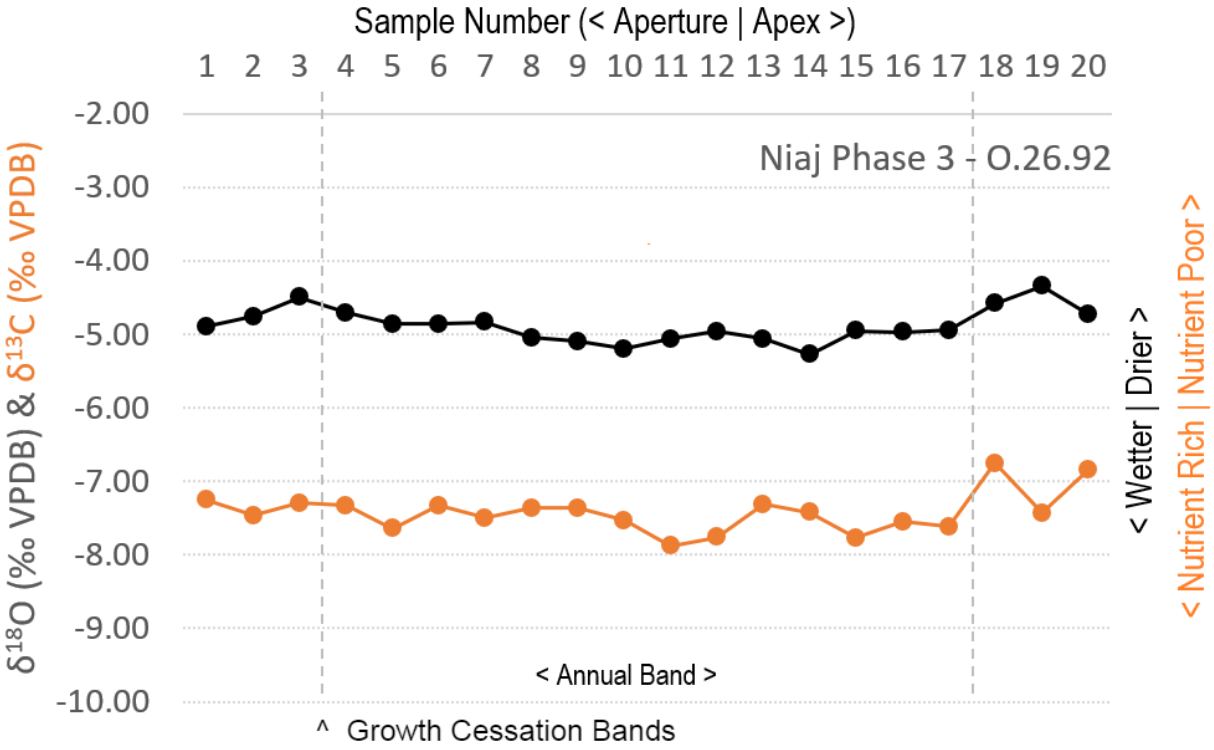

Figure 8.5 Values of $\delta^{18}O$ (black) and $\delta^{13}C$ (orange) from the shell of *Melanopsis buccinoidea* recovered from Tell Abu en-Ni'aj, Jordan Phase 3. Sample numbers are listed at the top with 1 starting at the shell aperture. Time runs from sample 20 to 1, with sample 1 roughly representing the organism's demise. Bands of growth cessation are noted with vertical dashed lines.

In Phase 2, the shell shows a rapid increase in both ^{18}O and ^{13}C at the final band, and between samples 10-3 the two isotope trends followed a u-shaped pattern with peaks at the seasonal growth bands, more visible in the $\delta^{13}C$ profile (Figure 8.6). Trends between $\delta^{18}O$ and $\delta^{13}C$ did not correlate well, with $\delta^{13}C$ fluctuating more between samples 20-11 and $\delta^{18}O$ fluctuating in the designated annual profile between samples 10-3. The $\delta^{18}O$ values did not reach the same minimum of -5.5‰ as for shells in Phases 4 and 3, but the profile was shorter and exhibited more variance than others. The variance of $\delta^{18}O$ was also much higher in Phase 2, around 3‰, due to a peak at the end of the profile around samples 3-1 that nears 2‰.

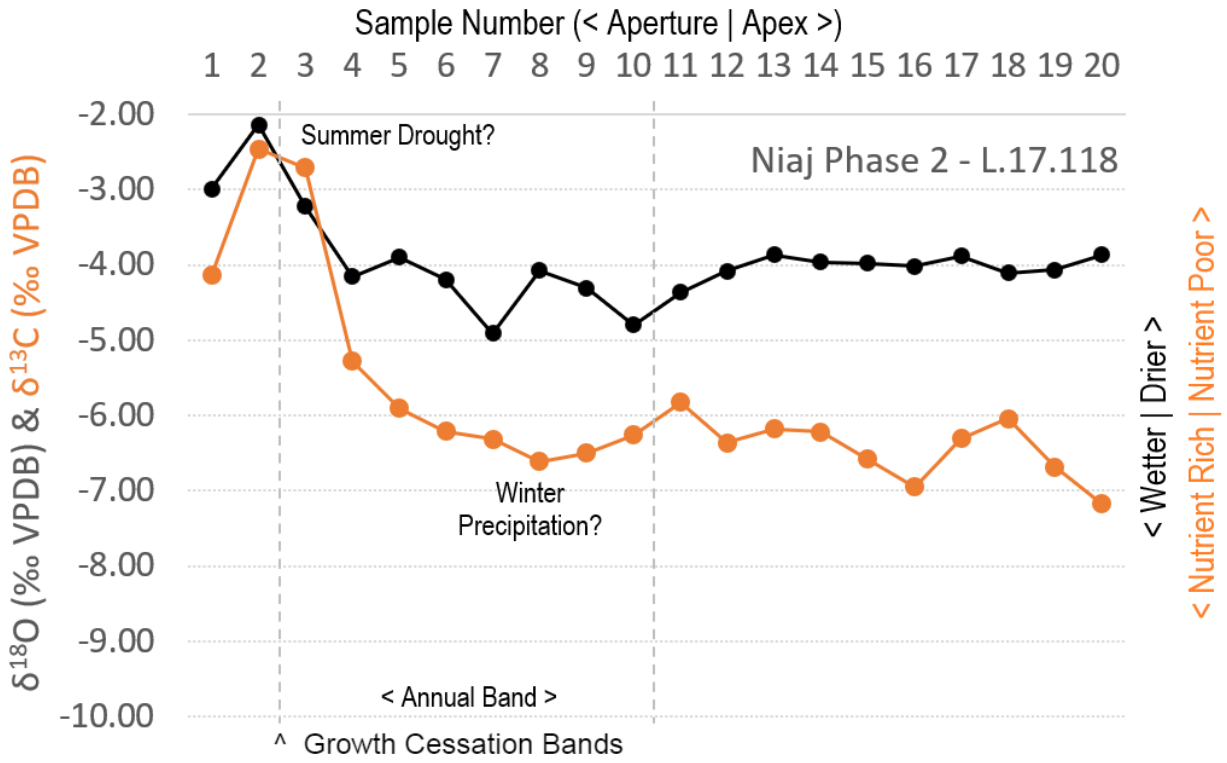

Figure 8.6 Values of $\delta^{18}O$ (black) and $\delta^{13}C$ (orange) from the shell of *Melanopsis buccinoidea* recovered from Tell Abu en-Ni'aj, Jordan Phase 2. Sample numbers are listed at the top with 1 starting at the shell aperture. Time runs from sample 20 to 1, with sample 1 roughly representing the organism's demise. Bands of growth cessation are noted with vertical dashed lines.

The shells from Tell Abu en-Ni'aj show some correlation between oxygen and carbon stable isotope trends, but this was not consistent. The mean values from the full, 20-sample profile for shells from each phase are significantly distinct for both $\delta^{18}O$ and $\delta^{13}C$ values using single-factor ANOVAs ($p < 0.001$). Values for each of the three shells indicate a minimum winter $\delta^{18}O$ value of around -5.5‰. The variation in $\delta^{13}C$ in all three shells mimics the variation in $\delta^{18}O$, with a range of up to around 2-3‰ in a profile.

Tell el-Hayyat

Four shells were sampled from Tell el-Hayyat, with values of $\delta^{18}O$ and $\delta^{13}C$ plotted in Figures 8.7-8.10 (Table A4). Values of $\delta^{18}O$ from Hayyat again show low variation throughout the annual profiles of several shells, with lightly u-shaped profiles in Phases 5, 3, and 2.

The Phase 5 shell reaches lower $\delta^{18}O$ values than from Ni'aj, with a maximum of around -5.75‰ (Figure 8.7). Its annual profile is depicted between samples 20-3. The profile may roughly suggest a u-shaped pattern towards the end. Close proximity of the banding between samples 3-2 and 2-1 very likely indicates intra-annual cessation either at the start or end of an annual band, which is further supported by the relatively high $\delta^{18}O$ value from sample 2. The

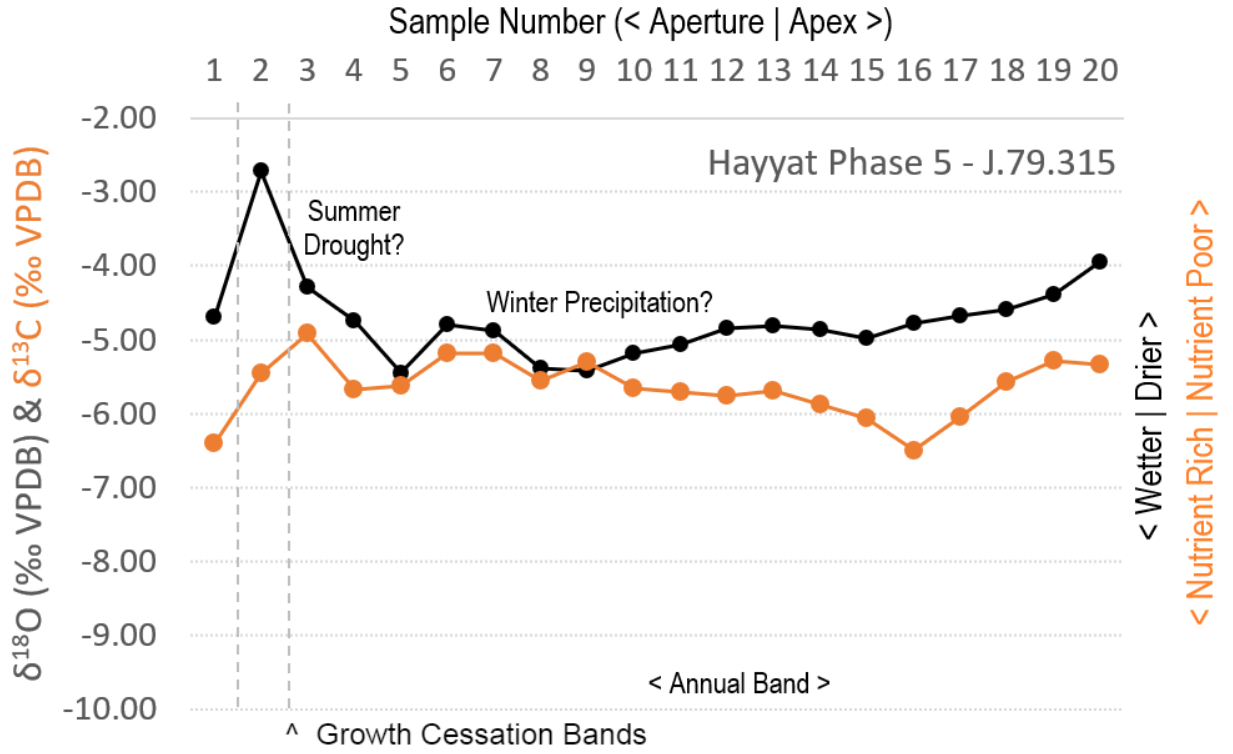

Figure 8.7 Values of $\delta^{18}O$ (black) and $\delta^{13}C$ (orange) from the shell of *Melanopsis buccinoidea* recovered from Tell el-Hayyat, Jordan Phase 5. Sample numbers are listed at the top with 1 starting at the shell aperture. Time runs from sample 20 to 1, with sample 1 roughly representing the organism's demise. Bands of growth cessation are noted with vertical dashed lines.

$\delta^{13}C$ values from this shell show a similar pattern to values of $\delta^{18}O$, but the profile has an inverse slope at some periods, such as around samples 12-9.

The Phase 4 shell has a steady profile akin to that from Phase 3 at Ni'aj. Relatively little variance occurs in the entire profile, around 1‰ (Figure 8.8). This shell has the highest minimum values at around -4.5‰, indicating that more ^{18}O was than present during the winter than in the other Hayyat shells. The $\delta^{13}C$ profile matches the steady slope of the $\delta^{18}O$ profile, but was significantly lower than that of other $\delta^{13}C$ profiles at Hayyat, ($p < 0.001$), at around -9‰ or 5‰ lower. These values are unlikely to be erroneous as standards were processed three times during the measurement period.

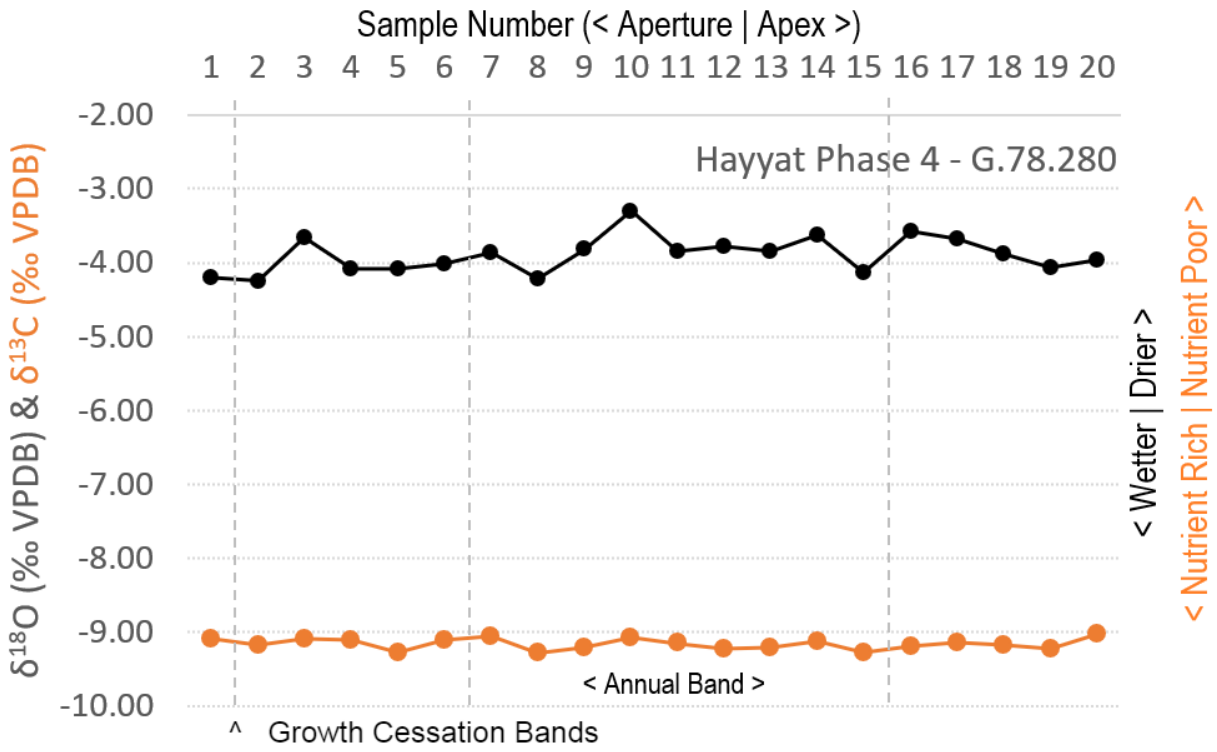

Figure 8.8 Values of $\delta^{18}O$ (black) and $\delta^{13}C$ (orange) from the shell of *Melanopsis buccinoidea* recovered from Tell el-Hayyat, Jordan Phase 4. Sample numbers are listed at the top with 1 starting at the shell aperture. Time runs from sample 20 to 1, with sample 1 roughly representing the organism's demise. Bands of growth cessation are noted with vertical dashed lines.

The $\delta^{18}O$ profile for Phase 3 exhibits a deep u-shaped annual profile between samples 16-7 (Figure 8.9). Values reach the lowest $\delta^{18}O$ of around -6‰ around samples 14-10 and also appear to show a similar trend in the previous and next seasons, around samples 20 and 2. The $\delta^{13}C$ trends roughly match the slope of $\delta^{18}O$ between samples 20-7, but between samples 6-1 were highly distinct, with $\delta^{13}C$ values fluctuating more than 3‰ and sloping rapidly upwards. The sharp contrast seems to correlate with multiple darker bands on the outside of the shell and may indicate multiple periods of intra-annual growth cessation. This portion of the shell may suggest either drier conditions or disturbance to the mollusk (Hallmann et al., 2009; Andrus, 2011).

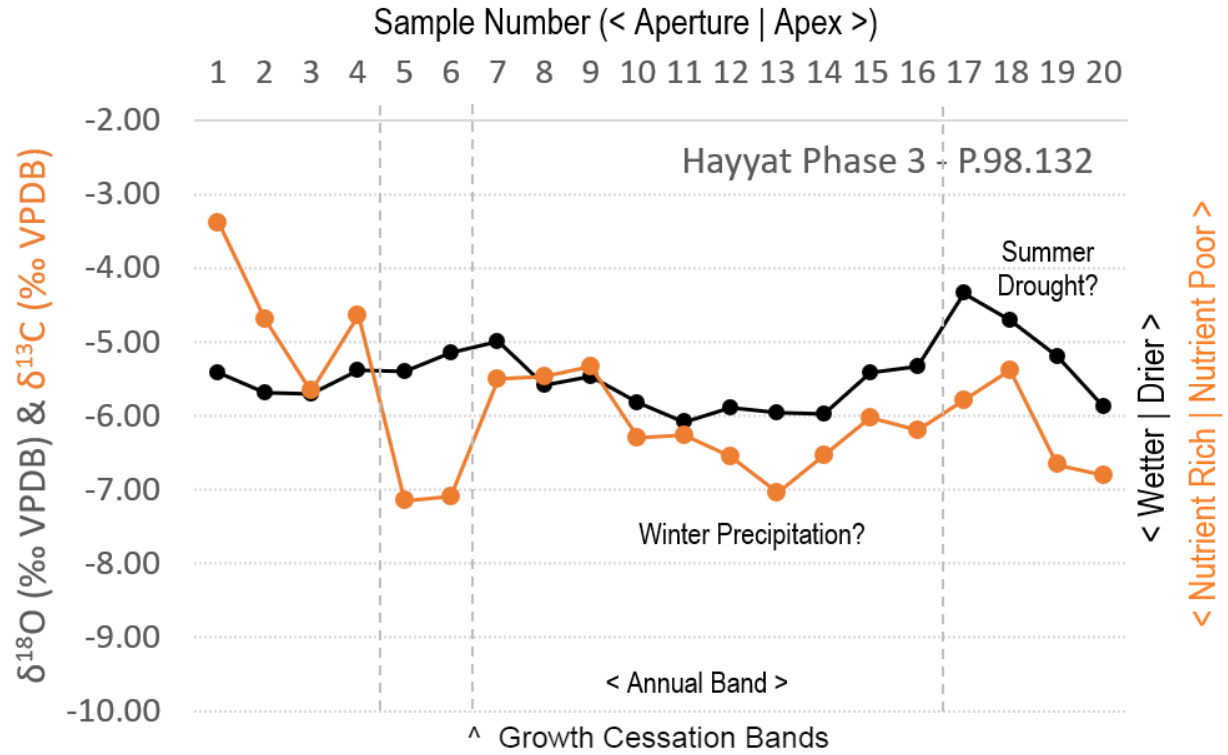

Figure 8.9 Values of $\delta^{18}O$ (black) and $\delta^{13}C$ (orange) from the shell of *Melanopsis buccinoidea* recovered from Tell el-Hayyat, Jordan Phase 3. Sample numbers are listed at the top with 1 starting at the shell aperture. Time runs from sample 20 to 1, with sample 1 roughly representing the organism's demise. Bands of growth cessation are noted with vertical dashed lines.

In Phase 2 the annual profile exhibits the least change (Figure 8.10). There is only a slight rise in values towards the annual growth band between samples 8-7, but values slope upward

more quickly in samples 5-1. The slopes of $\delta^{13}C$ for this phase roughly correspond to those of $\delta^{18}O$ but did disassociate toward the end of the profile.

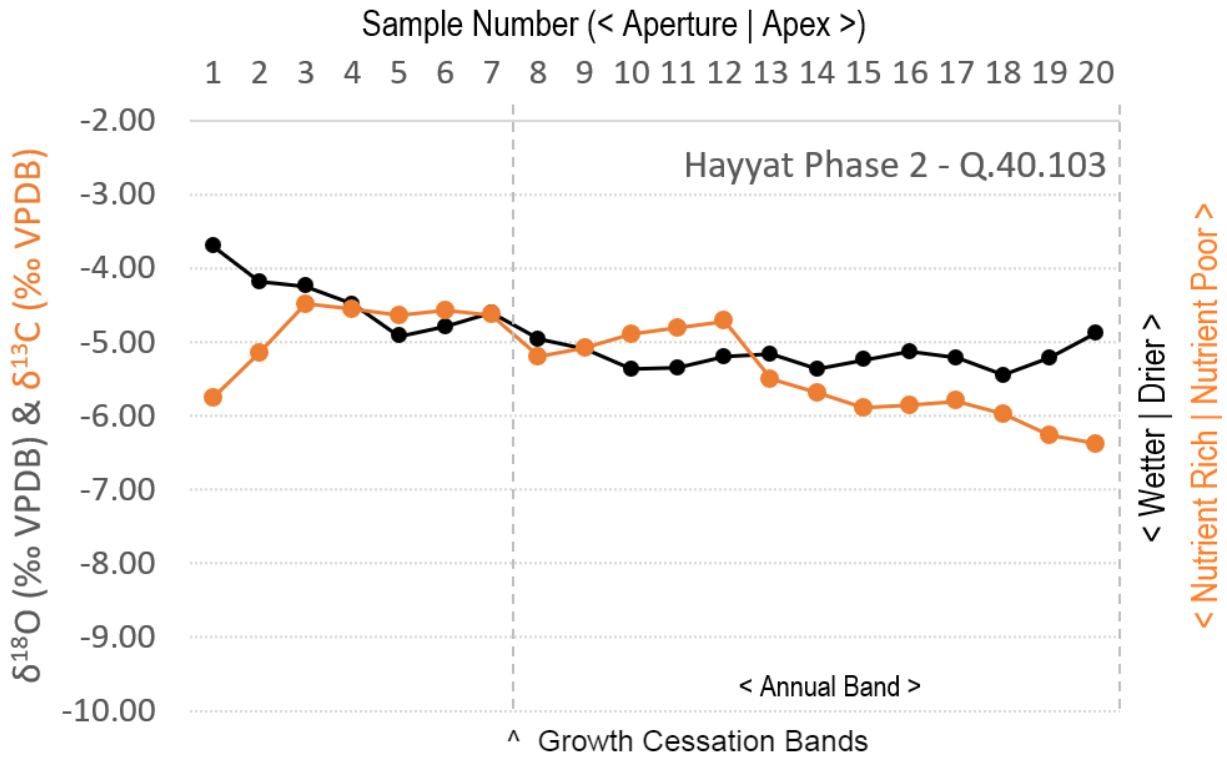

Figure 8.10 Values of $\delta^{18}O$ (black) and $\delta^{13}C$ (orange) from the shell of *Melanopsis buccinoidea* recovered from Tell el-Hayyat, Jordan Phase 2. Sample numbers are listed at the top with 1 starting at the shell aperture. Time runs from sample 20 to 1, with sample 1 roughly representing the organism's demise. Bands of growth cessation are noted with vertical dashed lines.

The mean values for both $\delta^{18}O$ and $\delta^{13}C$ from the full, 20-sample profile for each shell are significantly different from one another values using single-factor ANOVAs ($p < 0.001$). Analysis of overall $\delta^{18}O$ suggest these shells have ranges of around -3‰ to -6‰. The relatively small fluctuation in several annual profiles indicate similarity in the annual $\delta^{18}O$ signal. The lowest values are found in Phases 3 and 2 reaching around -6‰, but high value are reached in Phase 5, at nearly -2.5‰. Values of $\delta^{13}C$ vary considerably more at Hayyat, while trends rarely follow the patterns from $\delta^{18}O$. Fluctuation in the carbon profile, particularly in the Phase 3 shell,

suggests that seasonal environmental differences may play a factor in the appearance of interannual growth cessations noted in two of the shells (Çakirlar and Şeşen, 2013).

Temporal Comparisons Between Ni'aj and Hayyat

A comparison of summary data from the seven shells from Ni'aj and Hayyat (Figure 8.11) shows their mean values of $\delta^{18}O$ and $\delta^{13}C$ with 1σ standard deviations. The ranges from individual phases show low standard deviations with little overlap between individual shells. Comparison of mean values with two-sample *t*-tests with unequal variances for $\delta^{18}O$ and $\delta^{13}C$ values from the values in annual bands shows significant differences between the values at Ni'aj and Hayyat ($p < 0.1$) for both variables. This trend suggests slightly lower values of $\delta^{18}O$ for shells from Hayyat than Ni'aj, with exception of the outlier Hayyat Phase 4, which had the highest value. Hayyat Phases 3 and 2 have the lowest overall values.

In terms of mean $\delta^{13}C$, Ni'aj generally had lower values than Hayyat, with exception of the Hayyat Phase 4 outlier. Hayyat shows more overlap, but 1σ ranges do not overlap Ni'aj Phases 3 and 2 well. However, the values between both sites, if omitting Hayyat Phase 4, are not significantly distinct ($p > 0.5$). When the results from both sites are viewed jointly in terms of $\delta^{18}O$ and $\delta^{13}C$, they show some clustering among the shells from each site, but also suggest some distinction may be present in the values of each variable within each site.

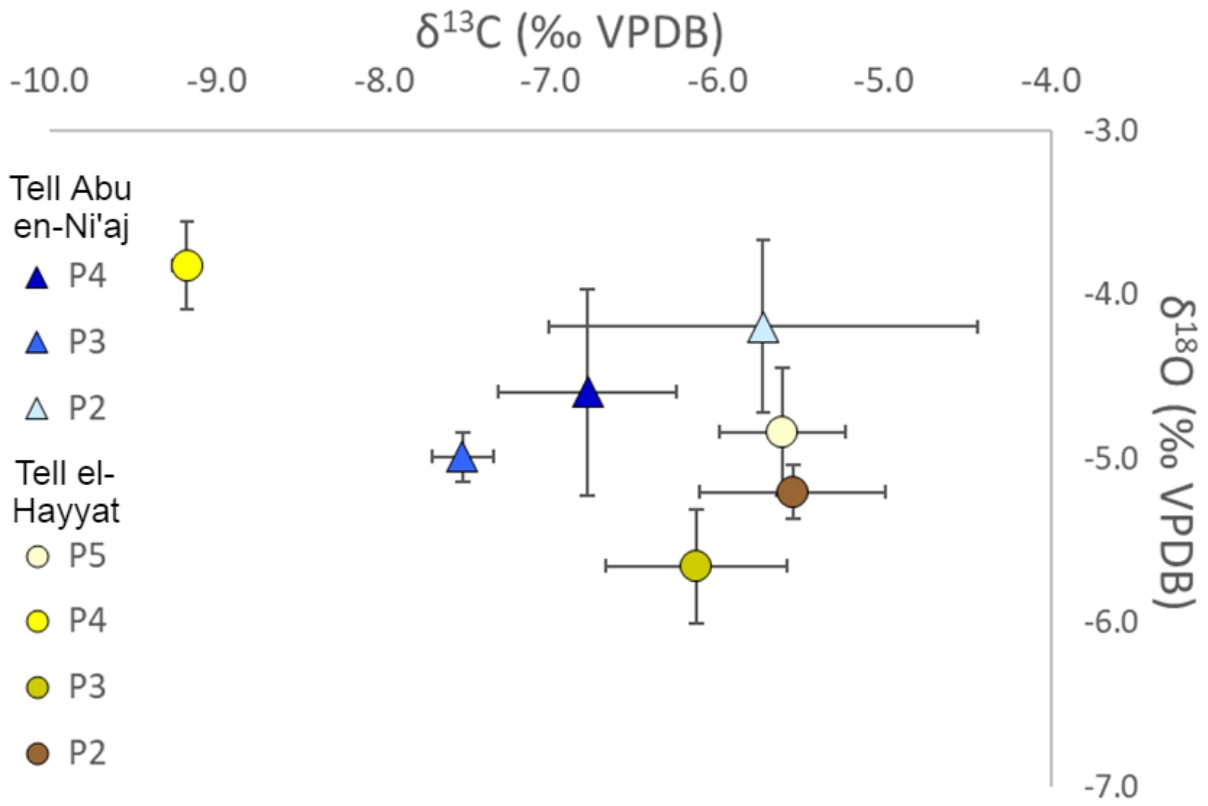

Figure 8.11 Mean values of $\delta^{18}O$ and $\delta^{13}C$ with bars for 1-sigma standard deviations for the values from the samples within the identified one-year growth cycle of all seven shells sampled at Tell Abu en-Ni'aj and Tell el-Hayyat, Jordan. Tell Abu en-Ni'aj Phase 4 through Phase 2 are shown as triangles. Tell el-Hayyat Phase 5 through Phase 2 are shown as circles.

Figure 8.12 shows the distributions of $\delta^{18}O$ values plotted according to the median value and quartile ranges of each phase at each site. Higher values are seen in EB IV and the early Middle Bronze Age, while the lower values are seen in MB II. This plot makes the distinctions at Hayyat more noticeable, where median $\delta^{18}O$ shifts almost 2‰ around the time of the MB I-II transition.

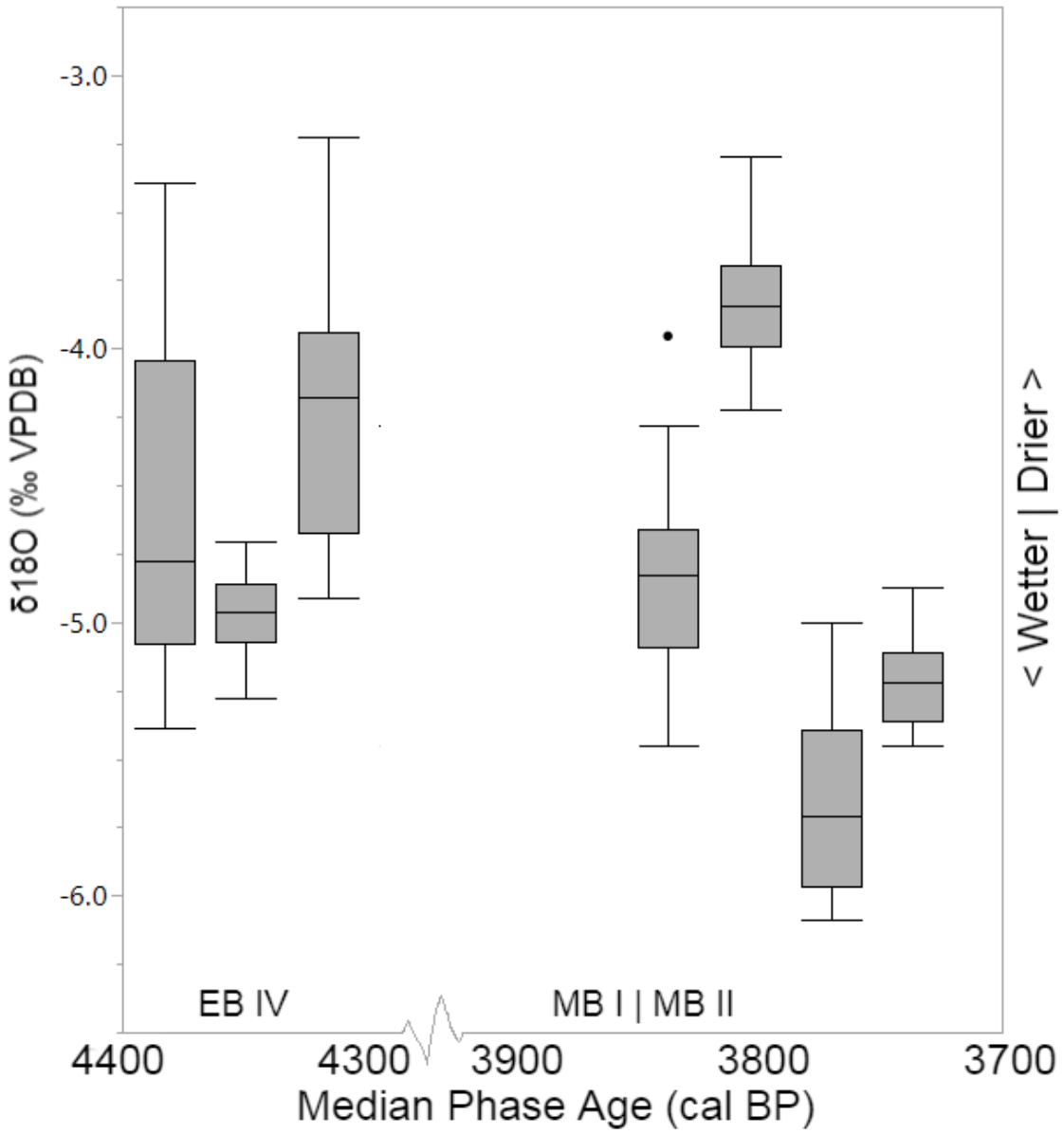

Figure 8.12 Boxplot of median values and quartile ranges for $\delta^{18}O$ values from the samples within the identified one-year growth cycle of the shells from Tell Abu en-Ni'aj and Tell el-Hayyat, Jordan, plotted per shell by median phase age.

Figure 8.13 shows the distributions of $\delta^{18}O$ and $\delta^{13}C$ values plotted according to the median value and quartile ranges of each site. The quartile ranges reflect the high seasonal range of $\delta^{18}O$ of up to roughly 3‰, the large range of $\delta^{13}C$ values of up to roughly 6‰, and the overlap between the distributions of $\delta^{18}O$ and d13C values from Tell Abu en-Ni'aj and Tell el-Hayyat. For $\delta^{18}O$, while the large variation in Hayyat Phase 5 to 4 does average out, the median value

shifts slightly lower than for Ni‘aj. Comparison of $\delta^{13}C$ values shows greater distinction between the values of each site, with little overlap of the inner quartile ranges.

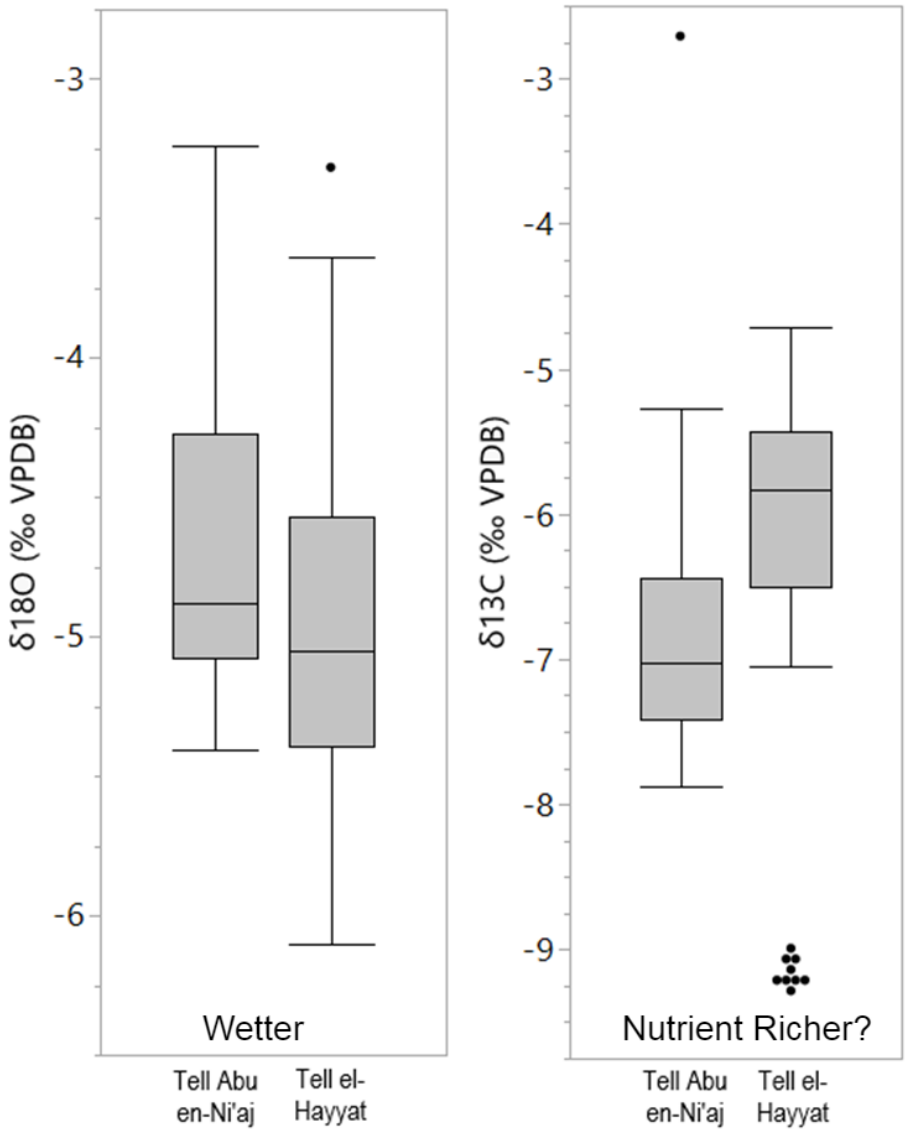

Figure 8.13 Boxplots of median values and quartile ranges for grouped $\delta^{18}O$ and $\delta^{13}C$ values from the samples within the identified one-year growth cycle of the shells from Tell Abu en-Ni‘aj and Tell el-Hayyat, Jordan. Dots signify outlying values, including the entirety of Hayyat Phase 4 in terms of $\delta^{13}C$.

Discussion

Environmental trends in EB IV and the MBA

Oxygen stable isotopes from shells of *Melanopsis buccinoidea* from Tell Abu en-Ni'aj and Tell el-Hayyat are used to infer regional climate trends in the northern Jordan Valley during Early Bronze IV and Middle Bronze I-II. Of particular interest is whether this comparison may reveal if there were differences in the local climate, hypothesized from my preliminary study of carbonized seed isotopes, between Early Bronze IV and the Middle Bronze Ages.

In each annual band the shells show a pattern exhibiting either a flat profile or slight u-shaped depression, indicating a winter recharge in ^{16}O from precipitation (Leng and Lewis, 2016; Zaarur et al., 2016; Rice et al., 2023). Samples from around the growth bands exhibited higher values of $\delta^{18}O$, forming caret-shaped intervals which may be indicative of increased evaporation and lower stream discharge until reaching a point of growth cessation (e.g., Hayyat Phase 5 Bands 1-3). Intermittent drying of smaller tributaries is commonplace in the region (Mabry and Palumbo, 1988), but temperature changes and seasonal stream discharge fluctuation could explain these termini. Shells with flat profiles suggest static conditions year-round, with no visible winter recharge, such as in Phase 3 at Ni'aj and during portions of Phases 5 and 2 at Hayyat. These may indicate a season with a low amount of winter precipitation or heightened evaporation.

Looking in-depth at each site, the Ni'aj shells paint a picture of variable seasonal climate with potentially slightly lower precipitation and or higher evaporation than at Hayyat. The minimum $\delta^{18}O$ values per annual sequence, which are around 0.25‰ to 0.5‰ higher at Ni'aj than from Hayyat, could indicate that the stream these snails lived in during EB IV had a higher concentration of the heavy isotope and thus less precipitation/more evaporation. Only the Phase

4 profile at Ni‘aj has a strong seasonal signal, while Phases 3 and 2 indicate similar and likely drier conditions year-round.

The shells from Hayyat also show evidence of years with little winter precipitation and with potentially low intra-annual variance in overall precipitation, suggesting that both settlements had years with low and infrequent winter rainfall or high winter evaporation. The lack of sharp peaks along the annual growth bands of the Hayyat shells may indicate no growth cessation in the summers, but the lack of sinusoidal pattern of seasonal variation and the higher proportion of ^{18}O suggests infrequent ^{16}O recharge and possibly indicates more pronounced drought conditions, particularly for the earlier phases. The relatively high minimum winter peak in Hayyat Phase 4 reinforces the notion that this shell may have formed during a drier year. On the other hand, the MB II shells from the Hayyat Phase 3 and 2 shells reach lower minimum $\delta^{18}O$ values and display profiles with shallow u-shaped annual trends, suggesting these organisms experienced a wetter climate.

Further interpretation can be drawn from aforementioned studies of Pleistocene fossils of *Melanopsis* in the Hula Valley north of Lake Kinneret (Moshkovitz and Margaritz, 1987; Zaarur et al., 2016; Rice, 2023). These concluded that differences of only around 1-2‰ between shell $\delta^{18}O$ in different time periods may reflect large scale changes in paleoprecipitation. The differences between the mean values of some phases (see Figure 8.11) certainly fall within this range between shells.

Trends of $\delta^{13}C$ are more complicated to interpret because they are products of several variables (Boutton 1991a), so $\delta^{13}C$ is typically used as a secondary indicator of paleoenvironmental change to augment $\delta^{18}O$ interpretations (Surge and Walker, 2006; Roach et al., 2016). Shell $\delta^{13}C$ values primarily reveal trends about the hydrological environment. It is

likely that stream discharge, related to precipitation rate, was a large driver on $\delta^{13}C$ values, particularly for timespans in which the oxygen and carbon profiles line up. When these profiles do not line up, the carbon profile may be more affected by other variables (Spiro et al., 2009). Differences in the slopes of the $\delta^{18}O$ and $\delta^{13}C$ profiles in multiple instances at Ni‘aj and Hayyat suggest that factors other than evaporation and discharge are driving shell $\delta^{13}C$ values, at least partially. Thus, although the net precipitation/evaporation rates of EB IV and MB I may have been roughly similar, the microenvironments around Ni‘aj and Hayyat in the lower Jordan Valley must have been distinct. This is most true for the outlying values from the shell in Phase 4, which likely indicate that this shell was collected from a different location than the other shells. If so, the removal of this point would result in Hayyat having a lower median $\delta^{18}O$ (see Figure 8.13) and thus reinforce earlier arguments.

Large shifts in mean $\delta^{13}C$ within and between shells have also been used to suggest differences in the sources of organically derived carbon (Spiro et al., 2009), which may reflect the $\delta^{13}C$ in algae that *Melanopsis* feeds on (Lev et al., 2007; Ekin et al., 2011). These changes could be caused by differences in upstream plant composition and soil respiration that alter stream water $\delta^{13}C$ (Leng et al., 1999; McConnaughey and Gillikin, 2008; Cole and Prairie, 2009; Murelaga, 2012; Roach et al., 2016; Zaarur et al., 2016; Jenkins et al., 2023). Lower values would suggest nutritional richness, whereas higher values may indicate nutrient-poor waters (Çakirlar and Şeşen, 2013). In this context, the higher trending profiles at Hayyat could potentially be indicative of nutrient-poorer conditions. In this hypothesis, the higher values of $\delta^{13}C$ for Middle Bronze Tell el-Hayyat and lower values at EB IV Tell Abu en-Ni‘aj may indicate heightened use of nutrient application via manuring in floodplain-adjacent fields at Ni‘aj.

As a counter-argument, the $\delta^{13}C$ of algae, the food source of *Melanopsis*, has been shown to roughly correlate with the $\delta^{13}C$ of dissolved inorganic carbon and atmospheric $\delta^{13}C$ (Finlay, 2004). Additionally, the paleoethnobotanical analysis in Chapters 4 and 5 show that there was not a dramatic difference in the composition of wild taxa between these sites. Thus, the shell $\delta^{13}C$ patterns observed at Hayyat may be responding to other variables, including river discharge, stream order, pCO_2, or alkalinity (Aucour et al., 2003; Roach et al., 2016).

Comparing the trends between EB IV and MB I-II, the $\delta^{18}O$ values from *Melanopsis buccinoidea* at Ni'aj and Hayyat show substantial variation but overlap in range and average. The trends at Tell el-Hayyat could suggest greater rainfall during MB II than in the preceding MB I, but the relatively smaller differences between EB IV and MB I suggests that these periods may have had a more similar climate. The overall precipitation/evaporation rate may have been highest around MB I. Differences in the $\delta^{13}C$ between shells from Ni'aj and Hayyat indicate the environmental distinction between EB IV and MB I-II was not driven by precipitation differences alone, and suggests the hydrology of the upstream ecosystem may have varied between periods. In conjunction, these results imply a minor distinction in paleoclimates and a potentially larger distinction in the paleoenvironments between EB IV and MB I-II in the Jordan Valley.

Modern Comparisons of $\delta^{18}O$ and Implications

Modern water samples are used here to supplement isotope investigations in the Jordan Valley. Figure 8.14 compares mean shell $\delta^{18}O$ values from Tell Abu en-Ni'aj and Tell el-Hayyat with modern spatial patterns of precipitation, ground/spring-water, and stream water $\delta^{18}O$ values

across the Southern Levant (Table A5). This comparison is drawn to visually indicate the relationship between rainwater $\delta^{18}O$ and surface water, driven by groundwater $\delta^{18}O$.

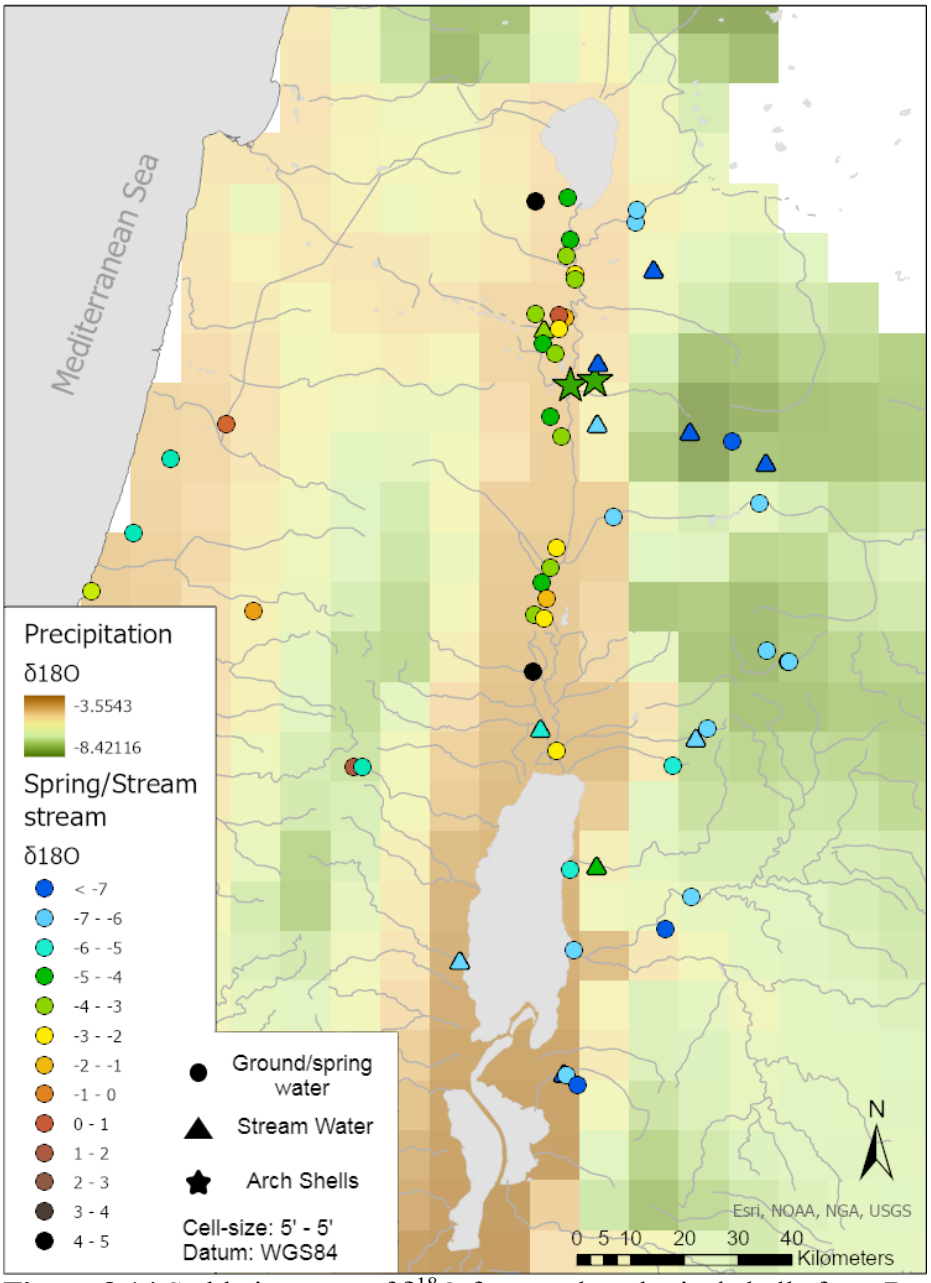

Figure 8.14 Stable isotopes of $\delta^{18}O$ from archaeological shells from Bronze Age Tell Abu en-Ni'aj and Tell el-Hayyat (stars) compared to published spring/groundwater values (circles; Farber et al., 2004; Waterisotopes Database, 2017), published stream water (squares; Farber et al., 2004; Waterisotopes Database, 2017), and unpublished spring/groundwater (circles) and stream water samples (triangles) collected by Drs. Fall, Falconer, and Ridder. The underlying map shows a raster of mean predicted growing season $\delta^{18}O$ values in precipitation with five arc minute resolution (5′) (Bowen et al., 2005; Waterisotopes Database, 2017). All point data are presented in Table A5.

From Figure 8.14, it is evident that modern precipitation follows a trend of lower $\delta^{18}O$ values at higher elevations and latitudes (Bowen et al., 2005). Precipitation $\delta^{18}O$ values were lowest in the Transjordanian highlands around -6.5‰ and transition to higher values around -3‰ in the foothills and valley bottom. Records from Israel show that $\delta^{18}O$ values in the valley can fluctuate in a wide spectrum of around -2‰ to -7‰, with lower values associated with winter rainfall, according to measurements from Israeli precipitation stations from 2000-2003 (Gat et al., 2005).

Groundwater and stream-water $\delta^{18}O$ values are lowest at high-elevation springs and increase along stream courses, with the highest values in the Dead Sea, the Sea of Galilee, and the southernmost stretch of the Jordan River due to evaporation (Hillel et al., 2019). Rapid groundwater recharge from upland limestone aquifers drives lower, more negative, winter $\delta^{18}O$ values while faulting between aquitards (water retardant geologies) allows $\delta^{16}O$-rich waters to permeate into the larger underlying sandstone aquifers in the lower valley (Akawwi et al., 2009; Gat and Dansgaard, 1972). Groundwater values from springs located near precipitation stations can thus fall several per mille lower than values from precipitation (Gat and Dansgaard, 1972; Gat, 1984; Farber et al., 2004; Roach et al., 2016), as is observed in Figure 8.14 around the lower Jordan Rift.

The $\delta^{18}O$ value from streams increases along a stream's course, as isotope composition reflects residence time in the above-ground reservoir (Gat, 1984; Farber et al., 2004; Roach et al., 2016). Values increase downstream as evaporation removes the lighter ^{16}O, so values in the lower Jordan River end up with higher values of $\delta^{18}O$. Thus, the Jordan River has modern values around -2.5‰ in the north to around 1‰ in the south (Hillel et al., 2019). Today, this region is

on the edge of a semi-arid to Mediterranean climate with roughly 300-400 mm of rainfall annually (Ziv et al., 2014; Tarawneh and Kadioglu, 2003).

The $\delta^{18}O$ values of archaeological *Melanopsis buccinoidea* shells, primarily around -4‰ to -5‰, suggest similar or potentially slightly lower values than those observed in the modern streams of the *ghor* in the northern Jordan Valley. Comparison with spring-water samples collected by our team near Ni'aj and Hayyat indicates that the archaeological shells have higher values than those of modern regional groundwater, averaging around -5‰ to -7‰ (Latel et al., 2004; Hamdan et al., 2016), but lower than those of the Jordan River, with are closer to roughly -1‰ to -4‰ (Farber et al., 2004).

Following the assumption that these shells were collected in waters near the site, broad assumptions can be made about how the precipitation at these sites may compare to that of the region today. If collected from the Jordan River, the similar or slightly higher stream water $\delta^{18}O$ in this region would suggest a similar or greater precipitation pattern may have existed during Early Bronze IV and the Middle Bronze Age. If collected from springs of the Wadi el-Yabis, which in the past may have been further up into the foothills, the modern signal would be lower than that of the shells, indicating a slightly drier climate in this age.

Archaeological Shell Summary

The overall interpretations from the archaeological shell analyses is twofold. First, there are potential characteristics of a dry, fluctuating climate through EB IV and MBA that potentially saw the wettest period in Middle Bronze II. The signal from all seven shells is potentially suggestive of a similarly semi-arid, drought-prone environment akin to the modern regional climate or drier, and does not suggest a large amount of climate change occurred

between the Early to Middle Bronze transition. The assumption of heightened precipitation in MB II would accord with previous findings from pollen studies (Langgut et al., 2013; 2015; Finklestein and Langgut, 2014; Kaniewski et al., 2020) and regional models suggesting higher precipitation early in the MBA (Soto Berelov et al., 2015; Fall et al., 2018).

Second, values of $\delta^{13}C$ suggest significant distinctions for the hydrological environments of several shells that most likely point to differences in the plant composition around or upstream of each site. Higher mean values in the Middle Bronze could suggest nutrient-poor waters during the occupation of Tell el-Hayyat, but the primary interpretation is simply that there are environmental differences between several shells. This could accord with a slight shift in vegetation associated with modest climate change.

There is a need for more comprehensive shell sampling for our sites and for another microclimate proxy that spans the missing centuries at the end of EB IV. More sampling along each shell would help elucidate the variability in the climate of the end EBA and early MBA, while bulk sampling of shells would provide a much better indicator of averaged environmental trends.

CHAPTER 9: CLIMATE AND CULTIVATION STRATEGIES: INVESTIGATIONS FROM STABLE ISOTOPES OF CARBONIZED SEEDS

Introduction

The stable isotopic analysis of carbonized seeds tells an important story of crop management in the early to middle bronze age southern levant. It hints at the presence of a steady, moderate drought throughout early EB IV through MB II, but mostly revealed patterns of practices like manuring of cultivated fields and careful management of a crop's access to water. It also revealed the greater scale of management prioritization for wheat, barley, and fruit production, particularly in the northern Jordan Valley. Finally, it revealed that certain sites were able to sustain sedentary agricultural societies in notably drier and possibly salt rich environments through intensive manure and water application.

Stable Isotope Background

Sampling Stable Isotopes of Carbon

Stable isotopes of carbon and nitrogen have routinely been used by paleoethnobotanists as indicators of ancient environmental conditions and management changes (Fiorentino et al., 2008; 2011; Riehl, 2008; 2011; Roberts et al., 2011; Riehl et al., 2014; Styring et al., 2017). The stable carbon isotope ^{13}C is introduced into plants from atmospheric CO_2 through carbon fixation. It is often found in lower concentrations in plants than in the atmosphere as plants undergo isotopic fractionation and selectively incorporate ^{12}C (Ehleringer, 1991). In C_3 plants, different ^{13}C:^{12}C ratios incorporated into plant matter can indicate the degree of carbon diffusion through a plant's stomata, linked to plant physiology and water availability and regulated by the phytohormone abscisic acid (Mengel et al., 2001 in Gouveia et al., 2020; Farquhar et al., 1982;

Ehleringer, 1991; Konvalina et al., 2014). Plants with a higher intake of CO_2 can discriminate and incorporate more ^{12}C, thus lowering the relative ^{13}C concentration (Farquhar et al., 1982; Ehleringer, 1991). In warm and dry environments, plants with higher water availability are able to open their stomata for longer periods and thus have lower (or more negative) values of $\delta^{13}C$. As a result, this metric serves as a fairly reliable indicator of a plant's water environmental conditions during the growing season of a plant (DeNiro and Hastorf, 1985).

Farquhar et al., (1989) introduced conversion of $\delta^{13}C$ values through the use of the $\Delta^{13}C$ notation. This metric is a product of $\delta^{13}C$, which focuses specifically on the ^{13}C:^{12}C ratio caused by biological action, allowing for more direct comparison between samples without having to consider changes to the atmospheric or soil carbon balance, which are already incorporated into this value. The $\Delta^{13}C$ value has been used as a metric for water availability in the Mediterranean and Near East (Araus et al., 1997a; Voltas et al., 2008) where higher values of $\Delta^{13}C$ indicate a lower concentration of the heavier ^{13}C isotope, correlating with lower values of $\delta^{13}C$ and thus greater water availability. Plant $\Delta^{13}C$ values can vary based on factors such as soil quality or temperature, so interpretation must be considered cautiously (Flohr et al., 2019). Interpretation of seed isotopes depends on the predicted watering range for each crop, which has been examined experimentally in a number of Eastern Mediterranean crop studies and has proven to be a useful determinant for differentiating between poorly and well-watered crops in drier climates (Wallace et al., 2013; 2015; Riehl et al., 2014; Styring et al., 2016; 2017; Flohr et al., 2019; Jones et al., 2021). Wallace et al. (2013; 2015) introduced the nomenclature 'poorly-watered, moderately-watered, and well-watered' in these experiments, which will be used in this dissertation to categorize levels of crop water availability.

Several other factors affect the initial $\delta^{13}C$ values which need to be accounted for, including differences in the environment and due to carbonization. To account for the effects of carbonization, authors have calculated numerical offsets for each species, suggesting values around -0.11‰ to -0.22‰ (Fiorentino et al., 2011; Fraser et al., 2013; Nitsch et al. 2015; Styring et al., 2017). A modification of -0.11‰ is used for all taxa in this study for the sake of consistency. For environmental differences, caution is used in interpreting distinctions between values any less dissimilar than roughly 0.5-0.7‰. Even under similar conditions, modern testing has shown that a single taxon sown across the same field can have a variance of around 0.7‰, as approximated from values in Heaton et al. (2009). There is also variation in the isotopic signature within different plant parts (DeNiro and Hastorf, 1985), which I minimize by sampling only seeds, and species-specific fractionation rates (Vogel, 1993), which I minimize by keeping interpretations to species level whenever possible.

Sampling Stable Isotopes of Nitrogen

The isotope ^{15}N is taken up by plants from the atmosphere and soils in the form of nitrate (NO_3^-) or ammonium (NH_4+) (Marshall et al., 2007). The ratio of ^{15}N:^{14}N is denoted by $\delta^{15}N$ with reference to the atmospheric standard. Nitrogen isotope values are useful indicators of soil quality, rainfall, and land use history (Bogaard et al., 2018a), especially in arid landscapes where the primary impact on plant $\delta^{15}N$ comes from nitrogen fractionation in the soil (West and Skujins, 1977, as cited in Fiorentino et al., 2011; Craine et al., 2015). Given the presence of nutrient-poor aridisols in the region, this stands to be a useful metric (Al-Bakri, 2008). Nitrogen discrimination does not occur in crops when plant nitrogen demand exceeds soil nitrogen supply, such as exists in a nitrogen limited soils in Mediterranean to semi-arid climates (Evans et al.,

1996, as cited in Marshall et al., 2007; Robinson et al., 2000; Passioura, 2002, as cited in Aguilera et al., 2008), thus soil nitrogen values directly impact plant ^{15}N rates.

Nitrogen stable isotope analysis is useful for interpreting the presence of manuring (Bogaard et al., 2007; Aguilera et al., 2008; Senbayram et al., 2008; Kanstrup et al., 2011; Styring et al., 2016). Dung is typically greatly enriched in ^{15}N, so higher concentrations of $\delta^{15}N$ will be found in agricultural fields where manure is used as fertilizer (Senbayram et al., 2008). Many Near Eastern sites have evidence that ancient people collected manure as a fuel (Miller and Smart, 1984; Charles, 1998; Spengler, 2019), and it has been suggested that manuring has long been practiced in ancient Near Eastern settlements as a method of revitalizing over-farmed agricultural fields (Bogaard, 2005).

Nitrogen isotope values are also prone to alteration due to carbonization and digestion. Carbonization appears to cause an increase of around 1‰ for nitrogen (Aguilera et al., 2008; Fiorentino et al., 2011; Fraser et al., 2013), and the pre-cleaning process for sampling carbonized seeds can cause a decrease of up to around 1‰ (Vaiglova et al., 2014). Given that these values may compensate for one another, no correction was applied to $\delta^{15}N$ values.

Environmental nitrogen incorporation will affect $\delta^{15}N$. The value for certain taxa, such as *Hordeum* or *Triticum*, has been shown to correlate positively with manure application, while for most pulses the correlation is not as strong as that of the cereals, leading to lower $\delta^{15}N$ values in experimentation (Fraser et al., 2011; Bogaard et al., 2013; Vaiglova et al., 2014). The multiple fractionation pathways of nitrogen (Marshall et al., 2007) also make comparison difficult. However, as this is not as impactful in semi-arid environments, this will mostly be a concern for intersite comparisons. A final factor is precipitation, which may skew values slightly higher in

drier climates, and could be an influencing factor in arid climates, such as those that experience low rainfall of around 50 mm/year or less (Hartman and Danin, 2010).

In summary, I use $\delta^{13}C$ and $\delta^{15}N$ values to study paleoenvironmental factors. Since seeds record the isotopic signature of their environments during formation, I will use stable isotope data to infer paleoclimatic and paleoenvironmental conditions during the plant's growing season, specifically during the grain-filling period. Values of $\delta^{13}C$ reveal water availability to plants, with high values indicating high water availability. I use $\delta^{15}N$ values to indicate soil nutrient availability, with high values indicating soil nutrient richness. It is also important to be aware that every species incorporates isotopes differently due to their metabolic pathways and phenological differences (Merah et al., 2001; Aguilera et al., 2008; Werner et al., 2012). Interpretation of $\delta^{13}C$ and $\delta^{15}N$ must carefully consider the taxa being compared and cannot simply be based on comparison of stable isotopic ranges (Araus et al., 1997b; Voltas et al., 1999; Konvalina et al., 2010; 2011; 2014; Bogaard et al., 2013; Wallace et al., 2013; 2015; Styring, 2016).

Other Considerations for Interpretation

The most important consideration is that the $\delta^{15}N$ and $\Delta^{13}C$ values of different species grown under the same environmental conditions may greatly differ across even relatively small spatial scales (Heaton et al., 2009; Hartman and Danin, 2010; Werner et al., 2012). This is especially important when the differences in the thresholds between crops being poorly-watered to well-watered may be about 1‰ difference or smaller (Wallace et al., 2013). In response, most interpretation of baselines values of manuring and water availability is in reference to the cereals or select, well-studied taxa.

Few species from my sites have undergone intensive stable isotopic study aside from the common species of *Hordeum* and *Triticum* (Araus et al., 1999; Ferrio et al., 2005; Riehl et al., 2008; Voltas et al., 2008; Fiorentino et al., 2015). Some experiments have included study of regional pulse and fruit crops (Araus et al., 1999; Fiorentino et al., 2008; Bogaard et al., 2013; 2018a; Wallace et al., 2013; 2015; Nitsch et al., 2017; 2019; Styring et al., 2017), but less is known about the expected baselines of these species. Thus, the discussion of other cultigens is primarily made via relative comparisons between the four focal sites or with other Eastern Mediterranean, mid-Holocene settlements

Laboratory Methods and Sampling Procedure

Stable isotopic analysis of $\delta^{13}C$ and $\delta^{15}N$ from carbonized seeds was conducted in several stages to interpret intra- and inter-site patterns of watering and manuring of common varieties of cereals, pulses and fruits. Taxa were selected with a primary focus on the cereals *Triticum dicoccum* and *Hordeum vulgare*, two of the most common taxa used in stable isotope analyses across the ancient Mediterranean and Near East. Sampling also targeted the cultivated cereals *H. vulgare* var. *nudum*, *H. vulgare hexastichum, T. aestivum*, and *T. monococcum*. Cultivated pulses chosen for sampling included *Lens culinaris, Pisum sativum*, *Lathyrus sativus, Cicer arietinum, Vicia ervilia,* and *V. faba.* Cultivated fruits sampled included *Ficus carica, Vitis vinifera* and the oil crop *Olea europaea.* Finally, non-cultigens sampled include *Pistacia terebinthus* and *Prosopis farcta.* Minimums of five samples of seeds for each cereal taxon and two samples for each non-cereal taxon from each phase of occupation were analyzed whenever possible. Analysis included 190 seeds from Tell Abu en-Ni‘aj, 254 from Tell el-Hayyat, 63 from Zahrat adh-Dhra‘ 1, and 52 from Khirbat Iskandar. Prior to my dissertation research, stable isotope values had been

published as part of larger radiocarbon analyses at Ni‘aj, Hayyat and ZAD 1 (Falconer and Fall, 2016; 2017; Fall et al., 2019). Additional investigation was conducted for stable isotopes at Ni‘aj for my MS thesis (Porson et al., 2021a). Tables 9.1 through 9.4 indicate the number of seeds analyzed for $\delta^{13}C$ and $\delta^{15}N$ by site and phase.

Table 9.1 Numbers of samples analyzed for stable isotopes of $\delta^{13}C$ and $\delta^{15}N$ by phase at Tell Abu en-Ni‘aj, Jordan. Radiocarbon age ranges are based on modeled phase boundary medians in Fall et al. 2021.

Age Range (cal BCE)	Phase	Sample Count
2294–2264	1	1
2331–2294	2	37
2375–2331	3	36
2418–2375	4	30
2456–2418	5	23
2487–2456	6	35
2524–2487	7	28
Total		190

Table 9.2 Numbers of samples analyzed for stable isotopes of $\delta^{13}C$ and $\delta^{15}N$ by phase at Tell el-Hayyat, Jordan. Radiocarbon age ranges are based on modeled phase boundary medians in Fall et al. 2021.

Age Range (cal BCE)	Phase	Sample Count
1711–1660	1	1
1779–1711	2	22
1798–1779	3	38
1834–1798	4	49
1887–1834	5	38
1921–1887	6	3
Total		254

Table 9.3 Numbers of samples analyzed for stable isotopes of $\delta^{13}C$ and $\delta^{15}N$ by phase at Khirbat Iskandar, Jordan. Radiocarbon age ranges are based on modeled phase boundary medians in Fall et al. 2022.

Age Range (cal BCE)	Phase	Sample Count
2469-2459	3	12
2481-2470	2	0
2506-2492	1	2
2514-2506	Pre-1A	22
2523-2514	Pre-1B	13
2536-2523	Pre-1D	0
Total		49

Table 9.4 Numbers of samples analyzed for stable isotopes of $\delta^{13}C$ and $\delta^{15}N$ by phase at Zahrat adh-Dhra‘ 1, Jordan. Radiocarbon age ranges are based on modeled phase boundary medians in Fall et al. 2023.

Age Range (cal BCE)	Phase	Sample Count
1802–1761	2	35
1879–1829	3	44
2029–1950	4	5
Total		63

Seeds in each sample were chosen for analysis until reaching a threshold weight, with priority given to samples with no fragmentation and minimal degradation. A weight of 12 mg and a minimum of two seeds was suitable for sampling carbon and nitrogen from most cereal grains, while a minimum weight of 20 mg, rather than a minimum seed count, was needed for many nitrogen deficient taxa like *Olea europaea* and *Vitis vinifera* to ensure successful analysis.

All selected seeds were weighed and measured before processing. A morphological analysis was conducted of 442 grains from the most common taxa: *Hordeum vulgare, H. vulgare* var. *nudum, Triticum aestivum, T. dicoccum, Lens culinaris,* and *Vitis vinifera* (Appendix B) to

examine the potential for grain yield differences between the same taxa in different sites, reflected as grain size and weight differences (Abd el Rahman et al., 1967; Craufurd et al., 1991). No significant distinctions in seed morphologies are recorded, suggesting that yield changes are not large enough to note.

Seeds were sent for analysis at the UGA Center for Applied Isotope Studies (CAIS) where they were processed by Dr. Suzanne Pilaar Birch. Ancient seeds were pretreated with an acid-base-acid wash to remove modern contaminants before analysis (Fraser et al; 2013; Vaiglova et al., 2014; Brinkkemper et al., 2018). Stable isotopes concentrations for all seeds were measured using a Delta-V elemental analyzer isotope ratio mass spectrometer (EA-IRMS). Seeds were flash combusted to CO_2 and N_2, and concentrations of stable isotopes in the gases were measured against in-lab gas standards in reference to the standards Vienna Pee Dee Belemnite (VPDB) and modern air, respectively.

Seeds co-analyzed for radiocarbon ages were processed at the University of Arizona Accelerator Mass Spectrometry Laboratory, the University of Groningen Centre for Isotope Research, the Vienna Environmental Research Accelerator, and the Oxford Radiocarbon Accelerator Unit. At Groningen (GrM), Oxford (OxA) and Arizona (AA), $\delta^{13}C$ was measured with an isotope ratio mass spectrometer, while values from Vienna (VERA) were measured directly by accelerated mass spectrometry (AMS). Only five values from the VERA lab were used in this study and all came from samples of either *Olea europaea* or *Triticum aestivum* from Hayyat.

Values of $\delta^{13}C$ were measured in reference to VPDB (Farquhar et al., 1982), adjusted by -0.11‰ to correct the carbonization offset. The calculations for $\delta^{13}C$ and $\delta^{15}N$ are similar.

$$\delta^{13}C = \left(\frac{13C\ sample/12C\ sample}{13C\ standard/\ 12C\ standard} - 1\right) * 1000 - 0.11 \quad (4)$$

$$\delta^{15}N = \left(\frac{15N\ sample/14N\ sample}{15N\ standard/\ 14N\ standard} - 1\right) * 1000 \quad (5)$$

Values of $\delta^{13}C$ were then converted to $\Delta^{13}C$. Carbon discrimination ($\Delta^{13}C$) was calculated using values of $\delta^{13}C$ from atmospheric CO_2 estimated from Ferrio's AIRCO2_LOESSv2 system (Ferrio et al., 2005; 2012) and Farquhar's isotope calibration formula (Farquhar et al., 1989).

$$\Delta^{13}C = \frac{\delta 13C\ air - \delta 13C\ sample}{1+(\delta 13C\ sample/1000)} \quad (6)$$

Four samples of *Triticum* sp.*,* were also collected from the modern northern Jordan Valley in 2018 by Drs. Patricia Fall, Elizabeth Ridder, and Steven Falconer. Modern values provide another method of intersite comparison. Plants were initially dried and transported in brown bags. At UNC Charlotte, seeds were stored in a freezer. Plants were later removed and ground into a fine powder with mortar and pestle, sieved through 500-micron mesh, and poured into pre-weighed vials until a weight of at least 200 mg was reached. These were also sampled at UGA's CAIS using IRMS.

Values of $\Delta^{13}C$ and $\delta^{15}N$ from the labs were then compared between taxa, phases, and sites. For data visualization and interpretation, biplots indicate the mean nitrogen and carbon stable isotopic values for a variety of cultigens, with results compared statistically using pairwise two-sample *t*-tests with unequal variance, and single-factor ANOVA. Data are also plotted as means and standard deviations per phase to examine temporal changes. For Iskandar and ZAD 1, phase distinctions are not used in the analysis for the stable isotopic investigation due to the smaller sample sizes from these sites.

Stable Isotope Profiles of $\Delta^{13}C$ and $\delta^{15}N$ at four Southern Levantine Sites

Introduction

Stable isotope analysis was conducted on 619 samples of common cultigens and wild taxa between four archeological sites in western Jordan. A total of 556 samples provided species-specific data used in this analysis. At each site, $\Delta^{13}C$ and $\delta^{15}N$ values from *Hordeum vulgare* and *Triticum dicoccum* are compared to offer intrasite metrics of similarity. An array of commonly cultivated cereals, legumes, and fruits are analyzed to broaden the range of studied taxa. One-sigma confidence intervals are plotted to indicate variance, which can range several units per mille. All raw data used in these figures can be found in Tables A6-A9 and Figures A16-A19.

Tell Abu en-Ni'aj

Figures 9.1-9.4 show the results from stable isotope analysis of seeds at Ni'aj for each taxon plotted according to mean $\Delta^{13}C$ and $\delta^{15}N$ values and 1σ confidence intervals. *Hordeum* and *Triticum* 1σ intervals overlap substantially among the other barleys and wheats, but *Hordeum vulgare* var. *hexastichum* (Figure 9.1) and *Triticum aestivum* (Figure 9.2) had notably higher $\Delta^{13}C$ values. Cereal $\Delta^{13}C$ values had similar ranges from around 17‰ to 18.5‰ and $\delta^{15}N$ bands ranging from about 6‰ to 7‰. *Hordeum vulgare* var. *nudum* has higher $\Delta^{13}C$ values than those of *H. vulgare* by around 1‰. Mean values for several legumes, including *Prosopis farcta*, also roughly clustered, with overlapping 1σ ranges and a mean around 3‰ for $\delta^{15}N$. Pulse $\Delta^{13}C$ values hovered around 17‰ with *Pisum sativum* notably higher (Figure 9.3). The fruit taxa do not cluster and show vary high $\delta^{15}N$ variation. Of the fruits, *Vitis vinifera* has the highest mean value for both $\Delta^{13}C$ and $\delta^{15}N$, while *Olea europaea* had the lowest of each (Figure 9.4).

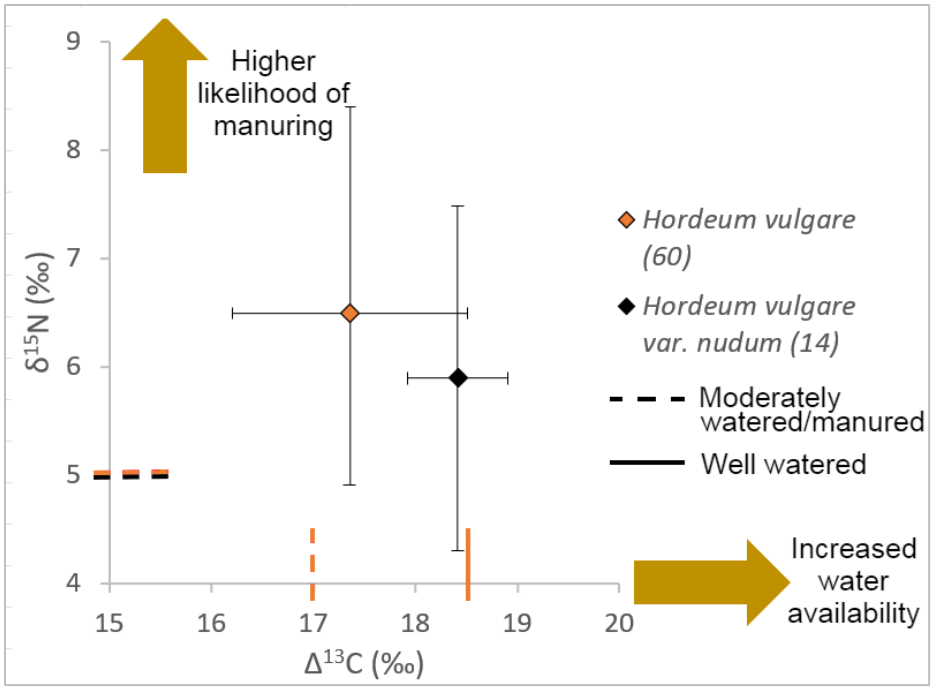

Figure 9.1 Scatterplot of mean $\Delta^{13}C$ and $\delta^{15}N$ values and 1σ standard deviations for *Hordeum* from Tell Abu en-Ni'aj, Jordan. Dashed and solid lines by the axes indicate the thresholds for poorly- to moderately- to well-watered or manured signals.

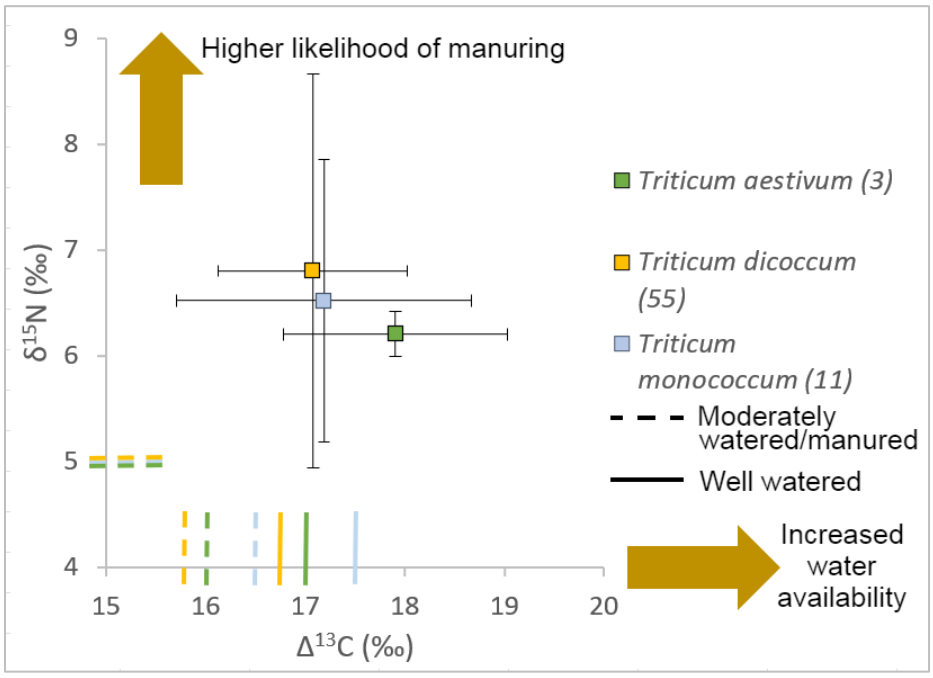

Figure 9.2 Scatterplot of mean $\Delta^{13}C$ and $\delta^{15}N$ values and 1σ standard deviations for *Triticum* from Tell Abu en-Ni'aj, Jordan. Dashed and solid lines by the axes indicate the thresholds for poorly- to moderately- to well-watered or manured signals.

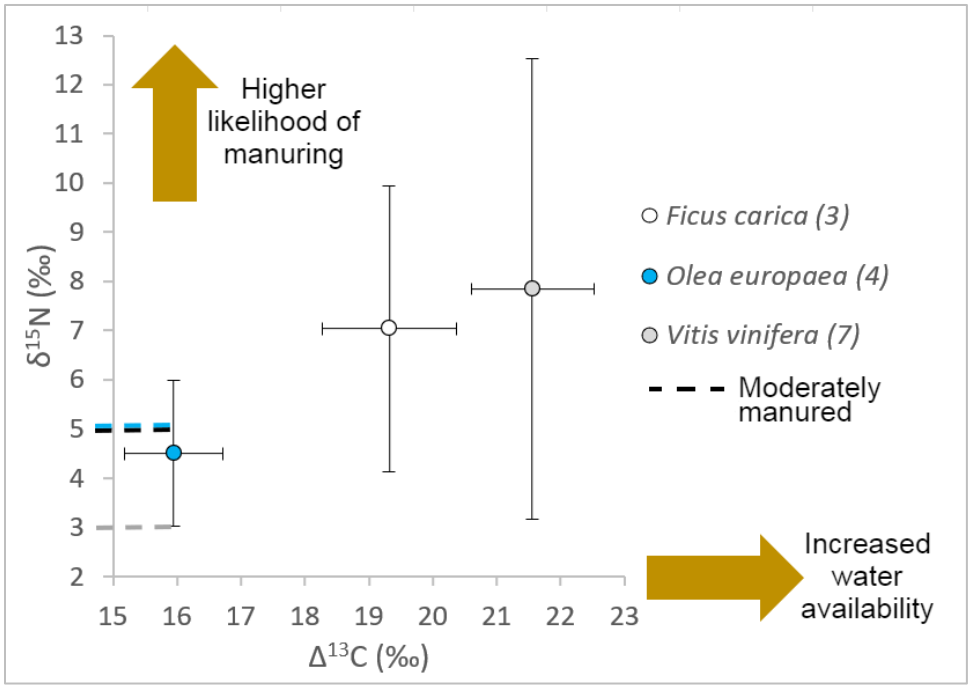

Figure 9.3 Scatterplot of mean $\Delta^{13}C$ and $\delta^{15}N$ values and 1σ standard deviations for fruit taxa from Tell Abu en-Ni'aj, Jordan. Dashed and solid lines by the axes indicate the thresholds for poorly- to moderately- to well-watered or manured signals.

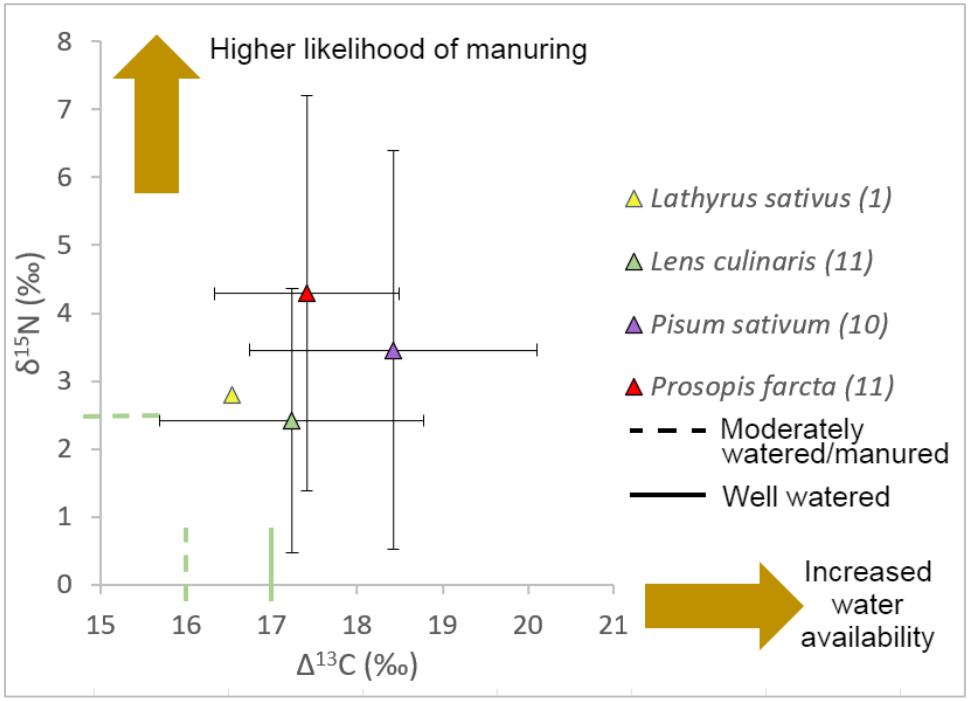

Figure 9.4 Scatterplot of mean $\Delta^{13}C$ and $\delta^{15}N$ values and 1σ standard deviations for pulses and *Prosopis farcta* from Tell Abu en-Ni'aj, Jordan. Dashed and solid lines by the axes indicate the thresholds for poorly- to moderately- to well-watered or manured signals.

A comparison of medians and quartile ranges for $\Delta^{13}C$ between phases at Tell Abu en-Ni‘aj is illustrated in Figure 9.5 for the primary cultigens *Hordeum vulgare* and *Triticum dicoccum*. To compare overlap, significance tests were conducted on values of $\Delta^{13}C$ as well as $\delta^{15}N$ from the whole assemblage, Table 9.5. Little temporal change occurred between phases for either grain or between sites, with values statistically insignificant for $\Delta^{13}C$ as well as $\delta^{15}N$. None of the comparisons of $\Delta^{13}C$ and $\delta^{15}N$ at Ni‘aj are significant between the two cereal types, which does indicate a slight difference in water availability for *H. vulgare* and *T. dicoccum,* as these taxa are purported to have a roughly 1‰ difference when cultivated in similar climate conditions based on the experimental tests on $\Delta^{13}C$ between these taxa (Araus, 1997b; Voltas et al., 1999; Wallace et al., 2013; 2015; Styring, 2016; Flohr, 2019). Based on the Wallace et al. 2015 watering categories, values of *H. vulgare* $\Delta^{13}C$ sit primarily in the moderately-watered category, with more values in the poorly-watered than the well-watered range. For *T. dicoccum,* values sit primarily in the well-watered category or the moderately-watered category. The full list of stable isotope results from Ni‘aj is presented in Table A6.

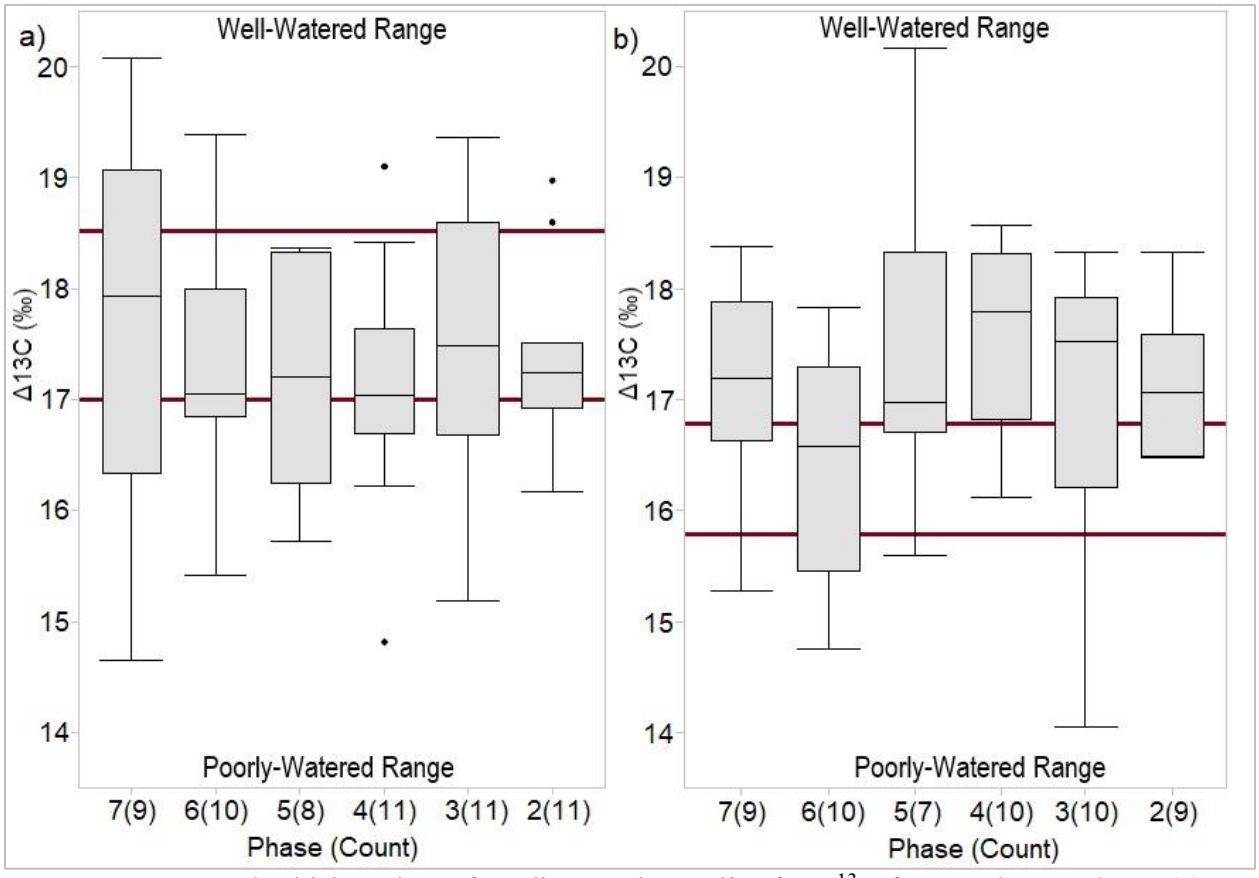

Figure 9.5 Box-and-whisker plots of medians and quartiles for $\Delta^{13}C$ for *Hordeum vulgare* (a) and *Triticum dicoccum* (b) by phase from Tell Abu en-Ni'aj, Jordan. The number of samples per phase is indicated in parentheses. The moderately-watered range (from Wallace et al., 2015) for each taxon is bounded by red lines. The poorly-watered range lies below the lower red line and the well-watered range lies above the upper red line.

Table 9.5 Statistical comparisons of *Hordeum vulgare* and *Triticum dicoccum* $\Delta^{13}C$ and $\delta^{15}N$ values from Tell Abu en-Ni'aj, Jordan.

What was Compared?	Statistical Test	*α* value	*p* value	Significant?
Ni'aj $\Delta^{13}C$ of *H. vulgare* between phases	Single-factor ANOVA	0.1	0.99	No
Ni'aj $\Delta^{13}C$ of *T. dicoccum* between phases	Single-factor ANOVA	0.1	0.99	No
Ni'aj $\delta^{15}N$ of *H. vulgare* between phases	Single-factor ANOVA	0.1	0.77	No
Ni'aj $\delta^{15}N$ *of T. dicoccum* between phases	Single-factor ANOVA	0.1	0.89	No
Ni'aj $\Delta^{13}C$ between all *H. vulgare* and *T. dicoccum*	two-sample *t*-test with unequal variance	0.1	0.15	No
Ni'aj $\delta^{15}N$ between all *H. vulgare* and *T. dicoccum*	two-sample *t*-test with unequal variance	0.1	0.44	No

Tell el-Hayyat

Figures 9.6-9.9 indicates the stable isotope results from cultivated plants and selected wild plants found at Hayyat. All three *Hordeum* taxa have strongly overlapping mean $\Delta^{13}C$ values of roughly 17.2‰ while mean $\delta^{15}N$ values ranged between 6‰ and 6.5‰ (Figure 9.6). *Triticum* values have slightly less overlap and lower $\Delta^{13}C$ values, with means ranging around 16.5‰. *Triticum* have $\delta^{15}N$ mean values between a relatively wide 6‰ and 8‰, with values for *Triticum monococcum* highest in $\delta^{15}N$ but lowest in $\Delta^{13}C$ values (Figure 9.7).

Fruits at Hayyat have $\Delta^{13}C$ values around 17-19‰ and the cultivated fruits had mean $\delta^{15}N$ values over 7.5‰, though values for the wild *Pistacia terebinthus* plot much lower, around 5‰. *Olea europaea* has the lowest mean value among fruits for $\Delta^{13}C$, while *V. vinifera* had the highest value (Figure 9.8). Most sampled legumes have similar $\Delta^{13}C$ values, with overlapping 1σ ranges. The pulse taxa have a low $\delta^{15}N$ signal, with values ranging from roughly 3-4‰, with the uncultivated *Prosopis farcta* has a slightly higher range at around 5‰ (Figure 9.9).

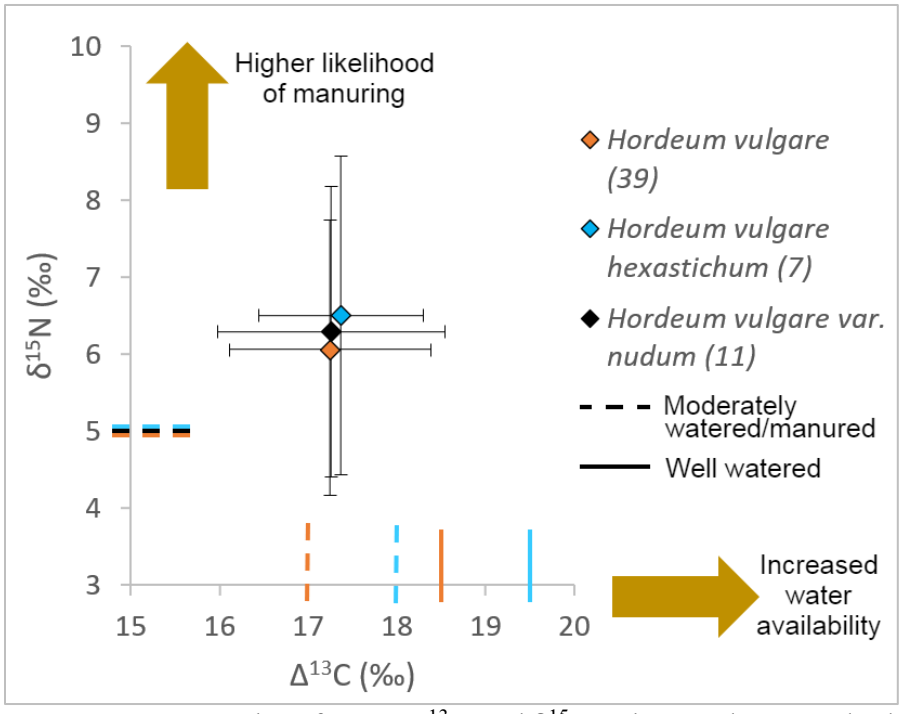

Figure 9.6 Scatterplot of mean $\Delta^{13}C$ and $\delta^{15}N$ values and 1σ standard deviations for *Hordeum* from Tell el-Hayyat, Jordan. Dashed and solid lines by the axes indicate the thresholds for poorly- to moderately- to well-watered or manured signals.

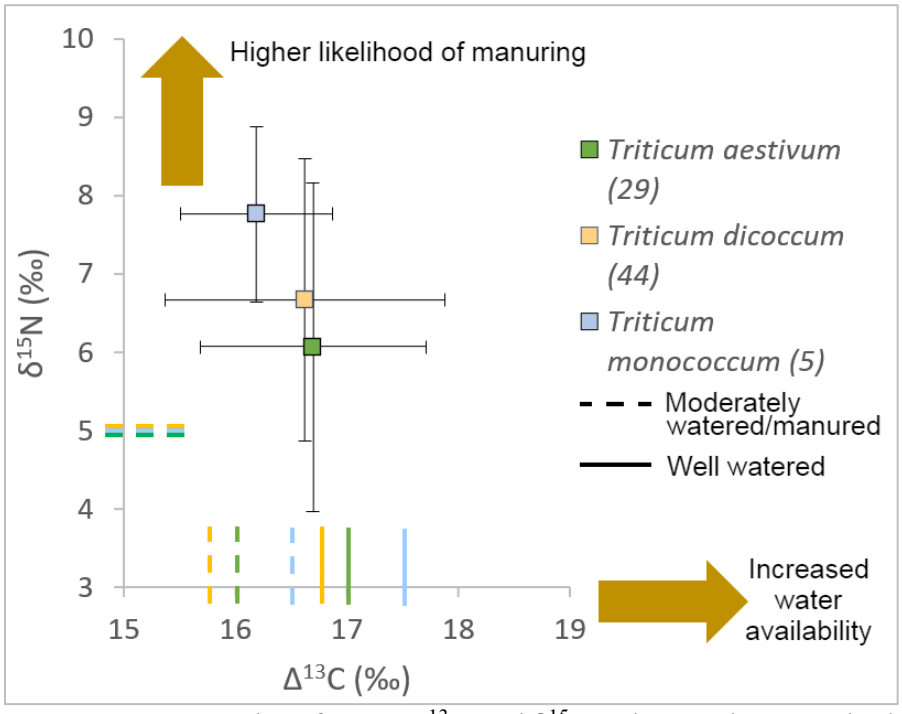

Figure 9.7 Scatterplot of mean $\Delta^{13}C$ and $\delta^{15}N$ values and 1σ standard deviations for *Triticum* from Tell el-Hayyat, Jordan. Dashed and solid lines by the axes indicate the thresholds for poorly- to moderately- to well-watered or manured signals.

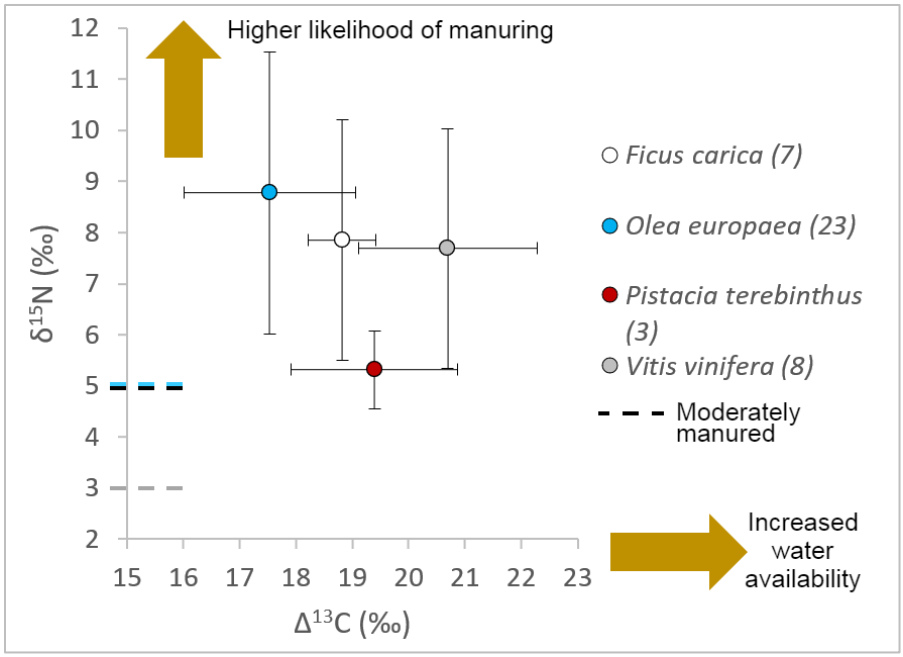

Figure 9.8 Scatterplot of mean $\Delta^{13}C$ and $\delta^{15}N$ values and 1σ standard deviations for fruit from Tell el-Hayyat, Jordan. Dashed and solid lines by the axes indicate the thresholds for poorly- to moderately- to well-watered or manured signals.

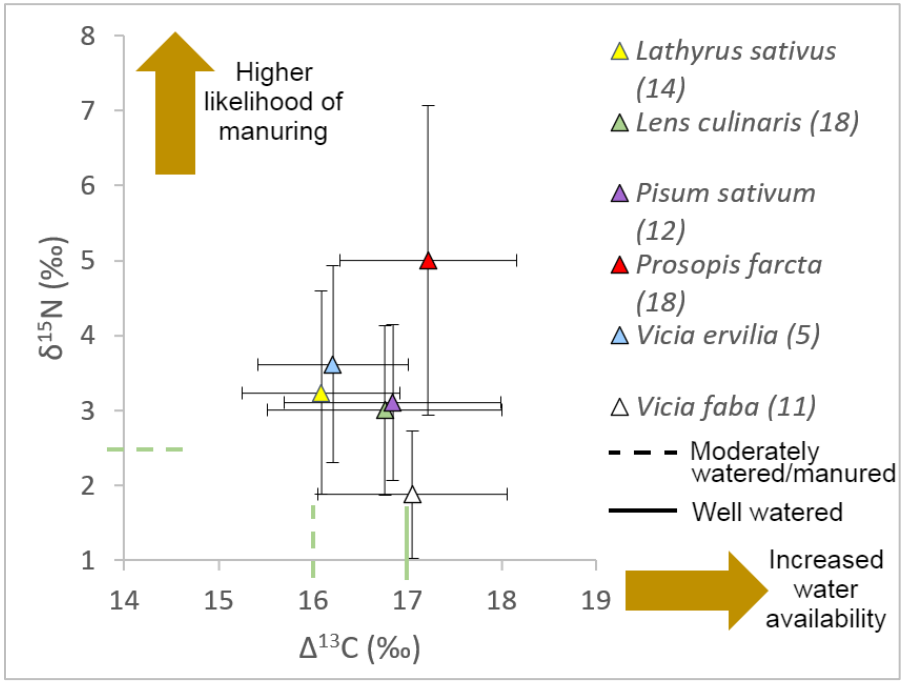

Figure 9.9 Scatterplot of mean $\Delta^{13}C$ and $\delta^{15}N$ values and 1σ standard deviations for pulse and *Prosopis farcta* from Tell el-Hayyat, Jordan. Dashed and solid lines by the axes indicate the thresholds for poorly- to moderately- to well-watered or manured signals.

Median values of $\Delta^{13}C$ for *Hordeum vulgare* and *Triticum dicoccum* are compared between four Hayyat occupational phases in Figure 9.10. Mean values, compared for statistical difference in Table 9.6, are significantly distinct between the taxa ($p < 0.1$). However, comparing median $\Delta^{13}C$ values for *H. vulgare* and *T. dicoccum* between phases does not suggest temporal shifts over the site's lifetime for either taxon. *Hordeum vulgare* $\Delta^{13}C$ values remain primarily in the moderately-watered range, with few values extending above the well-watered threshold. The values of *T. dicoccum* are much more variable, with an increased number of samples indicating well-watered conditions in Phases 3 and 2 (Wallace et al., 2013; 2015; Styring, 2016; Flohr, 2019). The full list of stable isotope results from Hayyat is presented in Table A7.

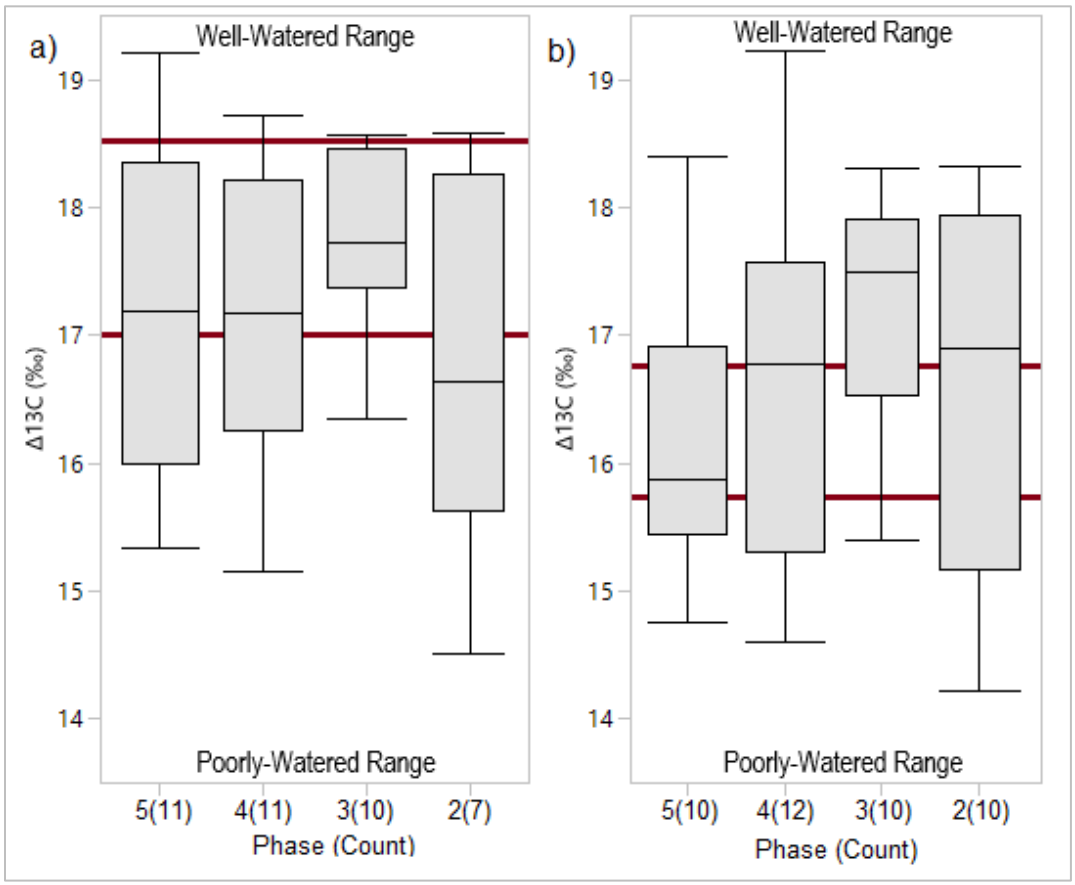

Figure 9.10 Box-and-whisker plots of medians and quartiles for $\Delta^{13}C$ for *Hordeum vulgare* (a) and *Triticum dicoccum* (b) by phase from Tell el-Hayyat, Jordan. The number of samples per phase is indicated in parentheses. The moderately-watered range (from Wallace et al., 2015) for each taxon is bounded by the red lines. The poorly-watered range lies below the lower red line and the well-watered range lies above the upper red line.

Table 9.6 Statistical comparisons of *Hordeum vulgare* and *Triticum dicoccum* $\Delta^{13}C$ and $\delta^{15}N$ values from Tell el-Hayyat, Jordan.

What was Compared?	Statistical Test	*α* value	*p* value	Significant?
Hayyat $\Delta^{13}C$ *of H. vulgare* between phases	Single-factor ANOVA	0.1	0.89	No
Hayyat $\Delta^{13}C$ of *T. dicoccum* between phases	Single-factor ANOVA	0.1	0.86	No
Hayyat $\delta^{15}N$ of *H. vulgare* between phases	Single-factor ANOVA	0.1	0.96	No
Hayyat $\delta^{15}N$ of *T. dicoccum* between phases	Single-factor ANOVA	0.1	0.53	No
Hayyat $\Delta^{13}C$ between *H. vulgare* and *T. dicoccum*	two-sample *t*-test with unequal variance	0.1	0.02	Yes
Hayyat $\delta^{15}N$ between *H. vulgare* and *T. dicoccum*	two-sample *t*-test with unequal variance	0.1	0.09	Yes

Khirbat Iskandar

Stable isotope values for $\Delta^{13}C$ and $\delta^{15}N$ from Iskandar are plotted in Figure 9.11-9.13, with *Hordeum* and *Triticum* plotted together. The mean *Hordeum vulgare* $\Delta^{13}C$ value is around 17.1‰, just above the mean value for *Triticum dicoccum* at roughly 17‰. The mean $\delta^{15}N$ values were higher for *T. dicoccum* than *H. vulgare*, plotting just outside the 1σ range of *H. vulgare* (Figure 9.11). However, due in part to the small sample size, statistical comparison suggests no significant difference in either $\Delta^{13}C$ or $\delta^{15}N$ between the two cereals (see Table 9.7).

Only *Vitis vinifera* was sampled for the fruits from Iskandar. *Vitis* has a $\Delta^{13}C$ around 20‰ and a $\delta^{15}N$ value just over 4‰. Pulse taxa cluster with relatively low mean values for both $\Delta^{13}C$ and $\delta^{15}N$, around 16‰ and 2‰ respectively.

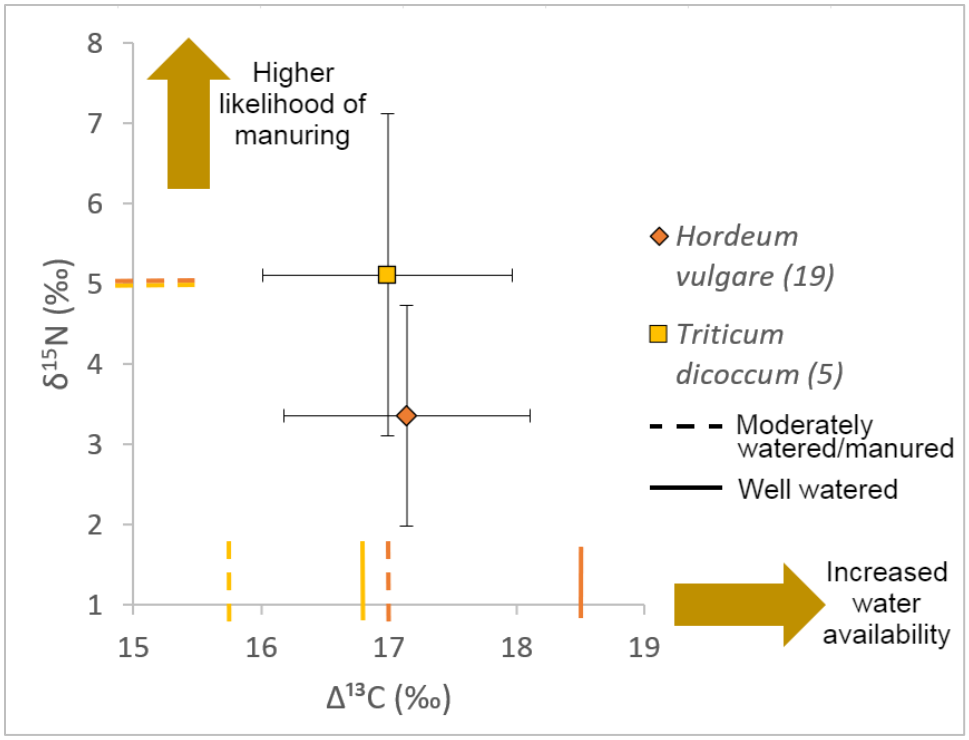

Figure 9.11 Scatterplot of mean $\Delta^{13}C$ and $\delta^{15}N$ values and 1σ standard deviations for *Hordeum* and *Triticum* from Khirbat Iskandar, Jordan. Dashed and solid lines by the axes indicate the thresholds for poorly- to moderately- to well-watered or manured signals.

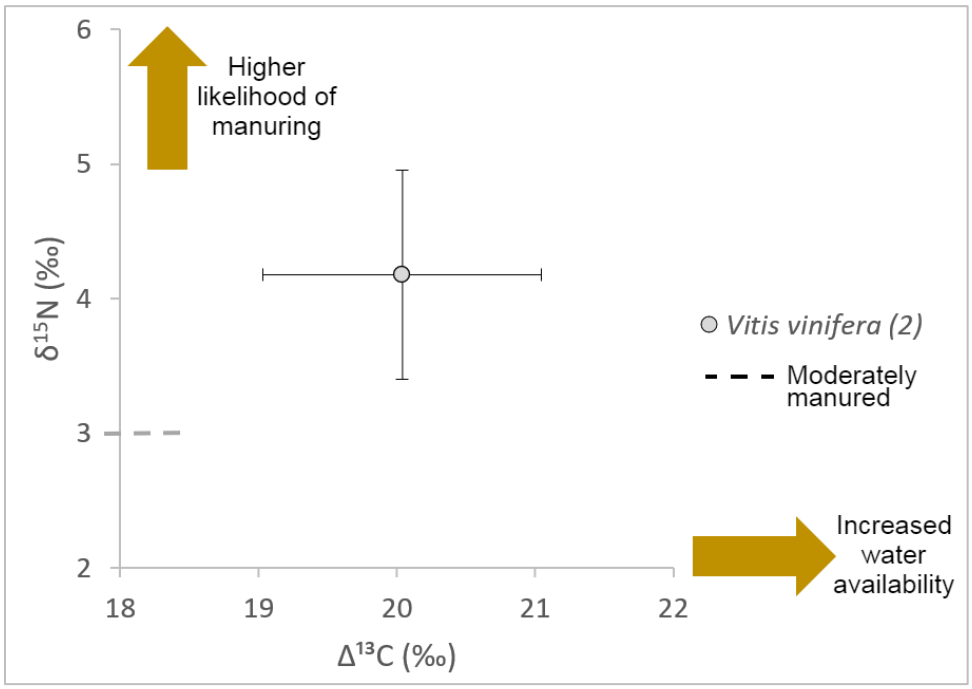

Figure 9.12 Scatterplot of mean $\Delta^{13}C$ and $\delta^{15}N$ values and 1σ standard deviations for *Vitis vinifera* from Khirbat Iskandar, Jordan. Dashed and solid lines by the axes indicate the thresholds for poorly- to moderately- to well-watered or manured signals.

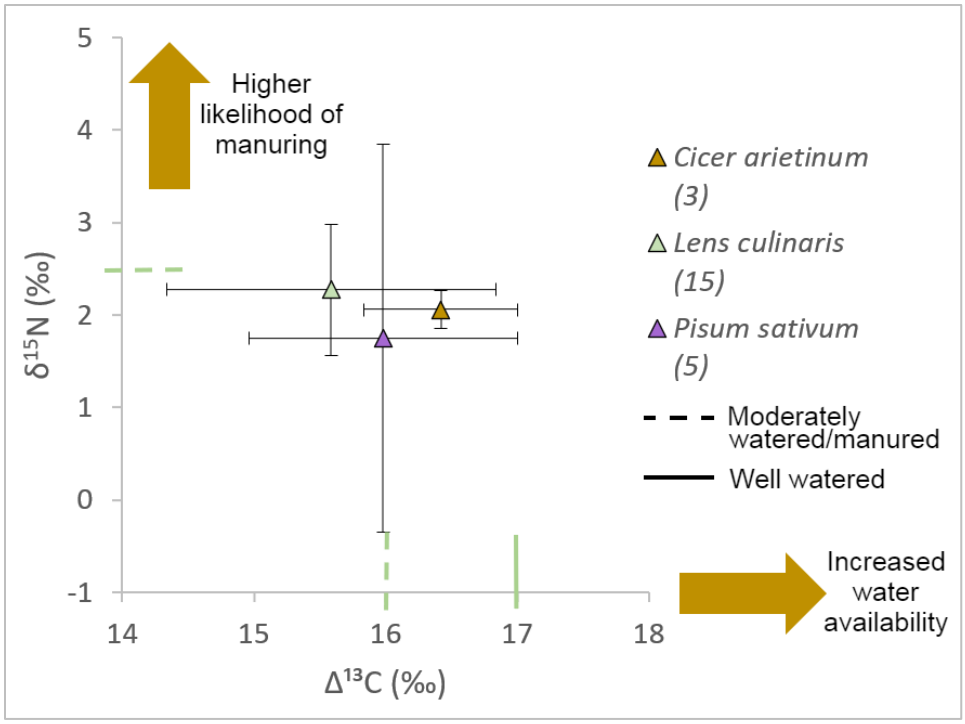

Figure 9.13 Scatterplot of mean $\Delta^{13}C$ and $\delta^{15}N$ values and 1σ standard deviations for pulses from Khirbat Iskandar, Jordan. Dashed and solid lines by the axes indicate the thresholds for poorly- to moderately- to well-watered or manured signals.

Medians and quartile ranges for $\Delta^{13}C$ from *Hordeum vulgare* and *Triticum dicoccum* are shown in Figure 9.14. Values for *H. vulgare* seeds plot in the poorly and moderately-watered categories, with only one of the 19 seeds plotting in the well-watered range. *Triticum dicoccum* values range between all three categories, with a majority indicative of well-watered conditions (Wallace et al., 2013; 2015; Styring, 2016; Flohr, 2019). The full list of stable isotope results from Iskandar is presented in Table A8.

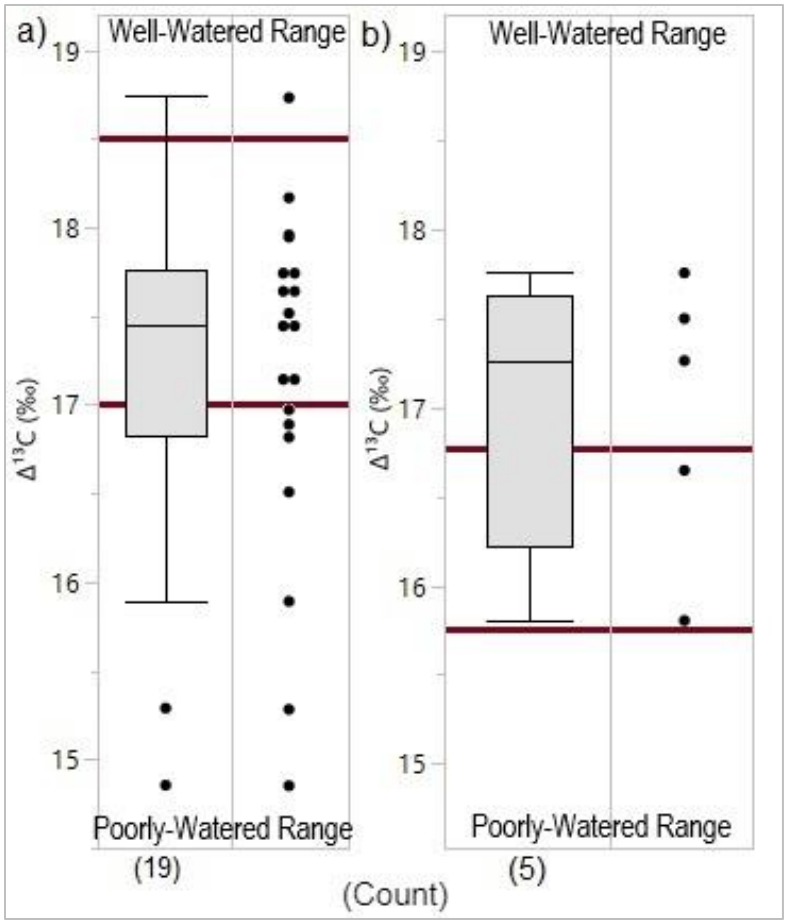

Figure 9.14 Box-and-whisker plots of $\Delta^{13}C$ of medians and quartiles for *Hordeum vulgare* (a) and *Triticum dicoccum* (b) by phase from Khirbat Iskandar, Jordan. The number of samples per phase is indicated in parentheses. The moderately-watered range (from Wallace et al., 2015) for each taxon is bounded by the red lines. The poorly-watered range lies below the lower red line and the well-watered range lies above the upper red line.

Table 9.7 Statistical comparisons of *Hordeum vulgare* and *Triticum dicoccum* $\Delta^{13}C$ and $\delta^{15}N$ values from Khirbat Iskandar, Jordan.

What was Compared?	Statistical Test	*α* value	*p* value	Significant?
Iskandar $\Delta^{13}C$ between *H. vulgare* and *T. dicoccum*	two-sample *t*-test with unequal variance	0.1	0.32	No
Iskandar $\delta^{15}N$ between *H. vulgare* and *T. dicoccum*	two-sample *t*-test with unequal variance	0.1	0.35	No

Zahrat adh-Dhra' 1

Results of $\Delta^{13}C$ and $\delta^{15}N$ analyses from ZAD 1 are illustrated in Figures 9.15-9.18.

Hordeum vulgare var. *nudum* and *Triticum aestivum* are the most abundant seeds, but did not

have the highest values of $\Delta^{13}C$ and $\delta^{15}N$. *Hordeum vulgare*, with a mean $\Delta^{13}C$ value around 19.3‰, is roughly 1‰ higher than *H. vulgare* var. *nudum*. Each has a $\delta^{15}N$ value around 9‰ (Figure 9.15). Each *Triticum* has a $\Delta^{13}C$ value around 18‰, but *Triticum aestivum* has a $\delta^{15}N$ value around 1.5‰ lower than *T. dicoccum* (Figure 9.16). The wheat *T. aestivum* reported as *T. aestivum/durum* in the paleoethnobotanical analysis, but seeds chosen for isotopic analysis most likely belong to *T. aestivum*.

Vitis vinifera and *Ficus carica* each have high values for mean $\delta^{15}N$, above 7‰. *Vitis vinifera* has a $\Delta^{13}C$ value around 20‰ (Figure 9.17). Pulse crops continued the pattern of having mean $\Delta^{13}C$ values around 16‰ or lower, while $\delta^{15}N$ values fell in the low 2-5‰ range, with mean $\delta^{15}N$ for *Vicia faba* falling nearly 2‰ higher (Figure 9.18).

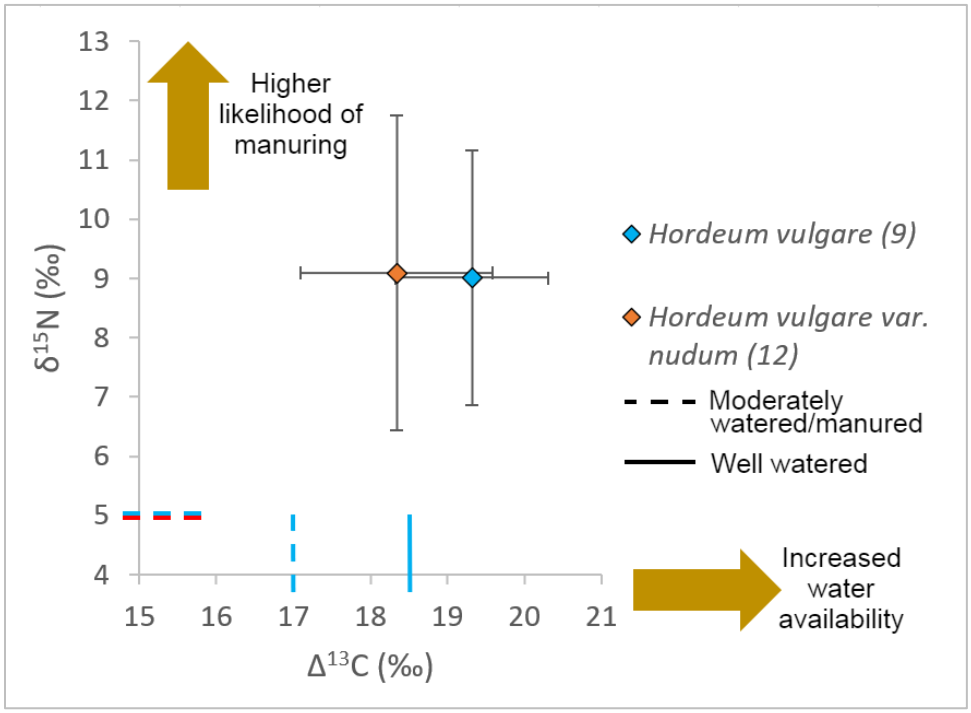

Figure 9.15 Scatterplot of mean $\Delta^{13}C$ and $\delta^{15}N$ values and 1σ standard deviations for *Hordeum* from Zahrat adh-Dhra‘ 1, Jordan. Dashed and solid lines by the axes indicate the thresholds for poorly- to moderately- to well-watered or manured signals.

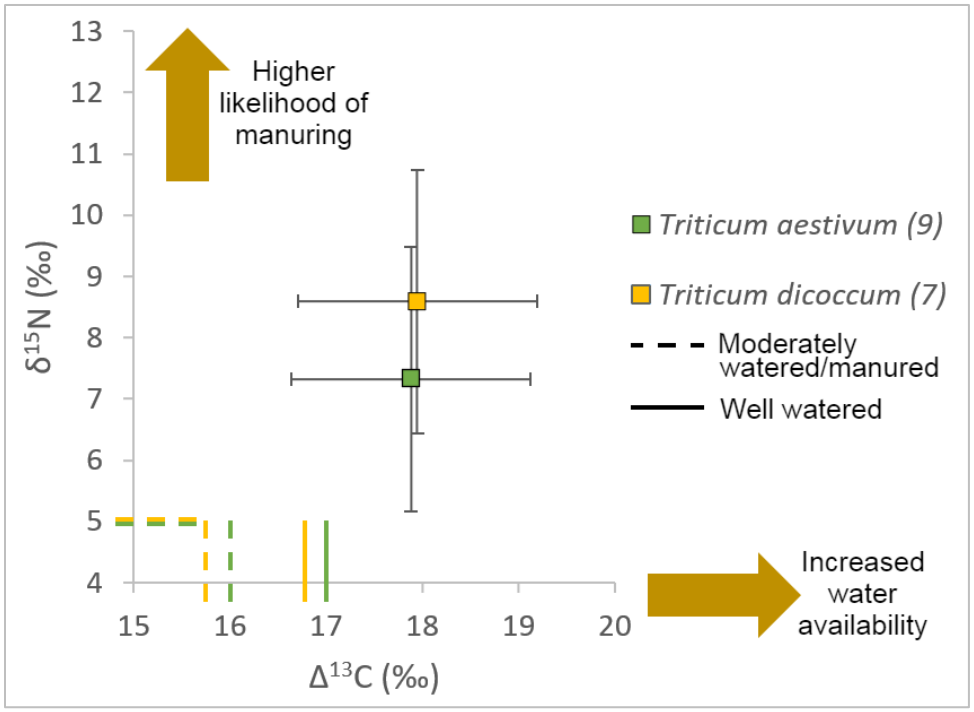

Figure 9.16 Scatterplot of mean $\Delta^{13}C$ and $\delta^{15}N$ values and 1σ standard deviations for *Triticum* from Zahrat adh-Dhra‘ 1, Jordan. Dashed and solid lines by the axes indicate the thresholds for poorly- to moderately- to well-watered or manured signals.

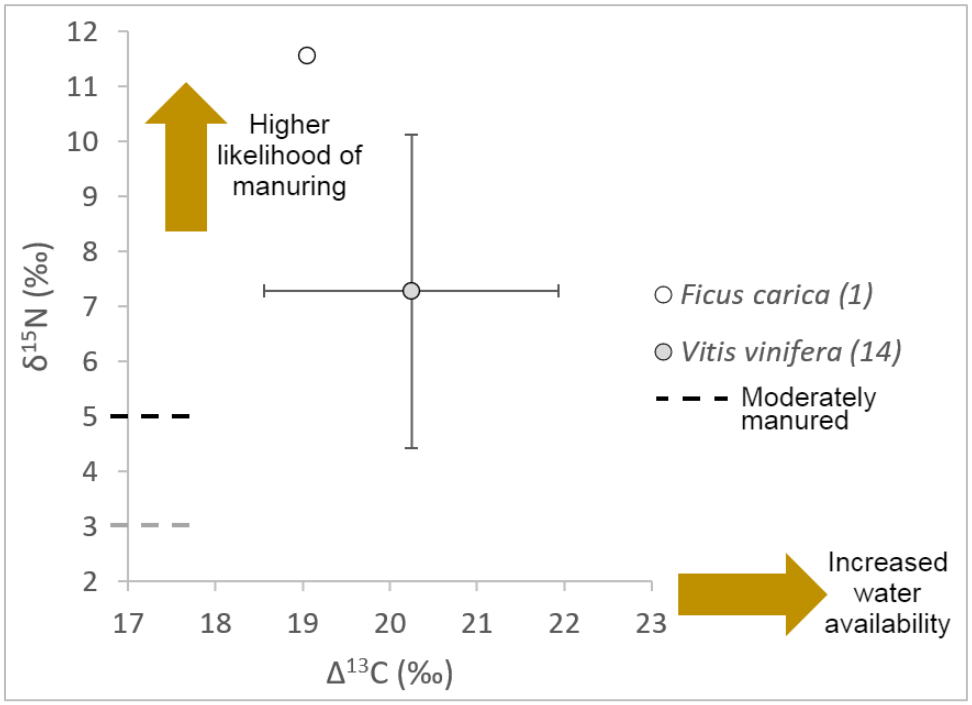

Figure 9.17 Scatterplot of mean $\Delta^{13}C$ and $\delta^{15}N$ values and 1σ standard deviations for fruit from Zahrat adh-Dhra‘ 1, Jordan. Dashed and solid lines by the axes indicate the thresholds for poorly- to moderately- to well-watered or manured signals.

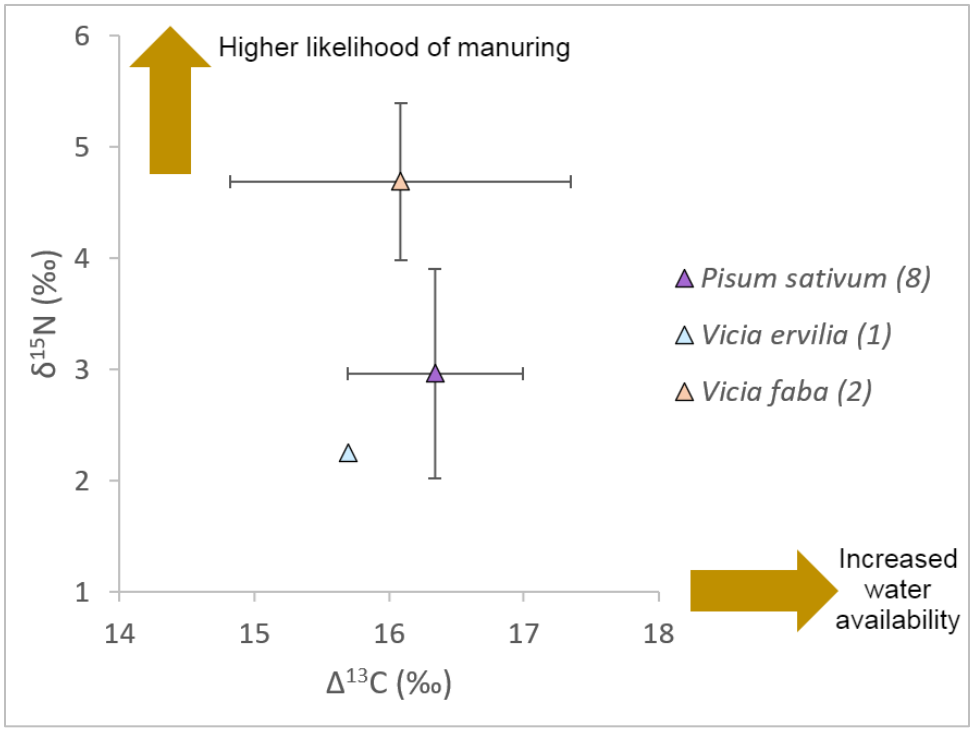

Figure 9.18 Scatterplot of mean $\Delta^{13}C$ and $\delta^{15}N$ values and 1σ standard deviations for pulses from Zahrat adh-Dhra‘ 1, Jordan.

Comparing the *Hordeum vulgare* and *Triticum dicoccum* from ZAD 1, values of $\Delta^{13}C$ differ significantly (Table 9.8). Notably, while mean values of $\delta^{15}N$ between these taxa are roughly 2‰ apart, the difference is not statistically significant due to the variance. The distributions of median $\Delta^{13}C$ values for *Hordeum vulgare* and *Triticum dicoccum* are plotted in Figure 9.19 to assess watering ranges. The range of $\Delta^{13}C$ values is firmly in the well-watered category for both taxa, with the inner quartile ranges entirely above the threshold for well-watered grains of each species. Of seven samples of *Triticum dicoccum,* all plot above the well-watered threshold (Wallace et al., 2013; 2015; Styring, 2016; Flohr, 2019). The full list of stable isotope results from ZAD 1 is presented in Table A9.

Results from ZAD 1 show a markedly different trend than for the previous three sites. However, this is not believed to be an artifact of small sample size. The cereal seeds from this

site were analyzed in three batches with similar results and with the appropriate use of stable isotopic standards.

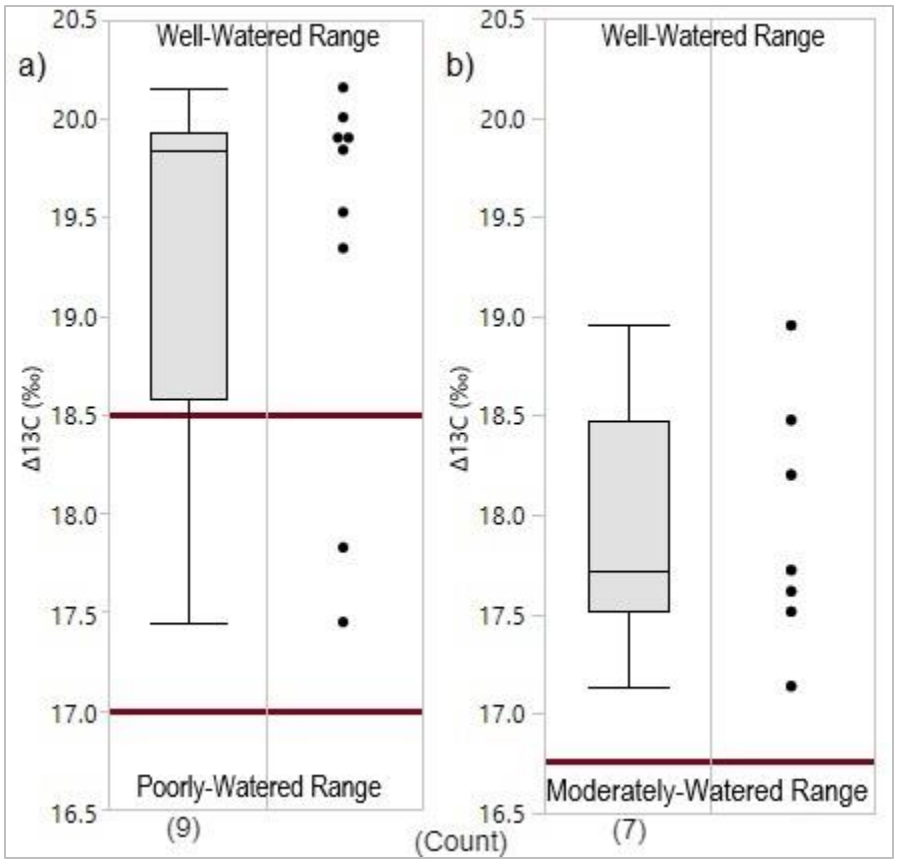

Figure 9.19 Box-and-whisker plots of $\Delta^{13}C$ of medians and quartiles for *Hordeum vulgare* (a) and *Triticum dicoccum* (b) by phase from Zahrat adh-Dhra‘ 1, Jordan. The number of samples per phase is indicated in parentheses. The moderately-watered range (from Wallace et al., 2015) for each taxon is bounded by red lines. The poorly-watered range lies below the lower red line and the well-watered range lies above the upper red line.

Table 9.8 Statistical comparisons of *Hordeum vulgare* and *Triticum dicoccum* $\Delta^{13}C$ and $\delta^{15}N$ values from Zahrat adh-Dhra‘ 1, Jordan.

What was Compared?	Statistical Test	*α* value	*p* value	Significant?
ZAD 1 $\Delta^{13}C$ between *H. vulgare* and *T. dicoccum*	two-sample *t*-test with unequal variance	0.1	0.02	Yes
ZAD 1 $\delta^{15}N$ between *H. vulgare* and *T. dicoccum*	two-sample *t*-test with unequal variance	0.1	0.77	No

Intersite Comparisons

Comparison of $\Delta^{13}C$ between the four sites is illustrated in Figures 9.20 and 9.21. This comparison examines the mean values between each phase at each site. Figure 9.20 shows the mean $\Delta^{13}C$ per phase for *Hordeum vulgare*. Values from Ni'aj, Hayyat, and Iskandar have similar mean values of around 17‰ to 17.5‰, whereas only the latest phase of ZAD 1 has a comparable value. Phases 4 and 3 at ZAD 1, dating to roughly the middle to late MB I, have values closer to 19.8‰. The comparison of $\Delta^{13}C$ between sites suggests that similar values existed in EB IV and MB II, whereas potentially higher values existed in MB I at ZAD 1.

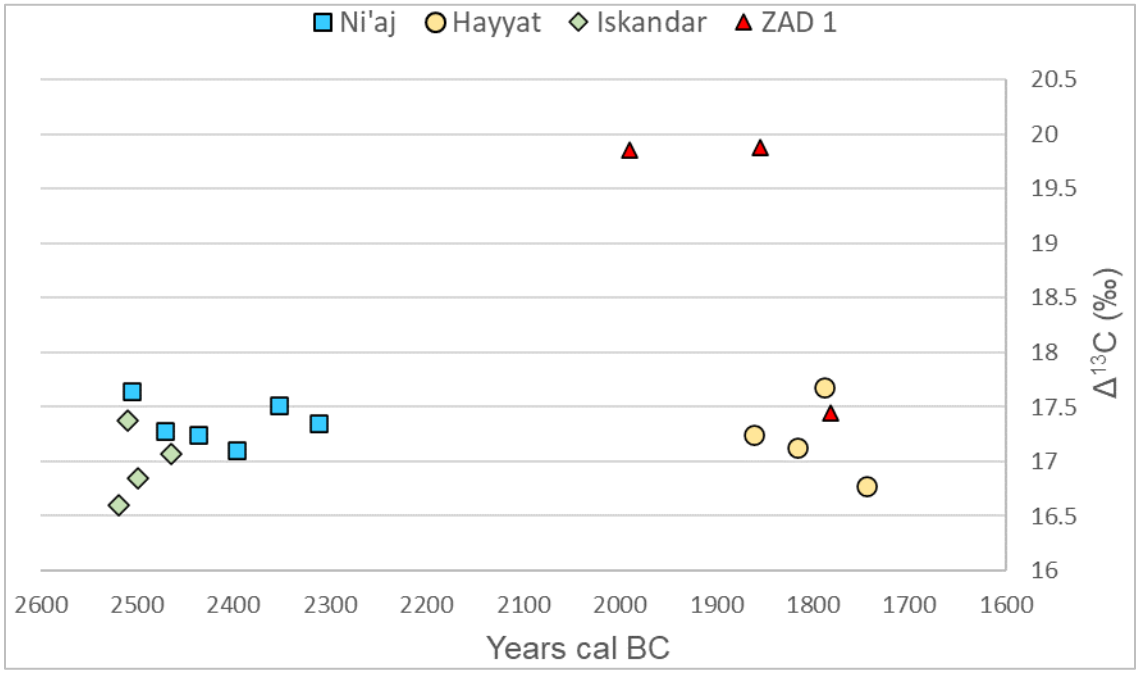

Figure 9.20 Comparison of mean $\Delta^{13}C$ values by phase for *Hordeum vulgare* seeds from Tell Abu en-Ni'aj (blue), Tell el-Hayyat (yellow), Khirbat Iskandar (green), and Zahrat adh-Dhra' 1 (red) plotted using median phase ages.

Figure 9.21 shows the mean $\Delta^{13}C$ per phase for *Triticum dicoccum*. *T. dicoccum* follows a similar trend, with values hovering around 17‰ for all three sites except ZAD 1, which had notably higher values around 18‰. However, there is a slight downward trend from EB IV Ni'aj and Iskandar to MB II Hayyat.

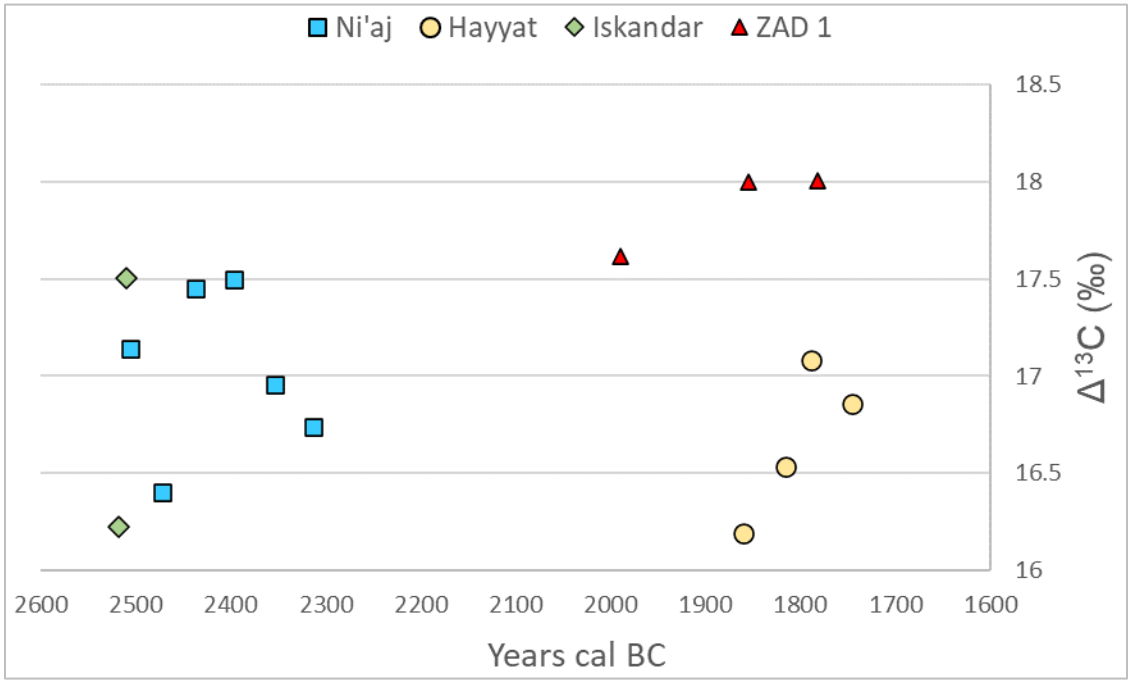

Figure 9.21 Comparison of mean $\Delta^{13}C$ values by phase for *Triticum dicoccum* seeds from Tell Abu en-Ni'aj (blue), Tell el-Hayyat (yellow), Khirbat Iskandar (green), and Zahrat adh-Dhra' 1 (red) plotted using median phase ages.

Figure 9.22 compares mean $\Delta^{13}C$ and $\delta^{15}N$ values from each site for the two cereal cultigens found at all four sites, *Hordeum vulgare* and *Triticum dicoccum*. Values from four modern *Triticum dicoccum* samples are included as a reference. Notable patterns include the closely overlapping mean ranges of $\Delta^{13}C$ and $\delta^{15}N$ values for both cereals at Ni'aj and Hayyat and the $\Delta^{13}C$ range from Iskandar. *Hordeum vulgare* from Iskandar stands out as particularly low in $\delta^{15}N$, while both cereals at ZAD 1 stand out as relatively high in terms of both $\Delta^{13}C$ and $\delta^{15}N$ values. The modern wheat samples sit at a mean $\Delta^{13}C$ of roughly 17‰ and a mean $\delta^{15}N$ of roughly 0‰. Most importantly, this suggests that modern, non-manured regional cereals can have a nitrogen signal much lower than the carbonized seeds from all four of the focal sites.

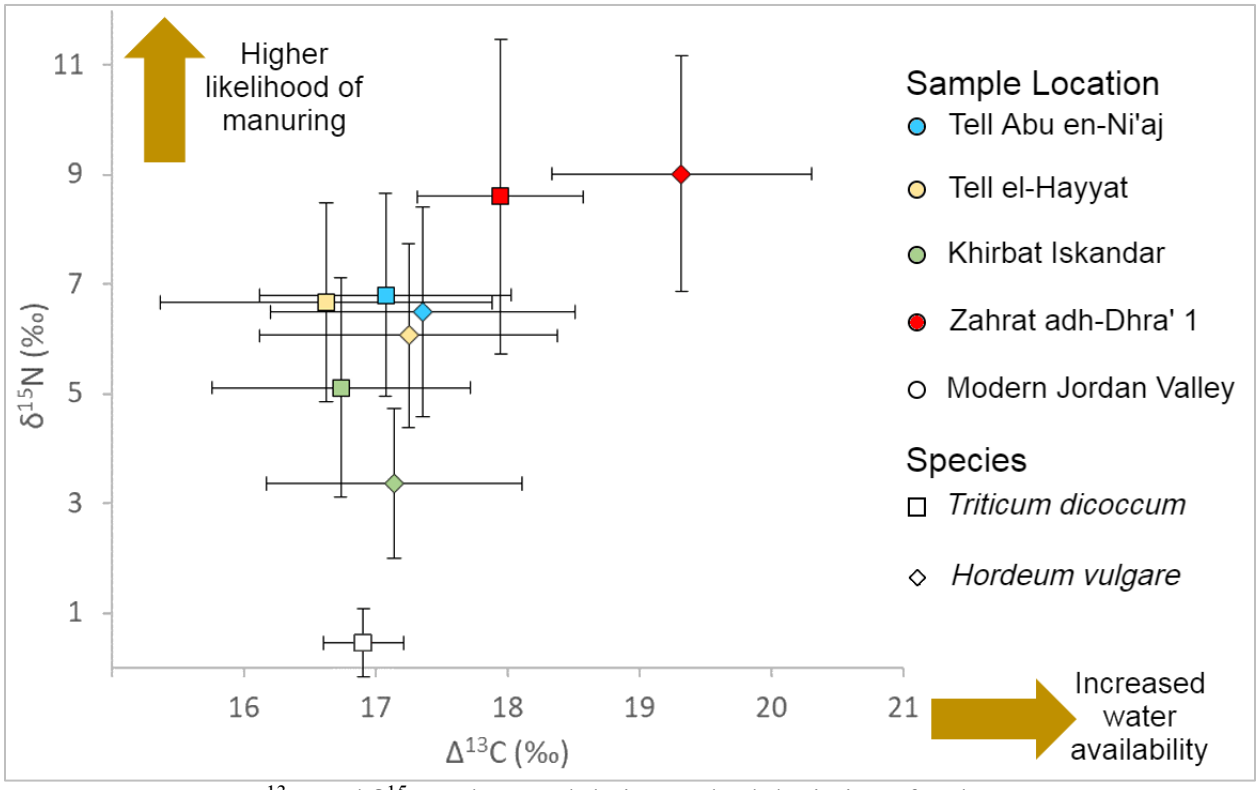

Figure 9.22 Mean $\Delta^{13}C$ and $\delta^{15}N$ values and their standard deviations for the most common Bronze Age cereal crops compared to modern *Triticum* from Jordan. Archaeological sites are Tell Abu en-Ni'aj (TAN), Tell el-Hayyat (TH), Khirbat Iskandar (KI), and Zahrat adh-Dhra' 1 (ZAD 1), Jordan. Error bars indicate 1σ confidence intervals.

Median $\Delta^{13}C$ values of *Hordeum vulgare* and *Triticum dicoccum* at each site are plotted with box-plots to further aid in interpretation. Figure 9.23 shows the box-and-whisker plot for *H. vulgare* with water-availability bands identified by Wallace et al., (2013; 2015). Median values are clearly distinct as falling in the well-watered range for ZAD 1, while the overall signal from all three other sites is of poorly- to moderately-watered *H. vulgare.*

Figure 9.24 shows the same comparison and the same general trend for *Triticum dicoccum.* The pattern reflects the heightened $\Delta^{13}C$ values at ZAD 1 over those from all three of the other sites, providing more detail for the pattern from Figure 9.22. It is also notable that all four focal sites feature well-watered *T. dicoccum.*

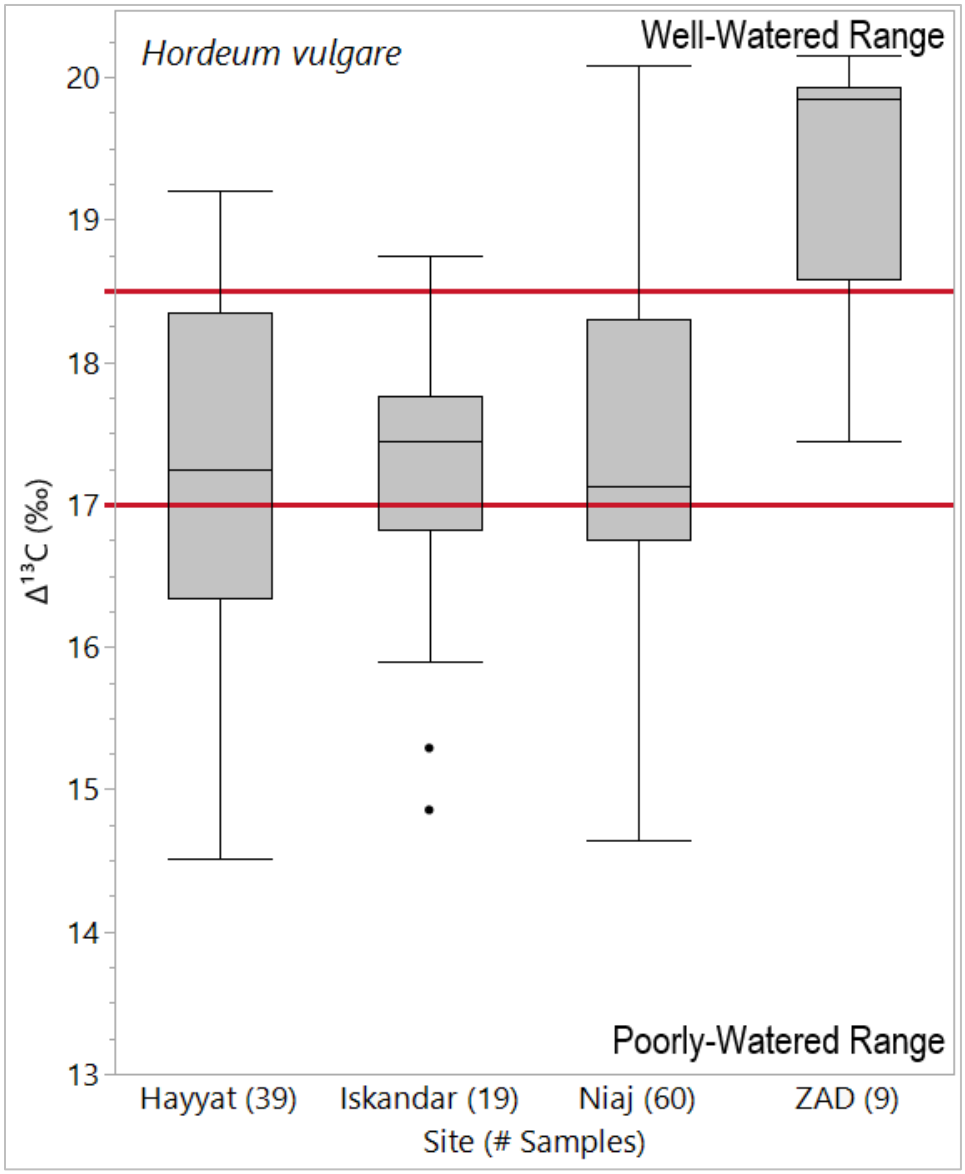

Figure 9.23 Box-and-whisker plots of $\Delta^{13}C$ medians and quartiles for *Hordeum vulgare* from Tell Abu en-Ni'aj, Tell el-Hayyat, Khirbat Iskandar, and Zahrat adh-Dhra' 1, Jordan. The number of samples per phase is indicated in parentheses. Moderately-watered range (from Wallace et al., 2015) for each taxon is bounded by red lines. The poorly-watered range lies below the lower red line and the well-watered range lies above the upper red line.

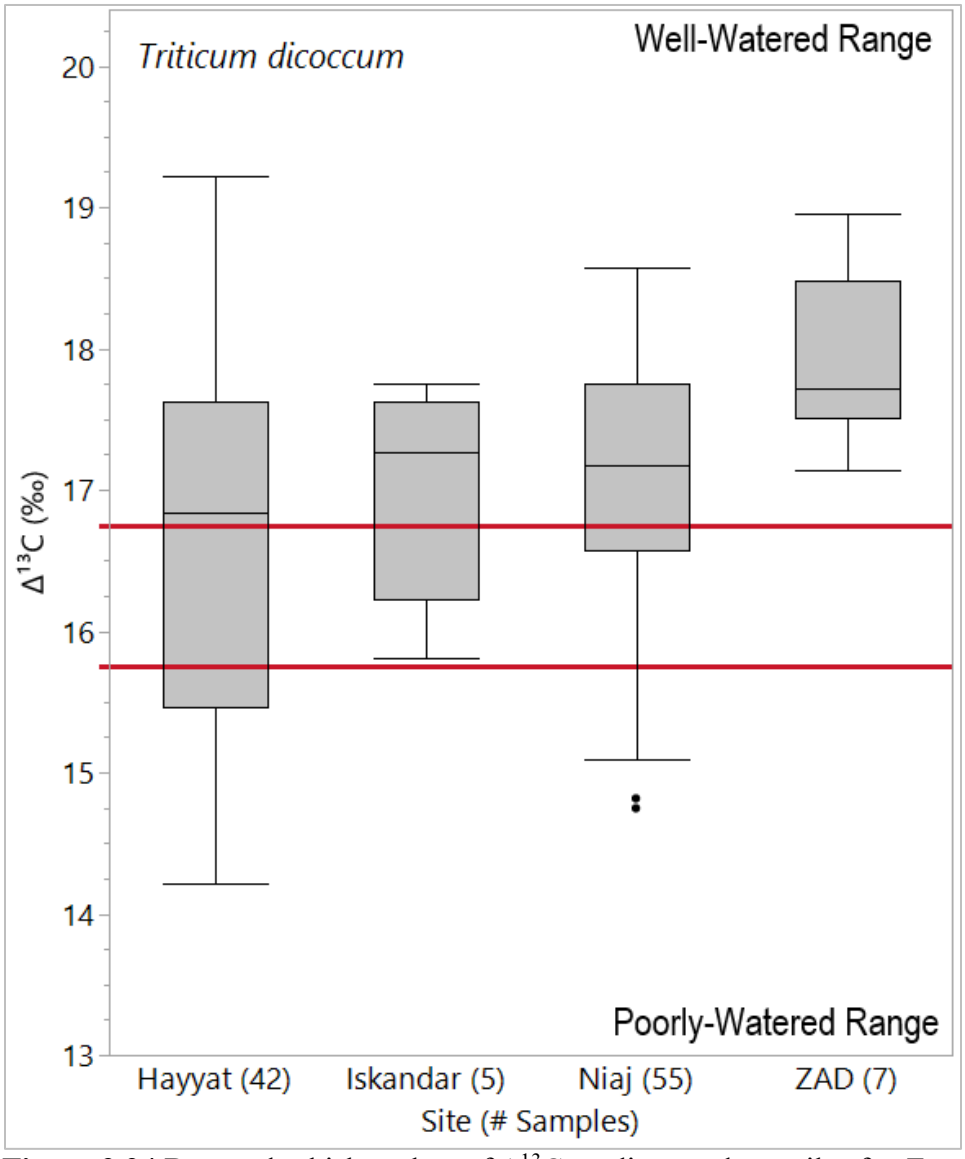

Figure 9.24 Box-and-whisker plots of $\Delta^{13}C$ medians and quartiles for *Triticum dicoccum* from Tell Abu en-Ni'aj, Tell el-Hayyat, Khirbat Iskandar, and Zahrat adh-Dhra' 1, Jordan. The number of samples per phase is indicated in parentheses. Moderately-watered range (from Wallace et al., 2015) for each taxon is bounded by red lines. The poorly-watered range lies below the lower red line and the well-watered range lies above the upper red line.

Discussion

Tell Abu en-Ni'aj

Stable isotopic values are determined for samples from Ni'aj for all major cereals as well as common fruit, pulse, and oil crops. Given the estimated difference of carbon fractionation in

cereal grains, *Hordeum vulgare* $\Delta^{13}C$ should be around 1.25‰ higher than *Triticum dicoccum* when grown in the same environmental conditions (Heaton et al., 2009; Konvalina et al., 2011). The difference between these taxa suggests that they are receiving different amounts of water, with *H. vulgare* experiencing relatively more drought stress than *T. dicoccum* (see Figure 9.22). The overlap of $\Delta^{13}C$ from *T. monococcum* with *T. dicoccum* is also suggestive of slight differences in water availability, with the $\Delta^{13}C$ of *T. monococcum* expected to be roughly 0.75‰ higher than those for *T. dicoccum* if these taxa were grown under similar conditions (Heaton et al., 2009). This may be indicative of seasonal cropping of taxa like *T. monococcum*, which prefers dry cultivation compared to emmer or bread wheat and is suitable for fall/winter production (McCreery, 1980; Zohary and Hopf, 1988).

Mean values of cereal $\delta^{15}N$ values tightly cluster for all grains around approximately 6-7‰, with *Triticum dicoccum* maintaining the highest values among wheat taxa and *Hordeum vulgare* the highest among barley taxa. Nitrogen values have not been shown to be notably distinct between cereal taxa, but cereal values around 5-6‰ or higher are generally indicative of high soil nitrogen availability for the semi-arid Eastern Mediterranean, so are indicative of manure application (Bogaard et al., 2007; Kanstrup et al., 2011). Based on the consistency of $\delta^{15}N$ values across all cereals from Niʻaj, it may be inferred that these crops were grown in fields with similar soil-nutrient conditions. It may also be that some cereals were intermixed in the same fields, or farmed in the same fields between different crop rotation cycles.

For the temporal variance of *Hordeum vulgare,* water availability remains low to moderate across the first six phases at Niʻaj, near the threshold for poorly-water conditions (Wallace et al., 2013; 2015). There is a considerable amount of variability in Phase 7, indicating that water availability may have fluctuated more profusely early in EB IV, which could be

attributed to a number of factors including field position, sowing date, or climate variations associated with environmental conditions. *Triticum dicoccum*'s water availability varied slightly less, with only two phases suggesting moderately- to well-watered conditions and four suggesting well-watered conditions (see Figure 9.5). It can be suggested that *T. dicoccum* was relatively well maintained and generally received enough water throughout the site's occupation given this taxon's high nitrogen and carbon stable isotope values. The heightened water availability for *Triticum* may indicate a higher prioritization for *T. dicoccum* and less reliance on *H. vulgare* at Ni'aj, as the water availability needs for the drought-intolerant species were met for *T. dicoccum*. While this contradicts the paleoethnobotanical analysis, suggestive of increased *Hordeum vulgare* reliance, it nevertheless appears likely that *T. dicoccum* was more heavily managed at Ni'aj.

Among fruit taxa, *Vitis vinifera* has relatively higher mean $\Delta^{13}C$ and $\delta^{15}N$ values with high variability in $\delta^{15}N$. *Vitis* also may be indicative of well-watered conditions at Ni'aj, given a notably higher relative mean $\Delta^{13}C$ value compared to the other focal sites. *Olea europaea* has the lowest $\Delta^{13}C$ mean value of all cultigens and a lower $\delta^{15}N$ value than other fruits, but $\Delta^{13}C$ may be suggestive of moderate to well-watering (Ehrlich et al., 2022). *Olea* wood is relatively well-represented in stable isotope studies (Bronk Ramsey et al., 2002; Golani and Segal, 2002; Fiorentino et al., 2008), but the signal in seeds is less well known and not all studies have incorporated nitrogen, so a threshold for $\delta^{15}N$ values is not known. It appears *Vitis vinifera* was well maintained at Ni'aj, but it is not clear if *Olea europaea* or *Ficus carica* were managed to the same extent.

For cultivated pulse taxa, comparisons are drawn between the pulses *Lens culinaris, Lathyrus sativus,* and *Pisum sativum*. The $\Delta^{13}C$ values expected under similar watering conditions

between pulse taxa have not been well established, but *L. culinaris* has received some previous study which suggests it to have similar watering thresholds of *Triticum aestivum* (Wallace et al., 2013; Bogaard et al., 2018a). Values of $\Delta^{13}C$ may thus suggest that *Lens culinaris* were cultivated under moderate to well-watered conditions. There is variation in the signals of other pulse taxa, indicating a range of soil nutrients and water availabilities, but not enough is known about these species' metabolic effects to determine thresholds for nutrient or water availability. It seems likely that pulses were not manured to the same degree as cereal crops, or that they received no manuring at all given that values recorded in modern, unfertilized pulses fall around 1-3‰ (Bogaard et al., 2013; Vaiglova et al., 2014; Bogaard et al., 2018a; Stroud et al., 2021). Thus, the primary trends are low to moderate soil nutrient availability for all pulses and a moderate to high signal of water availability for at least *Lens culinaris*.

Tell el-Hayyat

The stable isotopic data from Hayyat suggest patterns similar to those of Ni'aj for most taxa (see Figures 9.6-9.9). Cereal grains had high soil nutrient levels for all taxa, likely indicative of manuring (Bogaard et al., 2007; Kanstrup et al., 2011). Values of $\Delta^{13}C$ around 16-17‰ for *Triticum* generally are suggestive of moderately- to well-watered conditions, while values in the same range for *Hordeum* suggest poorly- to moderately-watered conditions (Wallace et al., 2013; 2015). A slight gap around 1‰ in $\Delta^{13}C$ values between *Hordeum vulgare* and *Triticum dicoccum* suggests more similarity in the water availability of the two genera, which is reflected as slightly lower water-availability for *Triticum dicoccum* at Hayyat (see Figure 9.22). *Triticum dicoccum* maintained a median value above the well-watered threshold but a mean value well within the moderately-watered range, suggesting some water stress for the crop (Wallace et al., 2013; 2015)

The cereals that plot higher in mean $\delta^{15}N$ are *T. monococcum* and *H. vulgare* var. *hexastichum*, which may indicate growth in different fields or a different manuring regime, but each suggest potentially increased manure application. Comparing $\Delta^{13}C$, *Triticum monococcum* should have a value roughly 0.5‰ higher value than *Triticum aestivum* growing in the same watering conditions (Heaton et al., 2009). A value roughly 0.5‰ lower than *T. aestivum* for *T. monococcum* thus suggests it experienced more drought stress, potentially indicative of winter rather than fall sowing and thus a later spring harvest when water was scarce. Part of this difference can be attributed to the negative correlation between manuring and the $\Delta^{13}C$ signal, which could indicate that only soil nutrient availability was increased (Maxwell et al., 2014). However, this trend occurred at both Ni'aj and Hayyat, so it seems more likely that this is related to time of harvest. It may also be that *T. monococcum* received more soil nutrient application in recognition of the difficulty in growing this crop.

Water availability trends at Hayyat though time indicate that variability was pronounced, with inner quartile ranges for *Hordeum vulgare* and *Triticum dicoccum* spanning nearly 2‰ for each phases (see Figure 9.10). Nearly all values for *Hordeum vulgare* fall below the well-watered threshold, with the lowest water availability indicated by poorly- to moderately-watered conditions in Phase 2, suggesting that at least mild drought conditions persisted well into MB II (Wallace et al., 2013; 2015). However, this pattern differs from that of *Triticum dicoccum*, which in the latter two phases showed indications of a moderate to high trend in water availability (Wallace et al., 2013; 2015). The heightened water availability for Phase 4-2 *Triticum* indicate a higher prioritization for *T. dicoccum* at Hayyat. This likely points to more resources and energy being utilized for production of high-yield wheat crops.

Between the fruit taxa, values of $\Delta^{13}C$ and $\delta^{15}N$ are highly distinct. The high values of $\delta^{15}N$ in *Olea europaea* strongly suggest the possibility of nutrient additions when compared to the values from Ni'aj. *Vitis vinifera* and *Ficus carica* may indicate manure input based on relatively high values compared to the other focal sites and compared to the wild taxa *Pistacia terebinthus*. In combination, these suggest that orchards were well maintained at Hayyat.

More overlap is apparent among $\Delta^{13}C$ and $\delta^{15}N$ values from the pulses in comparison to cereals or fruits from Hayyat (see Figure 9.9). The two common pulse crops *Lens culinaris* and *Pisum sativum* have clearly overlapping ranges of both $\Delta^{13}C$ and $\delta^{15}N$. Values of $\delta^{15}N$ around 3‰ indicate low soil nutrient availability and suggest low or potentially negligible nitrogen application, as this is only slightly higher than the signal of around 1-3‰ that may be expected in wild plants (Bogaard et al., 2013; Vaiglova et al., 2014; Bogaard et al., 2018a; Stroud et al., 2021). Values of $\Delta^{13}C$ for *Lens culinaris* suggest a water availability around the moderate to well-watered threshold, similar to that of wheat (Wallace et al., 2013; 2015). The crop may have received some management at Hayyat, but it is not evident if that included both water management and nutrient additions.

Prosopis farcta, used as a wild comparison, very likely did not receive manuring or water application given its lack of cultivation, but has relatively high $\delta^{15}N$ values for the pulses, approaching 5‰. This may be attributable to it being more of a woody shrub, as high $\delta^{15}N$ values are common for wild woody species in arid climates (Evans and Ehleringer, 1994; Handley et al., 1994; Gatica et al., 2017). However, it is possible *P. farcta* experienced some level of supplemental nutrient and water application due to its proclivity to grow in fallow fields or along the margins of arable fields (Zohary, 1950; Felker and Moss, 1996; Wasylikowa and Kolinski, 2013).

Khirbat Iskandar

The $\Delta^{13}C$ values of *H. vulgare* at Iskandar suggest a low to moderate water availability (see Figure 9.11; Heaton et al., 2009; Wallace et al., 2013; 2013). Comparing the primary cultigens at Iskandar, *Hordeum vulgare* maintains similar values of $\Delta^{13}C$ compared to those for *Triticum dicoccum*. The roughly 0.1‰ difference falls far below the estimated 1.25‰ difference between these species (Heaton et al., 2009; Konvalina et al., 2011) and suggests water availability differences for the crops. *H. vulgare* also has a notably lower $\delta^{15}N$ value than the other three focal sites, indicative of low to moderate soil nutrient availability, with a mean value around 3‰, which has been used to indicate manuring in the past but is not necessarily indicative of intensive manuring (Bogaard et al., 2013; Stroud et al., 2019). For *Triticum dicoccum*, $\delta^{15}N$ values fall roughly around similar values to those observed at Ni'aj and Hayyat, with a mean $\delta^{15}N$ around 5‰. This indicates moderate to high soil nutrient availability and is suggestive of manuring (Bogaard et al., 2007; Kanstrup et al., 2011).

From these comparisons, it is evident that *Hordeum vulgare* and *T. dicoccum* were cultivated in fields with different soil conditions and may have been cultivated at different times. The higher water availability and nutrient availability for *Triticum dicoccum* grains and relatively low values of each variable from *Hordeum vulgare* suggests a strong dichotomy between the management of these two prominent cereals. These results could even suggest that *H. vulgare* was not a very important crop for farmers at Iskandar, which could be evaluated via a paleoethnobotanical analysis.

Vitis vinifera from Iskandar was only represented by two seeds, but their mean $\Delta^{13}C$ values of roughly 20‰ fall only slightly below the values determined for seeds from Ni'aj and Hayyat. *Vitis vinifera* across all focal sites seems to have a wide range of $\Delta^{13}C$ and $\delta^{15}N$ values. This

variability can be partially attributed to the low sample sizes of *V. vinifera* analyzed at all four focal sites, but given how high the variation is it could suggest that certain plots received heightened levels of management. This would also suggest cultivation in separate locations and by separate peoples, as would occur if the crop was being managed more independently.

The pulse crops *Lens culinaris*, *Pisum sativum,* and *Cicer arietinum* have similar mean values of both $\Delta^{13}C$ and $\delta^{15}N$. Low values of $\delta^{15}N$ around 2‰ indicate low soil nutrient availability and likely indicate a lack of manuring (Bogaard et al., 2013; Vaiglova et al., 2014; Stroud et al., 2021). The low $\Delta^{13}C$ values relative to Ni'aj and Hayyat also suggest potentially low to moderate water availability, particularly for *L. culinaris*. Given the low value of both variables, it can be inferred that farmers put less effort into managing the cultivation of pulses at Iskandar.

Zahrat adh-Dhra' 1

At Zahrat adh-Dhra' 1, values of $\Delta^{13}C$ and $\delta^{15}N$ for the cereal crops were far more distinct than those from previous sites (see Figures 9.15-9.18). The wheat crop *Triticum aestivum* has a $\delta^{15}N$ indicative of moderate to high soil nutrient content, but the $\delta^{15}N$ for both *Hordeum* and for *T. dicoccum* reached around 9‰ and suggest a very high soil nutrient content indicative of manuring (Bogaard et al., 2007; Kanstrup et al., 2011). Though all cereal taxa have high $\delta^{15}N$ values, the discrepancy between taxa may suggest cultivation of *Hordeum* sp. and both *Triticum* species in separate fields.

The high $\Delta^{13}C$ values for several species suggest high water-availability. This includes *Hordeum vulgare, Triticum dicoccum,* and the relatively drought-intolerant *Triticum aestivum* (Wallace et al., 2013; 2015). *Hordeum vulgare* var. *nudum* is the only cereal that falls relatively lower, with a mean value possibly sitting below the well-watered threshold for this species,

based on comparisons of *Hordeum* species and the phenology of naked cereals (Kanstrup et al., 2011; Djelel et al., 2020). Values of $\Delta^{13}C$ for both *Hordeum vulgare* and *Triticum dicoccum* are roughly 2‰ higher than those from the other three focal sites, but are not necessarily high enough to clearly indicate irrigation, which has been shown in modern experiments to drive cultivated crop $\Delta^{13}C$ values up anywhere from 1.5-5‰ compared to unirrigated values (Araus et al., 1997a; Gomez-Alonso and Garcia-Romero, 2008; Foulkes et al., 2016). However, they suggest a clearly heightened cereal management strategy existed at the site.

Regarding irrigation, the archaeological site of Zahrat adh-Dhra‘ 1 sits far above the adjacent wadis, which would be inopportune for the use of floodplain irrigation. First, evidence of extreme incision rates in the valley have been noted in modern times relating to the recent drops in the Dead Sea level (Bowman et al., 2010), so it is posited that the site sat much closer to streambank level in past. Second, increased floodplain alluviation is noted to have occurred throughout the Levant during EB IV (Rosen, 1995, as cited in Rosen, 2007), and could have supported soil health at this location through increased alluvial deposition during floods (Boettinger, 2005). Under these hypothesis, the two wadis may have provided substantial water availability and more fertile soils, needed for a sedentary agricultural settlement to survive here in the MBA. Another explanation for the high cereal $\Delta^{13}C$ values could be seasonal use, such as if cereals were only cultivated during the wettest portion of the year. However, this hypothesis is not supported by the rich presence of grapes, which take several years to fruit from initial sowing.

The proximity of ZAD 1 to tributaries of the Wadi al-Karak, the very high values of cereal $\delta^{15}N$ from manuring, and the potential lack of agriculture outside of the winter/early spring may help to explain the high $\Delta^{13}C$ values of cultigens. This settlement location may have

been chosen specifically due to its optimal location for agriculture, sitting between the Wadi Dhra‘ and Wadi Wa’ida and amidst landscape of multiple other intermittent tributaries of the Wadi al-Karak (Fall et al., 2019; 2023). The high $\delta^{15}N$ values for *Hordeum* sp. and *Triticum* sp. are likely skewing the $\Delta^{13}C$ values from these taxa even higher. Nevertheless, these results help support an inference of intensified agricultural management at ZAD 1.

Vitis vinifera maintains values of $\Delta^{13}C$ and $\delta^{15}N$ roughly comparable to those of Ni‘aj and Hayyat, indicative of slightly lower relative soil nutrient availability and slightly lower relative water availability. However, values may still suggest management of *Vitis vinifera* at this site. Values of $\Delta^{13}C$ and $\delta^{15}N$ for pulses like *Pisum sativum*, however, fell further below those from *Pisum sativum* at Ni‘aj and Hayyat, with values suggesting relatively less water and soil nutrient availability. Few *Lens culinaris* were recovered from ZAD 1, and none sampled, which in combination with these low values for *P. sativum* suggest that pulses may not have been managed intensively at ZAD 1.

Summary

Values of $\Delta^{13}C$ and $\delta^{15}N$ from both Tell Abu en-Ni‘aj and Tell el-Hayyat suggest an environment of moderate drought stress present from Early Bronze IV through Middle Bronze II, with limited water availability for the production of cereal crops. Sustained, low values of $\Delta^{13}C$ relative to categories of *Hordeum vulgare* water availability suggest that drought stress was prevalent at three of the four focal sites, while moderate to high water-availability signals for *Triticum dicoccum* suggest that farmers were able to provide for the water needs of at least some of their crops through management of water resources.

The seasonal differences from cereals harvested in winter versus spring might partially account for the distinctions in $\Delta^{13}C$ between barley and wheat. *Hordeum* taxa have a shorter growing season than *Triticum,* so could be sown later in the winter to early spring and still be harvested in time to avoid the worst of the summer drought (Leonard and Martin, 1970, as cited in Chernoff, 1988; Rawson et al., 1988). However, *H. vulgare* and *T. dicoccum* often appear in high densities in the same samples and contained similar $\delta^{15}N$ values at each site, so these taxa may have been cultivated simultaneously in at least some seasons.

A key interest in this study is the $\Delta^{13}C$ and $\delta^{15}N$ values from Zahrat adh-Dhra‘ 1, which tell a very different story than the results from the other sites. ZAD 1 sits in what should be a relatively arid climate (Black et al., 2011; Soto-Berelov et al., 2012; Fall et al., 2018), but the seeds indicate well-watered conditions for most cereal species. Given their high $\Delta^{13}C$ values, it is clear that the water requirements of the primary cereal crops were being met. However, there are still indications that water availability was a challenge. The $\Delta^{13}C$ values of *H. vulgare var. nudum* and each pulse cultigen is evidence of at least a moderate drought stress, while the array of wild taxa suggests a more dry, open landscape surrounds the site.

As a final note on cereal cultivation is the importance of *Hordeum*. The signal of heightened manuring for *Hordeum* crops suggests potentially more intensive cultivation of *Hordeum* than other non-cereal cultigens for these Jordan Rift settlements. This would make less sense if this taxa was not designed for human consumption rather than being fed to or grazed upon by livestock. This suggests a reliance on barley cultivation for food rather than fodder.

For fruits and pulses, the stable isotope signals help provide evidence for the selective intensification of certain crops at certain sites. The two Dead Sea area settlements exhibit pulse crops with a lower $\Delta^{13}C$ water availability signal than for those from the northern Jordan Valley,

which follows expectations based on modern rainfall isohyets. Almost all pulse crops display low $\delta^{15}N$ values suggestive of low to no manuring and, combined with the low macrofossil counts, likely signify a lower relative importance for the cultivation of these crops in the Southern Levantine Jordan Rift.

Vitis vinifera may have been one of the few non-cereal cultigens that was more intensively managed in the valley, as it may have received management at Ni'aj, Hayyat, and ZAD 1. *Vitis vinifera* seeds had relatively high $\delta^{15}N$ compared to values from Iskandar and modern values from experimentally cultivated fields even in gravelly vineyards. These experiments suggest values of $\delta^{15}N$ higher than around 3‰ are attributable to organic nitrogen and manure application (Santesteban et al. 2015). Prioritized water management for *V. vinifera* also likely occurred at ZAD 1, and would agree with findings from the macrofossil analysis that showed relatively heightened cultivation of *V. vinifera*.

Overall, the largest distinction was the geographical distinction between management in the northern Jordan Valley and Dead Sea Valley. The Dead Sea Valley settlements, specifically the lower Dead Sea Valley settlement, was more indicative of dry environments than the northern Jordan Valley settlements.

In terms of crop management, the intensification of crop management appears to be offsetting the stable isotope signals expected in some cereal crops. This points to a knowledge of climate impacts and associated strategies for continued agricultural practice. Crop management through manuring and floodplain irrigation or selective cropping near water sources appears to be applied during the Early to Middle Bronze Age. Regarding cultivation strategies, three distinct patterns of cultivation emerge based on which species received water and soil nutrient management. Ni'aj and Hayyat had management of a wide array of cereals, a selection of pulses,

and several common fruits. ZAD 1 applied careful management of grapes and select cereals, particularly *Hordeum vulgare*, *Triticum aestivum,* and *T. dicoccum*. Meanwhile, evidence available from Iskandar suggests intensive management of only its primary wheat crop, *T. dicoccum*.

CHAPTER 10: INTERREGIONAL INTERPRETATIONS AND DISCUSSION

Introduction

This chapter serves to integrate the results from the prior chapters and draw overarching conclusion about the Bronze Age Jordan Valley. Comparisons are discussed first within the Southern Levantine Bronze Age and then in the wider Eastern Mediterranean in order to frame my focal sites into a wider regional context. Data for these comparisons stem from a host of sources including primary literature (e.g., Miller, 1991; Riehl et al., 2014) and online data repositories like the *Archaeobotanical Database of Eastern Mediterranean and Near Eastern Sites* (ADEMNES, 2015). The composition of flora cultivated in early agrarian societies and the framework of Eastern Mediterranean climate change are considered in order to help address my original questions. These questions are: how did cultivation trends shift between the Early to Middle Bronze Ages at these Southern Levantine settlements, and what effect did climate change have on both the environment and agricultural practices in the region surrounding the 4.2 ka BP event in late Early Bronze IV? A map of the sites used for regional comparison is provided in Figure 10.1.

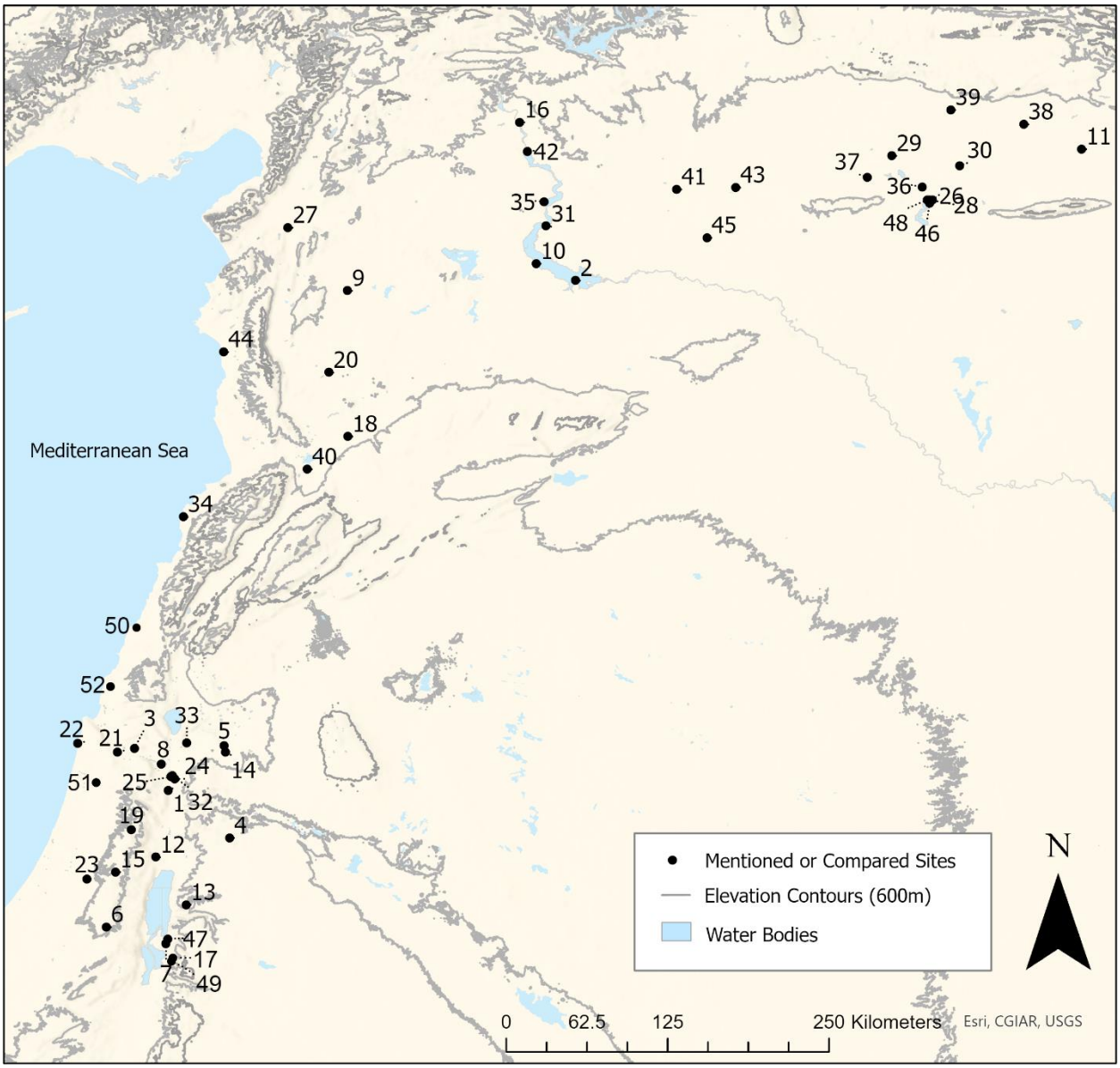

Figure 10.1 Archaeological sites referred to in comparisons in Chapter 10: 1 - Abu Hamid, 2 - Abu Hureyra, 3 - 'Afula, 4 - Ain Ghazal, 5 - Ain Rahub, 6 - Arad, 7 - Bab edh-Dhra', 8 - Beth-Shean, 9 - Ebla, 10 - Emar, 11 - Hamoukar, 12 - Jericho, 13 - Khirbat Iskandar, 14 - Khirbet ez-Zeraqon, 15 - Manahat, 16 - Mezraa Teleilat Hoyuk, 17 - Numeira, 18 - Qatna (Tell Mishrifeh), 19 - Shiloh, 20 - Shir, 21 - Tel Megiddo, 22 - Tel Nami, 23 - Tel Yarmuth, 24 - Tell Abu al-Kharaz, 25 - Tell Abu en-Ni'aj, 26 - Tell al-Raqa'i, 27 - Tell Atchana, 28 - Tell Atij, 29 - Tell Beydar III, 30 - Tell Brak, 31 - Tell el'Abd, 32 - Tell el-Hayyat, 33 - Tell esh-Shuna, 34 - Tell Fadous-Kfarabida, 35 - Tell Halula, 36 - Tell Kerma, 37 - Tell Kuran, 38 - Tell Leilan, 39 - Tell Mozan, 40 - Tell Nebi Mend (Qadesh), 41 - Tell Sabi Abyad, 42 - Tell Shioukh Faouqani, 43 - Tell Tawila, 44 - Tell Tweini, 45 - Tell Zeidan, 46 - Umm Qseir, 47 - Zahrat adh-Dhra' 1, 48 - Ziyade, 49 - Ras an-Numeyra, 50 - Sidon, 51 - Tell el Ifshar, 52 - Tell Kabri.

Discussion of Jordan Valley Cultivation Trends

Focal Site Comparisons

This section briefly presents the results of intersite comparisons between the carbonized floral assemblages of Tell Abu en-Ni‘aj, Tell el-Hayyat, and Zahrat adh-Dhra‘ 1, discussed in Chapters 4-6. This will be integrated into a more detailed summary of the focal site patterns in the following section.

Figure 10.2 uses ratios to illustrate distinctions in the agricultural focus of each settlement based on comparisons of four plant categories. At Tell el-Hayyat, the total proportion between the overall presence of *Hordeum* and *Triticum* is the closest to an even split that was reached at any of the three settlements, with each showing a preference towards *Hordeum*. At Ni‘aj and ZAD 1 there are distinctly higher frequencies of *Hordeum*. Hayyat existed in the Middle Bronze II and in the northern Jordan Valley, putting it in a more humid environment than either Ni‘aj or ZAD 1, which has been hypothesized to explain this pattern.

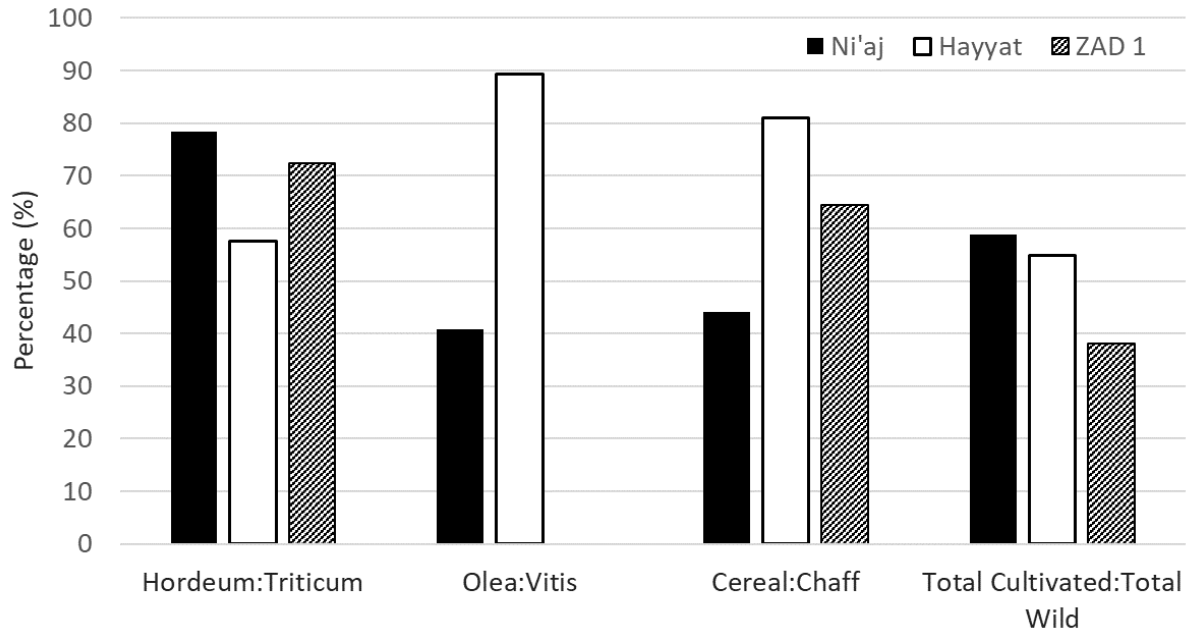

Figure 10.2 Ratios based on NISP of *Hordeum : Hordeum + Triticum*, *Olea : Olea + Vitis,* Cereal : Cereal + Chaff, and Cultivated : Cultivated + Wild Plant Fragments from Tell Abu en-Ni‘aj, Tell el-Hayyat and Zahrat adh-Dhra‘ 1, Jordan.

The evidence for fruit cultivation shows clear distinctions between the three sites. Hayyat was focused primarily on olive cultivation in the Middle Bronze Age, whereas ZAD 1 to the south was focused entirely on grapes. The evidence for olive cultivation is by far greatest at Hayyat (see Table 5.1), with its 532 olive remains, many of which were unbroken stones. Hayyat also provides evidence of grape production, as its 64 grape remains gives it a higher density than Ni‘aj. On the other end of the spectrum is ZAD 1, which had no olive presence at the site and a significantly greater reliance on grape cultivation, with 110 remains constituting almost 20% of the assemblages of Phases 3-2. Compared to Hayyat or ZAD 1, Ni‘aj had a fairly even assortment of both fruits, with neither standing out as particularly frequent among the macrofloral remains, but with enough remains of both to suggest managed cultivation by the community.

To examine larger trends, two additional comparisons were made, one to examine the ratios of all cereal crops to all chaff remains and one to compare the ratios of all cultivated to all wild taxa. One important observation is the relatively low chaff frequency and high cultivated crop frequency at Ni‘aj, which countered initial expectations. Being an EB IV settlement, Ni‘aj was expected to have relatively less agricultural focus and more foraging and utilization of wild plants to augment diet in what was hypothesized to be a drier period. However, Ni‘aj was a relatively larger settlement than either Hayyat or ZAD 1 and, though a wide array of wild plant taxa is indicated, Ni‘aj was clearly focused on agricultural production. The low ratio of cereal to chaff reflects the high quantities of chaff recovered from the site, which could be due to the integration of cereal processing by-products for dung-cakes or fuel.

The other notable characteristic about ZAD 1 is its lower abundance of cultivated crops. ZAD 1 clearly prioritized a few select cultigens, but the majority of plant remains were from wild species. This does accord with expectations for a site in an arid, agriculturally marginal region, and is likely indicative of less reliance on plant agriculture.

To further compare temporal trends in barley and wheat cultivation at the three focal sites, Figure 10.3 illustrates *Hordeum* to *Triticum* ratios per site plotted by median calibrated phase ages. The main trends are increased preference for barley at Ni'aj, shifts to more preference for wheat at Hayyat and ZAD 1, and generally greater reliance on wheat at Hayyat than at the other two settlements.

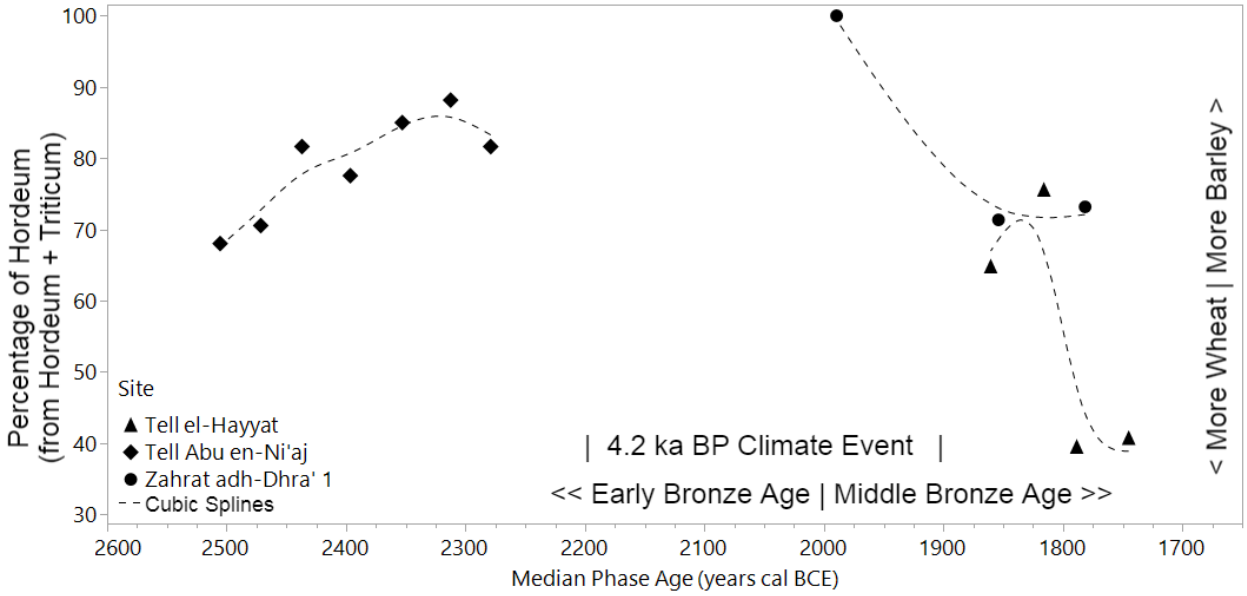

Figure 10.3 Ratios of *Hordeum* : *Hordeum* + *Triticum* NISP at each site plotted against median phase ages. Spline curves indicate the general trend of each site. Phases 6 and 1 from Tell el-Hayyat are omitted due to low sample sizes.

In Early Bronze IV, these ratios steadily climb into the low 80% range, indicating an increasing reliance on barley at Ni'aj. Given the relatively higher sample size per phase at Ni'aj (Table 4.1), the almost 10% increase between the early to middle EB IV and the consistent trend of much higher barley values are notable. There is a roughly 300-year gap in data between my

sites before the next data point in the Middle Bronze Age, starting around 1900 BCE. From 1900 to 1700 there is a wider scatter of points which range from around 40-75%, indicating a mixed reliance on both *Hordeum* and *Triticum* in the Middle Bronze Age.

The ratio from ZAD 1 in Phase 4 around 2000 BCE is anomalously high, as no wheat was found, and could be treated as an outlier. Regardless of whether this point is an outlier, the higher ratios around MB I-II transition at Hayyat and ZAD 1, and lower values around MB II, suggest a general decline in reliance on barley over time, and more preference for barley in EB IV at Ni'aj. At Hayyat, this trend is more apparent when focusing on Phases 5-2, which are far better sampled than Phases 6 and 1.

Notably, Hayyat and ZAD 1 have more pronounced changes between phases, with swings of almost 30% changes in the ratios of the two genera. Ratios at Ni'aj changed more gradually over almost 200 years, so the rapid change, particularly around MB I-II transition between Phases 5-4 and Phases 3-2 at Hayyat, could potentially be capturing a dramatic shift in agricultural cultivation preference.

Summary of Cultivation Trends at the Focal Sites

All three sites retained a rich array of field and orchard cultigens with the densities of *Hordeum* and *Ficus carica* indicating the most frequent plant taxa. In general, the most utilized cultigens are *Hordeum vulgare, H. vulgare* var. *nudum, Triticum dicoccum, T. aestivum, Vitis vinifera, Olea europaea,* and *Ficus carica.* Ni'aj and Hayyat prioritize a similar array of cultigens, with focus on *Hordeum vulgare* and *Triticum dicoccum*, all three fruit taxa, and a wider array of pulses, while at ZAD 1 the focus was on *H. vulgare* var. *nudum, T. aestivum,* the fruit crops *Ficus carica* and *Vitis vinifera,* and *Pisum sativum*.

Increased abundances of *Hordeum* and *Ficus carica* are apparent at all three sites, with the highest *Hordeum* to *Triticum* ratios appearing towards the end of EB IV and beginning of MB I. *Triticum* abundance eclipsed that of *Hordeum* only in the MB II phases of the northern Jordan Valley site Tell el-Hayyat, which could suggest more humid conditions. This follows the expectation of finding increased barley cultivation nearer the end of EB IV as an indication of drier conditions surrounding the 4.2 ka BP event.

ZAD 1 produced higher proportions of more drought-intolerant cereal varieties for both *Hordeum* and *Triticum* than at either Ni'aj or Hayyat, suggesting this southern site was able to meet water availability requirements for its fields during MB I and MB II. However, the arrays of wild taxa and charcoal point to a more arid environment than found at either of the northern Jordan Valley sites. This suggests that climate and location alone were not necessarily determinants of which taxa could be cultivated by any given community. Farmers at ZAD 1 had a preference for drought-intolerant taxa and were able to take measures to meet the water needs of these plants.

One curiosity is why there are more remains of *H. vulgare var. nudum* at ZAD 1 as they have a lower yield and are slightly more drought intolerant than *H. vulgare* (Sturite et al., 2019). This may be indicative of increased regional cultivation of *H. vulgare var. nudum* or local preference for production of this crop. Farmers may have simply preferred the crop due to its relatively higher drought tolerance compared to wheat (Tian et al., 2018; Djelel et al., 2020) and the ease of post-harvest processing in comparison to hulled cereals (Hillman et al., 1984; Lister and Jones, 2012). It could be that this taxon was more frequently consumed by animals and thus burnt in dung, which would explain their relatively lower $\Delta^{13}C$ and $\delta^{15}N$ values if they were less intensively managed, though values are still higher than would be expected from wild cereals.

For non-cereal cultigens, the importance of *Vitis vinifera*, *Olea europaea*, and *Ficus carica* has been suggested strongly in certain sites through the seed quantities, spatial patterning, and stable isotopic signals. These fruits could have been used for secondary products like oil, wine, or dried fruits, and the remains burnt, but it is likely much of their remains are due to consumption through animals. *Pisum sativum* and *Lens culinaris* may have also had a somewhat greater importance for the northern Jordan Valley settlements, but then is suggested by their seed densities, but stable isotopes suggest pulses may have only played a limited role in regional agriculture.

High densities of wild taxa, such as *Medicago/Onobrychis* or *Malva* at Ni'aj and Hayyat, appear to be more representative of grazing and may reflect local cultivation patterns and natural environments. They suggest grazing amid cultivated lands in the Jordan Valley and at ZAD 1. The arrays of cultivated taxa suggest slightly drier conditions at ZAD 1 compared to Hayyat, and wetter conditions at MB II Hayyat compared to MB I Hayyat or Ni'aj (Zohary, 1966; 1972; 1982; Feinbrun-Dothan 1978; 1986; Abu-Irmaileh, 1982; Riehl, 2010; Kreuz and Schäfer, 2011). However, it is evident that a drier ecosystem surrounded ZAD 1, including during MB II on the Dead Sea Plain, with the lands along wadis being uniquely conducive to agriculture. This understandably contrasts with the evidence from the northern Jordan Valley, as even today the gradient in vegetation moving from the northern to southern Jordan Valley is clearly apparent.

The trend from wild vegetation thus paints a picture of a semi-arid/arid steppe in the north, with open, anthropogenic landscapes through both EB IV and MB I-II, more akin to Irano-Turanian biogeography. This environment transitions into the foothills and likely out of the valley towards the south, as the lower valley becomes an arid scrub with drought and salt-tolerant vegetation more common and other vegetation clustered within the wadi bottoms.

Regarding seed densities, Ni‘aj had by far the highest seed densities from any of the focal sites. The densities did decline dramatically over time, but even later phases the site had densities comparable to Hayyat or ZAD 1. It is clear from these densities that Ni‘aj, as well as Hayyat, were agriculture intensive sites, and Ni‘aj was likely conducting larger-scale agricultural operations than at the other focal sites, at least in the early EB IV. ZAD 1, however, is also believed to be agriculturally intensive in at least Phase 3, around the MB I-II transition. The presence of potentially moderately- to well-watered *Vitis vinifera* at the site, a fall-fruiting crop with higher water requirements and more long-term maintenance than cereals or pulses (Riehl, 2009), supports an interpretation of a longer-term agricultural mindset at ZAD 1 (Lines, 1995). The spatiality of ZAD 1, potentially communally managing their grain and grape crops, further supports that this was an agriculturally-focused site.

Seed density at ZAD 1 may partially suggest decreased agriculture at the site. However, another reason for decreased seed quantity is the shallow, porous sediments at ZAD 1, which likely degraded some of the site’s macrofossil remains. Both carbonized seeds and animal bones were found to be in notably poor quality (Fall et al., 2019).

Finally, ZAD 1 presents a unique case of site use, and while abandonment is not the focus of this work, it is necessary to discuss this aspect in light of the evidence from this site. It is apparent that factors including the decline in sea level and the presence of salt-tolerant crops may shed light into the reason for the site’s abandonment. ZAD 1 sits at around 180 m b.s.l. In EB IV, a large regression of the Dead Sea occurred (Ken-Tor et al., 2004), as evidenced by gypsum and pebble deposits in the lower valley (Migowski et al., 2006; Kagan et al., 2015) and by increased EB IV river incision rates (Rosen, 1997). Given the location of ZAD 1, sitting on one of the lowest terraces and afront a steep scarp of the Dead Sea Basin, a knickpoint within this basin

could have strong downcutting potential (Dente et al., 2017). However, the timing of this phenomenon does not quite line up with the abandonment of ZAD 1 several centuries later. Geological data also suggests that by the Middle Bronze II, a rapid, large transgression was likely underway (Goldsmith et al., 2023), with a possible subsequent regression only occurring around the Late Bronze Age (Klinger et al., 2003; Migowski et al., 2006; Kagan et al., 2015). If the impact of the downcutting from the EB IV sea level decline was delayed until the mid to late Middle Bronze Age, then it could be responsible for the downcutting of local streams at ZAD 1. This seems unlikely as the EB IV regression is also slated as a potential cause for the gradual abandonment of nearby Khirbat Iskandar, several centuries earlier in mid EB IV (Richard, 2024), a settlement sitting much further up the valley.

A more plausible scenario for the abandonment of ZAD 1 could be related to the presence of the salt-tolerant *Aizoon* (Abu-Irmaileh, 1982). Highly saline soils would pose a large problem for agriculture (Qadir et al., 2000; Maggio et al., 2011) and could have led to a shift away from plant agriculture by Phase 2. If so, this would suggest that the abandonment of ZAD 1 was in part brought on by overexploitation of the settlement periphery by farmers. Further, though geological records suggest a sea level rise in Middle Bronze, rainfall models (Enzel et al., 2003; Soto-Berelov et al., 2015) do suggest a declining trend towards the end of the Middle Bronze Age, which would have increased the challenges of farming. Thus, a combination of factors including declining water level, salt leaching, or increasing drought conditions around MB III may be linked to the site's abandonment.

From macrofloral remains, it is evident that each of the agrarian settlements of Tell Abu en-Ni'aj, Tell el-Hayyat, and Zahrat adh-Dhra' 1 had their own trajectory in terms of how they focused their cultivation efforts. Ni'aj and Hayyat put emphasis on cereal production, with the

drought-tolerant *Hordeum vulgare* being the most abundant crop. Ni'aj appears to focus more on production of *H. vulgare,* while Hayyat spread its cereals between a larger array of wheat and barley taxa, but each has a healthy array of cultivated cereal, pulse, and fruit crops. ZAD 1, on the other hand, placed most of its attention to the management of its limited cereal crops, its grapes, and possibly pea cultivation.

Comparison with Macrofossil Assemblages from Other Regional Settlements

The array of crops found at the three focal sites from the paleoethnobotanical analyses generally mirrors that found at other Levantine sites (Helbaek, 1958; Zohary and Hopf, 1988; Liphschitz, 1989). Values from Early Bronze Age suggest a heavy reliance on *Triticum dicoccum* and diminished but high quantities of *Hordeum vulgare* through the EB III (Hopf, 1983). At Bab edh-Dhra', the dominant EBA crops mimic our sites very well, with *H. vulgare* and *T. dicoccum* most prominent, and *H. vulgare* var. *nudum*, *T. monococcum,* and *T. aestivum* appearing less frequently (McCreery, 2003a). A heavier reliance on wheat is noted at some Bronze Age sites, particularly to the north and in EB II or MB III (Melamed, 1996; Riehl, 2004; Fischer and Holden, 2006; Simchoni et al., 2007; Riehl and Orendi, 2019), but several suggest barley as a dominant crop from EB III to MB II (Mathias and Parr, 1989; Kislev, 1998). The combination of limited agricultural remains and a heavy focus on *T. aestivum* is noted at Tell Nimrin, another MB II settlement north of the Dead Sea (McCreery, 2003a). This is similar to the trend found at ZAD 1 in its limited cereal production with focus on a drought-intolerant variety, but few sites suggest dominant production of naked barley.

The ratio of barley and wheat is thought to be driven by differences in climate and water availability, with farmers opting to produce more barley crops, whether hulled or naked, when

drier conditions emerged in order to keep consistently high yields and produce enough food for the sedentary population. This characteristic has been used to support the notion that certain points in time were warmer or cooler (Fall, 1998). Figure 10.4 illustrates the *Hordeum* sp. and *Triticum* sp. ratios from a number of Levantine sites (primarily Southern Levantine) from the Early to Middle Bronze Age. Cereals across 16 regional settlements are plotted to show patterns of cultivation by early farmers. During EB IV in particular, but also MB I, there is a noticeable lack of sites prioritizing wheat cultivation. Data from recorded EB IV sites including Tell Nebi Mend, Bab edh-Dhra‘, Numeira, and Jericho show that higher ratios of barley production was more typical during this period (Hopf, 1978; 1983; Mathias and Parr, 1989; McCreery 2003a; 2003b). This lines up with similar findings from Tell Abu en-Ni‘aj (Fall et al. 1998; 2002; Falconer and Fall, 2006:126), providing a wider comparison and supporting the hypothesis that the preference for barley cultivation was a uniquely high at the end of the Early Bronze Age.

The social structure of EB IV through MB II may also have impacted the cultivated crop assemblages noted at my focal settlements. Early Bronze IV is known to be relatively sparce in terms of large settlements (Gophna and Portugali, 1988; Esse, 1989; Finkelstein, 1989; Falconer, 1994; Falconer and Savage, 1995), though trade of some secondary products on at least a local scale has been inferred for the EB IV Southern Levant (Goren, 1996). A possible reduction in regional trade compared to EB III among sedentary agricultural sites would mean a lower need for the production of goods designed for export. This would have a larger effect on secondary-product producing crops, which would thus have less value. While continual production of a variety of cultigens was noted at both northern Jordan Valley sites, cultigen density did decline at EB IV Ni‘aj, compared to those from regional EB II-III settlements (Hopf, 1983; McCreery

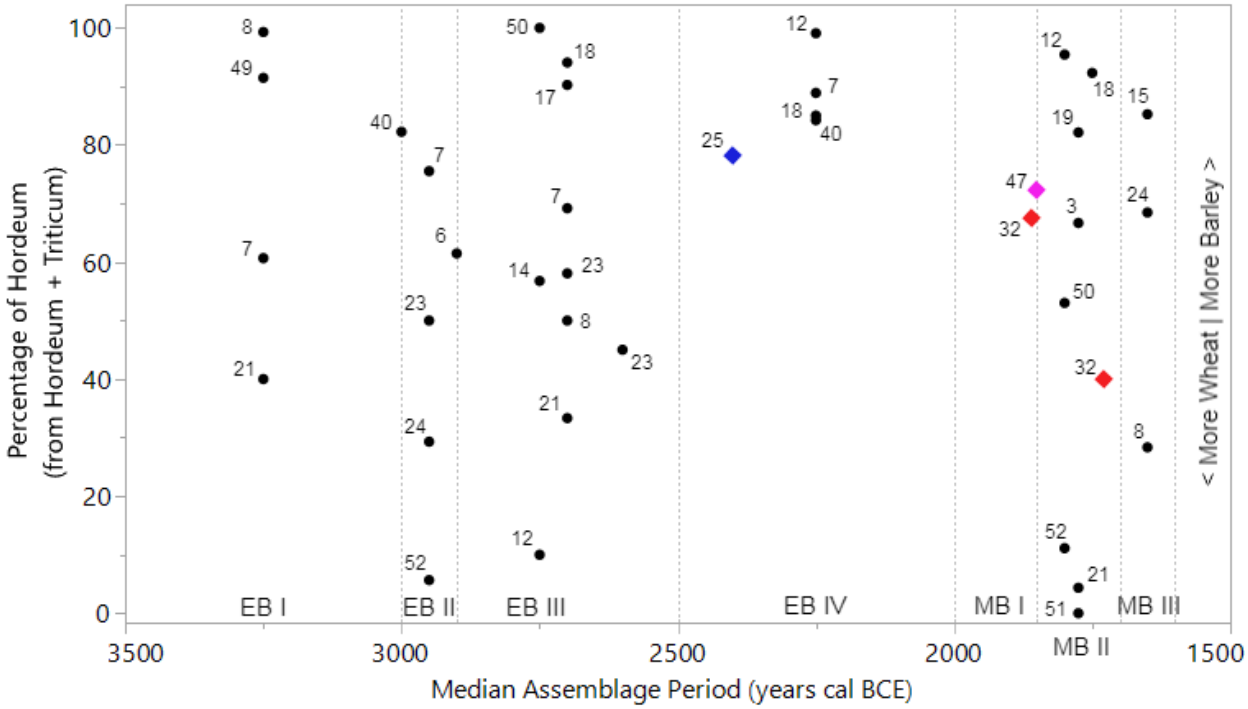

Figure 10.4 Ratios of *Hordeum* NISP to combined *Hordeum and Triticum* NISP for 16 archaeological sites from the Levant occupied during the Early and Middle Bronze Ages. The ratios are plotted against median radiocarbon ages for each site. Values are highlighted for Ni'aj (blue), Hayyat (red) and ZAD 1 (purple) with values averaged for all periods at each site. All values used in this comparison are included in Table A10. Sites include the following sites also shown in Figure 10.1: 3 – 'Afula, 6 - Arad, 7 - Bab edh-Dhra', 8 - Beth-Shean, 12 - Jericho, 14 - Khirbet ez-Zeraqon, 15 - Manahat, 17 - Numeira, 18 - Qatna (Tell Mishrifeh), 19 - Shiloh, 21 - Tel Megiddo, 23 - Tel Yarmuth, 24 - Tell Abu al-Kharaz, 25 - Tell Abu en-Ni'aj, 32 - Tell el-Hayyat, 40 - Tell Nebi Mend (Qadesh), 47 - Zahrat adh-Dhra' 1, 49 - Ras an-Numeyra, 50 - Sidon, 51 - Tell el Ifshar, 52 - Tell Kabri.

2003b; Riehl, 2004; Peña-Chocarro and Rottoli, 2007; Simchoni et al., 2007. If trade was a factor, this could suggest that Tell Abu en-Ni'aj shifted to focusing less on trade, though intraregional trade with smaller, regional peoples is still likely to have occurred (Goren, 1996; Fall et al., 1998; Richard and Long, 2008; Palumbo, 2008; Prag, 2014; Wilkinson et al., 2014).

In terms of cereal use, several aspects point to the centralized production of cereals in Ni'aj and Hayyat. The high maximum densities for barley in certain sectors at Hayyat and in certain samples at Ni'aj could suggest a processing or storage location. Contexts at Ni'aj had substantially higher NISP counts of barley (see Table S1), several reaching 200 seeds and one

reaching over 500. Furthermore, the strong spatial overlap in the contexts where barley and wheat remains are located, where other domestic clay-lined structures are found and burnt wood was found, more concretely points to processing activities. Cereal grains also have a very close association with fire-related loci at both site.

Finally, animal management certainly also played an important role in the assemblage differences noted between and within all three focal sites. As these are dung-burning sites, factors relating to animal management including where and which animals are herded, how animals are fed, how frequently dung is collected, and how it is utilized (whether for fuel or fertilizer), will all shape a site's paleoethnobotanical record. A slight shift in animal management at Ni'aj, alongside slightly increased wood burning, could have exacerbated the rapid decline in carbonized seed densities at the site over time, further explaining the relatively increased barley and overall decreased crop remains. At Ni'aj, faunal remains indicate a transition from predominantly *Ovis aries* (sheep) to *Capra hircus* (goat), and a trend of increased *Sus scrofa* (pig) bones over time (Falconer et al., 2004; Falconer and Fall, 2019: 29–33). While pigs are more poorly suited for herding, indicating a more sedentary lifestyle for farmers (Wapnish and Hesse, 1988: 93; Horwitz, 1989; Hesse, 1990), they are more likely to scavenge domestic food scraps than goat or sheep (Zeder 1991: 30). This implies that pigs are more likely to consume the cereal-processing and bread-making trash prevalent in domestic interiors and fire-associated remains. Hulled cereals also require more additional grain processing than free-threshing varieties, which are more likely to have been conducted near the site (Jones, 1983; Hillman, 1984; Reddy, 1997; Anderson, 1998; Alonso et al., 2014), a fact that could explain the larger frequency of hulled cereals.

For comparison of the fruit and oil crops, several regional sites exhibit a clear selection towards cultivation of certain fruits in the Early to Middle Bronze Ages. Fig, *Ficus carica,* was recorded in large quantities along the southern *ghor* at sites like ZAD 1, Bab edh-Dhra‘ and Numeira (McCreery, 2003b) and further north around Beth-Shean in the upper northern Jordan Valley, suggesting a wide regional presence (Simchoni et al., 2007). However, it was notably rare or absent at some sites like MB II Tell Nimrin or at further sites like Tel Yarmouth, Tell Nebi Mend, Abu al-Kharaz, and Tel Lachish (Helbaek, 1958; Mathias and Parr, 1989; McCreery, 2003a; Salavert, 2008; Fischer and Holden, 2006). Since high frequencies of this taxa in site macrofloral records are not a given, it suggests that this taxa had a relatively heightened importance as a cultigen at Ni‘aj, Hayyat, ZAD 1, and possibly in the Jordan Rift of the Southern Levant in general.

Olea europaea and *Vitis vinifera*, Olive and grape, are also found in large frequencies at several sites, such as with olive at Bab edh-Dhra‘ (McCreery, 1980; 2003b). In the northern Jordan Valley, the prevalence of *O. europaea* remains at Beth-Shean suggest its cultivation in MB II (Simchoni et al., 2007), and spatial trends at Hayyat further highlight the importance of both *Olea* and *Vitis* in the northern Jordan Valley. Presence of olive charcoal at sites, more frequent than carbonized seed remains, supports a similar presence of widespread cultivation and utilization of *Olea* throughout the Early Bronze Age (Lev-Yadun et al., 1996; Liphschitz, 2004; Salavert, 2008; Mazar, 2012), while pollen records suggest sustained or even heightened presence in EB IV throughout at least the north and central portions of the valley (Langgut et al., 2015; 2016).

Vitis vinifera is a particularly notable cultigen at my focal sites. *Vitis* is less drought tolerant than many common regional secondary-product crops (Riehl, 2009; Kamlah and Riehl,

2020), but its presence has been noted in drier settlements in past (Fall et al., 1998; 2002). Grape remains are relatively frequent at MB II Tell Nimrin (McCreery, 2003a) and MB I-II ZAD 1, each located in the southern portion of the Jordan Rift, and possibly also at EB II Ras an-Numayra (White et al., 2014). *Vitis vinifera* remains are commonplace in other studies in Israel and the Jordan Valley, though are typically found in relatively much lower frequencies than those noted at ZAD 1. *Vitis vinifera* remains are noted particularly from the Middle Bronze Age and have been found at sites like Khirbet ez-Zeraqon, Tel Nami, Jericho, and others (Helbaek, 1958; Liphschitz, 1989; Lev-Yadun et al., 1996; Neef, 1997; McCreery, 2003a; Riehl, 2004; Fischer and Holden, 2006; Simchoni et al., 2007; Hopf, 2008). Evidence of the importance of *Vitis* cultivation is attested regionwide through early pollen and paleoethnobotanical studies, and later through textual remains (Renfrew, 2003; Miller, 2008), and reports suggest it may have been most important in the lower Southern Levant.

Pulse density appears relatively low at most sites in part due to preservation challenges (McCreery, 2003b), but relatively high frequencies at my focal sites reflect a mix of site preference and regional availability. Regional sites like Jericho hosted a more unique array of pulse cultigens (Hopf, 1983), and sites in Western Israel and the Northern Levant tended to have more focus on pulse production (Nicoli et al., 2023), but many regional sites had lower proportions of these crops. Regional sites point to *Lens culinaris* (lentil)*, Cicer arietinum* (chickpea), and *Vicia* sp. (vetches) possibly being the most prominent pulse taxa during the Early to Middle Bronze (Miller, 1991; McCreery, 2003b; Riehl, 2004; Fischer and Holden, 2006; Simchoni et al., 2007; Mazar et al., 2012; White et al., 2014). Several sites also show limited quantities of *Pisum sativum* (garden pea) (Melamed, 1996; Mazar, 2012; McCreery, 2003b; Simchoni et al., 2007), but the assemblages from Ni‘aj, Hayyat, and ZAD 1 have almost no *C.*

arietinum or *Vicia* and a higher presence of *Pisum sativum*, particularly for ZAD 1, which has few *Lens culinaris* remains. Regardless, cultivation of pulses was limited in my focal sites, and may reflect the pattern of limited pulse importance in the region.

Regional Comparison of $\Delta^{13}C$ and $\delta^{15}N$ from Major Cultigens Across the Near East

Introduction

To compare regional water availability of common taxa data was collected on $\Delta^{13}C$ from past studies. The intention was to examine the larger-scale differences of isotope composition over time in order to understand the scale of long-term change witnessed regionally and better interpret the magnitude of change during the EB IV-MB II transition, and to see what larger scale patterns emerged following the addition of our data. Maps were composed in ArcGIS Pro to plot 37 Eastern Mediterranean sites ranging from Neolithic to Late Bronze, Figure 10.5. These time periods were chosen to provide climate contexts for the early to middle Holocene that can support the Early Bronze IV to Middle Bronze I-II comparison that is discussed throughout this dissertation. Site selection was expanded from the Southern Levantine Jordan and Dead Sea Valleys to the Northern Levant and Upper Mesopotamia to capture additional data points and provide a larger regional scale for the assessment of ancient water-availability trends. The region encompasses sites receiving precipitation from storm systems arriving from the northwest to west across the Atlantic and Mediterranean (Lionello et al., 2006; Black et al., 2010; 2011; Brayshaw et al., 2010; Ben Dor et al., 2018).

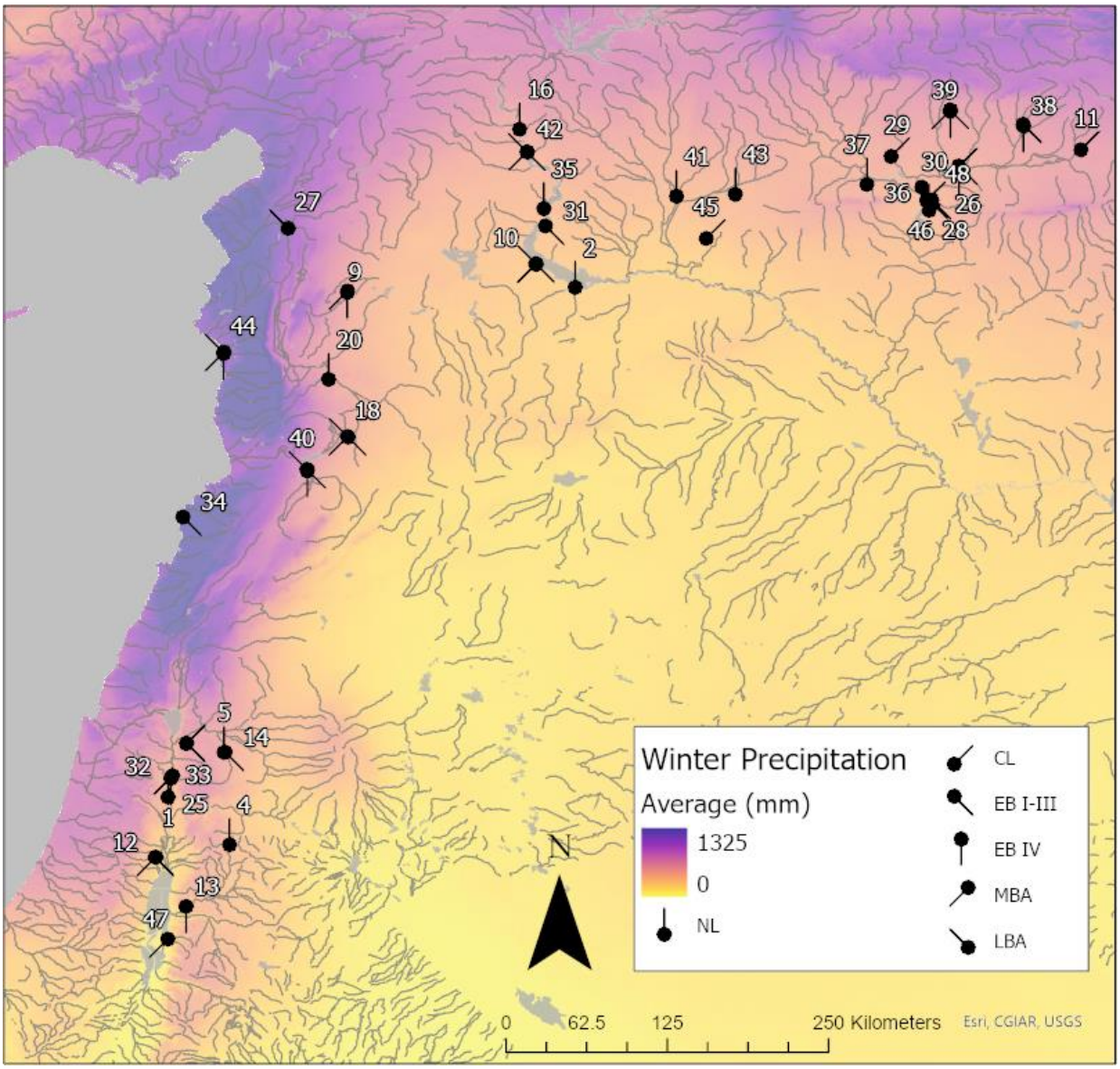

Figure 10.5 Map of mean winter precipitation in the lands east of the Mediterranean including sites and their periods of occupation that are used in the $\Delta^{13}C$ comparisons shown in Figures 10.6, 10.7 and 10.8. Periods of occupation include: Neolithic (NL), Chalcolithic (CL), Early Bronze I-III (EB I-III), Early Bronze IV (EB IV), Middle Bronze (MBA), and Late Bronze (LBA). Modern precipitation data is based on WorldClim 30s winter and spring precipitation (December to May) bands (Fick and Hijmans, 2017), and river data is from DIVA-GIS. All sites used in these comparisons and all *Hordeum* sp. and *Triticum* sp. values included in Table A11 include: 1 - Abu Hamid, 2 - Abu Hureyra, 4 - Ain Ghazal, 5 - Ain Rahub, 9 - Ebla, 10 - Emar, 11 - Hamoukar, 12 - Jericho, 13 - Khirbat Iskandar, 14 - Khirbet ez-Zeraqon, 16 - Mezraa Teleilat Hoyuk, 18 - Qatna (Tell Mishrifeh), 20 - Shir, 25 - Tell Abu en-Ni'aj, 26 - Tell al-Raqa'i, 27 - Tell Atchana, 28 - Tell Atij, 29 - Tell Beydar III, 30 - Tell Brak, 31 - Tell el'Abd, 32 - Tell el-Hayyat, 33 - Tell Esh-Shuna (Tell Nimrin), 34 - Tell Fadous-Kfarabida, 35 - Tell Halula, 36 - Tell Kerma, 37 - Tell Kuran, 38 - Tell Leilan, 39 - Tell Mozan, 40 - Tell Nebi Mend, 41 - Tell Sabi Abyad, 42 - Tell Shioukh Faouqani, 43 - Tell Tawila, 44 - Tell Tweini, 45 - Tell Zeidan, 46 - Umm Qseir, 47 - Zahrat adh-Dhra' 1, 48 – Ziyade.

Regional comparison suggests the high $\delta^{15}N$ values noted at my focal sites were not anomalies, as similar values have been reported from other regional sites. In the Bronze Age, Tell Brak, Tell Leilan, and Ebla (Fiorentino et al., 2011; Styring, 2017) contained nitrogen values around 3.5-5.5‰ that were still attributed to manure application. The lowest values of $\delta^{15}N$ seen at my focal sites at Khirbat Iskandar fall within this range, which support the inference that Iskandar's cereal crops may have received some level of manure application. Higher values of nitrogen that more closely align with our values from ZAD 1 have been noted from earlier sites like Tell Zeidan, Abu Hureyra, and Hamoukar (Styring et al. 2017) as evidence of intensified manuring; however, few sites in the Bronze Age appear to have values as high as those reported at ZAD 1.

Water Availability for Common Cereal Grains

Mean $\Delta^{13}C$ values from regional sites (Figure 10.5) are plotted according to cereal taxa in Figure 10.6 for sites with species-specific data. Values are split between four common cereal taxa showing change over time in $\Delta^{13}C$ signatures. Water availability thresholds are provided for each genus to indicate the poorly-, moderately-, and well-watered ranges. The comparison shows that certain cereal species were generally provided higher water availability than others. Comparing the data regionally across the Eastern Mediterranean (Riehl et al., 2014; Wallace et al., 2015; Styring et al., 2017), the trends of wheat and barley from my focal sites roughly fall in line. The pattern for the Southern Levant tends to be slightly on the drier side in comparison to EB III/IV Upper Mesopotamian sites but similar or slightly wetter than sites in the Northern Levant.

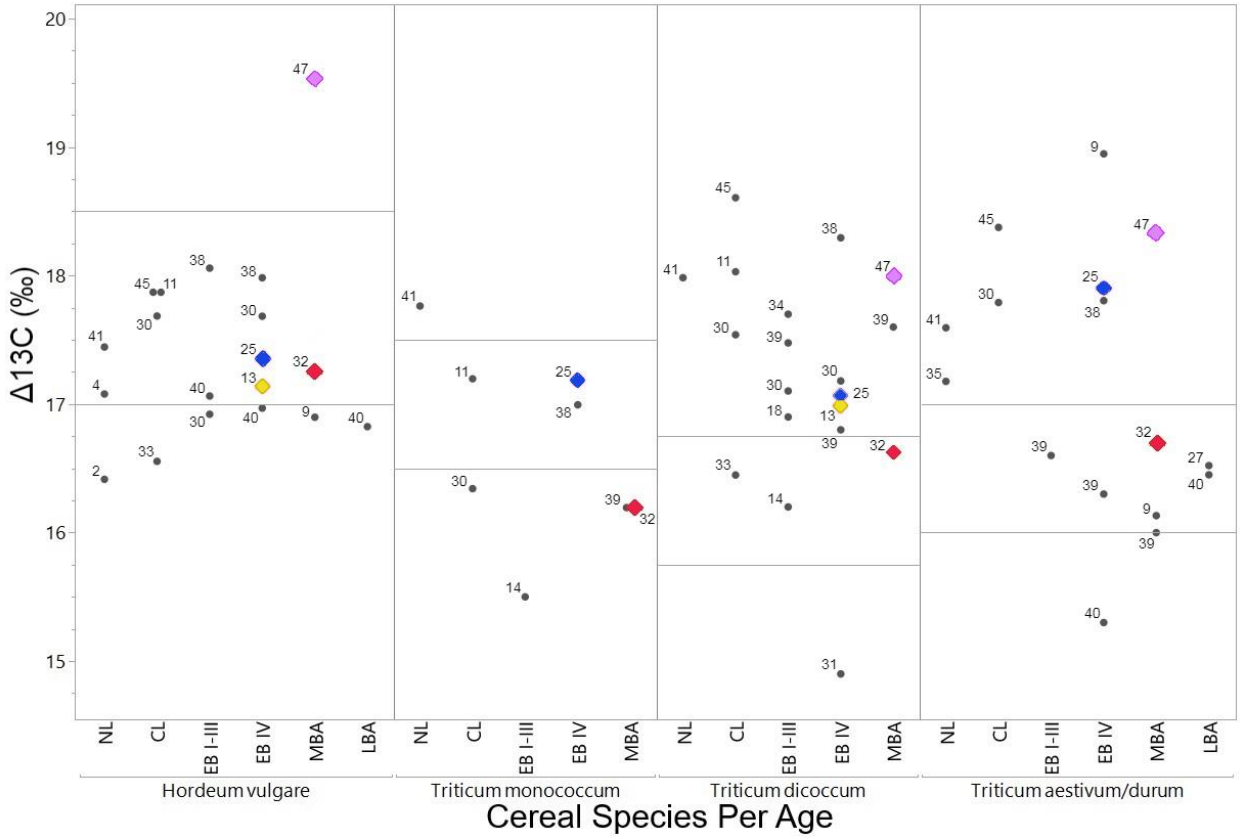

Figure 10.6 Values of $\Delta^{13}C$ for cultivated cereal taxa showing the mean from all samples at a settlement according to period of occupation. Time periods include the Neolithic, Chalcolithic, Early Bronze I-III, Early Bronze IV, Middle Bronze Age, and Late Bronze Age. Mean values are highlighted for Ni'aj (blue), Hayyat (red), Iskandar (yellow), and ZAD 1 (purple). Sites include: 2 - Abu Hureyra, 4 - Ain Ghazal, 9 - Ebla, 11 - Hamoukar, 13 - Khirbat Iskandar, 14 - Khirbet ez-Zeraqon, 18 - Qatna (Tell Mishrifeh), 25 - Tell Abu en-Ni'aj, 27 - Tell Atchana, 30 - Tell Brak, 31 - Tell el'Abd, 32 - Tell el-Hayyat, 33 - Tell esh-Shuna, 34 - Tell Fadous-Kfarabida, 35 - Tell Halula, 38 - Tell Leilan, 39 - Tell Mozan, 40 - Tell Nebi Mend (Qadesh), 41 - Tell Sabi Abyad, 45 - Tell Zeidan, 47 - Zahrat adh-Dhra' 1.

When breaking down $\Delta^{13}C$ values according to individual species, it becomes clear that not all wheat species were prioritized to the same degree across the region and at my focal sites. The values of *Triticum aestivum* often greatly surpass the estimated well-watered threshold of the species, indicating well-watered conditions. *Triticum dicoccum*, which displays a slightly lower $\Delta^{13}C$ signature under the same experimental water conditions as *T. aestivum*, are routinely reported with values roughly matching or surpassing those of *T. aestivum*. Both of these taxa are

indicated primarily by well-watered conditions. Preferential watering of *T. aestivum* makes sense as it is drought-intolerant, although the more drought intolerant *T. monococcum* falls primarily in the poorly- to moderately-watered range (Riehl, 2009).

The $\Delta^{13}C$ values for *T. monococcum* plot more similarly to those of *Hordeum vulgare*, each suggesting relatively low water availability. The differences in water availability between these four cereals may be due in part to cultivation in different seasons, such as for *Triticum monococcum,* which can be grown under winter rainfall (Fall et al., 2002). For *H. vulgare*, field localization may be a feasible reason for distinctions in water availability.

Water availability patterns from the moderately- to poorly-watered species in each taxonomic category could suggest that slightly dry conditions persisted through the entire mid-Holocene, but do not form a consensus. On the other hand, the $\Delta^{13}C$ values from *T. dicoccum* and *T. aestivum* crops indicate that water availability needs were met at most settlements despite the potential of climatic constraints, though it could also suggest that these taxa were less cultivated in dry years or were less likely to survive carbonization if the plant experienced drought conditions. The discrepancy between poorly-watered drought-tolerant species and well-watered drought-intolerant species is reinforced by the $\Delta^{13}C$ data from the focal sites in this dissertation. It suggests that patterns of likely enhanced water availability for *Triticum* in EB IV and MB II are not outliers but reflective of a wider, continuous trend of water maintenance for both certain species.

The water availability patterns at the focal sites ultimately agree with models suggestive of similar water availability between early EB IV and EB III with moderate to high water availability in MBA (Bryson and DeWall, 2007; Soto-Berelov et al., 2012; Fall et al., 2018). The data also fits well into the overall scope of $\Delta^{13}C$ values across the region, which suggest

continuous moderate drought stress with potential gradual drying into the Middle to Late Bronze Ages. The data helps constrain the timing of the 4.2 ka BP event to a roughly 300-year period, fitting in very well with prior expectations (Weiss, 2016; Pokharia et al., 2017; Railsback et al, 2018; Xiao et al., 2018; Bini et al., 2019; Kaniewski et al., 2020).

Hordeum Water Availability in the mid-Holocene Eastern Mediterranean

For additional comparison of regional cereal stable isotope data, Figures 10.7 and 10.8 present stable isotope and modern rainfall data to infer spatio-temporal relationships of water availability for barley and wheat crops. Regional comparison is made across six time slices from the Pre-Pottery Neolithic through the Late Bronze Ages for the following periods: Neolithic, Chalcolithic, Early Bronze I-III, Early Bronze IV, Middle Bronze, and Late Bronze.

Figure 10.7 presents published $\Delta^{13}C$ data from *Hordeum vulgare*, *H. vulgare* var. *nudum* and *Hordeum* sp. Much of the *Hordeum* sp. comes from Riehl et al. (2014). Water availability ranges are based on Wallace et al.'s (2013; 2015) studies of *Hordeum vulgare* $\Delta^{13}C$, with values grouped into three categories:

- Well-watered barley: $\Delta^{13}C > 18.5‰$: Green symbol
- Moderately-watered barley: $\Delta^{13}C$ between 17-18.5‰: Yellow symbol
- Poorly-watered barley: $\Delta^{13}C < 17‰$: Red symbol

No sites other than Tell el-Hayyat contained stable isotopic data on *H. vulgare hexastichum*, so this taxon is not incorporated. The watering ranges for *H. vulgare* var. *nudum* are undetermined, so the predicted watering range of around 17‰ to 18.5‰ for moderately-watered barley was used for all three taxa: *Hordeum vulgare*, *H. vulgare* var. *nudum* and *Hordeum* sp. The taxa *Hordeum vulgare hexastichum* is shown to produce values 1‰ higher

than *H. vulgare,* so if this taxon is incorporated into the signal of *Hordeum* sp., the signal would shift towards higher values of $\Delta^{13}C$ (Araus et al., 1997b; Voltas et al., 1999).

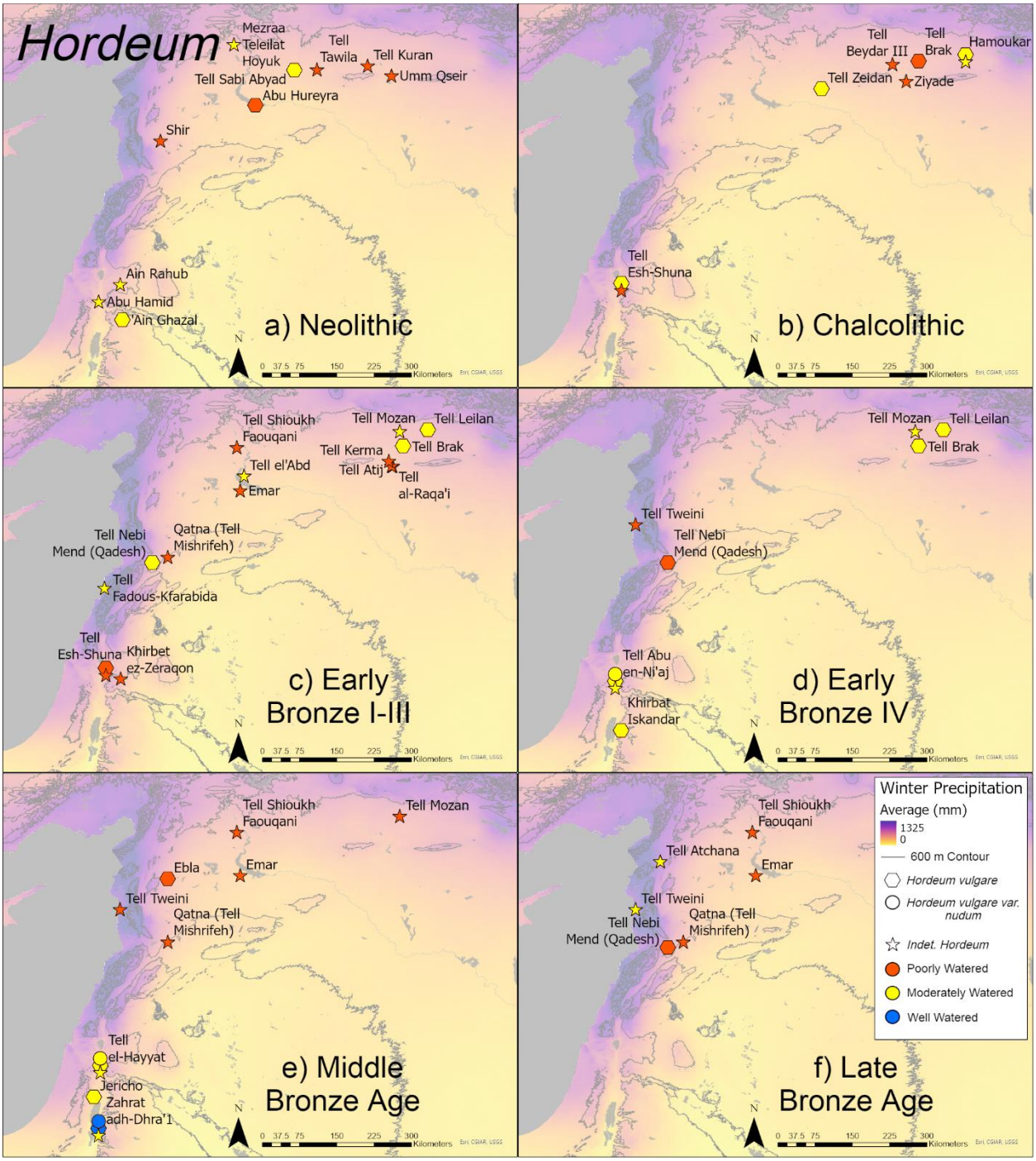

Figure 10.7 Levels of water availability for *Hordeum vulgare* (hexagon), *H. vulgare* var. *nudum* (circle), and *Hordeum* sp. (star) based on mean $\Delta^{13}C$ values (Wallace et al., 2013; 2015): Well-watered – Green; Moderately-watered – Yellow; Poorly-watered – Red. Variation in modern precipitation shown in color based on WorldClim 30s mean winter and spring precipitation data (December to May) (Fick and Hijmans, 2017).

Figure 10.7 shows a similar spatial pattern for barley through all six time slices, suggestive of cultivation in conditions of moderate to severe drought stress. A substantial proportion of the sites within each period contained barley values indicative of more severe drought stress (Wallace et al., 2013; 2015; Styring et al., 2016; 2017). This does not indicate that each of these settlements was in a drought from the Neolithic through Late Bronze Ages, but suggests that the barley crops were routinely not provided sufficient watering to reach maximum yields. This pattern is shared by both *Hordeum vulgare* and *Hordeum* sp. The spatial patterns of sites with moderate to high drought stress do not correspond to the precipitation gradients across the region, and may correlate better with the proximity of each site's agricultural fields to the nearest spring or stream. The low stable isotope values may thus reflect an understanding of barley's drought tolerance and its ability to produce sufficient yields for cultivation under less-than-optimal watering conditions.

The exceptions to the pattern of poorly-watered barley come from the Southern Levantine Middle Bronze Age communities. The Southern Levant appears to contain values associated with greater water availability than shown elsewhere in the Near East. Zahrat adh-Dhra' 1 is the only site with barley values plotting above the well-watered threshold for *Hordeum vulgare*, some of which lie well above the threshold. The MB data from these sites plot comparatively better in terms of water availability than those from the same region in EB I-III (Riehl et al., 2014; Styring et al., 2017).

While a myriad of important factors, such as the distance to the nearest water source, are not incorporated in this comparison, the regional patterning of barley data reveals an important fact. Stable isotope comparison of barley $\Delta^{13}C$ values do not capture the larger-scale Holocene paleoclimatic trends shown by other proxies like speleothem, pollen, or sediment analyses. The

main Holocene-scale trends visible through these proxies suggest humid conditions in the early Holocene and drier conditions in the mid-Holocene, patterns which are not shown by stable isotope data for *Hordeum* presented here. This may suggest that *Hordeum* sp. $\Delta^{13}C$ data are not ideal indicators of regional climate signals, as this genus maintains values indicating dry conditions through wetter and drier periods alike.

Instead of regional climate, the water availability data for *Hordeum* species are more useful for interpreting crop management patterns. In the Southern Levant, and particularly at MB I ZAD 1, $\Delta^{13}C$ data alongside $\delta^{15}N$ values reveal particularly intensive crop management. While ZAD 1 was likely positioned in one of the driest environments, its well-watered stable isotope signal seems to be an indication of more intensive crop management to ensure sufficient crop watering.

Triticum Water Availability in the mid-Holocene Eastern Mediterranean

To evaluate spatio-temporal patterns of wheat cultivation, I plot sites with published $\Delta^{13}C$ data from *T. aestivum*, *T. dicoccum*, *T. monococcum*, and *Triticum* sp. (Figure 10.8). Water availability ranges are based on Wallace et al.'s (2013; 2015) studies of *Triticum dicoccum* $\Delta^{13}C$, with values grouped into three categories:

- Well-watered wheat: $\Delta^{13}C > 17‰$: Green symbol
- Moderately-watered wheat: $\Delta^{13}C$ between 16-17‰: Yellow symbol
- Poorly-watered wheat: $\Delta^{13}C < 16‰$: Red symbol

Triticum aestivum and *Triticum* sp. each used the above categories, but *T. dicoccum* and *T. monococcum* have slightly different ranges based on experimental studies of the optimal watering ranges for these species. Values for *T. dicoccum* fall roughly 0.25‰ lower than those

for *T. aestivum*, so a moderate watering range of 15.75 - 16.75‰ is applied for this species (Konvalina et al., 2011). Values for *T. monococcum* fall roughly 0.5‰ higher than those for *T. aestivum*, so a moderate watering range of 16.5 - 17.5‰ is applied for this species (Heaton, 2009).

While there are fewer data available for *Triticum* than for *Hordeum*, there are notably more *Triticum* values indicative of well-watered conditions in each of the time periods. Many sites that maintained moderate- to poorly-watered conditions for *Hordeum* cultivation show higher water availability for *Triticum* species. There are few moderately- or poorly-watered crops at Neolithic and Chalcolithic sites, with the only examples coming from *Triticum monococcum* (Bronk Ramsey et al., 2002; Wallace et al., 2015; Styring et al., 2017; Bogaard et al., 2018a). Through all time periods, *T. monococcum* accounts for more of the poorly- to moderately-watered values. In the Early to Middle Bronze Ages, sites in the Levant and Upper Mesopotamia provide well-watered values, while poorly- to moderately-watered values only come from sites in the Levant (Riehl et al., 2008). Fewer well-watered values are noted in the Levant through the Middle to Early Bronze ages, with most *Triticum aestivum* indicative of moderately-watered conditions.

As with barley, the Levantine wheat values appear to be most indicative of crop management rather than climate change. Wheat values do not seem to reflect the general Holocene trend of regional, gradual drying (Bryson and DeWall, 2007; Soto-Berelov et al., 2012). Wheat in Upper Mesopotamia has a well-watered pattern for all taxa in the Neolithic and Chalcolithic with the exception of *T. monococcum*. More moderately-watered values appear for *T. aestivum* and *T. dicoccum* in the Early to Middle Bronze Ages, which could indicate drier conditions. In the Levant, values from the Early to Middle Bronze generally show moderate- to

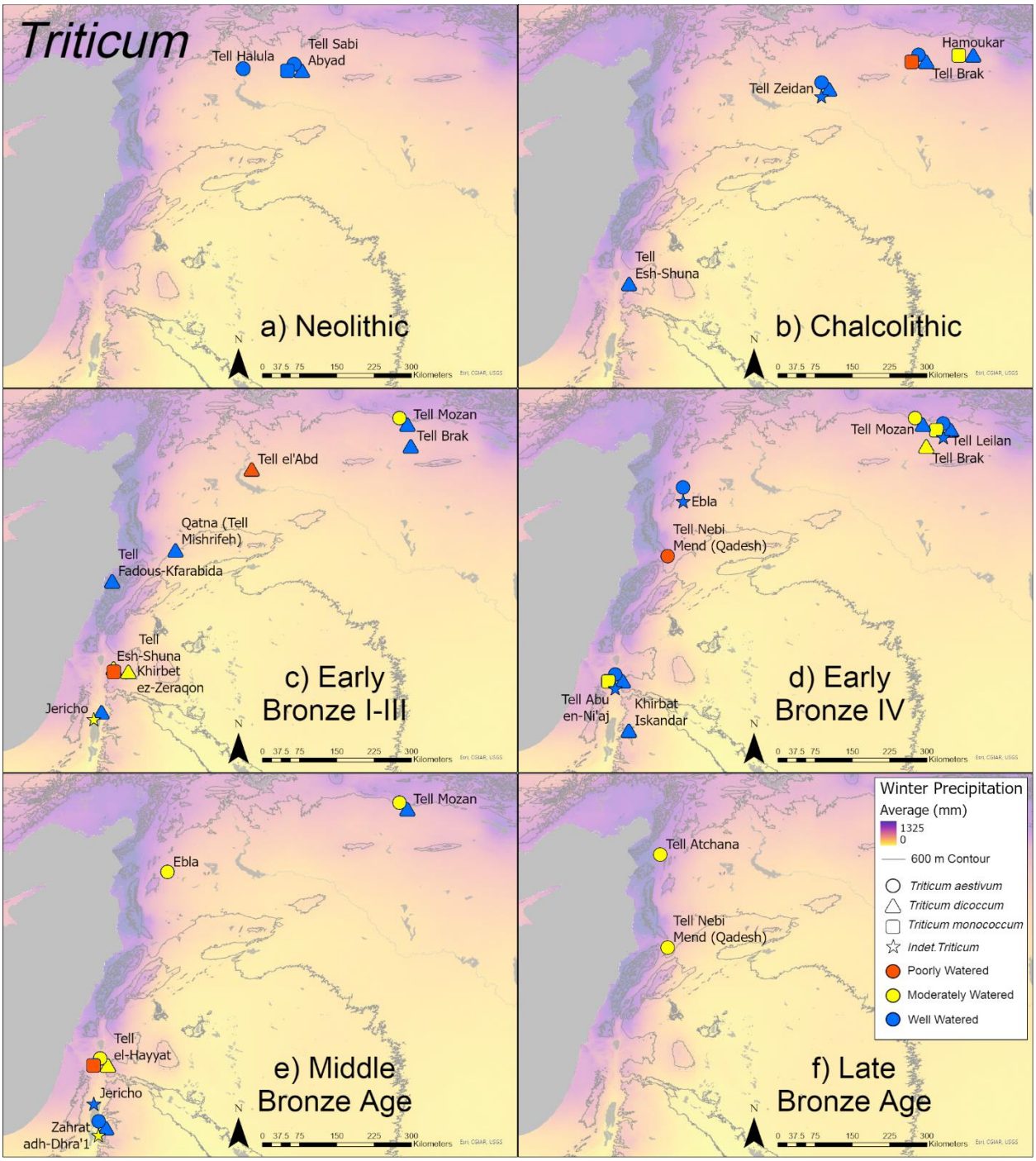

Figure 10.8 Levels of water availability for *Triticum aestivum* (circle), *T. dicoccum* (triangle), *T. monococcum* (square), and *Triticum* sp. (star), based on mean $\Delta^{13}C$ values (Wallace et al., 2013; 2015): Well-watered – Green; Moderately-watered – Yellow; Poorly-watered – Red. Variation in modern precipitation shown in color based on WorldClim 30s mean winter and spring precipitation data (December to May) (Fick and Hijmans, 2017).

well-watered conditions for wheats, with a few exceptions of poorly-watered wheat values. Values indicating the driest conditions are found in EB I-III and the MBA in the northern Jordan Valley. This does not follow the expectations from climate and vegetation models that suggest EB I-III being more humid than EB IV, and the northern Jordan Valley being more humid than the southern Jordan Valley and Dead Sea Valley.

Interestingly, the $\Delta^{13}C$ data for both barley and wheat suggest increased water availability from EB I-III to EB IV in the Southern Levantine Jordan Rift, through the opposite trend appears in the Northern Levant. The EB I cereal $\Delta^{13}C$ data from Tell esh-Shuna (Bronk Ramsey et al., 2002; Riehl et al., 2014) and EB II-III Khirbet ez-Zeraqon (Riehl 2004, Riehl et al., 2008; 2014) in the northern Jordan Valley, two sites located in an area with relatively higher modeled annual precipitation than in the southern Jordan Valley (Soto-Berelov et al., 2015), but their $\Delta^{13}C$ data indicate poor to moderate water availability for cereals. In EB IV, these values are replaced by the relatively higher watering values for barley and wheat crops at Tell Abu en-Ni‘aj. It is possible that the region around the northern Jordan Rift received additional rainfall in EB IV, which could correspond to findings of steady lake levels in the Sea of Galilee (Vossel et al., 2018) and offsetting records from speleothems (Cheng et al., 2015; Burstyn et al., 2019). However, it is also likely that strategies were implemented by early farmers to offset low rainfall, such as the selective site location and maintenance observed at ZAD 1. This would support the idea of more intensified cereal management at Ni‘aj. Since wheat crops are more drought-intolerant, and appear to be carefully managed, the inability to provide sufficient water could be indicative of climate stresses, but due to the many considerations needed, wheat isotopes are also not ideal indicators of paleoclimate signals and likely reveal more about how ancient peoples managed their crops.

These cereal stable isotope trends support the hypothesis of intentional land management towards providing increased water availability to wheat crops. The presence of well-watered barley may be indicative of intensified cereal management and possibly irrigation, while the presence of poorly-watered wheats could be indicative of drier local conditions or less prioritization for cereal management. My investigation reveals that in the Early to Middle Bronze Ages there may have been relatively intensified cereal management at my focal sites, in what is predicted to be some of the driest times and locations, e.g., EB IV of the Jordan Valley and the MBA (MB I-II) around the Dead Sea Plain.

Water Availability for Other Common Cultigens

Brief comparisons are also made for other common regional cultigens. Figure 10.9 shows mean $\Delta^{13}C$ values from seven fruit and pulse taxa found frequently at our sites. Comparison spans the Neolithic to Bronze Age from the Southern Levant to Upper Mesopotamia. Taxa include *Hordeum vulgare* var. *nudum, Lens culinaris, Pisum sativum, Vicia faba, Lathyrus sativus, Vitis vinifera,* and *Olea europaea*. Several of these taxa have not been thoroughly studied in experimental settings and so lack information as to their predicted $\Delta^{13}C$ values under different watering profiles. Each species in this comparison is included in the isotopic sampling from at least one of my focal sites in order to bolster the regional record for these taxa.

For *Hordeum vulgare* var. *nudum*, no values of carbon stable isotopic measurements are noted from other regional sites. Averages for Ni‘aj and Hayyat suggest this cereal has values around 1‰ greater than those for *Hordeum vulgare*, but the opposite relationship is observed from seeds at ZAD 1, so both experimental testing and additional macrofossil sampling is required for interpretation.

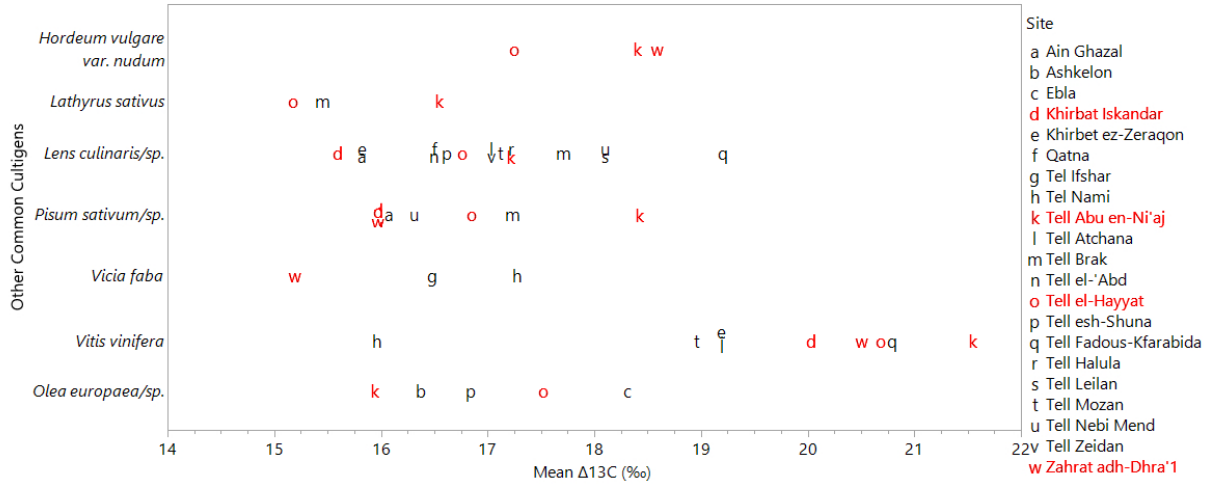

Figure 10.9 Mean $\Delta^{13}C$ values for carbonized seeds from seven common cultigen crops from archaeological sites across the Levant and Upper Mesopotamia during the Early to Middle Holocene. Values from the four focal sites Tell Abu en-Ni‘aj, Tell el-Hayyat, Khirbat Iskandar, and Zahrat adh-Dhra‘ 1 are highlighted in red.

Lens culinaris is perhaps the most well sampled species among these taxa. Thresholds of water availability may be close to or just below those of *Triticum aestivum* (Wallace, 2013; 2015; Styring, 2017; Stroud et al., 2021). The values of $\Delta^{13}C$ for *Lens* from Ni‘aj, Hayyat, and ZAD 1 plot in the poorly-, moderately-, and well-watered category depending on the site. Compared to the general distribution of data from other sites, around 16.5-17.5‰, the values from my focal sites in the Southern Levantine Jordan Rift are relatively low, with Iskandar having the lowest mean $\Delta^{13}C$ value for the crop. *Lens* appears to have been better watered at sites in Western Israel, Northern Levant, and Upper Mesopotamia. These results support the hypothesis of low cultivation intensity of pulses regionally, as interpreted from low $\delta^{15}N$ values (Stroud et al., 2021).

Of the remaining five taxa, *Pisum sativum*, *Vitis vinifera*, and *Olea europaea* had enough data from other regional sites to draw relative comparisons. Values of $\Delta^{13}C$ from *Pisum* are relatively higher for Ni‘aj and Hayyat and relatively lower for both ZAD 1 and Iskandar,

compared to other regional sites. For *Vitis,* all four of my focal sites have relatively high values, and comparatively, only Fadous-Kfarabida in the Northern Levant has reported similarly high values (Riehl et al., 2014). For *Olea*, Hayyat may have a relatively high value, but the mean value from Ni'aj falls towards the lower end of the spectrum. With olives likely being rain-fed, this supports that Hayyat had higher precipitation. Studies of modern olive also suggest that values of roughly 15.5‰ or higher may indicate well-watered conditions in semi-arid to arid environments (Ehrlich et al., 2022), so seeds from both focal sites and all regional sites in this comparison may have had a high plant water availability.

These comparisons suggest areas of regional importance for certain taxa. Though frequency of this *Pisum sativum* was high at ZAD 1, it appears that water management for both *Lens* and *Pisum* only occurred in the northern Jordan Valley sites. Pulses may have been more intensively managed in the Northern Levant or Mesopotamia. Likewise, *Olea europaea* did not appear at either Dead Sea Basin site, but was clearly an important cultigen in the northern Jordan Valley. It is evident from pollen records that *Olea* was present in the Dead Sea Basin throughout the early to middle Holocene (Langgut et al., 2016; 2019), so its absence from these southern focal sites may suggest a temporary shift northward or a lack of preference for oil production. *Vitis*, with its relatively high $\Delta^{13}C$ values and potentially moderate to high $\delta^{15}N$ values, may have been more intensively cultivated in the Jordan Rift of the Southern Levant, and it is clear that this extended through the Dead Sea Basin. This trend is partially supported by similar findings at EB III Bab edh-Dhra' (McCreery, 2003b), though few sites exist in the region in EB IV and MB I to offer comparison, and it is clear that all of these cultigens were present in the valley in the remainder of the Early to Middle Bronze Age (Hopf, 1983).

Overview and Contextual Interpretations of Ancient Crop Cultivation

Crop Cultivation in the Southern Levant During EB IV to the Middle Bronze Ages

It is clear that Tell Abu en-Ni'aj and Tell el-Hayyat were settlements highly invested in agricultural production, with coordination of crop management that evolved over time. The floral assemblages of Ni'aj and Hayyat are generally similar to those noted towards the central and southern portions of the Levant and reported in even the earliest paleoethnobotanical studies (Helbaek, 1958; 1960). Both sites indicate cultivation of a typical array of hulled cereals, pulses like lentil and garden pea, and fruit crops like grape, fig or olive (Zohary and Spiegel-Roy, 1975; Hopf, 1983; Zohary and Hopf, 1988; Liphschitz, 1989; Liphschitz et al., 1991; Miller, 1992; McCreery, 2003a; 2003b; Fuller and Harvey, 2006; Bonacossi, 2014; Caracuta et al., 2015; Dighton et al., 2016). The lack of cultigens like *Linum usitatissimum* or *Cicer arietinum*, more frequent in Early Bronze sites to the east and north (Hopf, 1978; Kislev et al., 2009; Simchoni and Kislev, 2012; White et al., 2014) support notions from pottery typology and settlement structure that these sites, and possibly EB IV in general, had less regional connectivity (Wilkinson, 2003; Greenberg and Iserlis, 2014; Prag, 2014; Kennedy, 2015; Greenberg, 2019), as these non-native cultigens were not being traded into these Jordan Valley settlements.

Zahrat adh-Dhra' 1 stands in clear contrast to Ni'aj and Hayyat in terms of its carbonized macrofossil assemblage. Despite the increased climate stress, cereal production was an important feature of local crop cultivation. Its agricultural focus in late MB I-early MB II is attested by greater abundances of cereal crops and a plethora of grape remains. While no basin features for wine production were recovered, the grouping of cereal and fruit remains in relatively isolated central structures at the center of the site could indicate a larger communal structure that may

have participated in the production, processing, and possibly protection of these stored food and food products.

Along with the primary cereals, the fruit cultigens fig, grape, and olive all show distinct spatial trends at Hayyat and ZAD 1. In conjunction with the stable isotope values, these patterns not only indicate the heightened importance of these goods at Ni'aj, Hayyat, and ZAD 1 but suggest how they may have been processed and utilized as well. Locus type analysis indicates that barley, wheat, grape, and fig may have played the largest roles in the Bronze Age diet, while all three fruits may have had secondary uses as dried fruits, wine, or oil.

The differences in the cereal assemblages of each site appear to be closely linked to crop management but are also partially indicative of climate stress. With the incorporation of stable isotope data, region-wide commonalities emerged in the treatment of certain crops, suggesting that cereal cultivation was a primary interest for all four settlements, including Khirbat Iskandar. Ancient farmers were carefully selecting and managing high-maintenance, drought-intolerant but high-yield crops to ensure that water and soil nutrient thresholds could be met. *Hordeum vulgare* was consistently found with $\Delta^{13}C$ values indicative of low to moderate water availability and cultivation practices distinct from those of *Triticum* species, in which *Hordeum* crops may have been farmed in drier times or farmed in fields further from water sources. It is plausible that ancient farmers understood the tolerance of certain plants to drought and how to prioritize placement of crops near water sources, as surficial irrigation strategies emerged across the region in the late Early Bronze Age (Rosen, 1997).

The proportional increase in wheat in the Middle Bronze Age and increased cultivation of olive at Hayyat or grape at Hayyat and ZAD 1 may also be signs of renewed production of marketable goods in the Middle Bronze Age, particularly during Middle Bronze II (Fall et al.,

2002). The MBA saw increased cultivation of secondary product taxa at some Southern Levantine sites with trade said to return to roughly pre-EB IV levels in the MBA (Gaastra et al., 2020). Cultivation of olive and grape (Chernoff and Paley, 1998; Fall et al., 2002; Kislev et al., 2009), as well as other agricultural crops like wheats and pulses (Fall et al., 2002; Hopf, 2008), and goods not seen at the focal sites here like chickpea or flax are each presumed to have increased sometime around MB II, which accords with my results.

Interpretations on the Extent of Regional Climate Change

The investigation of ancient cultivation trends along the Jordan Rift sets the stage for a deeper dive into climate and climate change during the Early to Middle Bronze Age transition and the effect of climate stresses on human society. Quantification of the macrofossil assemblages show that each settlement used selective cultivation practices for specific crops and distinct crop management patterns that potentially prioritized drought-resistant taxa in drier periods and regions, which indicate agrarian responses to climate stress. Preference for wheat and olive over barley and grape has been used to suggest wetter conditions in past (Fall et al., 1998; 2002), and this pattern emerges in many instances at my sites.

Temporal patterns of *Hordeum* and *Triticum* shows a clear trend toward increased water availability in EB IV and MB I, with values highest surrounding the 4.2 ka bp event. Ni‘aj primarily produced the drought-tolerant barleys while Hayyat shifted towards wheat, but both settlements produced large frequencies of *Hordeum* compared to EB III or even other MB II settlements. This transition is slightly later at Hayyat, suggesting a climate change in the early to middle MB II, but a climate shift seems to begin earlier looking at cultivation from ZAD 1. The other climate signal comes from the seeds of wild taxa. Wild taxa are primarily being carbonized

through their incorporation in animal dung from sheep and goat. Since these seeds best reflect what the animals are grazing, they reflect the environments surrounding and beyond agricultural fields. The overarching signal was of similar, semi-arid climates during EB IV and MB II at Ni‘aj and Hayyat but of a distinct, more arid climate at ZAD 1 that suggests potentially drier conditions in MB I than compared to early EB IV or MB II.

Some palynological studies point to the reduction of olive in the valley from the end EB IV throughout the Middle Bronze Age (Baruch, 1986; Schiebel and Litt, 2018), tying this to regional drying. The clear presence of olive at Ni‘aj and particularly increased relative frequencies through the phases at Hayyat supplements paleoethnobotanical and charcoal studies (Neef, 1990; Willcox, 1999; Benzaquen et al., 2019) that point to its increased cultivation and regional importance, particularly in the Middle Bronze Age. The subsequent lack of olive in the Dead Sea Basin settlements, however, could be a signal of increased aridity in EB IV and early MBA.

These climate trends are supported by the archaeological shell stable isotope data from Ni‘aj and Hayyat that suggest points of distinction in the climates of EB IV and MB I-II, with potentially higher water availability in MB II and driest conditions in MB I. The significant overlap of shell $\delta^{13}C$ for six of the seven shells corresponds with the overlap in wild taxa between Ni‘aj and Hayyat, suggestive of similar natural environments around these sites, which from the wild weed assemblages is indicative of an open, semi-arid, possibly scrubland environment (Zohary, 1982; Abu-Irmaileh, 1982), rich with wild grasses, weedy clovers and amaranths, and shrubby mallows and mesquites.

The climate and environment around ZAD 1 are revealed to be distinct from that of my other focal sites from both the wild weed assemblage and then through stable isotope analysis.

The evidence from ZAD 1 suggests high water availability for its cereal crops, but the wild taxa assemblage and relatively lower water availability for its possibly rain-fed fruit and pulse taxa indicate this to be a dry environment.

One of the most important findings from the cereal $\Delta^{13}C$ analysis was the timing of climate-driven shifts. Figure 10.10 shows the relationships of the climate trends inferred from the combined data in this dissertation compared to those from regional paleoclimate proxies (Bar-Matthews et al., 1997; 1999; Soto-Berelov et al., 2012; Kaniewski et al., 2013; Cheng et al., 2015; Kagan et al., 2015). Data from this dissertation point to potentially increasing drought stress in the Jordan Valley and Dead Sea Basin from the start of Early Bronze IV to the abandonments of Ni'aj and Iskandar around 4450 BP, and to increasing water availability in Middle Bronze I and II, with a notable rise in water availability around the MB I-II transition. The driest timespan may have existed following the abandonments of EB IV and shortly after reurbanization in MB I, somewhere around 4200 BP to 3900/3850 BP, though data from some models (Soto-Berelov et al., 2015) suggest there may be an even drier period between this time.

This pattern (Figure 10.10f), hypothesizes EB IV to be slightly more humid than MB I, which would fit best with the Soreq Cave profile (Bar-Matthews et al., 1997; 1999), but the predicted rise in MB I and II accords better with the Jeita Cave (Cheng et al., 2015) or gradual trends from Dead Sea level and pollen trends (Kaniewski et al., 2013; Kagan et al., 2015). While these latter three proxies and models do not agree on the length of the driest period, they all agree with the suggestion of gradual drying conditions beginning earlier in EB IV, ranging from around 4400 BP to 4250 BP. My findings also roughly coincide with other interpretations from pollen (Baruch, 1990; Langgut et al., 2013; 2015), speleothem (Bar-Matthews et al., 1997; Verheyden et al., 2008; Bar-Matthews and Ayalon, 2011; Burstyn et al., 2019) and sea level

proxies (Kagan et al., 2015; Goldsmith et al., 2023) suggesting a drier climate in the late EB IV to early MBA. The results do disagree with some proxies (Arikan, 2015; Guiot and Kaniewski, 2015) but show an overall consistency with the general pattern of a 300-year 4.2 ka BP event ending around the start of MB II (Weiss, 2016; Pokharia et al., 2017; Railsback et al, 2018; Xiao et al., 2018; Bini et al., 2019; Kaniewski et al., 2020).

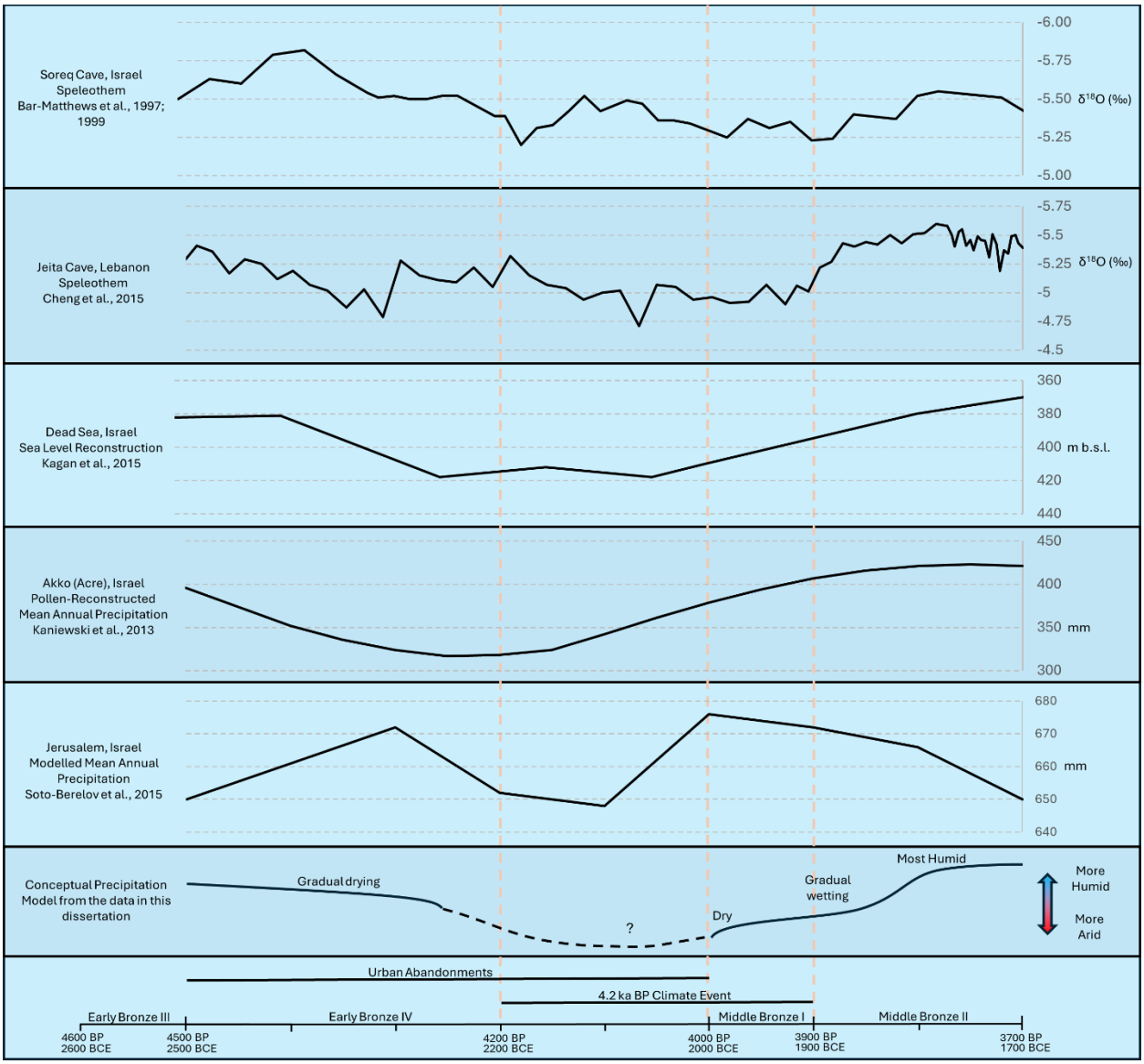

Figure 10.10 Regional climate models and proxy data compared to the climate trend inferred from archaeological seeds and shells from Tell Abu en-Ni'aj, Tell el-Hayyat, Khirbat Iskandar, and Zahrat adh-Dhra' 1, Jordan presented in this dissertation.

Results have also spurred a reevaluation of a primary finding from my preliminary studies of Tell Abu en-Ni‘aj which concluded that Ni‘aj was not indicative of a regional decline in precipitation because a significant water-availability gradient was not noted between phases (Porson et al., 2021a). Within the wider context of the Bronze Age, it is clear now that the site is indicative of a longer-term climatic phenomenon involving relatively diminished precipitation starting earlier in EB IV.

CHAPTER 11: CONCLUSIONS

This dissertation investigates how Early to Middle Bronze Age agrarian societies in the Southern Levant utilized agriculture and how they responded to one of the larger climatic events of the Holocene, the 4.2 ka BP global climate event. For decades, authors have attempted to unravel the mysteries of this climate phenomenon in order to understand its global variability and its effects on the evolution of ancient human society. As such, this dissertation includes a dual paleoethnobotanical and paleoclimatic investigation to uncover the extent, timing, and environmental and agricultural changes associated with this event.

My hypotheses for this dissertation centered on my investigation of cultigen variety and climate change, but my results also reveal important trends regarding agricultural management strategy. Macrofossil, sclerochronological, and stable isotopic analyses of carbonized seeds and archaeological shells are used to explore variable expressions of agricultural response to climate change along the Southern Levantine Jordan Rift. Comparison of proxies with regional data from across the Near Eastern Holocene help reveal the extent of change experienced in the Southern Levantine Bronze Age landscape. These variations are not simply matters of just time or space; instead, they illustrate settlement-by-settlement and taxon-by-taxon differences, many of which are interestingly unexpected.

Results from the paleoethnobotanical analyses reveal distinct patterns of crop management that suggest at least three different agricultural strategies practiced among the four focal settlements of Tell Abu en-Ni‘aj, Tell el-Hayyat, Khirbat Iskandar, and Zahrat adh-Dhra‘ 1. Ni‘aj and Hayyat in the northern Jordan Valley, practiced intensive agriculture, harvested a wide variety of cereal, pulse, and fruit cultigens, and likely practiced moderate amounts of landscape

management through manuring, multi-seasonal cropping, and the selective sowing of drought-intolerant crops. Khirbat Iskandar in the upper Dead Sea Basin practiced limited agriculture, with selective management of *Triticum dicoccum* but minimal management of any other crops. ZAD 1 on the Dead Sea Plain had the most intensive agricultural management through manuring, watering and selective-crop placement, but cultivated only a slim array of taxa with a preference towards cereal and grape crops. These characteristics, in tandem with the drier climate at ZAD 1, suggest that farmers likely took extra care of drought-intolerant crops in order to ensure healthy yields, likely cultivating crops on the banks of local streams, heavily manuring crop fields, and/or cultivating crops primarily in the winter.

The high frequencies and $\Delta^{13}C$ and $\delta^{15}N$ values for *Hordeum vulgare* and *Triticum dicoccum* throughout most of the occupations of each of the four focal sites reveal these taxa to be the most influential cereal cultigens for many Southern Levantine farmers in the Early to Middle Bronze Ages, particularly for the two northern Jordan Valley settlements. Furthermore, the spatial patterns, relative frequencies, stable isotopic values, and possible architectural features for processing grapes or olives (such as the three-basin feature at Ni‘aj) show that these taxa also were highly valued in the region. On the other hand, despite relatively moderate frequencies in the northern Jordan Valley, $\Delta^{13}C$ values suggest that pulses were less intensively managed at these sites, and reflect a preference for cereal and fruit/oil production.

My results further reveal that climate in the Jordan Rift in EB IV through MB II was relatively arid throughout. Regional comparisons of paleoethnobotanical assemblages reveal that the period from the beginning of EB IV through MB I may have been relatively drier than the subsequent MB II period, and archaeological shell results suggest that regional drying may have persisted throughout much of EB IV. Analyses also suggest that, while semi-arid climate

conditions persisted in the northern Jordan Valley, MB I around the Dead Sea Plain was a period with a much more arid environment. The relative dryness of the Dead Sea Plain roughly mimics the modern climate for the region, with the Dead Sea Basin being a particularly arid locale.

Overall, my climate proxies suggest a climatic transition that accords with a roughly 300-year interval of maximum drying starting around 4200 BP and terminating around 3900 BP in late EB IV and early MB I, which was bracketed by a relatively dry climate in early EB IV and early MB II. A summary of the primary findings from this dissertation is presented in Figure 11.1.

Further work that could most help to fill gaps in this dissertation include the paleoethnobotanical analysis of carbonized remains from Khirbat Iskandar, further stable isotopic investigation of shells at Tell Abu en-Ni‘aj and Tell el-Hayyat, and a general study of stable isotopic baselines for $\delta^{15}N$ and $\Delta^{13}C$ from cultivated taxa present at the four focal sites. Study of the floral assemblage of Khirbat Iskandar would allow for further interpretation of the stable isotopic results, revealing what crops were more frequent at the site and how people might have used them. This would help ascertain whether wheat was managed more intensively than other crops.

A more in-depth study of *Melanopsis* shells would help provide a potentially local climate signal for the northern Jordan Valley. Obtaining sub-annual data helped reveal patterns of yearly climate variability while still providing a limited snapshot of climate for seven occupation phases at Tell Abu en-Ni‘aj and Tell el-Hayyat, so the next step would be to bulk sample shells from each site. Bulk sampling, incorporating multiple shells from each phase, would fill out the temporal range and provide a more accurate signal of mean paleoprecipitation.

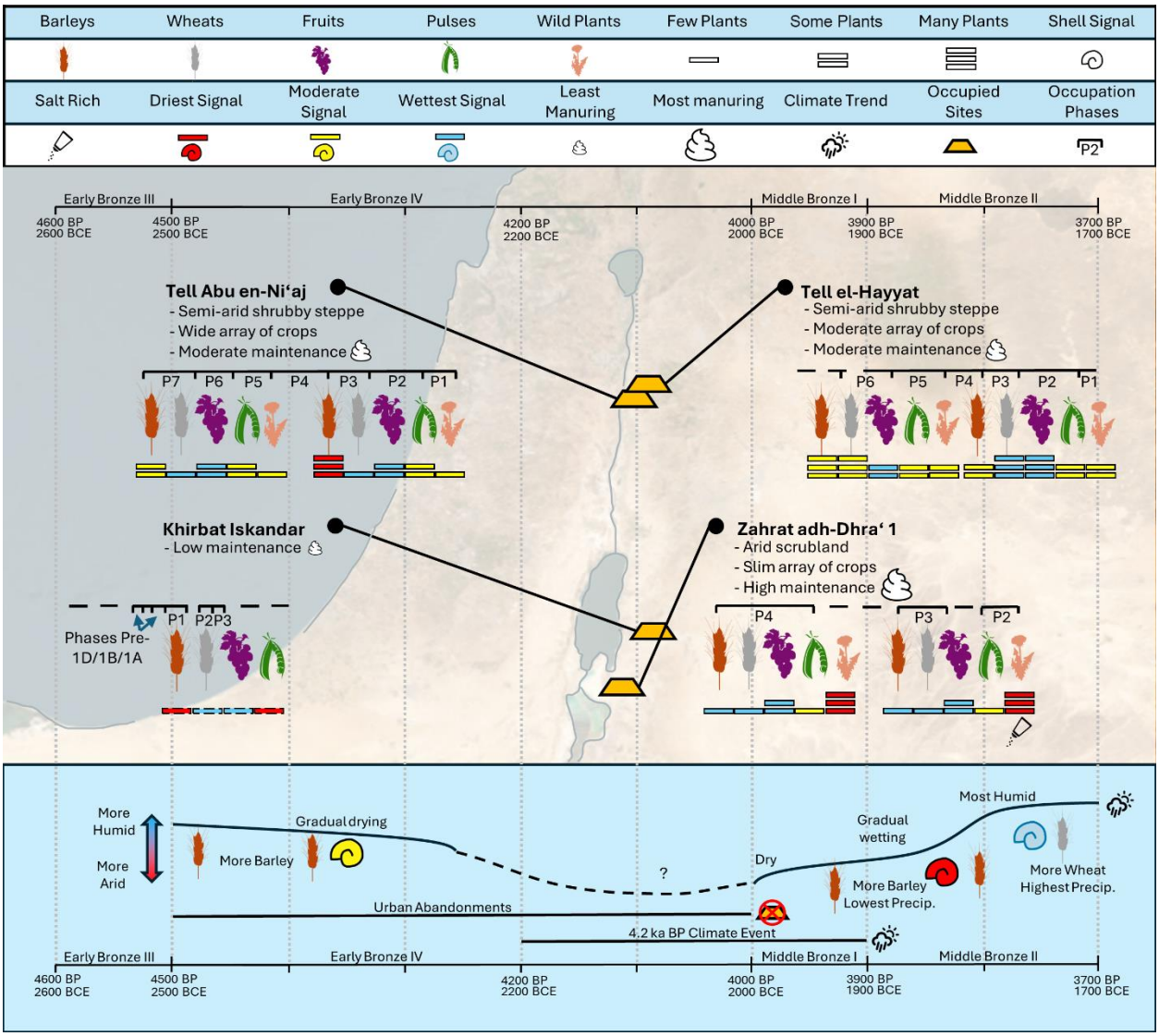

Figure 11.1 A summary of the main findings from the paleoethnobotanical and stable isotopic analyses of Tell Abu en-Ni'aj, Tell el-Hayyat, Khirbat Iskandar, and Zahrat adh-Dhra' 1, Jordan. Top depiction shows relative abundances of crops and vegetation (indicated by the number of stacked bars), and water availability signals (indicated by the color of the bars) compared from roughly the early and later portion of each site. Bottom timeline shows a curve of regional water availability inferred from the combined signals from the archaeological seed and shell proxies. The scale of change (few/some/many and driest/moderate/wettest) are approximated and relative to the amount of change at each site and for each proxy.

Finally, the most important and challenging step would be to conduct experiments on modern crops in semi-arid climates to determine the expected range of stable isotopes of carbon and nitrogen under a variety of environmental conditions. Experimental testing could expand the study of cereal cultigens or focus on the less well-known signals from fruit and pulse cultigens,

examining how varying factors such as soil nutrient composition and water availability from various sources may affect an isotope profile.

The combination of approaches utilized in the multiple avenues of this study constitute an innovative approach for inferring ancient use of agricultural landscapes and potential human responses to environmental stress. I present a novel contribution to the field in several avenues, including my comparative methodology and spatial analyses. My methodology is focused on an interwoven analysis of local climate and agriculture. The proxies of archaeological seeds and archaeological shells were selected specifically to offer comparative signals of climate. These proxies build on one another, allowing me to draw interpretations with heightened confidence where the patterns of these proxies correlate, such as the transition to a more humid climate during Middle Bronze II, around Hayyat Phase 3.

My analysis of spatial patterns was also novel in certain aspects. In Chapter 5, I utilized multiple methods for analyzing the spatial patterns of seed deposition. In particular, the consideration for locus types helped reveal the potential use for various plants, such as how chaff was incorporated into mudbricks or barley was more frequently used in food preparation activities.at Ni‘aj. In Chapter 8, I considered spatial patterns of stable carbon isotopes values for cereal crops. I compare the watering thresholds to expected spatio-temporal patterns to show how $\Delta^{13}C$ values from cultivated crops, in times used as a proxy of climate (Riehl et al., 2014; Flohr et al., 2019), may be better indicators of crop management than climate. Regional comparison shows that this consideration may be true even in water-limited, rain-fed fields and confirms, though well-known by now, that species-specific data must be used for future study.

Tell Abu en-Ni‘aj and Tell el-Hayyat provide case studies for interpretation of sedentary agrarian behavior within a limited spatial scope that helps to isolate the effects of climate

through time. Zahrat adh-Dhra‘ 1 and Khirbat Iskandar, on the other hand, offer invaluable comparisons from unique archaeological contexts that help frame the extent and variable expressions of agricultural management and response to climate shifts along the Jordan Rift. Results ultimately refute my initial hypothesis of a transition from drier conditions through the entire EB IV to more humid conditions starting at the outset of the MBA, or MB I. However, they offer intriguing comparisons that reveal how ancient farmers applied differing agricultural practices, thereby helping present these settlements in a new light.

REFERENCES

Abd el Rahman, A. A., Batanouny, K. H., & Ezzat, N. H. (1967). Effect of water supply on growth and yield of barley. *Plant and Soil*, *27*(3), 369–382.

Abdullah, M. T., & Al-Dosari, M. E. (2002). *Vegetation of the State of Kuwait*. IUCN and Kuwait, State of Kuwait: Environment Public Authority.

Abu-Irmaileh, B. E. (1982). *Weeds of Jordan (Weeds of crop fields)*. Author.

ADEMNES: The GRF (German Research Foundation) and University of Tübingen funded Archaeobotanical Database of Eastern Mediterranean and Near Eastern Sites, last update 2015. www.ademnes.de

Aguilera, M., Araus, J. L., Voltas, J., Rodriguez-Ariza, M. O., Molina, F., Buxó, R., & Ferrio, J. P. (2008). Stable carbon and nitrogen isotopes and quality traits of fossil cereal grains provide clues on sustainability at the beginnings of Mediterranean agriculture. *Rapid Communications in Mass Spectrometry*, *22*, 1653–1663.

Akawwi, E., Kakish, M., & Hadadin, N. (2009). Geological model and groundwater aspects of the area surrounding eastern shores of Dead Sea (DS)-Jordan. *WSEAS Transactions on Information Science and Applications*, *6*(4), 670–683.

Al-Bakri, J. T. (2008). Soils of Jordan. *Status of Mediterranean Soil Resources: Actions Needed to Support Their Sustainable Use*, 16.

Albright, W. F. (1962). The Chronology of Middle Bronze I (Early Bronze-Middle Bronze). *Bulletin of the American Schools of Oriental Research*, *168*, 36–42.

Alhejoj, I., Bandel, K., & Salameh, E. (2017). Aquatic Mollusks: Occurrences, identification and their use as bioindicators of environmental conditions (salinity, trace elements and pollution parameters) in Jordan. In O. Abdalla (Ed.), *Water Resources in Arid Areas: The Way Forward* (pp. 295–318). Springer International.

Ali, W., Glaser, J., Hötzl, H., Lenz, S., Salameh, E., Thiel, M., & Werz, H. (2009). Groundwater conditions of the Jordan Rift escarpment northeast of the Dead Sea. In H. Hötzl, P. Möller, & E. Rosenthal (Eds.), *The Water of the Jordan Valley: Scarcity and Deterioration of Groundwater and its Impact on the Regional Development* (pp. 385–412). Springer-Verlag, Berlin, Heidelberg.

Alonso, N., Cantero, F. J., Jornet, R., Lopez, D., Montes, E., Prats, G., & Valenzuela, S. (2014). Milling wheat and barley with rotary querns: The Ouarten women (Dahmani, Kef, Tunisia). *AmS-Skrifter*, *24*, 11–30.

Al-Zoubi, A., & Abu-Hamatteh, Z. S. H. (2009). Geological evolution of the Jordan Valley. In T. Ahmad, F. Hirsch, & P. Charusiri (Eds.), *Geological Anatomy of India and the Middle East* (Vol. 32). Journal of the Virtual Explorer.

Amr, Z., Alnasarat, H., & Neubert, E. (2014). Notes on the current and past freshwater snail fauna of Jordan. *Jordan Journal of Natural History*, 83–115.

Anderson, P. C. (1998). History of Harvesting and Threshing Techniques for Cereals in the Prehistoric Near East. In A. B. J. Valkoun, G. Willcox, & C. O. Qualset (Eds.), *The Origins of Agriculture and Crop Domestication* (pp. 145–159). ICARDA.

Anderson, S., & Ertug-Yaras, F. (1998). Fuel Fodder and Faeces: An Ethnographic and Botanical Study of Dung Fuel Use in Central Anatolia. *Environmental Archaeology*, *1*, 99–109.

Andrus, C. F. T. (2011). Shell midden schlerochronology. *Quaternary Science Reviews*, *30*, 2892–2905.

Antolin, F., & Buxó, R. (2011). Proposal for the systematic description and taphonomic study of carbonized cereal grain assemblages: A case study of an early Neolithic funerary context in the cave of Can Sadurni (Begues, Barcelona province, Spain). *Vegetation History and Archaeobotany*, *20*, 53–66.

Araus, J. L., Febrero, A., Buxo, R., Camalich, M. D., Martin, D., Molina, F., Rodriguez-Ariza, M. O., & Romagosa, I. (1997). Changes in carbon isotope discrimination in grain cereals from different regions of the western Mediterranean Basin during the past seven millennia. Palaeoenvironmental evidence of a differential change in aridity during the late Holocene. *Global Change Biology*, *3*, 107–118.

Araus, J. L., Febrero, A., Buxó, R., Rodriguez-Ariza, M. O., Molina, F., Camalich, M. D., Martin, D., & Voltas, J. (1997). Identification of Ancient Irrigation Practices based on the Carbon Isotope Discrimination of Plant Seeds: A Case Study from the South-East Iberian Peninsula. *Journal of Archaeological Science*, *24*, 729–740.

Araus, J. L., Febrero, A., Catala, M., Molist, M., Volta, J., & Romagosa, I. (1999). Crop water availability in early agriculture: Evidence from carbon isotope discrimination of seeds from a tenth millennium BP site on the Euphrates. *Global Change Biology*, *5*, 201–212.

Arikan, B. (2015). Modeling the paleoclimate (ca. 6000-3200 cal BP) in eastern Anatolia: The method of Macrophysical Climate Model and comparison with proxy data. *Journal of Archaeological Science*, *57*, 158–167.

Arranz-Otaegui, A., Colledge, S., Zapata, L., Teira-Mayolini, L. C., & Ibáñez, J. J. (2016). Regional diversity on the timing for the initial appearance of cereal cultivation and domestication in southwest Asia. *PNAS*, *113*(49).

Asouti, E., & Fuller, D. Q. (2012). From foraging to farming in the southern Levant: The development of Epipalaeolithic and Pre-pottery Neolithic plant management strategies. *Vegetation History and Archaeobotany*, *21*, 149–162.

Asouti, E., & Fuller, D. Q. (2013). A contextual approach to the emergence of agriculture in Southwest Asia: Reconstructing Early Neolithic plant-food production. *Current Anthropology*, *54*(3), 299–345.

Aucour, A.-M., Sheppard, S. M. F., & Savoye, R. (2003). δ13C of fluvial mollusk shells (Rhone River): A proxy for dissolved inorganic carbon? *Limnology and Oceanography*, *48*(6), 2186–2193.

Bandel, K., Sivan, N., & Heller, J. (2007). Melanopsis from Al-Qarn, Jordan Valley (Gastropoda: Cerithioidea). *Palaontologische Zeitschrift*, *81*(3), 304–315.

Bar-Matthews, M., & Ayalon, A. (2011). Mid-Holocene climate variations revealed by high-resolution speleothem records from Soreq Cave, Israel and their correlation with cultural changes. *The Holocene*, *21*(1), 163–171.

Bar-Matthews, M., Ayalon, A., & Kaufman, A. (1997). Late Quaternary Paleoclimate in the Eastern Mediterranean Region from Stable Isotope Analysis of Speleothems at Soreq Cave, Israel. *Quaternary Research*, *47*, 155–168.

Bar-Matthews, M., Ayalon, A., Kaufman, A., & Wasserburg, G. J. (1999). The Eastern Mediterranean paleoclimate as a reflection of regional events: Soreq cave, Israel. *Earth and Planetary Science Letters*, *166*, 85–95.

Baruch, U. (1986). The Late Holocene vegetational history of Lake Kinneret (Sea of Galilee), Israel. *Paléorient*, *12*(2), 37–48.

Baruch, U. (1990). Palynological evidence of human impact on the vegetation as recorded in Late Holocene lake sediments in Israel. In S. Bottema, G. Entjes-Nieborg, & W. van Zeist (Eds.), *Man's Role in the Shaping of the Eastern Mediterranean Landscape* (pp. 283–293). Balkema.

Bar-Yosef, D. E., & Heller, J. (1987). Mollusca from Yiftah'el, Lower Galilee, Israel. *Paleorient*, *13*(1), 131–135.

Bejenaru, L., Bodi, G., Stanc, S., & Danu, M. (2018). Middle Holocene subsistence east of the Romanian Carpathians: Bioarchaeological data from the Chalcolithic site of Poduri-Dealul Ghindaru. *The Holocene*, *28*(10), 1653–1663.

Ben Dor, Y., Armon, M., Ahlborn, M., Morin, E., Erel, Y., Brauer, A., Schwab, M. J., Tjallingii, R., & Enzel, Y. (2018). Changing flood frequencies under opposing late Pleistocene eastern Mediterranean climates. *Scientific Reports*, *8*, 11.

Benzaquen, M., Finkelstein, I., & Langgut, D. (2019). Vegetation history and human impacts on the environs of Tel Megiddo in the Bronze and Iron Ages: A dendroarchaeological analysis. *Tel Aviv*, *46*, 42–64.

Bieniada, M. E. (2016). Intermediate Bronze Age in Southern Levant (4200-4000 BP)—Why did four cities in Transjordan survive urban collapse? *Studia Quaternaria*, *33*(1), 5–10.

Bini, M., Zanchetta, G., Perşoiu, A., Cartier, R., Catalá, A., Cacho, I., Dean, J., Di Rita, F., Drysdale, R., Finnè, M., Isola, I., Jalali, B., Lirer, F., Magri, D., Masi, A., Marks, L., Mercuri, A. M., Peyron, O., Sadori, L., … Brisset, E. (2019). The 4.2 ka BP Event in the Mediterranean region: An overview. *Clim. Past*, *15*, 555–577.

Black, E., Brayshaw, D. J., & Rambeau, C. M. (2010). Past, present, and future precipitation in the Middle East: Insights from models and observations: Philosophical Transactions. *Mathematical, Physical and Engineering Sciences*, *368*(1931), 5173–5184.

Black, E., Hoskins, B., Slingo, J., & Brayshaw, D. (2011). The present-day climate of the Middle East. In S. Mithen & E. Black (Eds.), *Water, Life and Civilization: Climate, Environment and Society in the Jordan Valley* (pp. 13–24). Cambridge University Press.

Boardman, S., & Jones, G. (1990). Experiments on the effects of charring on cereal plant components. *Journal of Archaeological Science*, *17*, 1–11.

Bobrowsky, P. T. (1984). The history and science of gastropods in archaeology. *American Antiquity*, *49*(1), 77–93.

Boettinger, J. L. (2005). Alluvium and alluvial soils. In D. Hillel (Ed.), *Encyclopedia of Soils in the Environment* (pp. 45–49). Elsevier.

Bogaard, A. (2005). "Garden Agriculture" and the Nature of Early Farming in Europe and the Near East. *World Archaeology*, *37*(2), 177–196.

Bogaard, A., Ater, M., & Hodgson, J. G. (2018b). Arable weeds as a case study in plant-human relationships beyond domestication. In C. Stepanoff & J.-D. Vigne (Eds.), *Hybrid Communities: Biosocial Approaches to Domestication and Other Trans-Species Relationships* (1st ed., pp. 97–112). Routledge.

Bogaard, A., Fraser, R., Heaton, T. H. E., Wallace, M., Vaiglova, P., Charles, M., Jones, G., Evershed, R. P., Styring, A. K., Anderson, N. H., Arbogast, R.-M., Bartosiewicz, L., Gardeisen, A., Kanstrup, M., Maier, U., Marinova, E., Ninov, L., Schafer, M., & Stephan, E. (2013). Crop manuring and intensive land management by Europe's first farmers. *PNAS*, *110*(31), 12589–12594.

Bogaard, A., Heaton, T. H. E., Poulton, P., & Merbach, I. (2007). The impact of manuring on nitrogen isotope ratios in cereals: Archaeological implications for reconstruction of diet and crop management practices. *Journal of Archaeological Science*, *34*, 335–343.

Bogaard, A., Styring, A., Ater, M., Hmimsa, Y., Green, L., Stroud, E., Whitlam, J., Diffey, C., Nitsch, E., Charles, M., Jones, G., & Hodgson, J. (2018a). From Traditional Farming in Morocco to Early Urban Agroecology in Northern Mesopotamia: Combining Present-day Arable Weed Surveys and Crop Isotope Analysis to Reconstruct Past Agrosystems in (Semi-)arid Regions. *Environmental Archaeology*, *23*(4), 303–322.

Bonacossi, D. M. (2014). Early Bronze Age storage techniques at Mishrifeh, Central-Western Syria. In L. Milano (Ed.), *Paleonutrition and Food Practices in the Ancient Near East* (pp. 237–252). Sargon Editore.

Bonhomme, V., Forster, E., & Wallace, M. (2017). Identification of inter- and intra-species variation in cereal grains through genometric morphometric analysis, and its resilience under experimental charring. *Journal of Archaeological Science*, *86*, 60–67.

Bourke, S. (2006). Pella and the Jordanian Middle and Late Bronze Ages (response to Chapter IV). In P. M. Fischer (Ed.), *The Chronology of the Jordan Valley During the Middle and Late Bronze Ages: Pella, Tell Abu Al-Kharaz and Tell Deir 'Alla* (pp. 243–256). Publishing house of the Austrian Academy of Sciences.

Bourke, S. J. (2014). The Southern Levant (Transjordan) during the Middle Bronze Age. In M. L. Steiner & A. E. Killebrew (Eds.), *The Oxford handbook of the archaeology of the Levant c. 8000-332 BCE* (pp. 465–481). Oxford University Press.

Bourke, S., Zoppi, U., Meadows, J., Hua, Q., & Gibbins, S. (2009). The beginning of the Early Bronze Age in the North Jordan Valley: New 14C determinations from Pella in Jordan. *Radiocarbon*, *51*(3), 905–913.

Boutton, T. W. (1991a). Stable Carbon Isotope Ratios of Natural Materials: II. Atmospheric, Terrestrial, Marine, and Freshwater Environments. In D. C. Coleman & B. Fry (Eds.), *Carbon Isotope Techniques* (pp. 173–185). Academic Press.

Boutton, T. W. (1991b). Tracer studies with 13C-enriched substrates: Humans and large animals. In D. C. Coleman & B. Fry (Eds.), *Carbon isotope techniques* (pp. 219–242). Academic Press.

Bowen, G. J., Wassenaar, L. I., & Hobson, K. A. (2005). Global application of stable hydrogen and oxygen isotopes to wildlife forensics. *Oecologia*, *143*(3), 337–348.

Bowman, D., Svoray, T., Devora, S., & Laronne, S. J. B. (2010). Extreme rates of channel incision and shape evolution in response to a continuous, rapid base-level fall, the Dead Sea, Israel. *Geomorphology*, *114*, 227–2378.

Braadbaart, F. (2008). Carbonisation and morphological changes in modern dehusked and husked Triticum dicoccum and Triticum aestivum grains. *Vegetation History and Archaeobotany*, *17*, 155–166.

Bradley, R. S. (2015). Chapter 8—Speleothems. In R. S. Bradley (Ed.), *Paleoclimatology* (3rd ed., pp. 291–318). Academic Press.

Brayshaw, D. J., Hoskins, B., & Black, E. (2010). Some physical drivers of changes in the winter storm tracks over the North Atlantic and Mediterranean during the Holocene: Philosophical Transactions. *Mathematical, Physical and Engineering Sciences*, *368*(1931), 5185–5223.

Brinkkemper, O., Braadbaart, F., van Os, B., van Hoesel, A., van Brussel, A. A. N., & Fernandes, R. (2018). Effectiveness of different pre-treatments in recovering pre-burial isotopic ratios of charred plants. *Rapid Communications in Mass Spectrometry*, *32*, 251–261.

Bronk Ramsey, C. (2009). Bayesian analysis of radiocarbon dates. *Radiocarbon*, *51*(1), 337–360.

Bronk Ramsey, C., Higham, T. F. G., Owen, D. C., Pike, A. W. G., & Hedges, R. E. M. (2002). Radiocarbon dates from the Oxford AMS system: Archaeometry datelist 31. *Archaeometry*, *44*(3), 1–149.

Bruins, H. J., & van der Plicht, J. (1995). Tell es-Sultan (Jericho): Radiocarbon Results of Short-Lived Cereal and Multiyear Charcoal Samples from the End of the Middle Bronze Age. *Radiocarbon*, *37*(2), 213–220.

Bruins, H. J., & van der Plicht, J. (1998). Early Bronze Jericho: High-Precision 14C Dates of Short-Lived Palaeobotanic Remains. *Radiocarbon*, *40*(2), 621–628.

Bryson, R. A., & DeWall, K. M. (2007). *A paleoclimatology workbook: High resolution, site-specific, macrophysical climate modeling*. Hot Springs: The Mammoth Site.

Burchell, M., Stopp, M. P., Cannon, A., Hallmann, N., & Schone, B. R. (2018). Determining seasonality of mussel collection from an early historic Inuit site, Labrador, Canada: Comparing thin-sections with high-resolution stable oxygen isotope analysis. *Journal of Archaeological Science: Reports*, *21*, 1215–1224.

Burstyn, Y., Martrat, B., Lopez, J., Iriarte, E., Jacobson, M. J., Lone, M. A., & Deininger, M. (2019). Speleothems from the Middle East: An example of water limited environments in the SISAL database. *Quaternary*, *2*(16), 28.

Çakirlar, C., & Şeşen, R. (2013). Reading between the lines: δ18O and δ13C isotopes of *Unio elongatulus* shell increments as proxies for local palaeoenvironments in mid-Holocene northern Syria. *Archaeol Anthropol Sci*, *5*, 85–94.

Cappers, R. T. J., & Bekker, R. M. (2013). *A Manual for the Identification of Plant Seeds and Fruits* (Vol. 23). University of Groningen.

Caracuta, V., Barzilai, O., Khalaily, H., Milevski, I., Paz, Y., Vardi, J., Regev, L., & Boaretto, E. (2015). The onset of faba bean farming in the Southern Levant. *Scientific Reports*, 9.

Caracuta, V., Vardi, J., Paz, Y., & Boaretto, E. (2017). Farming legumes in the pre-pottery Neolithic: New discoveries from the site of Ahihud (Israel). *PLOS ONE*, *12*(5), 28.

Charles, M. (1998). Fodder from dung: The recognition and interpretation of dung-derived plant material from archaeological sites. *Environmental Archaeology*, *1*(1), 111–122.

Charles, M. P. (1984). Introductory remarks on the cereals. In J. N. Postgate & M. A. Powell (Eds.), *Bulletin on Sumerian agriculture* (Vol. 1, pp. 17–31). University Press, Cambridge.

Cheng, H., Sinha, A., Verheyden, S., Nader, F. H., Li, X. L., Zheng, P. Z., Yin, J. J., Yi, L., Peng, Y. B., Rao, Z. G., Ning, Y. F., & Edwards, R. L. (2015). The climate variability in northern Levant over the past 20,000 years. *Geophysical Research Letters*, *42*, 8631–8650.

Chernoff, M. C. (1988). *The archaeobotanical material from Tel el Ifshar, Israel: A diachronic study of agricultural strategies during the third and second millennia B.C.E.* [Dissertation]. Brandeis University.

Chernoff, M. C., & Paley, S. M. (1998). Dynamics of cereal production at Tell el Ifshar, Israel during the Middle Bronze Age. *Journal of Field Archaeology*, *25*(4), 397–416.

Chesson, M. S., & Philip, G. (2003). Tales of the city? "Urbanism" in the Early Bronze Age Levant from Mediterranean and Levantine perspectives. *Journal of Mediterranean Archaeology*, *16*(1), 3–16.

Cohen, S. L. (2022). The Early Bronze IV - Middle Bronze I transition in the southern Levant: Analysis and assessment. *Levant*, 13. https://doi.org/10.1080/00758914.2022.2073689

Cole, J. J., & Prairie, Y. T. (2009). Dissolved CO2. *Encyclopedia of Inland Waters*, *2*, 30–34.

Cossani, C. M., Slafer, G. A., & Savin, R. (2009). Yield and biomass in wheat and barley under a range of conditions in a Mediterranean site. *Field Crops Research*, *112*, 205–213.

Craine, J. M., Brookshire, E. N. J., Cramer, M. D., Hasselquist, N. J., Koba, K., Marin-Spiotta, E., & Wang, L. (2015). Ecological interpretations of nitrogen isotope ratios of terrestrial plants and soils. *Plant Soil*, *396*, 1–26.

Craufurd, P. Q., Austin, R. B., Acevedo, E., & Hall, M. A. (1991). Carbon isotope discrimination and grain-yield in barley. *Field Crops Research*, *27*, 301–313.

Cullen, H. M., DeMenocal, P. B., Hemming, S., Hemming, G., Brown, F. H., Guilderson, T., & Sirocko, F. (2000). Climate change and the collapse of the Akkadian empire: Evidence from the deep sea. *Geology*, *28*(4), 379–382.

D'Andrea, M. (2019). The periodization of Early Bronze IV in the Southern Levant: Bridging the gap between stratigraphy and absolute chronology. In E. Gallo (Ed.), *Conceptualizing Urban Experiences: Tell es-Sultan and Tall al-Hammam Early Bronze cities across the Jordan. Proceedings of a workshop held in Palermo, G. Whitaker Foundation, Villa Malfitano, June 19th 2017* (pp. 61–78). La Sapienza.

D'Andrea, M. (2020). About stratigraphy, pottery, and relative chronology: Some considerations for a refinement of the archaeological periodization of the Southern Levantine Early Bronze Age IV. In S. Richard (Ed.), *New Horizons in the Study of the Early Bronze III and Early Bronze IV of the Levant* (pp. 395–416). Eisenbrauns.

Danin, A. (1995). Man and the Natural Environment. In T. Levy (Ed.), *Archaeology of Society in the Holy Land* (pp. 24–39). Leicester University Press.

Dansgaard, W. (1964). Stable isotopes in precipitation. *Tellus XVI*, *4*, 437–468.

Davies, C. P., & Fall, P. L. (2001). Modern pollen precipitation from an elevational transect in central Jordan and its relationship to vegetation. *Journal of Biogeography*, *28*, 1195–1210.

Deith, M. R. (1983). Molluscan calendars: The use of growth-line analysis to establish seasonality of shellfish collection at the Mesolithic site of Morton, Fife. *Journal of Archaeological Science*, *10*, 423–440.

Delorit, R. J. (1970). *Illustrated Taxonomy Manual of Weed Seeds*. Agronomy Publications.

deMenocal, P. B. (2001). Cultural responses to climate change during the Late Holocene. *Science*, *292*(5517), 667–673.

DeNiro, M. J., & Hastorf, C. A. (1985). Alteration of 15N/14N and 13C/12C ratios of plant matter during the initial stages of diagenesis: Studies utilizing archaeological specimens from Peru. *Geochimica et Cosmochimica Acta*, *49*, 97–115.

Dennell, R. (1974). Botanical evidence for prehistoric crop processing activities. *Journal of Archaeological Science*, *1*, 275–284.

Dente, E., Lensky, N. G., Morin, E., Grodek, T., Sheffer, N. A., & Enzel, Y. (2017). Geomorphic Response of a Low-Gradient Channel to Modern, Progressive Base-Level Lowering: Nahal HaArava, the Dead Sea. *Journal of Geophysical Research: Earth Surface*, *122*, 2468–2487.

Dettman, D. L., & Lohmann, K. C. (1993). Seasonal change in Paleogene surface water 6180: Fresh-water bivalves of Western North America. In P. K. Swart, K. C. Lohmann, J. Mckenzie, & S. Savin (Eds.), *Climate Change in Continental Isotopic Records* (pp. 153–163). American Geophysical Union.

Dever, W. G. (1980). New Vistas on the EB IV ("MB I") Horizon in Syria-Palestine. *Bulletin of the American Schools of Oriental Research*, *237*, 35–64.

Dever, W. G. (1995). Social structure in the Early Bronze IV period in Palestine. In T. E. Levy (Ed.), *The Archaeology of Society in the Holy Land* (pp. 282–296). Leicester University Press.

Dickin, E., Steele, K., Edwards-Jones, G., & Wright, D. (2012). Agronomic diversity of naked barley (*Hordeum vulgare* L.): A potential resource for breeding new food barley for Europe. *Euphytica*, *184*, 85–99.

Dighton, A., Fairbairn, A., Bourke, S., Faith, J. T., & Habgood, P. (2016). Bronze Age olive domestication in the north Jordan Valley: New morphological evidence for regional complexity in early arboricultural practice from Pella in Jordan. *Vegetation History and Archaeobotany*, *26*, 403–413.

Djelel, R., Nabiha, B., Noureddine, Z., & Imene, F. (2020). Morphological and physiological response of naked and covered barley genotypes to water stress in Eastern Algeria. *Asian Jr. of Microbol. Biotech. Env. Sc.*, *22*(3), 567–572.

de Miroschedji, P. (2009). Rise and collapse in the Southern Levant in the Early Bronze Age. In A. Cardarelli, A. Cazzella, M. Frangipane, & R. Peroni (Eds.), *Scienze dell'antichità* (pp. 101–129). La Sapienza.

de Moulins, D. (2009). Sidon Grains from the Store-Rooms. *Archaeology & History in the Lebanon*, *29*, 11–15.

de Moulins, D., & Marsh, A. (2012). Sidon: Plant remains from the Middle Bronze Age. *Archaeology & History in the Lebanon*, *34–35*, 236–258.

Edelman-Furstenberg, Y., Almogi-Labin, A., & Hemleben, C. (2008). Palaeoceanographic evolution of the central Red Sea during the late Holocene. *The Holocene*, *19*(1), 117–127.

Edwards, P. C., Falconer, S. E., Fall, P. L., Berelov, I., Davies, C., Meadows, J., Meegan, C., Metzger, M. C., & Sayej, G. (2001). Archaeology and environment of the Dead Sea Plain: Preliminary results of the first season of investigations by the joint La Trobe University/Arizona State University project. *Annual of the Department of Antiquities of Jordan*, *45*, 135–157.

Ehleringer, J. R., Coleman, D. C., & Fry, B. (1991). 13C/12C fractionation and its utility in terrestrial plant studies. In *Carbon isotope techniques* (pp. 187–200). Academic Press.

Ehrlich, Y., Raj, H., Mintz, E., Regev, L., & Boaretto, E. (2022). Olive pits as a high-resolution proxy archive of climate: D13C in modern and archaeological olive pits reflecting environmental conditions. *Quaternary Science Reviews*, *294*, 1–13.

Ekin, I., Bashan, M., & Sesen, R. (2011). Possible seasonal variation of the fatty acid composition from *Melanopsis praemorsa* (L., 1758) (*Gastropoda: Prosobranchia*), from southeast Anatolia, Turkey. *Turkish Journal of Biology*, *35*, 203–213.

Elkarmi, A. Z., & Ismail, N. S. (2006). Allometry of the gastropod *Melanopsis praemorsa* (*Thiaridae: Prosobranchia*) from Azraq Oasis, Jordan. *Pakistan Journal Biological Sciences*, *9*(7), 1359–1363.

Enzel, Y., Ken-Tor, R. B., Sharon, D., Gvirtzman, H., Dayan, U., Ziv, B., & Stein, M. (2003). Late Holocene climates of the Near East deduced from Dead Sea level variation and modern regional winter rainfall. *Quaternary Research*, *60*(3), 263–273.

Erskine, W., Smartt, J., & Muehlbauer, F. J. (1994). Mimicry of Lentil and the Domestication of Common Vetch and Grass Pea. *Economic Botany*, *48*(3), 326–332.

Ertug, F. (2000). An ethnobotanical study in central Anatolia (Turkey). *Economic Botany*, *54*(2), 155–182.

Ertug-Yaras, F. (1997). *An ethnoarchaeological study of subsistence and plant gathering in central Anatolia* [Dissertation]. Washington University.

Esse, D. L. (1989). Secondary state formation and collapse in Early Bronze Age Palestine. In P. de Miroschedji (Ed.), *L'urbanisation de la Palestine a l'age du Bronze ancien: Bilan et perspectives des recherches actuelles* (pp. 81–96). BAR Publishing.

Falconer, S. E. (1987). Village pottery production and exchange: A Jordan Valley perspective. In A. Hadidi (Ed.), *Studies in the history and archaeology of Jordan III* (pp. 251–259). Routledge Kegan & Paul.

Falconer, S. E. (1994). The development and decline of Bronze Age civilization in the Southern Levant: A reassessment of urbanism and ruralism. In C. Mathers & S. Stoddart (Eds.), *Development and decline in the Mediterranean Bronze Age* (pp. 305–333). J.R. Collis Publications.

Falconer, S. E. (1995). Rural Responses to Early Urbanism: Bronze Age Household and Village Economy at Tell el-Hayyat, Jordan. *Journal of Field Archaeology*, *22*(4), 399–419.

Falconer, S. E., & Fall, P. L. (2006). *Bronze Age Rural Ecology and Village Life at Tell el-Hayyat, Jordan*. British Archaeological Reports.

Falconer, S. E., & Fall, P. L. (2016). A radiocarbon sequence from Tell Abu en-Ni‘aj, Jordan and its implications for Early Bronze IV chronology in the Southern Levant. *Radiocarbon*, *58*(3), 615–647.

Falconer, S. E., & Fall, P. L. (2017). Radiocarbon evidence from Tell Abu en-Ni‘aj and Tell el-Hayyat, Jordan, and its implications for Bronze Age Levantine and Egyptian chronologies. *Journal of Ancient Egyptian Interconnections*, *13*, 7–19.

Falconer, S. E., & Fall, P. L. (2019). *Early Bronze IV village life in the Jordan Valley: Excavations at Tell Abu en-Ni’aj and Dhahret Umm el-Marar, Jordan*. BAR Publishing.

Falconer, S. E., & Fall, P. L. (2022). Sacred spaces and liminal behavior in Levantine temples in antis. *Journal of Ancient Near Eastern History*, *9*, 259–284.

Falconer, S. E., Fall, P. L., & Jones, J. E. (1998). Jordan Valley Village Project. *American Journal of Archaeology*, *102*(3), 588–589.

Falconer, S. E., Fall, P. L., & Jones, J. E. (2001). The Jordan Valley Village Project: Excavations at Tell Abu en-Ni’aj, 2000. *American Journal of Archaeology*, *105*(3), 438–439.

Falconer, S. E., Fall, P. L., Metzger, M. C., & Lines, L. (2004). Bronze Age rural economic transitions in the Jordan Valley. *Annual of the American Schools of Oriental Research*, *58*, 1–17.

Falconer, S. E., Magness-Gardiner, B., & Metzger, M. C. (1984). Report of the First Season of the Tell el-Hayyat Project. *Bulletin of the American Schools of Oriental Research*, *255*, 49–74.

Falconer, S. E., & Savage, S. H. (1995). Heartlands and hinterlands: Alternative trajectories of Early urbanization in Mesopotamia and the Southern Levant. *American Antiquity*, *60*(1), 37–58.

Fall, P. L., Falconer, S. E., & Hoflmayer, F. (2021). New bayesian radiocarbon models for Early Bronze IV Tell Abu en-Ni’aj and Middle Bronze Age Tell el-Hayyat, Jordan. *Radiocarbon*, 63(1), 41-76.

Fall, P. L., Falconer, S. E., & Klinge, J. (2015). Bronze age fuel use and its implications for agrarian landscapes in the eastern Mediterranean. *Journal of Archaeological Science: Reports*, *4*, 182–191.

Fall, P. L., Falconer, S. E., & Lines, L. (2002). Agricultural Intensification and the Secondary Products Revolution along the Jordan Rift. *Human Ecology*, *30*(4), 445–482.

Fall, P. L., Falconer, S. E., & Porson, S. (2019). Archaeobotanical inference of intermittent settlement and agriculture at Middle Bronze Age Zahrat adh-Dhra’1, Jordan. *Journal of Archaeological Science: Reports*, *26*, 17.

Fall, P. L., Lines, L., & Falconer, S. E. (1998). Seeds of Civilization: Bronze Age Rural Economy and Ecology in the Southern Levant. *Association of American Geographers*, *88*(1), 107–125.

Fall, P. L., Richard, S., Pilaar Birch, S. E., Ridder, E., D'Andrea, M., Long, J. C. Jr., Hedges-Knyrim, G., Porson, S., Metzger, M., & Falconer, S. E. (2022). New AMS chronology for the Early Bronze III/IV transition at Khirbat Iskandar, Jordan. *Radiocarbon*, 64(2), 237-252. https://doi.org/10.1017/RDC.2022.22

Fall, P. L., Ridder, E., Pilaar Birch, S. E., & Falconer, S. E. (2023). Bayesian modeling of a peripheral Middle Bronze Age settlement at Zahrat adh-Dhra' 1, Jordan. *Radiocarbon*, *65*(5), 1022–1037. https://doi.org/doi:10.1017/RDC.2023.99

Fall, P. L., Soto-Berelov, M., Ridder, E., & Falconer, S. E. (2018). Toward a Grand Narrative of Bronze Age Vegetation Change and Social Dynamics in the Southern Levant. In T. E. Levy & I. W. N. Jones (Eds.), *Cyber-Archaeology and Grand Narratives* (pp. 91–110). Springer International.

Farber, E., Vengosh, A., Gavrieli, I., Marie, A., Bullen, T. D., Mayer, B., Holtzman, R., Segal, M., & Shavit, U. (2004). The origin and mechanisms of salinization of the Lower Jordan River. *Geochimica et Cosmochimica Acta*, *68*(9), 1989–2006.

Farquhar, G. D., Ehleringer, J. R., & Hubick, K. T. (1989). Carbon isotope discrimination and photosynthesis. *Annual Review of Plant Physiology and Plant Molecular Biology*, *40*, 503–537.

Farquhar, G. D., O'Leary, M. H. O., & Berry, J. A. (1982). On the relationship between carbon isotope discrimination and the intercellular carbon dioxide concentration in leaves. *Australian Journal of Plant Physiology*, *9*, 121–137.

Fastovsky, D. E., Arthur, M. A., Strater, N. H., & Foss, A. (1993). Freshwater Bivalves (*Unionidae*), Disequilibrium Isotopic Fractionation, and Temperatures. *PALAIOS*, *8*(6), 602–608.

Feinbrun-Dothan, N. (1978). *Flora Palaestina Three* (1–2). Israel Academy of Sciences and Humanity.

Feinbrun-Dothan, N. (1986). *Flora Palaestina Four* (1–2). Israel Academy of Sciences and Humanity.

Felker, P., & Moss, J. (Eds.). (1996). *Prosopis: Semiarid fuelwood and forage tree building consensus for the disenfranchised*. Texas A&M University-Kingsville.

Ferrio, J. P., Araus, J. L., Buxó, R., Voltas, J., & Bort, J. (2005). Water management practices and climate in ancient agriculture: Inferences from the stable isotope compositions of archaeobotanical remains. *Vegetation History and Archaeobotany*, *14*(4), 510–517.

Ferrio, J. P., Voltas, J., & Araus, J. L. (2012). *A smoothed curve of δ13C of atmospheric CO2 from 16,100 BCE to 2,010 CE*. http://web.udl.es/usuaris/x3845331/AIRCO2_LOESS.xls

Ferry, M., Meghraoui, M., Karaki, N. A., Al-Taj, M., Amoush, H., Al-Dhaisat, S., & Barjous, M. (2007). A 48-kyr-long slip rate history for the Jordan Valley segment of the Dead Sea Fault. *Earth and Planetary Science Letters*, *260*(3–4), 394–406.

Fick, S. E., & Hijmans, R. J. (2017). WorldClim 2: New 1km spatial resolution climate surfaces for global land areas. *International Journal of Climatology*, *37*(12), 4302–4315.

Filipović, D. (2012). *An archaeobotanical investigation of plant use, crop husbandry, and animal diet at early-mid Neolithic Catalhoyuk, Central Anatolia* [Dissertation]. Wolfson College Institute of Archaeology.

Finkelstein, I. (1989). Further observations on the socio-demographic structure of the intermediate Bronze Age. *Levant*, *21*, 129–140.

Finkelstein, I., & Langgut, D. (2014). Dry Climate in the Middle Bronze I and Its Impact on Settlement Patterns in the Levant and Beyond: New Pollen Evidence*. *Journal of Near Eastern Studies*, *73*(2), 219–234.

Finlay, J. C. (2004). Patterns and controls of lotic algal stable carbon isotope ratios. *Limnology and Oceanography*, *49*(3), 850–861.

Fiorentino, G., Caracuta, V., Calcagnile, L., D'Elia, M., Matthiae, P., Mavelli, F., & Quarta, G. (2008). Third millennium B.C. climate change in Syria highlighted by Carbon stable isotope analysis of 14C-AMS dated plant remains from Ebla. *Palaeogeography, Palaeoclimatology, Palaeoecology*, *266*, 51–58.

Fiorentino, G., Caracuta, V., Casiello, G., Longobardi, F., & Sacco, A. (2011). Studying ancient crop provenance: Implications from d13C and d15N values of charred barley in a Middle Bronze Age silo at Ebla (NW Syria). *Rapid Communications in Mass Spectrometry*, *26*, 327–335.

Fiorentino, G., Ferrio, J. P., Bogaard, A., Araus, J. L., & Riehl, S. (2015). Stable isotopes in archaeobotanical research. *Vegetation History and Archaeobotany*, *24*, 215–227.

Fischer, P. M., & Holden, T. (2006). Climate, Fauna and Flora: An overview. In *Tell Abu Al-Kharaz in the Jordan Valley* (Vol. 2, pp. 305-). Osterreichische Akademie Der Wissenschaften.

Flohr, P., Jenkins, E., Williams, H. R. S., Jamjoum, K., Nuimat, S., & Muldner, G. (2019). What can crop stable isotopes ever do for us? An experimental perspective on using cereal carbon stable isotope values for reconstructing water availability in semi-arid and arid environments. *Vegetation History and Archaeobotany*, *28*, 497–512.

Foulkes, M. J., DeSilva, J., Gaju, O., & Carvalho, P. (2016). Relationships between d13C, d18O and grain yield in bread wheat genotypes under favourable irrigated and rain-fed conditions. *Field Crops Research*, *196*, 237–250.

Fraser, R. A., Bogaard, A., Charles, M., Styring, A. K., Wallace, M., Jones, G., Ditchfield, P., & Heaton, T. H. E. (2013). Assessing natural variation and the effects of charring, burial and pre-treatment on the stable carbon and nitrogen isotope values of archaeobotanical cereals and pulses. *Journal of Archaeological Science*, *40*, 4754–4766.

Fraser, R. A., Bogaard, A., Heaton, T., Charles, M., Jones, G., Christensen, B. T., Halstead, P., Merbach, I., Poulton, P. R., Sparkes, D., & Styring, A. K. (2011). Manuring and stable nitrogen isotope ratios in cereals and pulses: Towards a new archaeobotanical approach to the inference of land use and dietary practices. *Journal of Archaeological Science*, *38*, 2790–2804.

Freeman, E. M. (1903). The seed-fungus of Lolium temulentum, L., the Darnel. *Philosophical Transactions of the Royal Society B*, *196*, 1–27.

Fritz, G., & Nesbitt, M. (2014). Laboratory Analysis and Identification of Plant Macroremains. In J. M. Marston, J. D. Guedes, & C. Wariner (Eds.), *Method and Theory in Paleoethnobotany* (pp. 115–146). University Press of Colorado.

Frumkin, A. (2009). Stable isotopes of a subfossil Tamarix tree from the Dead Sea region, Israel, and their implications for the Intermediate Bronze Age environmental crisis. *Quaternary Research*, *71*, 319–328.

Fuller, D. Q. (2006). Recent lessons from Near Eastern archaeobotany: Wild cereal use, pre-domestication cultivation and tracing multiple origins and dispersals. *Prāgdhārā*, *18*, 105–133.

Fuller, D. Q., & Harvey, E. L. (2006). The archaeobotany of Indian pulses: Identification, processing and evidence for cultivation. *Environmental Archaeology*, *11*(2), 219–246.

Fuller, D. Q., & Stevens, C. J. (2018). The making of the botanical battleground: Domestication and the origins of the world's weed floras. In E. Lightfoot, X. Liu, & D. Q. Fuller (Eds.), *Far from the Hearth: Essays in Honour of Martin K. Jones* (pp. 9–21). McDonald Institute for Archaeological Research.

Gaastra, J. S., Greenfield, T. L., & Greenfield, H. J. (2020). There and back again: A zooarchaeological perspective on Early and Middle Bronze Age urbanism in the southern Levant. *PLOS ONE*, *15*(3), 27.

Galán, C., García-Mozo, H., Vázquez, L., Ruiz, L., Díaz de la Guardia, C., & Domínguez-Vilches, E. (2008). Modeling Olive Crop Yield in Andalusia, Spain. *Agronomy Journal*, *100*(1), 98–104.

Garfunkel, Z., & Ben-Avraham, Z. (1996). The structure of the Dead Sea basin. *Tectonophysics*, *266*, 155–176.

Garrard, A. (1999). Charting the emergence of cereal and pulse domestication in south-west Asia. *Environmental Archaeology*, *4*, 67–86.

Gat, J. R. (1984). The stable isotope composition of Dead Sea waters. *Earth and Planetary Science Letters*, *71*, 361–376.

Gat, J. R. (2001). The lakes of the Jordan Rift Valley. *Final Research Co-Ordination Meeting on Use of Isotope Techniques in Lake Dynamics Investigations*, 105–114.

Gat, J. R., Ben-Mair, R., Yam, R., Yakir, D., & Wernli, H. (2005). *The isotope composition of atmospheric waters in Israel's coastal plain* (1453; Isotopic Composition of Precipitation in the Mediterranean Basin in Relation to Air Circulation Patterns and Climate, pp. 99–114). International Atomic Energy Agency.

Gat, J. R., & Dansgaard, W. (1972). Stable Isotope Survey of the Fresh Water Occurrences in Israel and the Northern Jordan Rift Valley. *Journal of Hydrology*, *16*, 177–212.

Gatica, M. G., Aranibar, J. N., & Pucheta, E. (2017). Environmental and species-specific controls on d13C and d15N in dominant woody plants from central-western Argentinian drylands. *Austral Ecology*, *42*, 553–543.

Gat-Tilman, G. (1994). Soil gases and the germination of Aizoon hispanicum. *Journal of Arid Environments*, *28*, 39–44.

Geary, D. H., Hoffmann, E., Magyar, I., Freiheit, J., & Padilla, D. (2012). Body size, longevity, and growth rate in Lake Pannon melanopsid gastropods and their predecessors. *Paleobiology*, *38*(4), 554–568.

Genz, H. (2003). Cash crop production and storage in the Early Bronze Age Southern Levant. *Journal of Mediterranean Archaeology*, *16*(1), 59–78.

Glaubrecht, M. (1993). Mapping the diversity: Geographical distribution of the freshwater snail *Melanopsis* (*Gastropoda*: ? *Cerithioidea: Melanopsidae*) with focus on its systematics in the Mediterranean Basin. *Mitt. Hamb. Zool. Mus. Inst.*, *90*, 41–97.

Golani, A., & Segal, D. (2002). Redefining the onset of the Early Bronze Age in Southern Canaan: New evidence of 14C dating from Ashkelon Afridar. In E. C. M. van der Brink

& E. Yannai (Eds.), *In Quest of Ancient Settlements and Landscapes* (pp. 135–154). Ramot Publishing.

Goldsmith, Y., Cohen, O., Stein, M., Torfstein, A., Kiro, Y., Kushnir, Y., Bartov, Y., Ben-Moshe, L., Frumkin, A., Lensky, N. G., Keinan, J., Gonen, L., & Enzel, Y. (2023). Holocene humid periods of the Levant—Evidence from Dead Sea lake-levels. *Quaternary Science Reviews*, *318*, 14.

Gómez-Alonso, S., & García-Romero, E. (2009). Effect of irrigation and variety on oxygen (d18O) and carbon (d13C) stable isotope composition of grapes cultivated in a warm climate. *Australian Journal of Grape and Wine Research*, *16*(2), 283–289.

Goor, A. (1966). The History of the Grape-Vine in the Holy Land. *Economic Botany*, *20*(1), 46–64.

Gophna, R. (1984). The Settlement Landscape of Palestine in the Early Bronze Age II-III and Middle Bronze Age II. *Israel Exploration Journal*, *34*(1), 24–31.

Gophna, R., & Portugali, J. (1988). Settlement and demographic processes in Israel's coastal plain from the Chalcolithic to the Middle Bronze Age. *Bulletin of the American Schools of Oriental Research*, *269*, 11–28.

Gordillo, S., Bayer, M. S., Boretto, G., & Charo, M. (2014). *Mollusk shells as bio-geo-archives: Evaluating environmental changes during the Quaternary*. Springer.

Goren, Y. (1996). The Southern Levant in the Early Bronze Age IV: The Petrographic. *Bulletin of the American Schools of Oriental Research*, *303*, 33–72.

Gouveia, C. S. S., Ganança, J. F. T., Slaski, J. J., Lebot, V., & de Carvalho, M. Â. A. P. (2020). Involvement of abscisic acid and other stress indicators in taro (*Colocasia esculenta* (L.) Schott) response to drought conditions. *Acta Physiologiae Plantarum*, *42*, 173.

Greenberg, R., & Iserlis, M. (2014). The Early Bronze Age Pottery Industries. In R. Greenberg (Ed.), *Bet Yerah—The Early Bronze Age Mound, Vol. II: Urban Structure and Material Culture, 1933–1986 Excavations* (pp. 53–149).

Greenberg, R. (2019). The Intermediate Bronze Age: Entering the orbit of Syria. In R. Greenberg (Ed.) *The Archaeology of the Bronze Age Levant: From Urban Origins to the Demise of City-States, 3700–1000 BCE* (pp. 136–179). Cambridge University Press.

Grimm, E. C. (1987). CONISS: A FORTRAN 77 program for stratigraphically constrained cluster analysis by the method of incremental sum of squares. *Computers & Geosciences*, *13*(1), 13–35.

Grimm, E. C. (2004). *TILIA and TGView Software* (Version 2.0.2) [Computer software].

Guiot, J., & Kaniewski, D. (2015). The Mediterranean basin and Southern Europe in a warmer world: What can we learn from the past? *Frontiers in Earth Science*, *3*(28), 16.

Gunn, C. R. (1972). Seed collecting and identification. In T. T. Kozlowski (Ed.), *Insects, and Seed Collection, Storage, Testing, and Certification* (pp. 55–143). Academic Press.

Hajar, L., Khater, C., & Cheddadi, R. (2008). Vegetation changes during the late Pleistocene and Holocene in Lebanon: A pollen record from the Bekaa Valley. *The Holocene*, *18*(7), 1089–1099.

Hald, M. M. (2010). Distribution of crops at late Early Bronze Age Titris Hoyuk, southeast Anatolia: Towards a model for the identification of consumers of centrally organised food distribution. *Vegetation History and Archaeobotany*, *19*, 69–77.

Hallmann, N., Burchell, M., Schone, B. R., Irvine, G. V., & Maxwell, D. (2009). High-resolution sclerochronological analysis of the bivalve mollusk *Saxidomus gigantea* from Alaska and British Columbia: Techniques for revealing environmental archives and archaeological seasonality. *Journal of Archaeological Science*, *36*, 2353–2364.

Hamdan, I., Wiegand, B., Toll, M., & Sauter, M. (2016). Spring response to precipitation events using δ18O and δ2H in the Tanour catchment, NW Jordan. *Isotopes in Environmental and Health Studies*, *52*(6), 682–693.

Handley, L. L., Odee, D., & Scrimgeour, C. M. (1994). δ15N and δ13C Patterns in Savanna Vegetation: Dependence on Water Availability and Disturbance. *Functional Ecology*, *8*(3), 306–314.

Hartman, G., & Danin, A. (2010). Isotopic values of plants in relation to water availability in the Eastern Mediterranean region. *Oecologia*, *162*, 837–852.

Hastorf, C. A., & Wright, M. F. (1998). Interpreting wild seeds from archaeological sites: A dung charring experiment from the Andes. *Journal of Ethnobiology*, *18*(2), 211–227.

Heaton, T. H. E., Jones, G., Halstead, P., & Tsipropooulos, T. (2009). Variations in the 13C/12C ratios of modern wheat grain, and implications for interpreting data from Bronze Age Assiros Toumba, Greece. *Journal of Archaeological Science*, *36*(10), 2224–2233.

Helbaek, H. (1958). Appendix A: Plant Economy in Ancient Lachish. In *Lachish IV: The Bronze Age* (pp. 309–317). Oxford University Press.

Helbaek, H. (1960). The palaeoethnobotany of the Near East and Europe. *Prehistoric Investigations in Iraqi Kurdistan*, 99–118.

Helbaek, H. (1964). First Impressions of the Çatal Hüyük Plant Husbandry. *Anatolian Studies*, *14*, 121–123.

Heller, J., Mordan, P., Ben-Ami, F., & Sivan, N. (2005). Conchometrics, systematics and distribution of *Melanopsis* (*Mollusca: Gastropoda*) in the Levant. *Zoological Journal of the Linnean Society*, *144*, 229–260.

Hesse, B. (1990). Pig lovers and pig haters: Patterns of Palestinian pork production. *Journal of Ethnobiology*, *10*(2), 195–225.

Hillel, N., Wine, M. L., Laronne, J. B., Licha, T., & Be'eri-Shlevin, Y. (2019). Identifying spatiotemporal variations in groundwater-surface water interactions using shallow pore water chemistry in the lower Jordan river. *Advances in Water Resources*, *131*, 15.

Hillman, G. C. (1981). Reconstructing crop husbandry practices from charred remains of crops. In R. Mercer (Ed.), *Farming practice in British prehistory* (pp. 123–162). Edinburgh University Press.

Hillman, G. C. (1984). Traditional husbandry and processing of archaic cereals in modern times: Part 1, the glume-wheats. In J. N. Postgate & M. A. Powell (Eds.), *Bulletin on Sumerian Agriculture* (Vol. 1, pp. 114–152). University Press, Cambridge.

Höflmayer, F. (2017). A radiocarbon chronology for the Middle Bronze Age Southern Levant. *Journal of Ancient Egyptian Interconnections*, *13*, 20–33.

Höflmayer, F., Dee, M. W., Genz, H., & Riehl, S. (2014). Radiocarbon evidence for the Early Bronze Age Levant: The site of Tell Fadous-Kfarabida (Lebanon) and the end of the Early Bronze III period. *Radiocarbon*, *56*(2), 529–542.

Höflmayer, F., Yasur-Landau, A., Cline, E. H., Dee, M. W., Lorentzen, B., & Riehl, S. (2016). New radiocarbon dates from Tel Kabri support a high Middle Bronze Age chronology. *Radiocarbon*, *58*(3), 599–613.

Holden, T. G. (1999). *The plant remains from Tell Esh-Shuna North, Jordan Valley*. 30.

Hopf, M. (1978). Plant Remains. *Early Arad: The Chalcolithic Settlement and Early Bronze City. I, First-Fith Seasons of Excavations, 1962-1966*, 64–82.

Hopf, M. (1983). Jericho Plant Remains. In K. M. Kenyon & T. A. Holland (Eds.), *Excavations at Jericho: The Pottery Phases of the Tell and Other Finds* (Vol. 5, pp. 576–621). British School of Archaeology in Jerusalem.

Hopf, M. (2008). Plant remains and early farming in Jericho. In G. W. Dimbleby (Ed.), *The domestication and exploitation of plants and animals* (1st ed., pp. 355–359). Routledge.

Horwitz, L. K. (1989). Sedentism in the Early Bronze IV: A Faunal Perspective. *Bulletin of the American Schools of Oriental Research*, *275*, 15–25.

Hubbard, R. N. L. B. (1980). Development of Agriculture in Europe and the Near East: Evidence from Quantitative Studies. *Economic Botany*, *34*(1), 51–67.

Hubbard, R. N. L. B. (1992). Dichotomous keys for the identification of the major Old World crops. *Review of Paleobotany and Palynology*, *73*, 105–115.

Hunt, C. O., Elrishi, H. A., Gilbertson, D. D., Grattan, J., McLaren, S., Pyatt, F. B., Rushworth, G., & Barker, G. W. (2004). Early-Holocene environments in the Wadi Faynan, Jordan. *The Holocene*, *14*(6), 921–930.

Hunt, C. O., Gilbertson, D. D., & El-Rishi, H. A. (2007). An 8000-year history of landscape, climate, and copper exploitation in the Middle East: The Wadi Faynan and the Wadi Dana National Reserve in southern Jordan. *Journal of Archaeological Science*, *34*, 1306–1338.

Ibrahim, M. M. (2009). The Jordan Valley during the Early Bronze Age. In E. Kaptijn & L. P. Petit (Eds.), *A Timeless Vale: Archaeological and related essays on the Jordan Valley in honour of Gerrit van der Kooij on the occasion of his sixty-fifth birthday* (pp. 81–96). Leiden University Press.

Isely, D. (1947). Investigations in seed classification by family characteristics. *Research Bulletin (Iowa Agriculture and Home Economics Experiment Station)*, *28*(351), 317–380.

Jacomet, S. (2006). *Identification of cereal remains from archaeological sites: 2nd edition*. Archaeobotany Lab IPAS, Basel University.

Jenkins, H., Andrews, J., Rowan, Y., Wasse, A., White, T., Philip, G., Marca, A., & Clarke, J. (2023). Local-scale environmental gradients in "snail-shell" stable isotopes from Holocene Jordanian archaeological sites. *The Holocene*, *33*(3), 255–266.

Jones, G. (1990). The application of present-day cereal processing studies to charred archaeobotanical remains. *Circaea*, *6*(2), 91–96.

Jones, G. E. M. (1983). *Interpretation of archaeological plant remains: Ethnographic models from Greece*. 43–61.

Jones, G. E. M. (1991). Numerical analysis in archaeobotany. In K. E. Behre, K. Wasylikowa, & W. van Zeist (Eds.), *Progress in Old World Palaeoethnobotany* (pp. 63–80). Balkema.

Jones, P. J., O'Connell, T. C., Jones, M. K., Singh, R. N., & Petrie, C. A. (2021). Crop water status from plant stable carbon isotope results: A test case for monsoonal climates. *The Holocene*, 1–12.

Kagan, E. J., Langgut, D., Boaretto, E., Neumann, F. H., & Stein, M. (2015). Dead Sea levels during the Bronze and Iron Ages. *Radiocarbon*, *57*(2), 237–252.

Kamlah, J., & Riehl, S. (2020). Agriculture in the Bronze Age Levant. In D. Hollander & T. Howe (Eds.), *A Companion to Ancient Agriculture* (pp. 193–209). Wiley-Blackwell.

Kaniewski, D., Marriner, N., Cheddadi, R., Fischer, P. M., Otto, T., Luce, P., & van Campo, E. (2020). Climate change and social unrest: A 6,000-year chronicle from the Eastern Mediterranean. *Geophysical Research Letters*, *47*, 10.

Kaniewski, D., Marriner, N., Cheddadi, R., Guiot, J., & Van Campo, E. (2018). The 4.2 ka BP event in the Levant. *Climate of the Past*, *14*, 1529–1542.

Kaniewski, D., Paulissen, E., Van Campo, E., Al-Maqdissi, M., Bretschneider, J., & Van Lerberghe, K. (2008). Middle East Coastal Ecosystem Response to Middle-to-Late Holocene Abrupt Climate Changes. *Proceedings of the National Academy of Sciences of the United States of America*, *105*(37), 13941–13946.

Kaniewski, D., Van Campo, E., Morhange, C., Guiot, J., Zviely, D., Shaked, I., Otto, T., & Artzy, M. (2013). Early urban impact on Mediterranean coastal environments. *Scientific Reports*, *3*(3540), 1–5.

Kanstrup, M., Thomsen, I. K., Andersen, A. J., Bogaard, A., & Christensen, B. T. (2011). Abundance of 13C and 15N in emmer, spelt, and naked barley grown on differently manured soils: Towards a method for identifying past manuring practice. *Rapid Communications in Mass Spectrometry*, *25*, 2879–2887.

Kelemen, Z., Gillikin, D. P., Graniero, L. E., Havel, H., Darchambeau, F., Borges, A. V., Yambele, A., Bassirou, A., & Bouillon, S. (2017). Calibration of hydroclimate proxies in freshwater bivalve shells from Central and West Africa. *Geochimica et Cosmochimica Acta*, *208*, 41–62.

Kennedy, M. A. (2015). Assessing the Early Bronze–Middle Bronze Age Transition in the Southern Levant in Light of a Transitional Ceramic Vessel from Tell Umm Hammad, Jordan. *Bulletin of the American Schools of Oriental Research*, *373*, 199–216.

Ken-Tor, R. B., Enzel, Y., Agnon, A., & Stein, M. (2004). Late Holocene lake levels of the Dead Sea. *GSA Bulletin*, *116*(5/6), 555–571.

Kintigh, K. W., & Ammerman, A. J. (1982). Heuristic approaches to spatial analysis in archaeology. *American Antiquity*, *47*(1), 31–63.

Kislev, M. E. (1993). In I. Finkelstein (Ed.), *Shiloh: The Archaeology of a Biblical Site* (pp. 354–361). Emery and Claire Yass Publications in Archaeology.

Kislev, M. E. (1998). The relative impact of pig husbandry versus goat browsing on ancient oak forests in Israel. In *Villages, Terraces, and Stone Mounds: Excavations at Manahat, Jerusalem, 1987-1989* (pp. 113–118). Israel Antiquities Authority.

Kislev, M. E., & Bar-Yosef, O. (1988). The legumes: The earliest domesticated plants in the Near East? *Current Anthropology*, *29*(1), 175–179.

Kislev, M. E., Simchoni, O., Melamed, Y., & Maroz, L. (2009). Food and industrial crops. In N. Panitz-Cohen & A. Mazar (Eds.), *Excavations at Tell Beth-Shean 1989-1996* (Vol. 3rd, pp. 764–771). The Israel Exploration Society.

Klinge, J., & Fall, P. L. (2010). Archaeobotanical inference of Bronze Age land use and land cover in the eastern Mediterranean. *Journal of Archaeological Science*, *37*, 2622–2629.

Klinger, Y., Avouac, J. P., Bourles, D., & Tisnerat, N. (2003). Alluvial deposition and lake-level fluctuations forced by Late Quaternary climate change: The Dead Sea case example. *Sedimentary Geology*, *162*, 119–139.

Konvalina, P., Capouchova, I., Stehno, Z., Moudry, J., Moudry jr., J., & Marton, L. (2011). Variation for carbon isotope ratio in a set of emmer (Triticum dicoccum Schrank) and bread wheat (*Triticum aestivum* L.) accessions. *African Journal of Biotechnology*, *10*(21), 4450–4456.

Konvalina, P., Moudry, J., Stehno, Z., & Moudry, J. Jr. (2010). Drought tolerance of Land Races of Emmer Wheat in Comparison to Soft Wheat. *Cereal Research Communications*, *38*(3), 429–439.

Konvalina, P., Suchy, K., Stehno, Z., Capouchova, L., & Moudry, J. (2014). Drought tolerance of different wheat species (Triticum L.). In M. Behnassi, M. S. Muteng'e, G. Ramachandran, & K. N. Shelat (Eds.), *Vulnerability of agriculture, water and fisheries to climate change* (pp. 207–216). Springer.

Kreuz, A., Marinova, E., Shafer, E., & Wiethold, J. (2005). A comparison of early Neolithic crop and weed assemblages from the Linearbandkeramik and the Bulgarian Neolithic cultures: Differences and similarities. *Vegetation History and Archaeobotany*, *14*, 237–258.

Kreuz, A., & Schäfer, E. (2011). Weed finds as indicators for the cultivation regime of the early Neolithic Bandkeramik culture? *Vegetation History and Archaeobotany*, *20*, 333–348.

Ladizinsky, G. (1979). Seed dispersal in relation to the domestication of Middle East legumes. *Economic Botany*, *33*(3), 284–289.

Langgut, D., Adams, M. J., & Finkelstein, I. (2016). Climate, settlement patterns and olive horticulture in the Souuthern Levant during the Early Bronze and Intermediate Bronze Ages (c. 3600-1950 BC). *Levant*, 18.

Langgut, D., Cheddadi, R., Carrion, J. S., Cavanagh, M., Colombaroli, D., Eastwood, W. J., Greenberg, R., Litt, T., Mercuri, A. M., Miebach, A., Roberts, C. N., Woldring, H., & Woodbridge, J. (2019). The origin and spread of olive cultivation in the Mediterranean Basin: The fossil pollen evidence. *The Holocene*, *29*(5), 902–922.

Langgut, D., Finkelstein, I., & Litt, T. (2013). Climate and the Late Bronze Collapse: New Evidence from the Southern Levant. *Tel Aviv*, *40*, 149–175.

Langgut, D., Finkelstein, I., Litt, T., Neumann, F. H., & Stein, M. (2015). Vegetation and climate changes during the Bronze and Iron Ages (~3600-600 BCE) in the Southern Levant based on palynological records. *Radiocarbon*, *57*(2), 217–235.

Latel, C., Piller, W. E., & Harzhauser, M. (2004). Palaeoenvironmental reconstructions by stable isotopes of Middle Miocene gastropods of the Central Paratethys. *Palaeogeography, Palaeoclimatology, Palaeoecology*, *211*, 157–169.

Leng, M. J., Lamb, A. L., Lamb, H. F., & Telford, R. J. (1999). Palaeoclimatic implications of isotopic data from modern and early Holocene shells of the freshwater snail *Melanoides turberculata*, from lakes in the Ethiopian Rift Valley. *Journal of Paleolimnology*, *21*, 97–106.

Leng, M. L., & Lewis, J. P. (2016). Oxygen isotopes in Molluscan shell: Applications in environmental archaeology. *Environmental Archaeology: The Journal of Human Palaeoecology*, *21*(3), 295–306.

Lennstrom, H. A., & Hastorf, C. A. (1995). Interpretation in Context: Sampling and Analysis in Paleoethnobotany. *American Antiquity*, *60*(4), 701–721.

Lev, L., Boaretto, E., Heller, J., Marco, S., & Stein, M. (2007). The feasibility of using *Melanopsis* shells as radiocarbon chronometers, Lake Kinneret, Israel. *Radiocarbon*, *49*(2), 1003–1015.

Levy, T. E. (1983). The emergence of specialized pastoralism in the Southern Levant. *World Archaeology*, *15*(1), 15–36.

Lev-Yadun, S., Artzy, M., Marcus, E., & Stidsing, R. (1996). Wood Remains from Tel Nami, a Middle Bronze IIA and Late Bronze IIB Port, Local Exploitation of Trees and Levantine Cedar Trade. *Economic Botany*, *50*(3), 310–317.

Lewis, J. P., Leng, M. J., Dean, J. R., Marciniak, A., Bar-Yosef Mayer, D. E., & Wu, X. (2017). Early Holocene palaeoseasonality inferred from the stable isotope composition of *Unio* shells from Çatalhöyük, Turkey. *Environmental Archaeology: The Journal of Human Palaeoecology*, *22*(1), 79–95.

Lines, L. (1995). *Bronze Age orchard cultivation and urbanization in the Jordan river valley* [Dissertation]. Arizona State University.

Lionello, P., Malanotte-Rizzoli, P., Boscolo, R., Alpert, P., Artale, V., Li, L., Luterbacher, J., May, W., Trigo, R., Tsimplis, M., Ulbrich, U., & Xoplaki, E. (2006). The Mediterranean Climate: An Overview of the Main Characteristics and Issues. In P. Lionello, P.

Malanotte-Rizzoli, & R. Boscolo (Eds.), *Mediterranean Climate Variability* (pp. 1–26). Elsevier.

Liphschitz, N. (1989). Plant Economy and diet in the Early Bronze Age in Israel: A summary of present research. In P. Miroschedji (Ed.), *L'Urbanisation de la Palestine a rage du Bronze ancien* (pp. 269–277). British Archaeological Reports.

Liphschitz, N. (1996). Analysis of botanical remains. In A. Gopher, B. Cresson, & E. Friedmann (Eds.), *Excavations at Tel Dalit: An Early Bronze Age Walled Town in Central Israel* (pp. 186–192). Ramot Publishing.

Liphschitz, N. (2004). Archaeobotanical remains from Ashqelon, Afridar. *'Atiqot*, *45*, 305–310.

Liphschitz, N., Gophna, R., Hartman, M., & Biger, G. (1991). The beginning of Olive (*Olea europaea*) cultivation in the Old World: A reassessment. *Journal of Archaeological Science*, *18*, 441–453.

Lister, D. L., & Jones, M. K. (2012). Is naked barley an eastern or western crop? The combined evidence of archaeobotany and genetics. *Vegetation History and Archaeobotany*, *22*, 439–446.

Mabry, J., & Palumbo, G. (1988). *The 1987 Wadi el-Yabis Survey* (32; Annual of the Department of Antiquities of Jordan, pp. 275–305).

Maggio, A., De Pascale, S., Fagnano, M., & Barbieri, G. (2011). Saline agriculture in Mediterranean environments. *Italian Journal of Agronomy*, *6*(7), 36–43.

Magness-Gardiner, B., & Falconer, S. E. (1991). Tell el-Hayyat, Tell Abu en-Ni'aj. *American Journal of Archaeology*, *95*(2), 264–265.

Magness-Gardiner, B., & Falconer, S. E. (1994). Community, Polity, and Temple in a Middle Brozne Age Levantine Village. *Journal of Mediterranean Archaeology*, *7*(2), 127–164.

Marinova, E., & Valamoti, S. M. (2014). Crop diversity and choices in the prehistory of SE Europe: The archaeobotanical evidence from Greece and Bulgaria. In E. Marinova, A. Chevalier, & L. Peña-Chocarro (Eds.), *Plants and people: Choices and diversity through time* (p. 23). Oxbow Books.

Marshall, J. D., Brooks, J. R., & Lajtha, K. (2007). Sources of variation in the stable isotopic compositions of plants. In K. Lajtha & R. Michener (Eds.), *Stable isotopes in ecology and environmental science* (2nd ed., pp. 22–60). Blackwell Publishing Ltd.

Martin, A. C., & Barkley, W. D. (1973). *Seed Identification Manual*. University of California Press.

Masi, A., Sadori, L., Baneschi, I., Siani, A. M., & Zanchetta, G. (2012). Stable isotope analysis of archaeological oak charcoal from eastern Anatolia as a marker of mid-Holocene climate change. *Plant Biology*, *15*(1), 83–92.

Mathias, V. T., & Parr, P. J. (1989). Early Bronze Age plant remains from Tell Nebi Mend. A preliminary account. *Levant*, *21*, 13–32.

Maxwell, T. D., Silva, L. C. R., & Horwath, W. R. (2014). *Using multielement isotopic analysis to decipher drought impacts and adaptive management in ancient agricultural systems* [PNAS Letter].

Mazar, A. (2012). Introduction and Synthesis. In *Excavations at Tel Beth-Shean 1989-1996* (Vol. 4, pp. 1–33). The Institute of Archaeology, The Hebrew University of Jerusalem.

McConnaughey, T. A., & Gillikin, D. P. (2008). Carbon isotopes in mollusk shell carbonates. *Geo-Mar Lett*, *28*, 287–299.

McCreery, D. W. (1980). *The nature and cultural implications of Early Bronze Age agriculture in the southern Ghor of Jordan—An archaeological reconstruction* [Dissertation]. University of Pittsburg.

McCreery, D. W. (2003a). Bronze Age agriculture in the Dead Sea Basin: The cases of Bab edh-Dhra', Numeira and Tell Nimrin. In D. M. Gunn & P. M. McNutt (Eds.), *"Imagining" Biblical Worlds: Stdies in Spatial, Social and Historical Constructs in Honor of James W. Flanagan* (pp. 250–263). Sheffield Academic Press.

McCreery, D. W. (2003b). The paleoethnobotany of Bâb edh-Dhrâ. In W. Rast & R. T. Schaub (Eds.), *Bâb edh-Dhrâ: Excavations at the Town Site (1975-1981)* (pp. 449–463). Eisenbrauns.

Meadows, J., & Jones, G. (1996). *The Final Straw: An archaeobotanical investigation of the economy of a fourth millennium BC site in the Wadi Fidan, southern Jordan* [Master's dissertation]. University of Sheffield.

Meegan, C. (2005). *Agrarian Ecology in the Bronze Age of the Southern Levant; an Archaeobotanical Study of Zahrat adh Dhra' 1* [Master's thesis]. Arizona State University.

Melamed, Y. (1996). Dry and charred grains from 'Afula—A taphonomic approach. *Israel Antiquities Authority*, *30*, 69–70.

Merah, O., Deleens, E., Al Hakami, A., & Monneveux, P. (2001). Carbon isotope discrimination and grain yield variations among tetraploid wheat species cultivated under contrasting precipitation regimes. *Journal of Agronomy & Crop Science*, *186*, 129–134.

Migowski, C., Stein, M., Prasad, S., Negendank, J. F. W., & Amotz, A. (2006). Holocene climate variability and cultural evolution in the Near East from the Dead Sea sedimentary record. *Quaternary Research*, *66*, 421–431.

Miksicek, C. H. (1987). Formation processes of the archaeobotanical record. *Advances in Archaeological Method and Theory*, *10*, 211–247.

Miller, N. (1991). The Near East. In K. E. Behre, K. Wasylikowa, & W. van Zeist (Eds.), *Progress in Old World Palaeoethnobotany* (pp. 133–160). Balkema.

Miller, N. (2002). Food, fodder, or fuel?: Harvesting the secrets of ancient seeds. *Expedition*, *44*(3), 5–6.

Miller, N. F. (1984). The use of dung as fuel: An ethnographic example and an archaeological application. *Paleorient*, *10*(2), 71–79.

Miller, N. F. (1988). Ratios in Paleoethnobotanical Analysis. In C. A. Hastorf & V. S. Popper (Eds.), *Current Paleoethnobotany*. University of Chicago Press.

Miller, N. F. (1992). The origins of plant cultivation in the Near East. In C. W. Cowan & P. J. Watson (Eds.), *The Origins of Agriculture: An International Perspective* (pp. 39–58). Smithsonian Institution Press.

Miller, N. F. (1997). Sweyhat and Hajji Ibrahim: Some Archaeobotanical Samples from the 1991 and 1993 Seasons. *MASCA Research Papers in Science and Archaeology*, *14*, 95–122.

Miller, N. F. (2008). Sweeter than wine? The use of the grape in early western Asia. *Antiquity*, *82*, 937–946.

Miller, N. F., & Enneking, D. (2014). Bitter Vetch (Vicia ervilia): Ancient medicinal crop and farmers' favorite for feeding livestock. In P. E. Minnis (Ed.), *New lives for ancient and extinct crops* (pp. 254–268). University of Arizona Press.

Miller, N. F., & Marston, J. M. (2012). Archaeological fuel remains as indicators of ancient west Asian agropastoral and land-use systems. *Journal of Arid Environments*, *86*, 97–103.

Miller, N. F., & Smart, T. L. (1984). Intentional burning of dung as fuel: A mechanism for the incorporation of charred seeds into the archaeological record. *Journal of Ethnobiology*, *4*(1), 15–28.

Moreno, B., Marin, B., Otero, A., Garcia, M., Raksa, H., Guijarro, M. I., Climent, M., Morales, M., Zabala, J., Loste, J. M., Acin, C., & Badiola, J. J. (2023). Peripheral neuropathy caused by fenugreek (*Trigonella foenum-graecum*) straw intoxication in cattle and experimental reproduction in sheep and goats. *Veterinary Pathology*, *60*(1), 115–122.

Morin, E., Ryb, T., Gavrieli, I., & Enzel, Y. (2019). Mean, variance, and trends of Levant precipitation over the past 4500 years from reconstructed Dead Sea levels and stochastic modeling. *Quaternary Research*, *91*(2), 751–767.

Moshkovitz, S., & Magaritz, M. (1987). Stratigraphy and isotope records of Middle and Late Pleistocene mollusks from a continuous corehole in the Hula Basin, Northern Jordan Valley, Israel. *Quaternary Research*, *28*, 226–237.

Murelaga, X., Ortega, L. A., Sancho, C., Munoz, A., Osacar, C., & Larraz, M. (2012). Succession and stable isotope composition of gastropods in Holocene semi-arid alluvial sequences (Bardenas Reales, Ebro Basin, NE Spain): Palaeoenvironmental implications. *The Holocene*, *22*(9), 1047–1060.

Murphy, C., Thompson, G., & Fuller, D. Q. (2013). Roman food refuse: Urban archaeobotany in Pompeii, Regio VI, Insula 1. *Vegetation History and Archaeobotany*, *22*, 409–419.

Neef, R. (1990). Introduction, development and environmental implications of olive culture: The evidence from Jordan. In S. Bottema, G. Entjes-Nieborg, & W. van Zeist (Eds.), *Man's role in the shaping of the Eastern Mediterranean Landscape* (pp. 295–306). Balkema.

Neef, R. (1997). Status and Perspectives of archaeobotanical research in Jordan. In H. G. K. Gebel & Z. Kafafi (Eds.), *The Prehistory of Jordan II. Perspectives from 1997* (pp. 601–609). Ex Oriente.

Neumann, F. H., Kagan, E. J., Leroy, S. A. G., & Baruch, U. (2010). Vegetation history and climate fluctuations on a transect along the Dead Sea west shore and their impact on past societies over the last 3500 years. *Journal of Arid Environments*, *74*, 756–764.

Neumann, F., Scholzel, C., Litt, T., Hense, A., & Stein, M. (2007). Holocene vegetation and climate history of the northern Golan heights (Near East). *Vegetation History and Archaeobotany*, *16*, 329–346.

Nicoli, M., Riehl, S., Cline, E. H., & Yasur-Landau, A. (2023). From Early Bronze Age domestic plant production to Middle Bronze Age regional exchange economy: The archaeobotanical assemblages from Tel Kabri. *Archaeological and Anthropological Sciences*, *15*(128), 1–24.

Nitsch, E., Andreou, S., Creuzieux, A., Gardeisen, A., Halstead, P., Isaakidou, V., Karathanou, A., Kotsachristou, D., Nikolaidou, D., Papanthimou, A., Petridou, C., Triantaphyllou, S., Valamoti, S. M., Vasileiadou, A., & Bogaard, A. (2017). A bottom-up view of food surplus: Using stable carbon and nitrogen isotope analysis to investigate agricultural strategies and diet at Bronze Age Archontiko and Thessaloniki Toumba, northern Greece. *World Archaeology*, *49*(1), 105–137.

Nitsch, E., Jones, G., Sarpaki, A., Hald, M. M., & Bogaard, A. (2019). Farming Practice and Land Management at Knossos, Crete: New Insights from δ13C and δ15N Analysis of

Neolithic and `Bronze Age Crop Remains. In D. Garcia, R. Orgeolet, M. Pomadere, & J. Zurbach (Eds.), *Country in the City: Agricultural Functions in Protohistoric Urban Settlements* (pp. 152–168). Archaeopress Archaeology.

Nitsch, E. K., Charles, M., & Bogaard, A. (2015). Calculating a statistically robust δ13C and δ15N offset for charred cereal and pulse seeds. *STAR: Science & Technology of Archaeological Research*, *1*(1), 1–8.

O'Connor, T. (2000). *The archaeology of animal bones*. Sutton Publishing Ltd.

Ön, Z. B., Macdonald, N., Akçer-Ön, S., & Greaves, A. M. (2023). A novel bayesian multilevel regression approach to the reconstruction of an eastern Mediterranean temperature record for the last 10,000 years. *The Holocene*, *33*(7), 807–815.

Palumbo, G. (2008). The Early Bronze Age IV. In R. B. Adams (Ed.), *Jordan: An Archaeological Reader* (pp. 227–262). Equinox Publishing.

Paz, S. (2015). (In)visible cities: The abandoned Early Bronze Age tells in the landscape of the Intermediate Bronze Age southern Levant. *Archaeological Review from Cambridge*, *30*(1), 28–36.

Pearsall, D. M. (1989). *Paleoethnobotany: A Handbood of Procedures*. Academic Press.

Peña-Chocarro, & Rottoli, M. (2007). Crop Husbandry Practices During the Bronze and Iron Ages in Tell Mishrifeh (Central-Western Syria). In D. M. Bonacossi (Ed.), *Urban and Natural Landscapes of an Ancient Syrian Capital. Settlement and Environment at Tell Mishrifeh/Qatna and in Central-Western Syria* (pp. 123–143).

Pető, Á., Kenéz, Á., Prunner, A. C., & Lisztes-Szabo, Z. (2015). Activity area analysis of a Roman period semi-subterranean building by means of integrated archaeobotanical and geoarchaeological data. *Vegetation History and Archaeobotany*, *24*, 101–120.

Pfister, L., Grave, C., Beisel, J. N., & McDonnell, J. J. (2019). A global assessment of freshwater mollusk shell oxygen isotope signatures and their relation to precipitation and stream water. *Scientific Reports*, *9*(4312), 6.

Pokharia, A. K., Agnihotri, R., Sharma, S., Bajpai, S., Nath, J., Kumaran, R. N., & Negi, B. C. (2017). Altered cropping pattern and cultural continuation with declined prosperity following abrupt and extreme arid event at ~4,200 yrs BP: Evidence from an Indus archaeological site Khirsara, Gujarat, western India. *PLOS ONE*, *12*(10), 17.

Polyak, V. J., & Denniston, R. F. (2012). Paleoclimate records from speleothems. In W. B. White & D. C. Culver (Eds.), *Encyclopedia of Caves* (pp. 577–585). Elsevier.

Popper, V. S. (1988). Selecting quantitative measurements in paleoethnobotany. In *Currnet Paleoethnobotany: Analytical methods and cultural interpretations of archaeological plant remains* (pp. 53–71). University of Chicago Press.

Poppi, D. P., Hendricksen, R. E., & Minson, D. J. (1985). The relative resistance to escape of leaf and stem particles from the rumen of cattle and sheep. *Journal of Agricultural Science*, *105*, 9–14.

Porson, S. (2018). *A paleoecological study of urban abandonment during Early Bronze IV in the Southern Levant* [Master's thesis]. University of North Carolina at Charlotte.

Porson, S., Falconer, S. E., Pilaar Birch, S., Ridder, E., & Fall, P. (2021a). Crop management and agricultural responses at Early Bronze IV Tell Abu en-Ni'aj, Jordan. *Journal of Archaeological Science*, *133*.

Porson, S., Fall, P. L., Falconer, S. E., Pilaar Birch, S. E., & Ridder, E. (2021b, November). *Middle Bronze Age agriculture at Tell el-Hayyat, Jordan* [Poster]. Annual Meeting of the American Society of Overseas Research, Chicago, Illinois.

Portillo, M., García-Suárez, A., Klimowicz, A., Barański, M. Z., & Matthews, W. (2019). Animal penning and open area activity at Neolithic Çatalhöyük, Turkey. *Journal of Anthropological Archaeology*, *56*, 16.

Postgate, J. N. (1984). Processing of cereals in the cuneiform record. In J. N. Postgate & M. A. Powell (Eds.), *Bulletin on Sumerian agriculture* (Vol. 1, pp. 103–113). University Press, Cambridge.

Powell, M. A. (1984). Sumerian cereal crops. In J. N. Postgate & M. A. Powell (Eds.), *Bulletin on Sumerian Agriculture* (Vol. 1, pp. 48–72). University Press, Cambridge.

Prag, K. (2014). The Southern Levant during the Intermediate Bronze Age. In M. L. Steiner & A. E. Killebrew (Eds.), *The Oxford handbook of the archaeology of the Levant c. 8000-332 BCE* (pp. 388–402). Oxford University Press.

Prendergast, A. L., & Stevens, R. E. (2014). Molluscs (Isotopes): Analyses in environmental archaeology. In C. Smith (Ed.), *Encyclopedia of Global Archaeology* (pp. 5010–5019). Springer.

Qadir, M., Ghafoor, A., & Murtaza, G. (2000). Amelioration strategies for saline soils: A review. *Land Degredation and Development*, *11*, 501–521.

Railsback, L. B., Liang, F., Brook, G. A., Riavo, N., Voarintsoa, G., Sletten, H. R., Marais, E., Hardt, B., Cheng, H., & Edwards, R. L. (2018). The timing, two-pulsed nature, and variable climatic expression of the 4.2 ka event: A review and new high-resolution stalagmite data from Namibia. *Quaternary Science Reviews*, *186*, 78–90.

Rambeau, C., & Black, S. (2011). Palaeoenvironments of the southern Levant 5,000 BP to present: Linking the geological and archaeological records. In *Water, Life and Civilization: Climate, Environment and Society in the Jordan Valley* (pp. 94–104). Cambridge University Press.

Rambeau, C. M. C. (2010). Palaeoenvironmental reconstruction in the Southern Levant: Synthesis, challenges, recent developments and perspectives. *Philosophical Transactions of the Royal Society A*, *368*, 5225–5248.

Ramsay, J., & Mueller, N. (2016). Telling seeds: Archaeobotanical investigations at Tall al-'Umayri, Jordan. In K. M. McGeough (Ed.), *The archaeology of agro-pastoralist economies in Jordan* (pp. 1–26). American Schools of Oriental Research.

Rawson, H. M., Richards, R. A., & Munns, R. (1988). An examination of selection criteria for salt tolerance in wheat, barley and Triticale genotypes. *Australian Journal of Agricultural Research*, *39*, 759–772.

Reed, K., Sabljic, S., Sostaric, R., & Essert, S. (2019). Grains from ear to ear: The morphology of spelt and free-threshing wheat from Roman Mursa (Osijek), Croatia. *Vegetation History and Archaeobotany*, 12.

Reddy, S. N. (1997). If the threshing floor could talk: Integration of agriculture and pastoralism during the Late Harappan in Gujarat, India. *Journal of Anthropological Archaeology*, *16*, 162–187.

Regev, J., De Miroschedji, P., Greenberg, R., Braun, E., Greenhut, Z., & Boaretto, E. (2012). Chronology of the Early Bronze Age in the Southern Levant: New Analysis for a High Chronology. *Radiocarbon*, *54*(3–4), 525–566.

Reitz, E. J., & Wing, E. S. (2008). Secondary data. In *Zooarchaeology* (2nd ed., pp. 182–250). Cambridge University Press.

Renfrew, J. M. (1973). *Palaeoethnobotany: The prehistoric food plants of the Near East and Europe*. Columbia University Press.

Renfrew, J. M. (2003). Archaeology and the origins of wine production. In M. Sandler & R. Pinder (Eds.), *Wine A Scientific Exploration* (pp. 56–69). Taylor & Francis.

Rice, A., Bunin, E., Plessen, B., Sharon, G., & Mischke, S. (2023). Implications of submonthly oxygen and carbon isotope variations in late Pleistocene Melanopsis shells for regional and local hydroglimate in the upper Jordan River valley. *Quaternary Research*, 14.

Richard, S. (1980). Towards a Consensus of opinion on the end of the Early Bronze Age in Palestine-Transjordan. *Bulletin of the American Schools of Oriental Research*, *237*, 5–34.

Richard, S. (1986). Excavations at Khirbet Iskandar, Jordan. *Expedition*, *28*(1), 3–12.

Richard, S. (1987). Archaeological Sources for the History of Palestine: The Early Bronze Age: The Rise and Collapse of Urbanism. *The Biblical Archaeologist*, *50*(1), 22–43.

Richard, S. (1990). The 1987 expedition to Khirbet Iskander and its vicinity: Fourth preliminary report. *Bulletin of the American Schools of Oriental Research Supplemental Studies*, *26*, 33–58.

Richard, S. (2014). Recent excavations at Khirbat Iskandar, Jordan. The EB III/IV fortifications. *Proceedings, 9th ICAANE, Basel*, 585–597.

Richard, S. (2024). Redefining "Collapse" in the Early Bronze Age: New evidence for recovery, resilience, and societal transformation at Khirbat Iskandar, Jordan. *Journal of Ancient Near Eastern History*, *11*(1), 1–37. https://doi.org/10.1515/janeh-2022-0011

Richard, S., & Long, J. C. Jr. (2006). Three seasons of excavations at Khirbat Iskandar, 1997, 2000, 2004. *Annual of the Department of Antiquities of Jordan*, *49*, 261–275.

Richard, S., & Long, J. C. Jr. (2008). Khirbet Iskander, Jordan and Early Bronze IV studies: A view from a tell. In P. J. Parr (Ed.), *The Levant in Transition* (pp. 90–100). Proceedings of a Conference held at the British Museum.

Richard, S., Long, J. C. Jr., D'Andrea, M., & Wulff-Krabbenhoft, R. (2018). Expedition to Khirbat Iskandar and its environs: The 2016 season. *Annual of the Department of Antiquities of Jordan*, *59*, 597–606.

Richard, S., Long, J. C. Jr., Holdorf, P. S., & Peterman, G. (Eds.). (2010). *Archaeological Expedition to Khirbat Iskander and its Environs, Jordan: Khirbat Iskander: Final Report on the Early Bronze IV Area C "Gateway" and Cemeteries* (Vol. 1). University of Chicago Press.

Richard, S., Long, J. C. Jr., Wulff-Krabbenhoft, R., & Ellis, S. (2013). Three seasons of excavations at Khirbat Iskandar: 2007, 2010 and 2013. *Annual of the Department of Antiquities of Jordan*, *57*, 447–461.

Riehl, S. (2004). Archaeobotany at the Early Bronze Age settlement of Hirbet ez-Zeraqon: A prliminary report. *Zeitschrift Des Deutschen Palastina-Vereins*, 101–122.

Riehl, S. (2008). Climate and agriculture in the ancient Near East: A synthesis of the archaeobotanical and stable carbon isotope evidence. *Vegetation History and Archaeobotany*, *17*(Suppl 1), S43–S51.

Riehl, S. (2009). Archaeobotanical evidence for the interrelationship of agricultural decision-making and climate change in the ancient Near East. *Quaternary International*, *197*, 93–114.

Riehl, S. (2010). Plant Production in a Changing Environment: The Archaeobotanical Remains from Tell Mozan. In P. Pfalzner, S. Riehl, M. Doll, & K. Deckers (Eds.), *The Development of the Environment, Subsistence and Settlement of the City of Urkeš and its Region* (Vol. 3, pp. 13–158). Harrassowitz.

Riehl, S. (2011). Climate and agriculture decision making: Environmental constraints and economic development in Near Eastern sites between 5000-3500 cal BP. In *Between Sand and Sea: The archaeology and human ecology of Southwestern Asia* (pp. 147–166). Kerns Verlag.

Riehl, S., & Bryson, R. (2007). Variability in human adaptation to changing environmental conditions in Upper Mesopotamia during the Early to Middle Bronze Age transition. In *Sociétés humaines et changement climatique à la fin du troisième millénaire—Une crise a-t-elle eu lieu en Haute-Mésopotamie ?* (pp. 523–548).

Riehl, S., Bryson, R., & Pustovoytov, K. (2008). Changing growing conditions for crops during the Near Eastern Bronze Age (3000e1200 BC): The stable carbon isotope evidence. *Journal of Archaeological Science*, *35*, 1011–1022.

Riehl, S., Orendi, A., Kamlah, J., & Sader, H. (2019). Archaeobotanical samples from Middle and Late Bronze Age contexts at Tell el-Burak. In *Tell el-Burak I: The Middle Bronze Age* (pp. 360–368). Harrassowitz Verlag.

Riehl, S., Pustovoytov, K. E., Weippert, H., Klett, S., & Hole, F. (2014). Drought stress variability in ancient Near Eastern agricultural systems evidenced by $\delta^{13}C$ in barley grain. *Proceedings of the National Academy of Sciences of the United States of America*, *111*(34), 12348–12353.

Roach, K. A., Rodriguez, M. A., Paradis, Y., & Cabana, G. (2016). *Controls of longitudinal variation in δ13C-DIC in rivers: A global meta-analysis*.

Roberts, N., Eastwood, W. J., Kuzucuoglu, C., Fiorentino, G., & Caracuta, V. (2011). Climatic, vegetation and cultural change in the eastern Mediterranean during the mid-Holocene environmental transition. *The Holocene*, *21*(1), 147–162.

Robinson, D., Handley, L. L., Scrimgeour, C. M., Gordon, D. C., Forster, B. P., & Ellis, R. P. (2000). Using stable isotope natural abundances (d15N and d13C) to integrate the stress responses of wild barley (*Hordeum spontaneum* C. Koch.) genotypes. *Journal of Experimental Botany*, *51*(342), 41–50.

Rosen, A. M. (1997). Environmental change and human adaptation at the end of the Early Bronze Age in the Southern Levant. In H. N. Dalfes, G. Kukla, & H. Weiss (Eds.), *Third Millenium BC Climate Change and Old World Collapse* (Vol. 49, pp. 25–38). Springer-Verlag, Berlin, Heidelberg.

Rosen, A. M. (2007). *Civilizing Climate: Social responses to climate change in the ancient Near East*. Altamira Press.

Salavert, A. (2008). Olive cultivation and oil production in Palestine during the Early Bronze Age (3500-2000 BC): The case of Tel Yarmouth, Israel. *Vegetation History and Archaeobotany*, 9.

Samuel, D. (1989). Their staff of life: Initial investigations on ancient Egyptian bread baking. In B. J. Kemp (Ed.), *Amarna Reports* (pp. 253–290). Egypt Exploration Society.

Santesteban, L. G., Barbarin, M. I., & Royo, J. B. (2015). Application of the measurement of the natural abundance of stable isotopes in viticulture: A review. *Australian Journal of Grape and Wine Research*, *21*, 157–167.

Schiebel, V., & Litt, T. (2018). Holocene vegetation history of the southern Levant based on a pollen record from Lake Kinneret (Sea of Galilee), Israel. *Vegetation History and Archaeobotany*, *27*, 577–590.

Scholl-Barna, G. (2011). An isotope mass balance model for the correlation of freshwater bivalve shell (*Unio pictorum*) carbonate δ18O to climatic conditions and water δ18O in Lake Balaton (Hungary). *Journal of Limnology*, *70*(2), 272–282.

Schöne, B. R., Dunca, E., Fiebig, J., & Pfeiffer, M. (2005). Mutvei's solution: An ideal agent for resolving microgrowth structures of biogenic carbonates. *Palaeogeography, Palaeoclimatology, Palaeoecology*, *228*, 149–166.

Schwab, M. J., Neumann, F., Litt, T., Negendank, J. F. W., & Stein, M. (2004). Holocene palaeoecology of the Golan Heights (Near East): Investigation of lacustrine sediments from Birkat Ram crater lake. *Quaternary Science Reviews*, *23*, 1723–1731.

Schwartz, G. M., Curvers, H. H., Dunham, S. S., & Weber, J. A. (2012). From Urban Origins to Imperial Integration in Western Syria: Umm el-Marra, 2006, 2008. *American Journal of Archaeology*, *116*(1), 157–193.

Senbayram, M., Dixon, L., Goulding, K. W. T., & Bol, R. (2008). Long-term influence of manure and mineral nitrogen applications on plant and soil 15N and 13C values from the Broadbalk Wheat Experiment. *Rapid Communications in Mass Spectrometry*, *22*, 1735–1740.

Setter, T. L., Waters, I., Stefanova, K., Munns, R., & Barrett-Lennard, E. G. (2016). Salt tolerance, date of flowering and rain affect the productivity of wheat and barley on rainfed saline land. *Field Crops Research*, *194*, 31–42.

Sharp, Z. D. (2017). Biogenic carbonates—Oxygen. In Z. D. Sharp (Ed.), *Principles of stable isotope geochemistry* (2nd ed., p. 32). University of New Mexico.

Sherratt, A. (1980). Water, Soil and Seasonality in Early Cereal Cultivation. *World Archaeology*, *11*(3), 313–330.

Sherratt, A. (1983). The Secondary Exploitation of Animals in the Old World. *World Archaeology*, *15*(1), 90–104.

Shin, N., Marston, J. M., Luke, C., Roosevelt, C. H., & Riehl, S. (2021). Agricultural practices at Bronze Age Kaymakçı, western Anatolia. *Journal of Archaeological Science: Reports*, *36*, 15.

Simchoni, O., & Kislev, M. E. (2012). Food and Fodder in Early Bronze Age Strata in Area M. In A. Mazar (Ed.), *The Beth-Shean Valley Archaeological Project* (Vol. 4, pp. 422–429). The Institute of Archaeology, The Hebrew University of Jerusalem.

Simchoni, O., Kislev, M. E., & Melamed, Y. (2007). Botanical remains. In A. Mazar & R. Muillins (Eds.), *Excavations at Tel Beth-Shean 1989-1996* (Vol. 2nd, pp. 702–715). The Israel Exploration Society.

Singer, A. (2007). Soils of the Yizreel and Jordan Valleys. In A. Singer (Ed.), *The Soils of Israel* (pp. 147–177). Springer-Verlag, Berlin, Heidelberg.

Snir, A., Nadel, D., & Weiss, E. (2015). Plant-food preparation on two consecutive floors at Upper Paleolithic Ohalo II, Israel. *Journal of Archaeological Science*, *53*, 61–71.

Sorrel, P., & Mathis, M. (2016). Mid- to late-Holocene coastal vegetation patterns in Northern Levant (Tell Sukas, Syria): Olive tree cultivation history and climatic change. *The Holocene*, *26*(6), 858–873.

Soto-Berelov, M., Fall, P. L., & Falconer, S. (2012). A revised map of plant geographical regions of the Southern Levant. *Geospatial Science Research*, *2*, 12.

Soto-Berelov, M., Fall, P. L., Falconer, S. E., & Ridder, E. (2015). Modeling vegetation dynamics in the Southern Levant through the Bronze Age. *Journal of Archaeological Science*, *53*, 94–109.

Spengler, R. N. III. (2019). Dung burning in the archaeobotanical record of West Asia: Where are we now? *Vegetation History and Archaeobotany*, *28*, 215–227.

Spiro, B., Ashkenazi, S., Meinis, H. K., Melamed, Y., Feibel, C., Delgado, A., & Starinsky, A. (2009). Climate variability in the Upper Jordan Valley around 0.78 Ma, inferences from time-series stable isotopes of Viviparidae, supported by mollusc and plant palaeoecology. *Palaeogeography, Palaeoclimatology, Palaeoecology*, *282*, 32–44.

Stroud, E., Bogaard, A., & Charles, M. (2021). A stable isotope and functional weed ecology investigation into Chalcolithic cultivation practices in Central Anatolia: Çatalhoyük, Çamlıbel Tarlası and Kuruçay. *Journal of Archaeological Science: Reports*, *38*, 13.

Sturite, I., Kronberga, A., Strazdina, V., Kokare, A., Aassveen, M., Olsen, A. K. B., Sterna, V., & Straumite, E. (2019). Adaptability of hull-less barley varieties to different cropping systems and climatic conditions. *Acta Agriculturae Scandinavica*, *69*(1), 11.

Styring, A. K., Ater, M., Hmimsa, Y., Fraser, R., Miller, H., Neef, R., Pearson, J. A., & Bogaard, A. (2016). Disentangling the effect of farming practice from aridity on crop stable isotope values: A present-day model from Morocco and its application to early farming sites in the eastern Mediterranean. *The Anthropocene Review*, *3*(1), 2–22.

Styring, A. K., Charles, M., Fantone, F., Hald, M. M., McMahon, A., Meadow, R. H., Nicholls, G. K., Patel, A. K., Pitre, M. C., Smith, A., Soltysiak, A., Stein, G., Weber, J. A., Weiss, H., & Bogaard, A. (2017). Isotope evidence for agricultural extensification reveals how the world's first cities were fed. *Nature Plants*, *3*(17076), 11.

Surge, D., & Walker, K. J. (2006). Geochemical variation in microstructural shell layers of the southern quahog (Mercinaria campechiensis): Implications for reconstructing seasonality. *Palaeogeography, Palaeoclimatology, Palaeoecology*, *237*, 182–190.

Tarawneh, Q., & Kadioglu, M. (2003). An analysis of precipitation climatology in Jordan. *Theoretical Applied Climatology*, *74*, 123–136.

Tian, D., Ma, J., Wang, J., Pilgram, T., Zhao, Z., & Liu, X. (2018). Cultivation of naked barley by Early Iron Age agropastoralists in Xinjiang, China. *Environmental Archaeology*, *23*(4), 416–425.

Tsuneki, A., & Miyake, Y. (1996). The earliest pottery sequence of the Levant: New data from Tell el-Kerkh 2, Northern Syria. *Paléorient*, *22*(1), 109–123.

Vaiglova, P., Snoeck, C., Nitsch, E., Bogaard, A., & Lee-Thorp, J. (2014). Impact of contamination and pre-treatment on stable carbon and nitrogen isotopic composition of charred plant remains. *Rapid Communications in Mass Spectrometry*, *28*, 2497–2510.

Valamoti, S. M., & Charles, M. (2005). Distinguishing food from fodder through the study of charred plant remains: An experimental approach to dung-derived chaff. *Vegetation History and Archaeobotany*, *14*, 528–533.

van Bommel, D., Bruins, H. J., Lazarovitch, N., & van der Plicht, J. (2021). Effect of dung, ash and runoff water on wheat and barley grain sizes and stable isotope ratios: Experimental studies in ancient desert agriculture (Negev, Israel). *Journal of Archaeological Science: Reports*, *39*, 14.

van der Veen, M. (1999). The economic value of chaff and straw in arid and temperate zones. *Vegetation History and Archaeobotany*, *8*, 211–224.

van der Veen, M. (2007). Formation processes of desiccated and carbonized plant remains—The identification of routine practice. *Journal of Archaeological Science*, *34*, 968–990.

van Zeist, W. (1970). Prehistoric and Early Historic food plants in the Netherlands. *Palaeohistoria*, *14*, 134.

van Zeist, W. (1974). Palaeobotanical studies of settlement sites in the coastal area of Netherlands. *Palaeohistoria*, *16*, 161.

van Zeist, W. (1976). On macroscopic traces of food plants in southwestern Asia (with some reference to pollen data). *Phil. Trans. R. Soc. Lond. B*, *275*, 27–41.

van Zeist, W. (1985). Past and Present Environments of the Jordan Valley. In *Studies in the History and Archaeology of Jordan 02* (pp. 199–204). Department of Antiquities of Jordan.

van Zeist, W. (1992). The origin and development of plant cultivation in the Near East. *Japan Review*, *3*, 149–165.

van Zeist, W., & Bakker-Heeres, J. A. H. (1982). Archaeobotanical studies in the Levant I: Neolithic sites in the Damascus basin: Aswad, Ghoriafe, Ramad. *Palaeohistoria*, *24*, 165–256.

van Zeist, W., & Bakker-Heeres, J. A. H. (1984a). Archaeobotanical studies in the Levant 2. Neolithic and Halaf levels at Ras Shamra. *Palaeohistoria*, *26*, 171–199.

van Zeist, W., & Bakker-Heeres, J. A. H. (1984b). Archaeobotanical studies in the Levant 3. Late-Palaeolithic Mureybit. *Palaeohistoria*, *26*, 151–170.

van Zeist, W., Baruch, U., & Bottema, S. (2009). Holocene Palaeoecology of the Hula Area, Northeastern Israel. In E. Kaptijn (Ed.), *A Timeless Vale* (pp. 29–64). Leiden University.

VanDerwarker, A. M., Alvarado, J. V., & Webb, P. (2014). Analysis and interpretation of intrasite variability in paleoethnobotanical remains: A consideration and application of methods at the Ravensford Site, North Carolina. In J. M. Marston, J. D. Guedes, & C. Wariner (Eds.), *Method and theory in paleoethnobotany* (pp. 205–234). University Press of Colorado.

Verheyden, S., Nader, F. H., Cheng, H. J., Edwards, L. R., & Swennen, R. (2008). Paleoclimate reconstruction in the Levant region from the geochemistry of a Holocene stalagmite from the Jeita cave, Lebanon. *Quaternary Research*, *70*, 368–381.

Vogel, J. C. (1993). Variability of Carbon Isotope Fractionation during Photosynthesis. In J. R. Ehleringer, A. E. Hall, & Farquhar G. D. (Eds.), *Stable Isotopes and Plant Carbon-Water Relations* (pp. 29–46). Academic Press.

Voltas, J., Ferrio, J. P., Alonso, N., & Araus, J. L. (2008). Stable carbon isotopes in archaeobotanical remains and palaeoclimate. *Contributions to Science*, *4*(1), 21–31.

Voltas, J., Romagosa, I., Lafarga, A., Armesto, A. P., Sombrero, A., & Araus, J. L. (1999). Genotype by environment interaction for grain yield and carbon isotope discrimination of barley in Mediterranean Spain. *Australian Journal of Agricultural Research*, *50*, 1263–1271.

Vossel, H., Roeser, P., Litt, T., & Reed, J. M. (2018). Lake Kinneret (Israel): New insights into Holocene regional palaeoclimate variability based on high-resolution multi-proxy analysis. *The Holocene*, *28*(9), 1395–1410.

Waines, J. G., & Price, N. P. S. (1975). Plant remains from Khirokitia in Cyprus. *Paléorient*, *3*, 281–284.

Wallace, M., & Charles, M. (2013). What goes in does not always come out: The impact of the ruminant digestive system of sheep on plant material, and its importance for the interpretation of dung-derived archaeobotanical assemblages. *Environmental Archaeology*, *18*(1), 18–30.

Wallace, M., Jones, G., Charles, M., Fraser, R., Halstead, P., Heaton, T. H. E., & Bogaard, A. (2013). Stable carbon isotope analysis as a direct means of inferring crop water status and water management practices. *World Archaeology*, *45*(3), 388–409.

Wallace, M. P., Jones, G., Charles, M., Fraser, R., Heaton, T. H. E., & Bogaard, A. (2015). Stable Carbon Isotope Evidence for Neolithic and Bronze Age Crop Water Management in the Eastern Mediterranean and Southwest Asia. *PLOS ONE*, *10*(6), 19.

Wapnish, P., & Hesse, B. (1988). Urbanization and the Organization of Animal Production at Tell Jemmeh in the Middle Bronze Age Levant. *Journal of Near Eastern Studies*, *47*(2), 81–94.

Wasylikowa, K., & Koliński, R. (2013). The role of plants in the economy of Tell Arbid, north-east Syria, in the Post-Akkadian Period and Middle Bronze Age. *Acta Palaeobotanica*, *53*(2), 263–293.

Waterisotopes Database (2017) http://waterisotopesDB.org. Accessed 6/2023. Query: Country=JO&IL&PS, Type=Precipitation&River_or_Stream&Spring&Tap

Weinstein, J. M. (1984). Radiocarbon dating in the Southern Levant. *Radiocarbon*, *26*, 297–366.

Weiss, E., Kislev, M. E., Simchoni, O., Nadel, D., & Tschauner, H. (2008). Plant-food preparation area on an Upper Paleolithic brush hut floor at Ohalo II, Israel. *Journal of Archaeological Science*, *35*, 2400–2414.

Weiss, E., & Zohary, D. (2011). The Neolithic Southwest Asian founder crops: Their biology and archaeobotany. *Current Anthropology*, *52*(54), S237–S254.

Weiss, H. (2017). Seventeen kings who lived in tents. In F. Hoflmayer (Ed.), *The late third millennium in the ancient Near East* (pp. 131–162). Oriental Institute of the University of Chicago.

Weiss, H. (2016). Global megadrought, societal collapse and resilience at 4.2-3.9 ka BP across the Mediterranean and west Asia. *PAGES Magazine*, *24*(2), 62–63.

Weiss, H., Courty, M.-A., Wetterstrom, W., Guichard, F., Senior, L., Meadow, R., & Curnow, A. (1993). The genesis and collapse of third millennium north Mesopotamian civilization. *Science*, *261*(5124), 994–1004.

Werner, C., Schnyder, H., Cuntz, M., Keitel, C., Zeeman, M. J., Dawson, T. E., Badeck, F.-W., Brugnoli, E., Ghashghaie, J., Grams, T. E. E., Kayler, Z. E., Lakatos, M., Lee, X., Maguas, C., Ogee, J., Rascher, K. G., Siegwolf, R. T. W., Unger, S., Welker, J., … Gessler, A. (2012). Progress and challenges in using stable isotopes to trace plant carbon and water relations across scales. *Biogeosciences*, *9*, 3083–3111.

White, C. E., Chesson, M. S., & Schaub, R. T. (2014). A recipe for disaster: Emerging urbanism and unsustainable plant economies at Early Bronze Age Ras an-Numayra, Jordan. *Antiquity*, *88*, 363–377.

Wilkinson, T. J. (2003). *Archaeological landscapes of the Near East*. University of Arizona Press.

Wilkinson, T. J., Philip, G., Bradbury, J., Dunford, R., Donoghue, D., Galiatsatos, N., Lawrence, D., Ricci, A., & Smith, S. L. (2014). Contextualizing Early Urbanization: Settlement Cores, Early States and Agro-pastoral Strategies in the Fertile Crescent During the Fourth and Third Millennia. *Journal of World Prehistory*, *27*(1), 42–108.

Willcox, G. (1999). Charcoal analysis and Holocene vegetation history in southern Syria. *Quaternary Science Reviews*, *18*, 711–716.

Willcox, G. (2005). The distribution, natural habitats and availability of wild cereals in relation to their domestication in the Near East: Multiple events, multiple centres. *Vegetation History and Archaeobotany*, 534–541.

Willcox, G. H. (1974). A History of Deforestation as Indicated by Charcoal Analysis of Four Sites in Eastern Anatolia: Anatolian Studies. *Anatolian Studies*, *24*, 117–133.

Woodbridge, J., Roberts, N., & Fyfe, R. (2018). Pan-Mediterranean Holocene vegetation and land-cover dynamics from synthesized pollen data. *Journal of Biogeography*, *45*(9), 2159–2174.

Xiao, J., Zhang, S., Fan, J., Wen, R., Xu, Q., Inouchi, Y., & Nakamura, T. (2019). The 4.2 ka event and its resulting cultural interruption in the Daihai Lake basin at the East Asian summer monsoon margin. *Quaternary International*, *527*, 87–93.

Zaarur, S., Affek, H. P., & Stein, M. (2016). Last glacial-Holocene temperatures and hydrology of the Sea of Galilee and Hula Valley from clumped isotopes in Melanopsis shells. *ScienceDirect*, *179*, 142–155.

Zarczynski, P. J., Sienkiewicz, S., Wierzbowska, J., & Krzebietke, S. J. (2021). Fodder Galega—A versatile plant. *Agronomy*, *11*(1797), 1–12.

Zeder, M. A. (1991). *Feeding Cities*. Smithsonian Institution Press.

Zhang, K., Bosch-Serra, A. D., Boixadera, J., & Thompson, A. J. (2015). Investigation of Water Dynamics and the Effect of Evapotranspiration on Grain Yield of Rainfed Wheat and Barley under a Mediterranean Environment: A Modelling Approach. *PLOS ONE*, *10*(8), 18.

Ziv, B., Saaroni, H., Pargament, R., Harpaz, T., & Alpert, P. (2014). Trends in rainfall regime over Israel, 1975-2010, and their relationship to large-scale variability. *Regional Environmental Change*, *14*, 1751–1764.

Zohary, D., & Hopf, M. (1973). Domestication of Pulses in the Old World. *Science*, *182*(4115), 887–894.

Zohary, D., & Hopf, M. (1988). *Domestication of Plants in the Old World: The origin and spread of cultivated plants in west Asia, Europe and the Nile Valley*. Clarendon Press.

Zohary, D., & Spiegel-Roy, P. (1975). Beginnings of Fruit Growing of the Old World. *Science*, *187*, 319–327.

Zohary, M. (1950). The segetal plant communities of Palestine. *Vegetatio*, *2*(6), 387–411.

Zohary, M. (1962). *Plant Life of Palestine (Israel and Jordan)*. The Ronald Press Company.

Zohary, M. (1966). *Flora Palaestina One* (1–2). Israel Academy of Sciences and Humanity.

Zohary, M. (1972). *Flora Palaestina Two* (1–2). Israel Academy of Sciences and Humanity.

Zohary, M. (1982). *Plants of the Bible*. Cambridge University Press.

APPENDIX A: TAXONOMIC IDENTIFICATION CRITERIA

Taxonomic Identification Criteria

Introduction

This section describes the traits I used to identify species from carbonized seed remains, prioritizing the most commonly encountered taxa from Tell Abu en-Ni'aj, Tell el-Hayyat, and Zahrat adh-Dhra' 1. Identification resources are described in Chapter 3 with primary reference to Zohary (1966; 1972); Delorit (1970); Martin and Barkley (1973); Feinbrun-Dothan (1978); (1986); Zohary and Hopf (1988); and Cappers and Bekker (2013). As my personal criteria for identifying species have evolved throughout this study, a discussion of my specific methods of identification is an important step not just for validation of identifications, but also to ensure reproducibility should future research be conducted on the carbonized remains of these sites. Figures A1-A5 show representative samples of each seed recovered from my focal sites.

Approximations of shape, size, texture, and the presence of unique morphological features gleaned from images and textual descriptions were the most commonly used characteristics for identification. Specific seed measurements, comparison with an in-lab collection of dried seeds, and comparison with images from online seed databases (e.g., Seed Identification Guide or The Image Database of Wild Plant Seeds) were also used as aids to identify less distinguishable specimens. The regional extent of a genera's species was sometimes used to identify taxon to species level if species-specific descriptions could not be found and only a single species of the genera is native to the Southern Levant. Information on regional extent was gathered from published paleoethnobotanical articles, overviews on ancient cultigen distribution (e.g., Zohary and Hopf 1973; 1988; Zohary and Spiegel-Roy 1975), and databases on native ranges of wild taxon (e.g., Plants of the World Online). Photos of well-preserved, representative seeds from common taxon are collated into Figures A1-A5, with descriptions of each seed below.

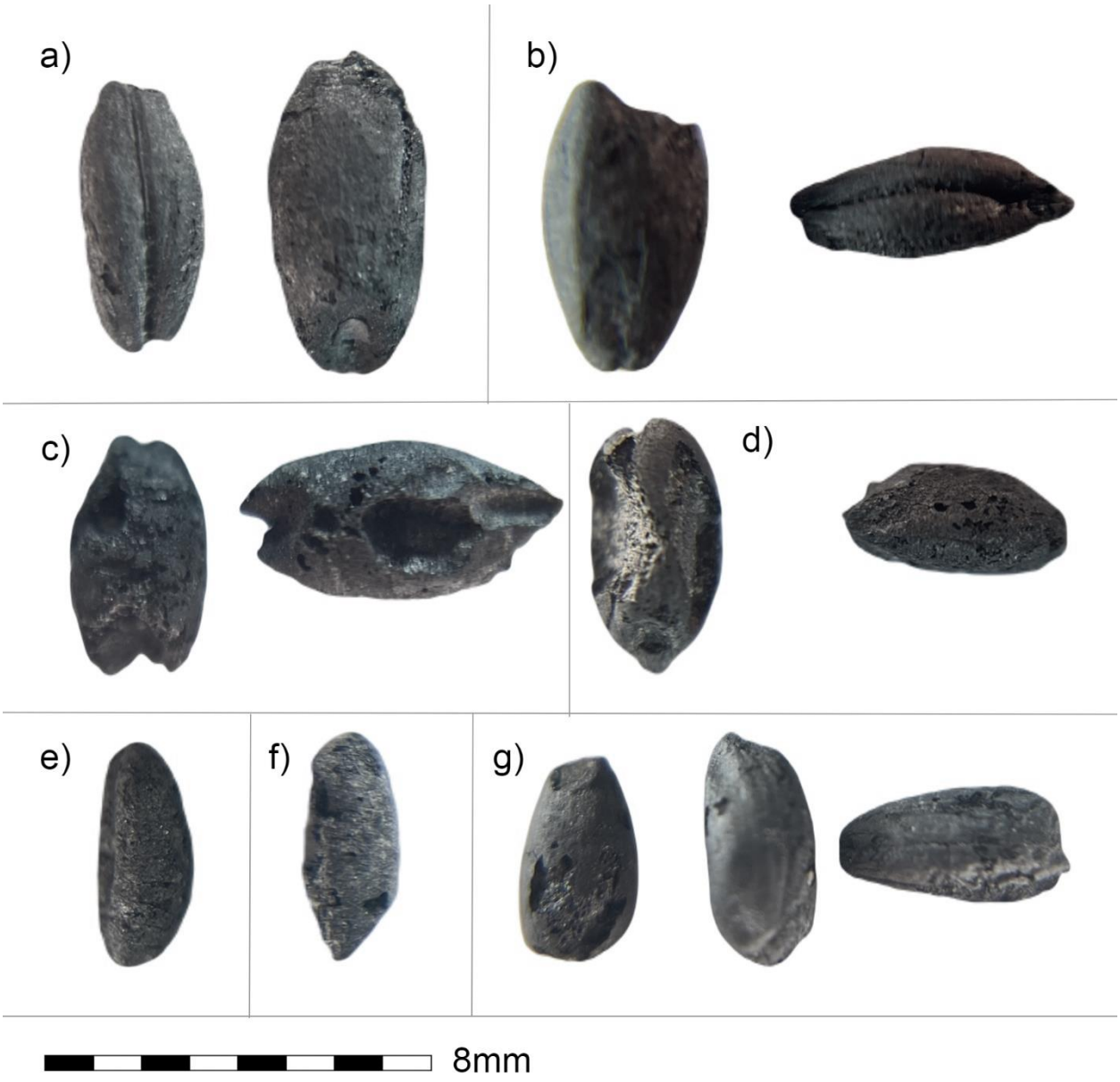

Figure A1. Carbonized seeds from Tell Abu en-Ni'aj and Tell el-Hayyat, Jordan. Species include: (a) *Hordeum vulgare*, (b) *H. vulgare hexastichum*, (c) *H. vulgare* var. *nudum*, (d) *Triticum aestivum*, (e) *T. dicoccum*, (f) *T. monococcum*, and (g) *T. spelta*.

Cultivated taxa

Hordeum vulgare* subsp. *distichum, two-row hulled barley, is typified by its flattened, elongate body. Prominent ridges are noted along the outer hull, most visible from the cross-sectional profile. Ridges appear in four corners of the rectangular cross-sectional profile, with an additional dorsal ridge sometimes visible and a deep ventral furrow. In the cross-section, seeds of the genus *Hordeum* have an ellipse shape, with the ventral and dorsal sides protruding roughly even distances from the center of the seed. This variant of hulled barley has no twisting along its length. All *Poaceae* grains have a concave embryo scar visible at the proximal end. In some cases for *Hordeum* and *Triticum*, the remnants of a radicle may be found, coming to a point just below embryo. For *Hordeum,* the embryo ridge is often noticeably lower than that of *Triticum*,

below an angle of about 45°. Striations are often noted along the outer hull, while signs of the hull bursting may be found on occasion. The internal structure of *Hordeum* and *Triticum* often appears fibrous and highly porous.

Hordeum vulgare* subsp. *hexastichum, six-row hulled barley, appears nearly identical to *Hordeum vulgare distichum*. This taxon produces three seeds per spikelet rather than the one seed of *H. vulgare distichum*, with the two outermost seeds taking on a slight twist in order to fit into the spikelet. *H. vulgare hexastichum* is similarly typified by a flattened, elongated body and distinct ridges running length-wise from the proximal to distal ends. It is distinguished from *H. vulgare distichum* by the roughly 30°-45° of twisting along its primary axis noted in cross-sectional view. The embryo shape, hull morphology, and internal structure are akin to that of *H. vulgare distichum*.

Hordeum vulgare* var. *nudum, naked barley, is typified by a flattened, ellipsoidal body with a roughly cardioid cross-section thanks to a deep ventral furrow. It lacks the distinct lengthwise ridges that denote the presence of a hull. As such, no striations are noted along the exterior. No twisting was noted in this variant of barley, suggesting only the two-row form was present throughout all of the sites. Grains have a shallow, concave embryo at the proximal end. *H. vulgare* var. *nudum* sometimes appears wider than the hulled varieties, and the distal end may appear more rounded.

Triticum aestivum, bread wheat, is defined by the puffy appearance of its seed, as compared to other wheats. It was combined with *T. durum* at ZAD 1 due to similarities between the two genera that could not be distinguished due to the poor seed quality at ZAD 1. *Triticum aestivum* was differentiated at Tell Abu en-Ni‘aj and Tell el-Hayyat based on rounding along each grain’s ventral face that seemed to more closely accord with this species. The genus *Triticum* typically has a triangular cross section with a pronounced, rounded dorsal ridge, a steeper embryo, and a flattened ventral profile. They also have a noticeable, but shallower ventral furrow than that of genus *Hordeum*. Both *Triticum aestivum* and *T. durum* are hull-less wheats. This taxon in particular has a rounder cross section than other wheats and is rounded at both its proximal and distal ends. Its cross-sectional view highlights the rounded corners and dorsal-lateral faces that give it a ‘puffy’ appearance. It has a shallow furrow on a slightly convex ventral face, a steep embryo ridge, and a maximum height occurring around the center of the seed in lateral view. *Triticum aestivum* is often wider and taller than other wheat seeds, but may be shorter in length from the proximal to distal ends. Internal structure again appears fibrous and highly porous.

Triticum dicoccum, emmer wheat, is one of the three hulled or glume wheats alongside *T. monococcum* and *T. spelta*. It is thinner than *T. aestivum* and has a cross sectional profile resembling an equilateral triangle, still with gently rounded corners. Most notably, this grain has a strong embryo ridge, with its tallest feature appearing very near the proximal end just above the embryo. It thus has the steepest embryo of the *Triticum* species discussed, at times approaching around 80°. It has a rounded apex at its distal end, but comes to more of a point along the proximal end of the ventral face. Two varieties of this grain are present between the sites, though undistinguished. The first has a flat ventral side and softer point at the distal end while the other has a slightly convex ventral face and comes to a sharper point at its distal end.

Cross-sectional profiles of emmer can have a good deal of diversity, sometimes being bilaterally asymmetrical, but typically will maintain an equilateral-triangle appearance if not slightly flattened. However, one distal-lateral face of the seed may protrude out further than the other, giving the seed a lop-sided appearance.

Triticum monococcum, einkorn wheat, has a cross-sectional profile approximating an isosceles triangle, with a larger dorsal ridge than other *Triticum* varieties. Two varieties of einkorn are noted at the sites. The first grain is notably thinner, has a steep embryo, a strong dorsal ridge similar to *T. dicoccum*, is typically much thinner, and has a strong lean towards one side. This variant also has a flat ventral face with sharp ventral edges that comes to a point at the distal end. The variant maintains a constant height until close to the distal point.

The second variety has a shallower embryo ridge more akin to *T. aestivum*, with the highest point occurring near the center of the seed. This variant is also thin and has a notable lean towards one side in cross-sectional view, but has a clearly convex ventral face and the distal point terminates nearer the center of the median plane rather than along the ventral plane. Other features including the shape of the embryo and the internal structure appear similar to other *Triticum*.

Triticum spelta, spelt wheat, has a wider and shorter triangular cross-sectional profile than other *Triticum* grains, though maintains a strong dorsal ridge and upright embryo that clearly mark it a *Triticum*. The grain is thinner at the proximal end but wide and rounded at its distal point. Though the ventral ridge is strong in cross section, it flattens out towards the distal end. It has a very shallow ventral furrow and is more rounded on its dorsal-lateral faces than *Triticum dicoccum* or *T. monococcum*. Grooves running laterally along the seed's lateral faces may denote the presence of a hull.

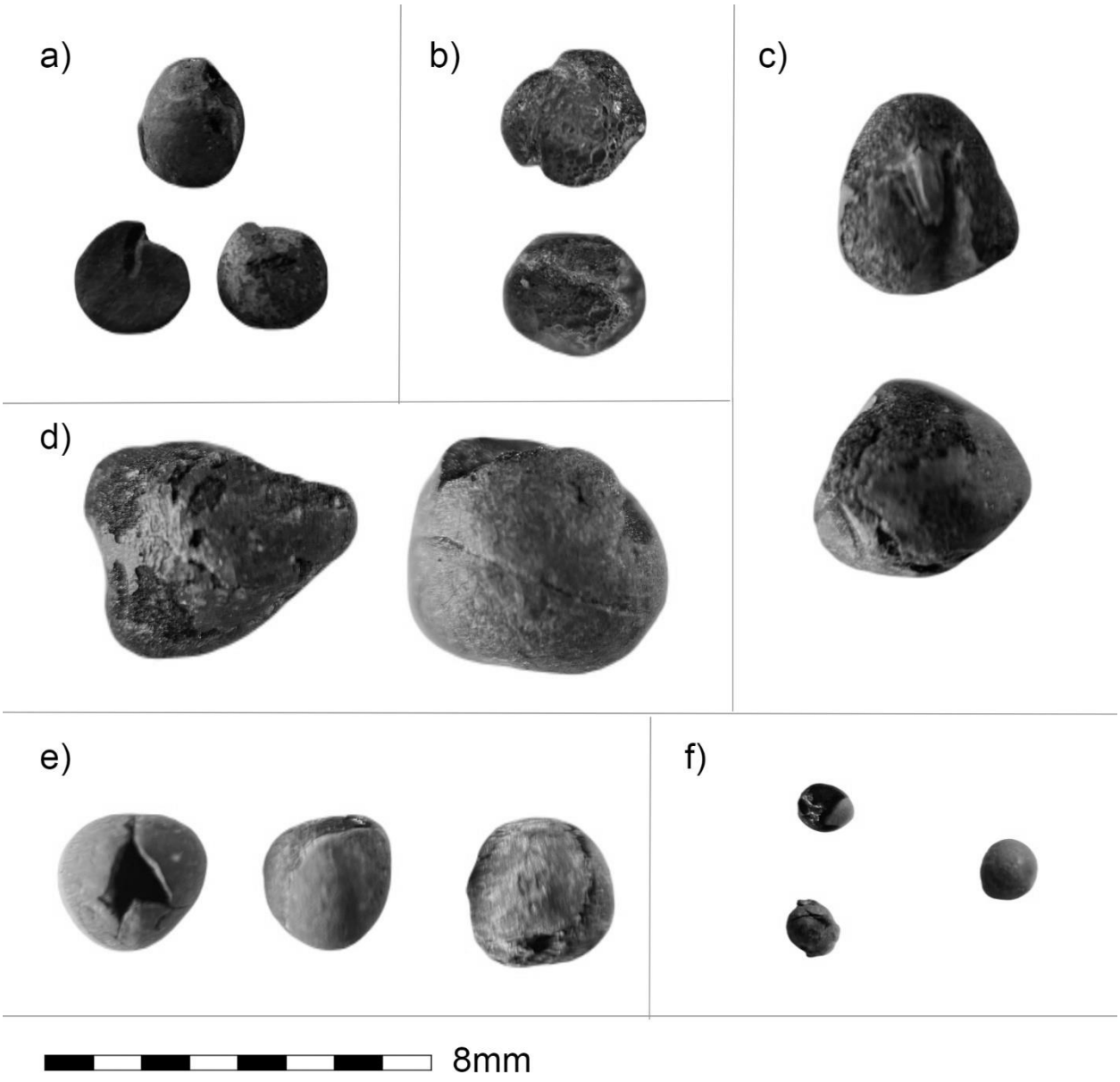

Figure A2. Carbonized seeds from Tell Abu en-Ni'aj and Zahrat adh-Dhra' 1, Jordan. Species include: (a) *Lens culinaris*, (b) *Pisum sativum*, (c) *Lathyrus sativus*, (d) *Vicia faba*, (e) *Vicia ervilia*, and (f) *Ficus carica*.

Lens culinaris, lentil, is a small grain with a namesake lenticular cross-section. It has a round profile from the dorsal view and a hilum scar visible on the edge of the seed along its circumference, where the seed can be seen pinching off. It may have a slight offset in the length of the seed near the radicle, which bulges slightly under the testa. If the testa is missing, cotyledons of the seeds can be found separately, with one flat side and one convex face giving a hemisphere shape. If broken, a starchy, non-porous texture is visible on the inner surfaces.

Pisum sativum, garden pea, are roughly spherical grains with a large hilum along one edge, tucked between two parallel ridges and below a third ridge that defines the position of the radicle. The parallel ridges are very slight, giving the hilum a gentle concavity. Each hemisphere

of the seed is roughly identical, giving bilateral symmetry. The internal structure resembles a Styrofoam-like texture with very low porosity.

Lathyrus sativus, grass pea, are larger and more angular than *Pisum sativum* and *Vicia ervilia*. The hilum is tucked in a concave furrow at the proximal end between three low ridges. The dorsal ridge at this end protrudes furthest, containing the radicle. The taxon maintains a bilateral symmetry. It has a roughly tooth-like shape overall, with the body shaped like a triangular prism, triangular cross section from the proximal end, and a rectangular shape from the ventral and dorsal-lateral views. At the distal end there may be a gentle concavity again formed by the three ridges that give the seed its shape. Internal structure again resembles a Styrofoam-like texture.

Vicia faba, horsebean, is a relatively flat and fabiform seed, and is noticeably larger than other beans. From a lateral view it may appear roughly ellipsoid, either with broad sides or with slight inward depressions on each side approaching the median plane. The seed is separated in two long, flattened segments and does not seem to retain bilateral symmetry in cross-section. At the proximal end, a long hilum is found along the circumference between the two cotyledons. This end of the seed is wider, with two thick ridges that run alongside the length of the hilum. If broken, the seed has a more porous internal texture than the aforementioned legumes.

Vicia ervilia, bitter vetch, closely resembles *Pisum sativum*. It is a small seed with rounded faces and a hilum positioned between two ridges in a deeply incised furrow. It has a smooth exterior and strong bilateral symmetry. The distinguishing feature is its notable overall shape, resembling a triangular pyramid with rounded points. From the proximal view, the strong triangular cross-section clearly differentiates the seed from *Pisum*. Internal texture is also more porous than that of pea.

Ficus carica, common fig, are small, lightweight, and roughly spherical seeds. If present, they tend to be found in large quantities and may be highly fragmented. The seed is notably thin-walled and hollow, susceptible to movement under slight force, making this seed exceedingly easy to distinguish even if not broken. A point may be found at one end with a thin ridge leading down one side of the seed away from the attachment point, but often no hilum is noted. Seeds are thus slightly ovoid and many have carbonized stem material still attached at the proximal end. If broken, the thickness of the testa and amount of curvature are the best indicators to use.

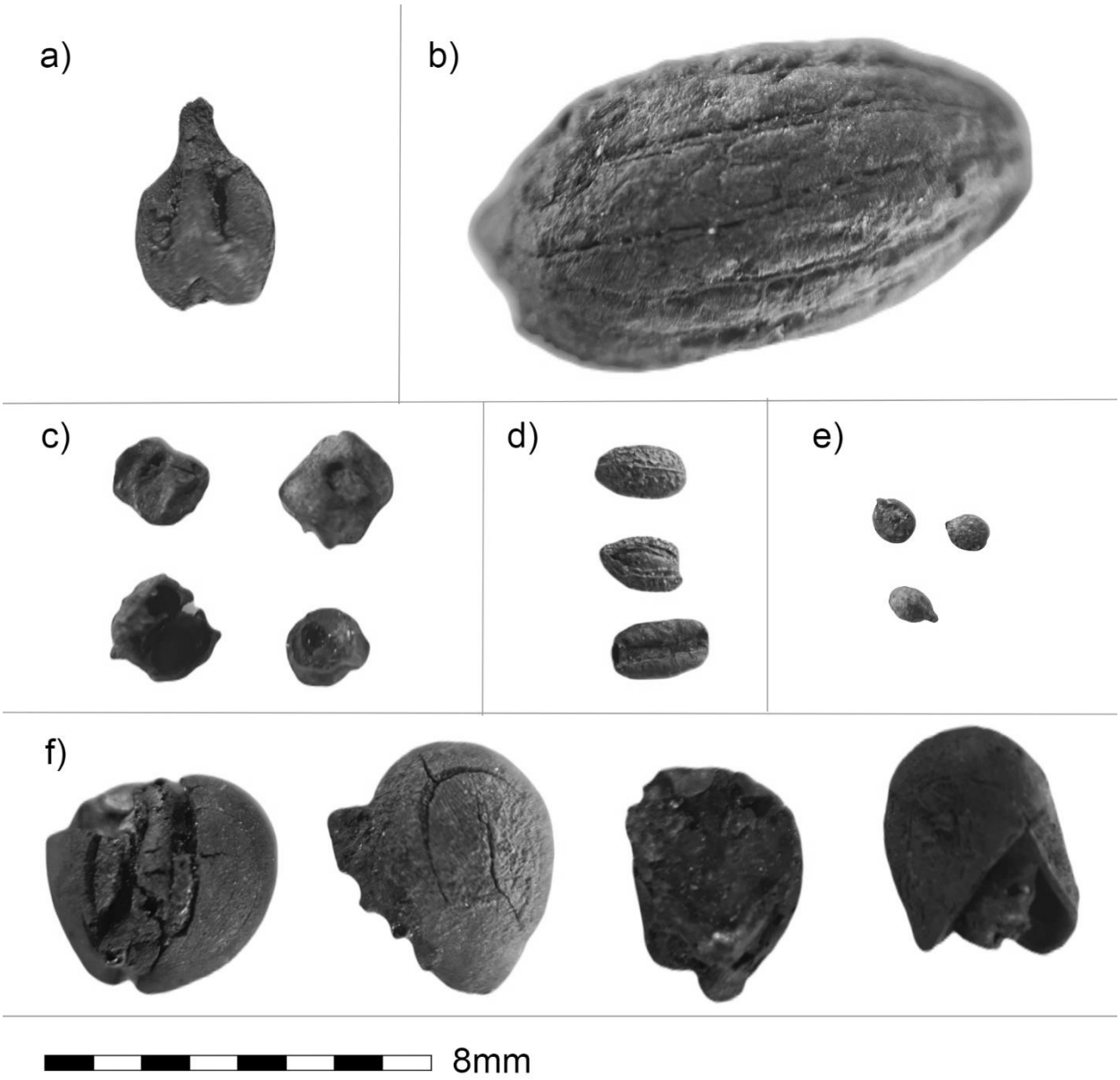

Figure A3. Carbonized seeds from Tell Abu en-Ni'aj, Tell el-Hayyat, and Zahrat adh-Dhra' 1, Jordan. Species include: (a) *Vitis vinifera*, (b) *Olea europaea*, (c) *Beta vulgaris*, (d) *Bupleurum* sp., (e) *Coriandrum sativum*, and (f) *Prosopis farcta*.

Vitis vinifera, common grape, has a distinct seed morphology. From the dorsal view, it has a pyriform shape with an elongated stem-like point at the proximal end and a small depression at the distal end. It has two large furrows running down the center on either side of a strong dorsal ridge. Across this ridge the seed has bilateral symmetry. In cross-sectional view the seed has a broad, oval shape, wider than it is thick. Grape seeds are hollow, but with thicker testa than either *Ficus* or *Prosopis*, thinner than *Prunus*, and occasionally a glassy looking texture that differentiates it from *Pistacia*. *Olea europaea* and *Vitis vinifera* each have very little difference in their seed morphology between the cultivated and wild varieties, with the primary distinction being as slight size difference of the stone or pip (Zohary and Spiegel-Roy, 1975; Liphschitz et al., 1991). The presence of cultivated varieties in the Southern Levant in the Chalcolithic and

Bronze Age (Goor, 1966; Neef, 1990; Liphschitz et al., 1991; Renfrew, 2003; Miller, 2008) supports the notion that these taxa were very likely cultivated. Further, based on the oblong shape of the seed and pip, grapes at our sites are very likely cultivated (Hopf, 1983).

Olea europaea, common olive, is defined by its large size and thick endocarp. On the exterior of this layer are a series of parallel ridges which undulate irregularly as they run from one end of the seed to the other. From a lateral view *Olea* is roughly ovoid in shape with a circular cross section. It may pinch at one or both ends, but this can vary. If fragmented, the endocarp is notably thicker than the remains from any other taxon described here. An embryo can be found preserved inside stones of *Olea*, though no remains of testa or endosperm were noted even in experiments with whole seeds. The embryo is large and ellipsoid with a circular cross section. It has a very rough, uneven exterior but few other noticeable features.

Beta vulgaris, beetroot, was identified most commonly by its angular endocarp which contains the base for two separated seeds. It has the shape of a flattened pentagonal prism with a rough exterior and small jutting points at each corner. Seeds were found both separate and still within the endocarps, with operculum opening on opposing ends. If found together, the seed was counted as two individuals. The seed is roughly lenticular, similar to that of *Atriplex,* but smaller and with a sharper depression around the outer edge where the radicle can be noted under the testa.

***Bupleurum* sp.**, thorow wax, is another seed typically found in its endocarp. The endocarp is elongated and ovoid, with the dorsal face appearing flattened. The exterior of the dorsal face has a thin furrow running the length of the seed, while the ventral face is lined by multiple thin, lateral ridges. The entire exterior of the endocarp is coated by small bumps which seem to occur irregularly. At the proximal end, the seed comes to a point, while the distal end is blunt and slightly rounded at the edges. If fragmented or missing, this seed coat is particularly thin, similar to that of fig, and the seed tends to be found intact. The seed has a similar overall shape but is smooth and rounded on each end. Instead of the flattened dorsal face, it has a wide and deep incision. It is differentiated from *Plantago* by the width of this incision, the straight sides, and the lack of other notable features on the seed. At my sites it was also easy to differentiate as many *Bupleurum* still had parts of the endocarp attached to the exterior of the seed. Figure A3 shows the seeds of *Bupleurum* sp. from Tell Abu en-Ni‘aj, Jordan. The picture from top to bottom indicates the bumps and ridges on ventral face, an example of an endocarp cracking open, and the seed of a large Bupleurum out of its endocarp.

Coriandrum sativum, coriander, was identified by its unique shape, almost perfectly hemispherical and occasionally slightly ovoid from a dorsal view, except for at the proximal end where the seed pinches out at its hilum. From a cross sectional view, the seed is dome shaped with relatively thick ridges running down from the stem on the exterior of the seed. Looking at the interior surface, there is a slight depression but the seed is otherwise featureless. These seeds were only ever found in half.

Prosopis farcta, Syrian mesquite, is a relatively large-seeded regional legume. The testa is rounded and obovate, more pointed at the proximal end. In cross-section it has an oval shape, thickest near the center of the seed towards the distal end. The seed is thicker than that of taxa

like *Vitis*, but thinner than taxa like *Olea* or *Prunus*. Its seed has several unique features including a thin, horseshoe-shaped incision on the exterior of its testa. In cross-sectional view, the incisions on the dorsal and ventral faces of *Prosopis* taper off before reaching the proximal end. Under the testa, there is a thin layer of highly porous, glassy, and fibrous-looking endosperm that can be seen holding the embryo in place, with endosperm thickest towards the median plane. The embryo, similar to the seed of *Olea*, appears dense, wrinkled, and lacks many defining features. Its shape is similarly obovate, but its cross section is oblong and flattened. This, alongside the overall shape and amount of endosperm helps differentiate it from *Vachellia.*

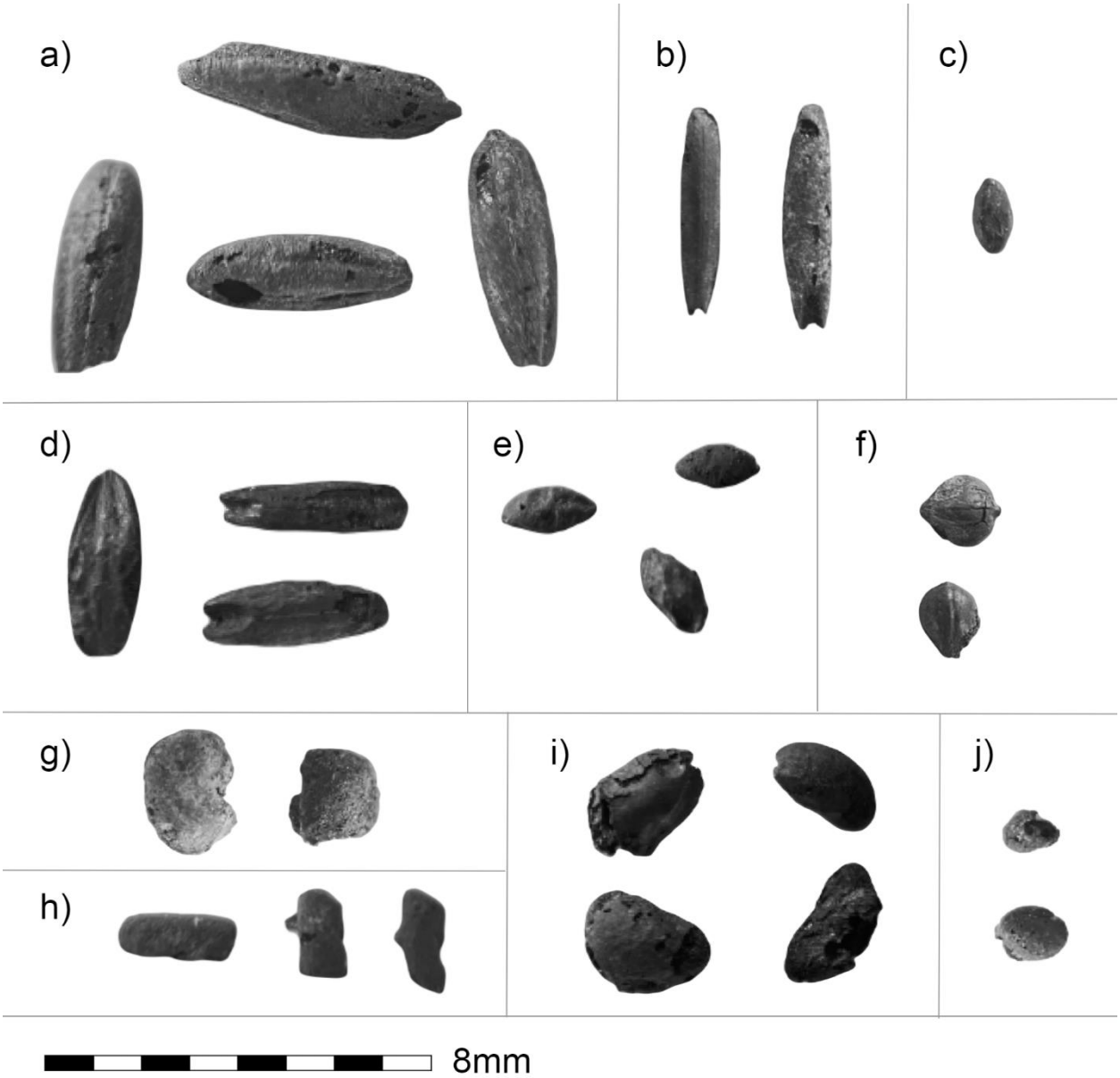

Figure A4. Carbonized seeds from Tell Abu en-Ni'aj and Zahrat adh-Dhra' 1, Jordan. Species include: (a) *Avena fatua*, (b) *Bromus* sp., (c) *Digitaria* spp., (d) *Lolium temulentum*, (e) *Phalaris canariensis*, (f) *Bolboschoenus maritimus,* (g) *Astragalus* sp., (h) *Trigonella* sp., (i) *Onobrychis* [left] and *Medicago* [right] spp., (j) *Melilotus* sp.

Avena fatua, wild oat, is a grass taxon with a thin, oblong seed. From lateral view it looks similar to a wheat seed, but it is typified by a notable bulge of the ventral face which gives the impression of an overhang. It has a roughly circular cross section, as opposed to the triangular cross sections of wheat and rye, and may have a flattened proximal end. A shallow furrow is noted on the ventral face. At the proximal end the embryo comes to a point, while the distal end is slightly wider and rounded. Occasionally, the distal end is slightly askew specifically on the ventral face, with one side of the seed swelling more than the other, giving the seed an asymmetrical appearance.

***Bromus* sp.**, brome, is a grass typified by its long, slender body. The species noted at our sites had ellipsoid cross sections, wider than tall, with small embryos and a clear ridge on the ventral face, as opposed to the furrows seen on other grasses. Both ends of the seed are slightly rounded, with the distal end rounder. The flattened profile and length of the seed, reaching around 8-9 mm at maximum, set it apart from other similar grains like *Stipa*. Unlike *Avena*, *Bromus* typically displays bilateral symmetry.

***Digitaria* spp.**, crabgrass, is one of the smallest grasses identified at my sites. A variety of seeds exhibiting the following characteristics were classified as cf./aff. *Digitaria* spp., and it is possible that several species are included in this designation. The taxa is typified by its length and roughly lenticular shape from lateral view. The embryo found is on the narrow side of the seed and may extend between ⅓ to ½ up the side of the seed. The dorsal and ventral ridge are thin, while the lateral faces are often more prominent. In cross-section, the taxon may exhibit circular to ovoid morphology, with the dorsal side thinner if ovoid. In lateral view both ends of the seed pinch out but remain rounded, with maximum width occurring towards the proximal end. In some seeds the distal end may come to more of a fine point. Unlike *Phalaris*, the dorsal and ventral faces are rounded.

Lolium temulentum, rye grass, is a grass whose seed is recognizable for its wide, flattened body. It has distinct groves on the ventral and dorsal faces including around the edges and along the central ridge on the ventral side. The overall shape is that of a flattened ellipsoid, with the proximal end having a short, deep embryo and the distal end being notably blunt. In lateral view, the seed may exhibit a slight curvature, with the proximal and distal ends curving upwards.

Phalaris canariensis, canary grass, is a small-seeded grass with a distinctive ~135° circular-sector shape from lateral view. It is flattened along the median plane similar to *Digitaria*, with the lateral faces most prominent. The ventral face is notably rounded, while the dorsal face has two straightened segments that come to a point near the transverse plane. The tallest point of the seed is towards the embryo, with a gentler slope from the tip of the embryo to the distal end. Both ends of the seed are relatively pointed, as is the apex of the seed at the top of the embryo. The seed is thin, extremely porous and crushes easily under light pressure.

Bolboschoenus maritimus, sea clubrush, is a sedge whose small, flattened seed exhibits an ovate to pyriform shape. Seeds of *Bolboschoenus* are primarily found within achenes, which have a relatively smooth exterior and strong dorsal ridge with a flat ventral face. The seed inside mimics the shape of the pericarp. The proximal end is wide and blunt while the distal end finishes at a fine point. From dorsal view, the edges of the seed begin curving off immediately at the proximal

end, while at the distal end the sides are straight. From cross-sectional view, the seed is much shorter than it is wide, giving an isosceles triangle shape with rounding on the dorsal-lateral faces. The seed is thickest and tallest roughly midway through the seed, towards the proximal end.

***Carex* spp.**, true sedges, are a wide genus of sedge plants. *Carex* species were not distinguished at my sites and were identified by several common traits shared at the genus level. Most notably, this includes the ovate shape from dorsal view, a thickening near the transverse plane, with rounding at the proximal end and pinching at the distal end. *Carex* seeds were also found primarily within their achenes, which survive carbonization. Their pericarps have strong lateral ridges along the edges and dorsal face. Some species had a high ridge, giving the seed a cross-sectional appearance resembling an equilateral triangle, with each lateral face of roughly similar size. In these cases, both the funicle at the proximal end and the point at the distal end remain parallel to the ventral face, separating it from similar taxon like the infrequent *Cyperus*.

***Astragalus* sp.** is a wide genus of leguminous plants typified by small, puffy seeds. Seeds are roughly fabiform from a lateral view, with each end wide and a notable depression where the hilum sits at the proximal side. *Astragalus* has an oblong shape from the top and side views. A groove may denote the radicle at one end of the seed near the hilum. The side with the radicle is thicker in cross section and may protrude out slightly farther on the face with the hilum than it does at the other side of the hilum. In cases where this is particularly notable, this gives these seeds an undulating, stairstep-like appearance on the proximal side in the lateral view, with the hilum appearing to jut out rather than recess inward. The interiors of *Astragalus* were extremely porous and shared the glassy texture commonly among in wild legumes.

Trigonella, fenugreek, is a leguminous crop with a roughly rectangular-prism shape. It has a flattened, elongated body with minimal rounding on its edges that gives the seed a rectilinear appearance. There is rounding on each end of the seed's relatively thin body, which is more than twice as long as it is wide. In cross-section, the seed pinches out at the lateral faces, with an oval shape. A shallow hilum is evident on one side of the seed. Internal structure shows the same highly porous texture common to wild legumes. *Trigonella* identification was challenging, and the species may be *Galega officinalis* based on the morphological similarity of these two taxa. Identification as *Trigonella* is more likely since *G. officinalis* is fairly poisonous to many ruminants (Zarczynski et al., 2021) while *Trigonella* is less poisonous (Moreno et al., 2022).

Medicago* and *Onobrychis, burclover and sainfoin respectively, are two species grouped together in this study, but which were generally easy to distinguish. Both are fabiform, with a depression on the proximal side where the hilum is located. *Medicago* is notably thinner from proximal to distal ends and flatter in cross-sectional view. In cross section these seeds may be two to three times as wide as they are tall and have an oblong appearance. *Medicago* seeds also tend to have a more noticeable depression at the hilum. *Onobrychis*, comparatively, is much thicker and more blunted on both ends. In cross-sectional view it more closely resembles an ovoid appearance, with the seed about as wide as it is thick. The hilum of *Onobrychis* is also less notable, and the proximal end may be nearly straight instead of slightly depressed. Each shares the porous, glassy internal texture of the wild legumes.

***Melilotus* sp.**, sweet clover, is a legume typified by its small seed and the unique shape it has due to the position of its radicle. The radicle, still identifiable inside the testa thanks to a strong groove, extends from one end of the seed vertically around ½ to ¾ of the way to the other end. It notably pinches from the seed at one end before hugging along the lateral face, ending in a flattened segment where the hilum is found. This part of the seed is much thinner than the main body of the seed. *Melilotus* is roughly oblong with rounded ends and is slightly wider in one direction, with the radicle further accentuating this.

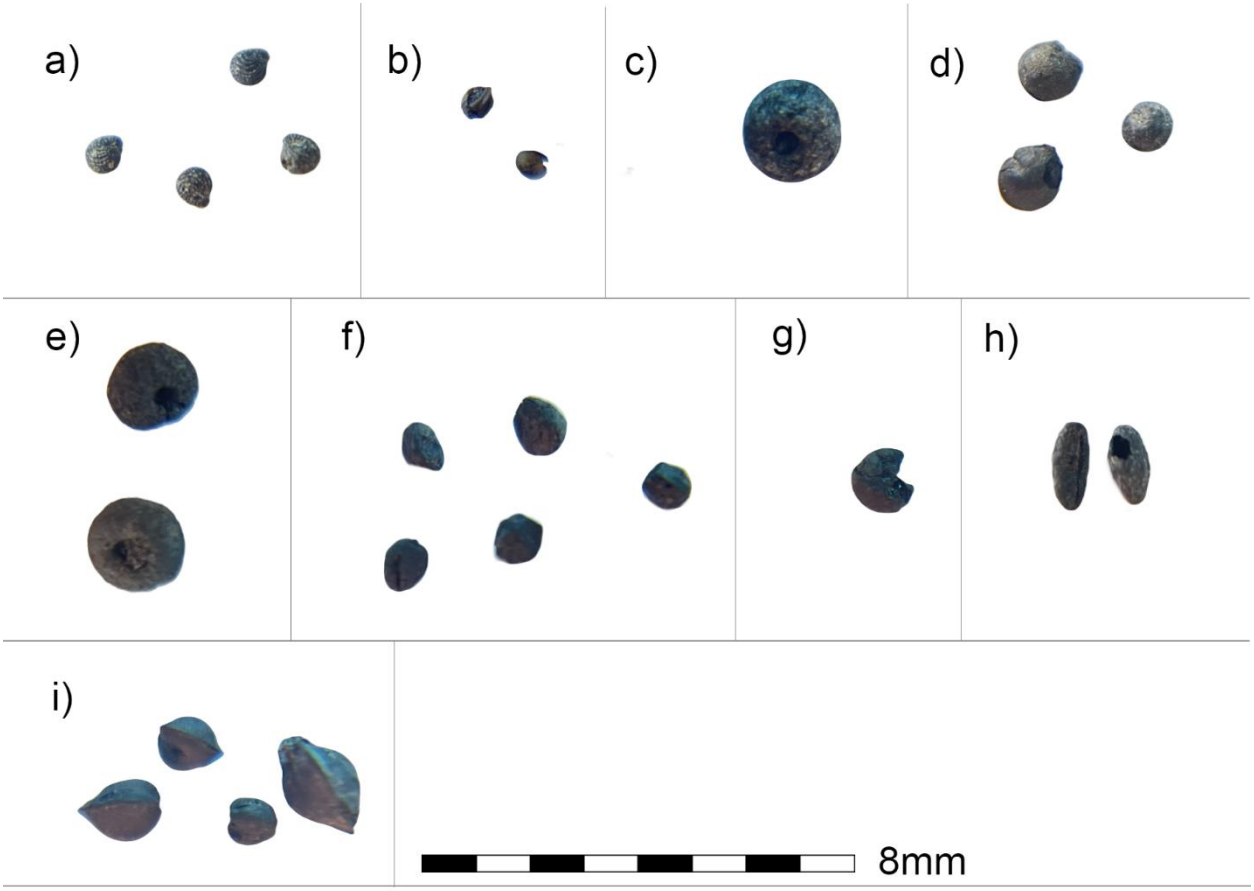

Figure A5. Carbonized seeds from Tell Abu en-Ni'aj, Jordan. Species include: (a) *Aizoon hispanicum*, (b) *Amaranthus graecizans,* (c) *Bellevalia* sp., (d) *Chenopodium* sp., (e) *Galium aparine*, (f) *Lysimachia arvensis,* (g) *Malva parviflora*, (h) *Plantago* sp. Carbonized seeds and an achene (i) from *Rumex/Polygonum* spp.

Aizoon hispanicum (syn. *Aizoanthemum*), Spanish aizoon, is typified by its small, light-weight seed. The seed is thin-walled and hollow. The extension of the radicle on one side gives the appearance of coiling, with a small furrow on each side denoting the radicle from the body of the embryo. On the exterior of the seed relatively thick, continuous ridges coil along the length of the testa of the seed. Two edges of the seed are slightly flattened, giving an ovoid appearance from lateral view. If broken, the seed has one of the thinnest testa, thinner than that of even *Ficus*.

Amaranthus graecizans, Mediterranean amaranth, is one of the smallest seeded plants to be collected in this study. It is typified by its smaller length and width, its proportional tall height, and its thick outer margin which pinches out to a thin rim. It has a circular shape from lateral view and a lenticular shape in cross section, similar to *Chenopodium*. From a top-down perspective there may be a slight ovoid shape pinching where the radicle is located. From this perspective one can see a slight fold in the testa near the edge of the seed that denotes an outer ring-like margin. In cross sectional view this margin is roughly ½ or greater than the height of the seed, but from lateral view the rim is less noticeable. The outer testa can have a smooth, glossy texture but this may be lost. If fragmented there is a spongy texture inside the seed that becomes more highly porous near the center of the seed where the endosperm would be.

***Bellevalia* sp**. is typified by its spherical shape with a hole on one face. On its exterior it is smooth, with no notable features outside of the single opening. The hole is radially symmetrical and is relatively small compared to other similar taxa like *Galium* or *Ornithogalum*. The hole penetrates around ¾ of the way through the seed but remains cylindrical and does not open into a larger space. If fragmented, cross-sectional view will show an impermeable, Styrofoam-like internal texture similar to that of the peas.

***Chenopodium* sp.**, goosefoot, have small seeds with embryos that wrap around forming a thickened outer rim, similar to that of *Amaranthus*. *Chenopodium* are about twice the length and width of *Amaranthus*, but are not notably taller, giving them more of a fusiform shape in cross-sectional view. The outer rim is also thinner in general but comes to a rounded edge. However, the rim is more noticeable from lateral view due to a circular groove following the exterior margin visible on the top face which roughly denotes the location of the embryo and radicle inside. A notch for the position of the hilum is also more visible in this genus, as a small depression which causes the rim to pinch in at one location. The external texture of *Chenopodium* is smooth and can be glossy, while texture internally is porous to spongy.

Galium aparine, catchweed, is a globose seed with two flattened faces. In most cases only the pericarp appears to remain, with the interior of the mericarp and embryo missing. If present, the hole appears as a large depression. The proximal face of *Galium* has a large, sub-rounded opening which gently curves inward. Small, scattered bumps coat the exterior of the pericarp irregularly. The interior of the seed is hollow and the endocarp thin, making *Galium* lightweight and fragile.

Lysimachia arvensis (syn. *Anagallis arvensis*)*,* scarlet pimpernel, has a very distinct yet flexible shape comprised of a series of gently curving faces. It generally takes the shape of a triangular pyramid, with five faces; however, it is not unusual for it to have three to six faces depending on the rounding of each side and how its edges intersect. Each edge is sharp and distinct with one face being more prominent than the others. The exterior is coated in small bumps of various sizes that give it a grainy and rough texture under magnification. If broken the seed is thin walled and hollow.

Malva parviflora, mallow, is somewhat fabiform from a lateral view, with each end curved inwards to form a ~270° circular-sector shape. The hilum is in the interior portion of the circular sector. One end of the seed is wider and rounder than the other, but both come to a relatively fine

point. Because of this, the side of the seed with the hilum and two ends is relatively thin, while the opposing curved face is thick, giving the seed a wedge shape from cross-sectional view. Rarely, *Malva* can be found connected together in a ring within the remains of the ovary. If this was present, each seed was counted individually

***Plantago* sp.**, fleaworts, are a small, flat seeded plant typified by a deep furrow which runs down the ventral face of the seed. The seed is ellipsoid shaped with slight tapering towards the ends and is relatively thinner than it is wide due to a flattening of the ventral face. The hilum is found at the center of the ventral furrow between two thick ridges. The dorsal face is convex, rounded, and may appear glossy and smooth. The shape and depth of the seed and furrow help to separate this taxon from the seed of *Bupleurum*.

***Rumex* and *Polygonum* spp.**, dock/sorrel and knotweed respectively, have a very similar morphology and distinction was not made during this study. It is likely that multiple species of each were combined in this category. Seeds from these taxa are typically recovered inside a thin-walled achene, but if fragmented the seed is inside. These achenes have several notable features including their triangular cross-section with three pronounced ridges. The thick ridges run from one end to the other dividing the achene into three faces, each with a pyriform to lanceolate shape. The distal end of the seed terminates at a fine point while the proximal end can either be pointed, flat, or concave. In cross-section, each face is slightly concave. Seeds of *Rumex*/*Polygonum* have a similar morphology to the achene, but are slightly smaller, do not possess strong ridges, have convex instead of concave faces, and do not terminate in a pointed distal end.

APPENDIX B: MORPHOLOGICAL COMPARISONS BETWEEN FOCAL SITES

Grain Morphology Introduction

Grain morphological investigations have proven to be useful for paleoethnobotanical taxon identifications (Portillo et al., 2019), but have also been shown to be valuable in studies of crop yield (Reed et al., 2019). Metrics regarding weight and size distribution between notable cultivated taxa are discussed here. Metrics of length, width, height, and weight were recorded for approximately 500 grains. Of those, the primary cereals, lentils, and grapes were measured in comparable sample sizes for analysis. Grain counts for each site are shown in Table A1, indicating the number of samples per species and the average proportions noted for each taxon. *Hordeum vulgare* and *Triticum dicoccum* were the most frequently sampled, with counts of 142 and 145 seeds respectively. Hordeum vulgare was the largest seed in both weight and estimated volume. Values for *Hordeum vulgare* var. *nudum* were roughly comparable to *Hordeum vulgare* with slightly lower weights, while *Triticum aestivum* values compared closely with *Triticum dicoccum* with slightly shorter and fatter grains.

Table A1. Seed metrics averaged between the four focal sites for the six most frequent taxa sampled for stable isotopes.

	Number of seeds	Length (mm)	Width (mm)	Height (mm)	Weight (mg)
Hordeum vulgare	142	5.49	2.98	2.37	9.32
Hordeum vulgare var. *nudum*	39	5.34	3.05	2.38	8.66
Triticum aestivum	41	4.53	3.05	2.89	9.17
Triticum dicoccum	145	4.93	2.50	2.41	7.30
Lens culinaris	49	3.29	3.08	2.28	6.82
Vitis vinifera	26	4.27	3.20	2.65	8.01

Grain Comparisons

Results for metrics comparing *Hordeum vulgare* and *Triticum dicoccum* between sites are graphed below showing similar distributions of size and shape, Figures A6 and A7. Pairwise chow tests of *Hordeum vulgare* and *Triticum dicoccum* between sites suggest there was no significant distinction of the morphological patterns. This suggests that there is no indication of significantly distinct grain sizes and thus no distinction in yield between settlements either between EB IV and MB I-II or between the northern Jordan Valley and Dead Sea Basin. While it is certain that environmental conditions were not identical across these spans, it can be presumed that the difference in these conditions was not large enough to leave a measurable effect on the seed proportions, or in this case grain yield.

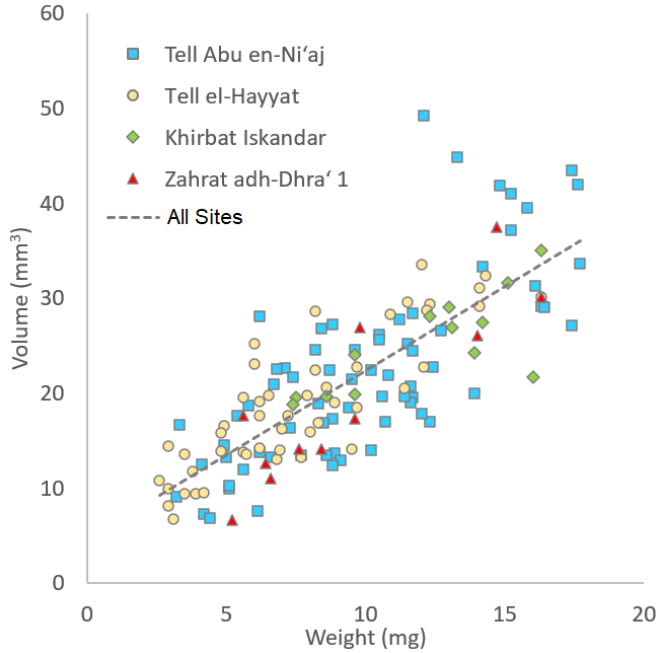

Figure A6. *Hordeum vulgare* morphometrics for each site. Trends of weight and volume suggest roughly similar morphology for grains at each site, as confirmed by pairwise Chow tests with all values falling below critical F-value when using a moderate alpha of 0.10.

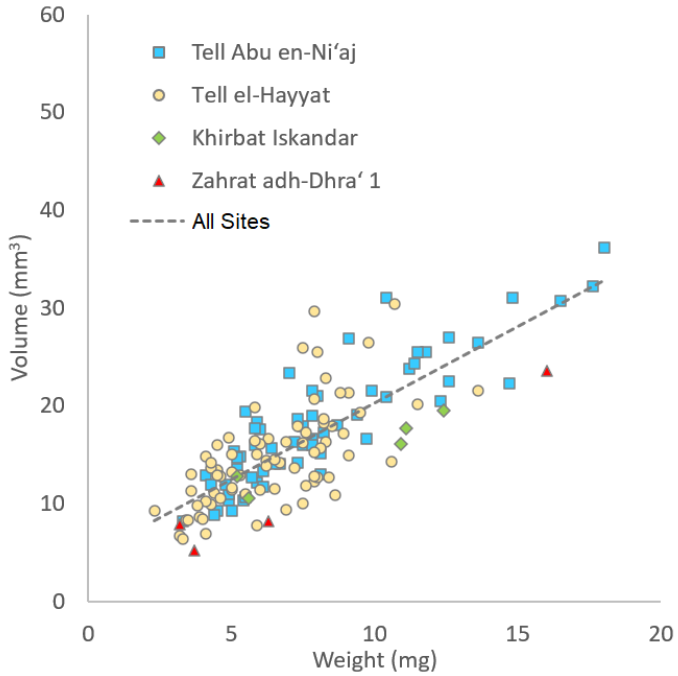

Figure A7. *Triticum dicoccum* for each site clustered closer than barley, with Chow test pairwise site comparisons also suggesting no significant difference (α 0.10).

APPENDIX C: MACROFOSSIL COUNT SUPPLEMENTARY TABLES

Macrofossil counts for the paleoethnobotanical assemblage and stable isotopic analyses in Chapters 4, 5, 6, and 9 are listed in Supplementary Tables S1-S3. Counts for Khirbat Iskandar seeds, used in stable isotopic analyses in Chapter 9, are available in Table S4. Data is provided in Microsoft Excel database format, 250 kb in size. The file, Supplement_MacrofossilCounts.xlsx, is available via ProQuest.

APPENDIX D: SECTOR CLASSIFICATION MAPS FOR TELL ABU EN-NI‘AJ

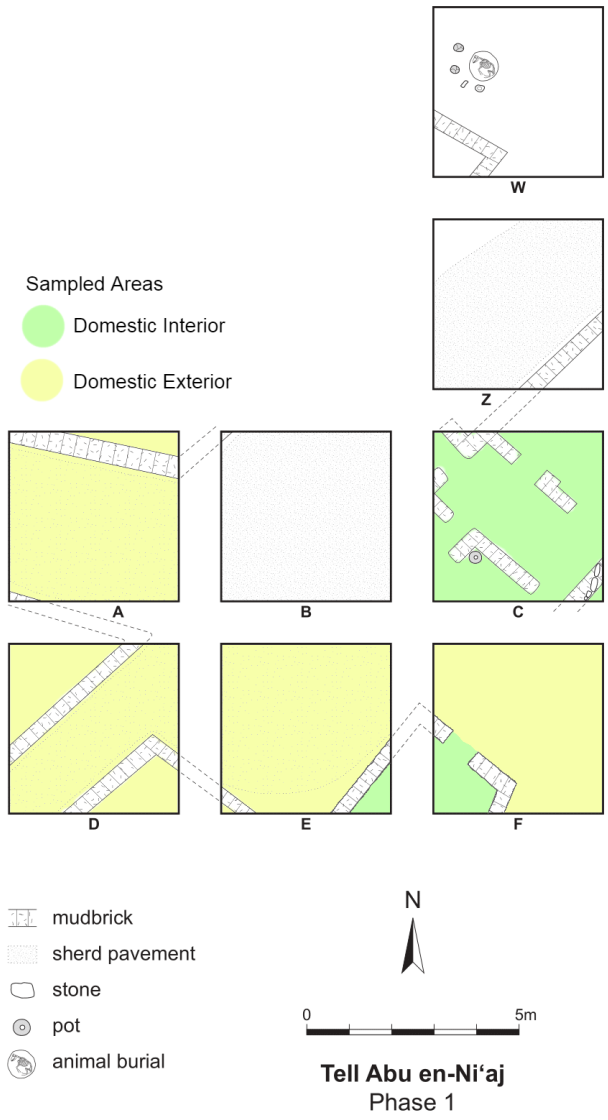

Figure A8. Archaeological plan of Tell Abu en-Ni‘aj Phase 1 showing the architectural layout of the site. Letters are used to designate each excavation unit (after Falconer and Fall 2019: fig 4.27). Colors are used to designate areas representing possible domestic interior sectors (green) and domestic exteriors (yellow) from the areas with carbonized material sampled in this dissertation.

Figure A9. Archaeological plan of Tell Abu en-Ni'aj Phase 2 showing the architectural layout of the site. Letters are used to designate each excavation unit (after Falconer and Fall 2019: fig 4.23). Colors are used to designate areas representing possible domestic interior sectors (green) and domestic exteriors (yellow) from the areas with carbonized material sampled in this dissertation.

Figure A10. Archaeological plan of Tell Abu en-Ni'aj Phase 3 showing the architectural layout of the site. Letters are used to designate each excavation unit (after Falconer and Fall 2019: fig 4.20). Colors are used to designate areas representing possible domestic interior sectors (green) and domestic exteriors (yellow) from the areas with carbonized material sampled in this dissertation.

Figure A11. Archaeological plan of Tell Abu en-Ni'aj Phase 4 showing the architectural layout of the site. Letters are used to designate each excavation unit (after Falconer and Fall 2019: fig 4.15). Colors are used to designate areas representing possible domestic interior sectors (green) and domestic exteriors (yellow) from the areas with carbonized material sampled in this dissertation.

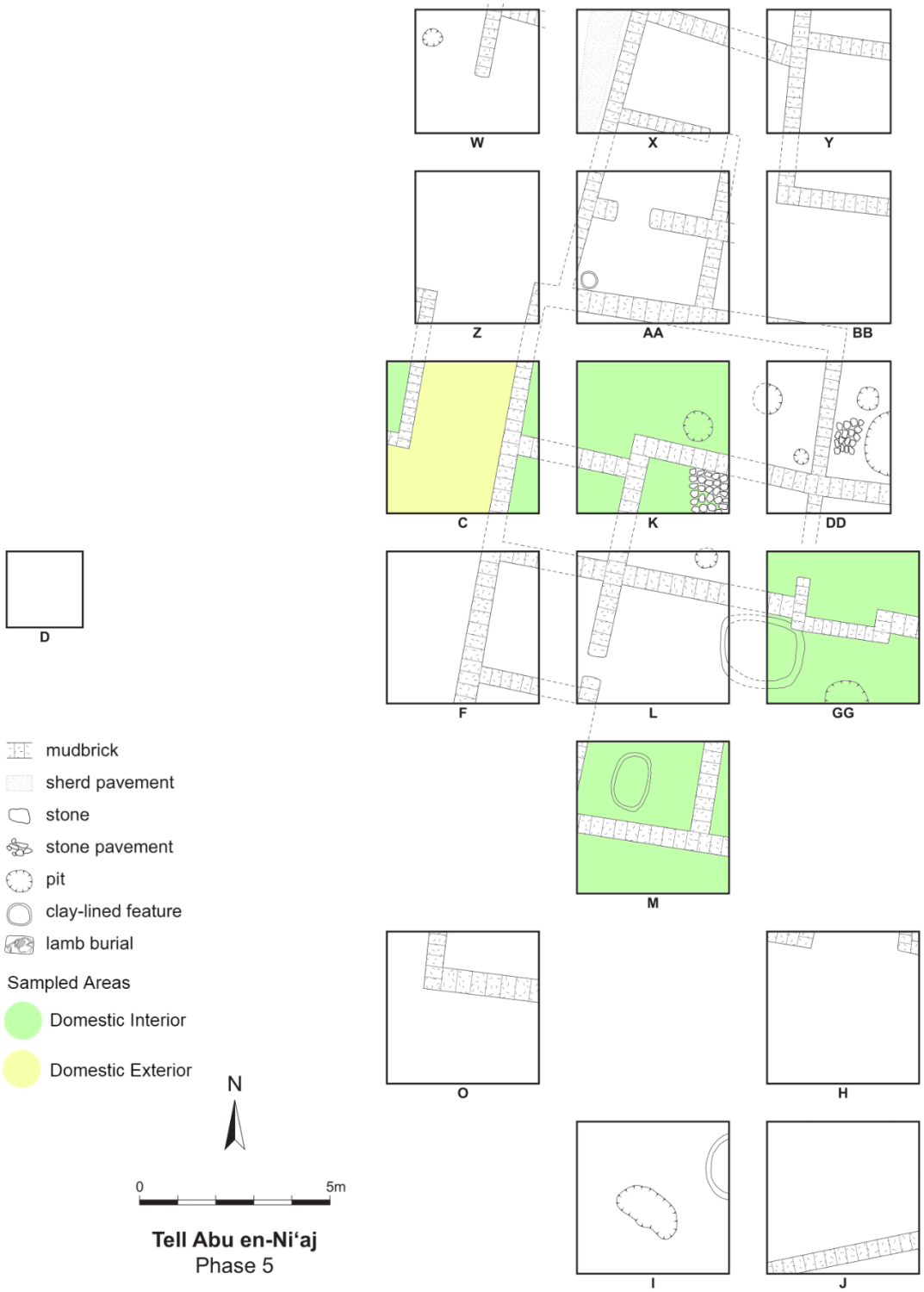

Figure A12. Archaeological plan of Tell Abu en-Ni'aj Phase 5 showing the architectural layout of the site. Letters are used to designate each excavation unit (after Falconer and Fall 2019: fig 4.10). Colors are used to designate areas representing possible domestic interior sectors (green) and domestic exteriors (yellow) from the areas with carbonized material sampled in this dissertation.

Figure A13. Archaeological plan of Tell Abu en-Ni'aj Phase 6 showing the architectural layout of the site. Letters are used to designate each excavation unit (after Falconer and Fall 2019: fig 4.6). Colors are used to designate areas representing possible domestic interior sectors (green) and domestic exteriors (yellow) from the areas with carbonized material sampled in this dissertation.

Figure A14. Archaeological plan of Tell Abu en-Ni'aj Phase 7 showing the architectural layout of the site. Letters are used to designate each excavation unit (after Falconer and Fall 2019: fig 4.4). Colors are used to designate areas representing possible domestic interior sectors (green) and domestic exteriors (yellow) from the areas with carbonized material sampled in this dissertation.

APPENDIX E: DENSITY VALUES FOR TELL EL-HAYYAT SPATIAL MAPS

Table A2. Density of seeds recovered per phase and sector for each taxon plotted in the maps of spatial distribution for Tell el-Hayyat, Jordan.

Phase	Sector	Volume	*Hordeum*	*Triticum*	*Ficus*	*Vitis*	*Olea*	*Lens*
2	CA	18	3.39	3.72	1.00	0.22	0.33	0.00
2	CE	6	6.67	4.67	1.33	0.00	0.00	1.50
2	EA	28	1.21	3.11	0.50	0.07	0.07	0.04
2	EB1	2	2.50	3.50	0.50	0.00	0.00	0.00
2	EB2	14.5	1.45	17.93	1.38	0.14	0.00	0.00
2	EB3	4	1.25	3.75	0.00	0.00	0.00	0.00
2	TF	8	0.00	0.75	1.13	0.25	0.00	0.00
2	TFE	8	0.25	0.13	0.00	0.38	0.00	0.00
2	TI	2	1.00	2.50	0.50	0.00	0.00	0.00
2	TS	14	2.07	2.36	1.50	0.07	0.00	0.14
3	CA	16	1.06	0.81	0.06	0.06	7.19	0.06
3	CE	18	4.83	16.28	0.28	0.17	0.00	0.28
3	EA	4	5.00	8.00	0.50	0.00	1.50	0.00
3	EB	13.5	1.19	12.30	1.26	0.37	0.00	0.07
3	EC	20	2.30	2.30	1.20	0.05	0.65	0.20
3	TF	25.87	2.98	2.78	14.57	0.19	0.12	0.58
3	TI	32.81	1.65	1.10	4.63	0.55	0.06	0.34
3	TS	1	2.00	0.00	0.00	0.00	0.00	0.00
3	WE	28	2.79	1.29	0.11	0.04	0.07	0.32
4	CA	4	2.25	2.00	0.50	0.00	0.00	1.00
4	CC	20	0.70	0.30	0.00	0.00	0.20	0.00
4	CE	1.47	10.22	0.00	0.00	0.00	0.00	0.00
4	CR	2	6.50	1.00	0.50	0.00	125.00	3.00
4	EA	9	8.56	3.56	0.78	0.00	1.00	0.00
4	EB	5.75	56.00	9.22	1.04	0.00	0.35	0.00
4	EC	32.87	7.54	1.52	0.43	0.06	1.00	0.15
4	TF	27	1.52	1.00	0.22	0.00	0.41	0.26
4	TI	41.74	2.11	1.05	2.25	0.07	0.00	0.17
4	TS	12	1.00	0.58	0.58	0.00	0.08	0.33
4	WR	8.87	11.72	1.13	0.90	0.11	0.79	0.11
5	OTE	111.44	13.61	7.56	2.86	0.03	0.38	0.48
5	TB	3	0.67	0.33	1.33	0.00	0.00	1.33
5	TF	30	1.23	0.60	1.17	0.03	0.00	0.03
5	TI	29.68	1.65	0.67	0.78	0.07	0.00	0.40
5	TS	2	10.50	2.50	9.00	0.50	0.00	2.50

APPENDIX F: ARAGONITE VERIFICATION

Analysis of shell composition was conducted from two shells of *Melanopsis buccinoidea,* one each from Tell Abu en-Ni‘aj and Tell el-Hayyat. Results from X-ray diffraction analysis indicated excellent preservation of original calcium carbonate from each shell. An example of the result from Tell Abu en-Ni‘aj is indicated in Figure A15 with the shell’s calcium carbonate compared to the baseline peaks for aragonite. Overlapping peaks indicated good preservation. Since the original aragonite was preserved, stable isotope sampling proceeded for the archaeological shells.

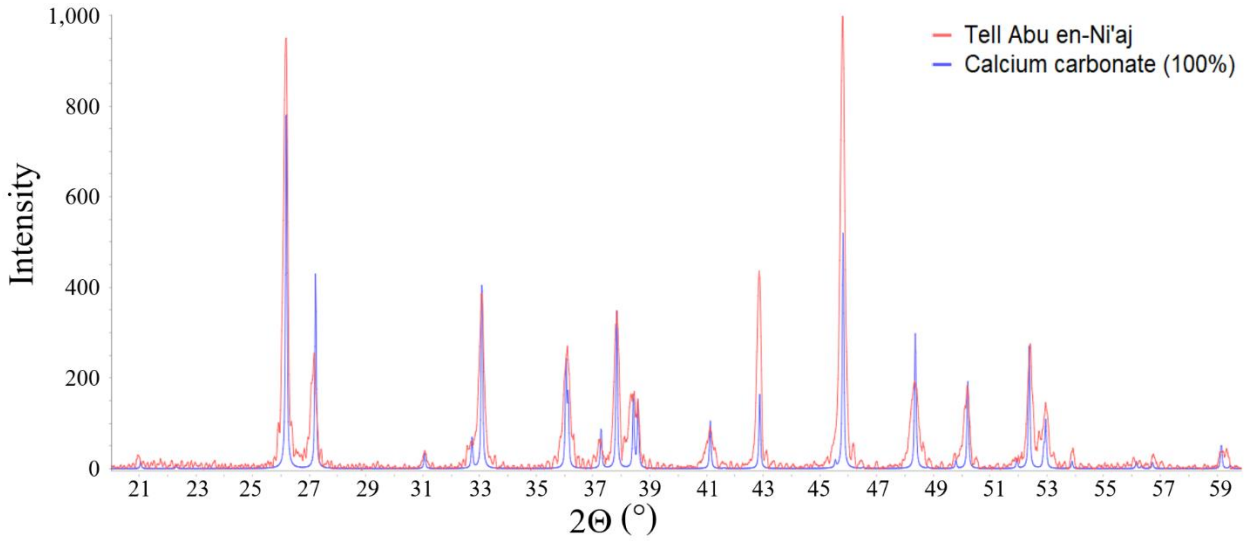

Figure A15. Result from preliminary X-ray fluorescence test of a Tell Abu en-Ni‘aj shell sample H.20.32 indicating matching peaks of shell aragonite and sample calcium carbonite, thus preservation of original aragonite microstructure.

APPENDIX G: ARCHAEOLOGICAL SHELL STABLE ISOTOPES FROM TELL ABU EN-NI'AJ AND TELL EL-HAYYAT

Table A3. Stable oxygen and carbon isotope measurements for each archaeological shell sample from Tell Abu en-Ni'aj, Jordan.
*Indicates values from the annual band used in isotopic analyses.

Context Area.Locus.Bag	Phase	Sample # (from aperture)	$\delta^{18}O$ (‰) Corrected	$\delta^{13}C$ (‰) Corrected
L.17.118	2	1	-2.99	-4.14
L.17.118	2	2	-2.14	-2.46
L.17.118	2	3*	-3.22	-2.71
L.17.118	2	4*	-4.16	-5.28
L.17.118	2	5*	-3.90	-5.90
L.17.118	2	6*	-4.20	-6.21
L.17.118	2	7*	-4.91	-6.31
L.17.118	2	8*	-4.07	-6.61
L.17.118	2	9*	-4.31	-6.50
L.17.118	2	10*	-4.80	-6.26
L.17.118	2	11	-4.36	-5.83
L.17.118	2	12	-4.09	-6.37
L.17.118	2	13	-3.87	-6.18
L.17.118	2	14	-3.96	-6.22
L.17.118	2	15	-3.97	-6.58
L.17.118	2	16	-4.02	-6.95
L.17.118	2	17	-3.88	-6.30
L.17.118	2	18	-4.11	-6.04
L.17.118	2	19	-4.06	-6.69
L.17.118	2	20	-3.86	-7.18
O.26.92	3	1	-4.89	-7.25
O.26.92	3	2	-4.76	-7.46
O.26.92	3	3	-4.50	-7.29
O.26.92	3	4*	-4.71	-7.33
O.26.92	3	5*	-4.86	-7.64
O.26.92	3	6*	-4.85	-7.33
O.26.92	3	7*	-4.83	-7.49
O.26.92	3	8*	-5.05	-7.36
O.26.92	3	9*	-5.09	-7.37
O.26.92	3	10*	-5.20	-7.53
O.26.92	3	11*	-5.06	-7.87
O.26.92	3	12*	-4.96	-7.76
O.26.92	3	13*	-5.06	-7.31
O.26.92	3	14*	-5.28	-7.42

O.26.92	3	15*	-4.95	-7.77
O.26.92	3	16*	-4.97	-7.55
O.26.92	3	17*	-4.95	-7.62
O.26.92	3	18	-4.58	-6.75
O.26.92	3	19	-4.34	-7.43
O.26.92	3	20	-4.73	-6.85
H.31.186	4	1	-4.83	-5.58
H.31.186	4	2	-5.08	-6.61
H.31.186	4	3	-4.91	-6.54
H.31.186	4	4	-4.22	-6.35
H.31.186	4	5*	-3.39	-5.39
H.31.186	4	6*	-3.54	-6.07
H.31.186	4	7*	-3.77	-6.87
H.31.186	4	8*	-4.04	-7.03
H.31.186	4	9*	-4.47	-6.89
H.31.186	4	10*	-4.96	-7.31
H.31.186	4	11*	-5.08	-6.88
H.31.186	4	12*	-5.11	-6.94
H.31.186	4	13*	-5.14	-6.40
H.31.186	4	14*	-5.39	-6.49
H.31.186	4	15*	-4.95	-6.63
H.31.186	4	16*	-5.05	-6.73
H.31.186	4	17*	-4.78	-7.23
H.31.186	4	18*	-4.47	-7.39
H.31.186	4	19*	-4.77	-7.38
H.31.186	4	20	-4.46	-7.32

Table A4. Stable oxygen and carbon isotope measurements for each archaeological shell sample from Tell el-Hayyat, Jordan. *Indicates values from the annual band used in isotopic analyses.

Context	Phase	Sample #	$\delta^{18}O$ (‰)	$\delta^{13}C$ (‰)
Area.Locus.Bag		(from aperture)	Corrected	Corrected
Q.40.103	2	1	-3.70	-5.76
Q.40.103	2	2	-4.18	-5.15
Q.40.103	2	3	-4.24	-4.49
Q.40.103	2	4	-4.49	-4.56
Q.40.103	2	5	-4.92	-4.64
Q.40.103	2	6	-4.79	-4.58
Q.40.103	2	7	-4.61	-4.63
Q.40.103	2	8*	-4.96	-5.19
Q.40.103	2	9*	-5.09	-5.08

Q.40.103	2	10*	-5.37	-4.90
Q.40.103	2	11*	-5.35	-4.80
Q.40.103	2	12*	-5.19	-4.72
Q.40.103	2	13*	-5.16	-5.50
Q.40.103	2	14*	-5.37	-5.69
Q.40.103	2	15*	-5.24	-5.90
Q.40.103	2	16*	-5.14	-5.86
Q.40.103	2	17*	-5.22	-5.80
Q.40.103	2	18*	-5.45	-5.98
Q.40.103	2	19*	-5.22	-6.27
Q.40.103	2	20*	-4.88	-6.38
P.98.132	3	1	-5.42	-3.39
P.98.132	3	2	-5.69	-4.69
P.98.132	3	3	-5.70	-5.67
P.98.132	3	4	-5.38	-4.64
P.98.132	3	5	-5.40	-7.15
P.98.132	3	6	-5.15	-7.09
P.98.132	3	7*	-5.00	-5.51
P.98.132	3	8*	-5.59	-5.47
P.98.132	3	9*	-5.47	-5.34
P.98.132	3	10*	-5.83	-6.30
P.98.132	3	11*	-6.09	-6.27
P.98.132	3	12*	-5.89	-6.55
P.98.132	3	13*	-5.97	-7.04
P.98.132	3	14*	-5.97	-6.53
P.98.132	3	15*	-5.41	-6.04
P.98.132	3	16*	-5.34	-6.20
P.98.132	3	17	-4.34	-5.79
P.98.132	3	18	-4.71	-5.38
P.98.132	3	19	-5.20	-6.66
P.98.132	3	20	-5.87	-6.81
G.78.280	4	1	-4.20	-9.10
G.78.280	4	2	-4.25	-9.18
G.78.280	4	3	-3.65	-9.09
G.78.280	4	4	-4.09	-9.10
G.78.280	4	5	-4.09	-9.28
G.78.280	4	6	-4.01	-9.10
G.78.280	4	7*	-3.86	-9.05
G.78.280	4	8*	-4.22	-9.28
G.78.280	4	9*	-3.82	-9.21
G.78.280	4	10*	-3.30	-9.07
G.78.280	4	11*	-3.84	-9.15

G.78.280	4	12*	-3.77	-9.23
G.78.280	4	13*	-3.84	-9.21
G.78.280	4	14*	-3.62	-9.13
G.78.280	4	15*	-4.13	-9.27
G.78.280	4	16	-3.58	-9.20
G.78.280	4	17	-3.67	-9.14
G.78.280	4	18	-3.88	-9.18
G.78.280	4	19	-4.07	-9.22
G.78.280	4	20	-3.97	-9.03
J.79.315	5	1	-4.70	-6.41
J.79.315	5	2	-2.72	-5.46
J.79.315	5	3*	-4.28	-4.91
J.79.315	5	4*	-4.75	-5.67
J.79.315	5	5*	-5.45	-5.63
J.79.315	5	6*	-4.79	-5.18
J.79.315	5	7*	-4.88	-5.19
J.79.315	5	8*	-5.38	-5.56
J.79.315	5	9*	-5.43	-5.30
J.79.315	5	10*	-5.18	-5.66
J.79.315	5	11*	-5.06	-5.71
J.79.315	5	12*	-4.85	-5.76
J.79.315	5	13*	-4.81	-5.68
J.79.315	5	14*	-4.86	-5.88
J.79.315	5	15*	-4.98	-6.07
J.79.315	5	16*	-4.77	-6.50
J.79.315	5	17*	-4.68	-6.05
J.79.315	5	18*	-4.60	-5.58
J.79.315	5	19*	-4.40	-5.28
J.79.315	5	20*	-3.95	-5.34

APPENDIX H: SURFACE AND GROUND WATER STABLE ISOTOPES USED IN SOUTHERN LEVANTINE REGIONAL COMPARISON

Table A5. Stream, spring/groundwater, and archaeological shell $\delta^{18}O$ values used in Figure 8.14. Archaeological shell values represent mean values from all shells at Tell Abu en-Ni'aj and Tell el-Hayyat, Jordan (Tables A3 and A4).

Date	Season	Sample ID	$\delta^{18}O$	Long	Lat	Source	Type
2018	Summer	JO W1	-6.29	35.8952	32.2822	Fall and Ridder unpublished	Ground
2018	Summer	JO W5	-4.07	35.6160	31.6091	Fall and Ridder unpublished	Ground
2000	Summer	21	-3.30	35.5241	32.5052	Farber et al., 2004	Ground
2000	Summer	53	-5.00	35.5182	31.8379	Farber et al., 2004	Ground
2005	Fall	JO-Amman	-5.70	35.9333	31.9500	Waterisotopes Database 2017	Ground
2004	Wnt/Spr	JO-Amman	-3.15	35.9330	31.9500	Waterisotopes Database 2017	Ground
2004	Wnt/Spr	IL-Tel Aviv	-4.78	34.7670	32.0670	Waterisotopes Database 2017	Ground
2004	Wnt/Spr	IL-Jerusalem	1.71	35.2208	31.7742	Waterisotopes Database 2017	Ground
2004	Wnt/Spr	IL-Natanya	-4.67	34.9000	32.2900	Waterisotopes Database 2017	Ground
2004	Wnt/Spr	IL-Natanya	-4.44	34.9000	32.2900	Waterisotopes Database 2017	Ground
2004	Wnt/Spr	IL-Jerusalem	-5.32	35.2208	31.7742	Waterisotopes Database 2017	Ground
2004	Wnt/Spr	IL-Jerusalem	-5.29	35.2208	31.7742	Waterisotopes Database 2017	Ground
2004	Summer	IL-Jerusalem	-4.36	35.2208	31.7742	Waterisotopes Database 2017	Ground
2004	Summer	IL-Herzlia	-4.30	34.8367	32.1658	Waterisotopes Database 2017	Ground
2004	Summer	IL-Gan Yoshia	0.28	34.9931	32.3461	Waterisotopes Database 2017	Ground
2004	Summer	IL-Beit Arye	-0.61	35.0378	32.0336	Waterisotopes Database 2017	Ground
2004	Summer	IL-Tel Aviv	-2.48	34.7670	32.0670	Waterisotopes Database 2017	Ground
2005	Wnt/Spr	JO-Amman	-5.92	35.9333	31.9500	Waterisotopes Database 2017	Ground
2008	Wnt/Spr	unnamed	-1.34	34.8011	30.6094	Waterisotopes Database 2017	Ground
2011	Summer	unnamed	-6.18	35.7278	31.5036	Waterisotopes Database 2017	Ground

2011	Summer	unnamed	-5.50	35.8975	31.9683	Waterisotopes Database 2017	Ground
2023	Spring	JW10	-2.68	35.6142	32.4491	Fall and Ridder unpublished	Ground
2023	Spring	JW11	-6.01	35.6142	32.4491	Fall and Ridder unpublished	Ground
2023	Spring	JW13	-3.87	35.6121	31.6084	Fall and Ridder unpublished	Ground
2023	Spring	JW16	-6.52	35.5567	31.2614	Fall and Ridder unpublished	Ground
2023	Spring	JW20	-6.56	35.5297	30.3949	Fall and Ridder unpublished	Ground
2023	Spring	JW21	-5.69	35.5618	30.5298	Fall and Ridder unpublished	Ground
2023	Spring	JW23	-6.40	35.8953	32.2820	Fall and Ridder unpublished	Ground
2023	Spring	JW24	-6.39	35.8953	32.2820	Fall and Ridder unpublished	Ground
2023	Spring	JW25	-6.37	35.7074	32.6051	Fall and Ridder unpublished	Ground
2023	Spring	JW29	-5.63	35.7781	31.8220	Fall and Ridder unpublished	Ground
2023	Spring	JW34	-6.38	35.7681	32.3341	Fall and Ridder unpublished	Ground
2023	Spring	JW37	-5.24	35.6132	32.3471	Fall and Ridder unpublished	Ground
2018	Summer	JO W2	-6.60	35.8397	32.3174	Fall and Ridder unpublished	Stream
2018	Summer	JO W3	-5.53	35.7395	31.7762	Fall and Ridder unpublished	Stream
2018	Summer	JO W4	-5.43	35.7979	31.8373	Fall and Ridder unpublished	Stream
2018	Summer	JO W6	-6.00	35.5803	31.2416	Fall and Ridder unpublished	Stream
2018	Summer	JO W7	-5.94	35.6142	32.4490	Fall and Ridder unpublished	Stream
2018	Summer	JO W8	-5.91	35.6138	32.4488	Fall and Ridder unpublished	Stream
2001	Wnt/Spr	3	4.60	35.5091	32.7201	Farber et al., 2004	Stream
2000	Summer	8	-4.20	35.5676	32.6545	Farber et al., 2004	Stream
2000	Summer	12	-3.60	35.5611	32.6286	Farber et al., 2004	Stream
2000	Summer	13	-2.70	35.5751	32.5968	Farber et al., 2004	Stream
2000	Summer	15	-3.30	35.5760	32.5881	Farber et al., 2004	Stream
2000	Summer	18	-1.40	35.5588	32.5239	Farber et al., 2004	Stream
2000	Summer	19	0.40	35.5485	32.5293	Farber et al., 2004	Stream
2000	Summer	20	-3.00	35.5108	32.5301	Farber et al., 2004	Stream

2000	Summer	22	-2.90	35.5485	32.5062	Farber et al., 2004	Stream
2000	Summer	23	-4.60	35.5225	32.4819	Farber et al., 2004	Stream
2000	Summer	24	-3.80	35.5423	32.4651	Farber et al., 2004	Stream
1999	Fall	27	-4.10	35.5356	32.3604	Farber et al., 2004	Stream
2000	Summer	28	-3.30	35.5542	32.3267	Farber et al., 2004	Stream
2000	Summer	36	-2.20	35.5459	32.1403	Farber et al., 2004	Stream
2000	Summer	38	-3.20	35.5353	32.1075	Farber et al., 2004	Stream
2000	Summer	39	-4.30	35.5208	32.0815	Farber et al., 2004	Stream
2000	Fall	44	-1.70	35.5286	32.0546	Farber et al., 2004	Stream
2000	Summer	46	-3.00	35.5078	32.0284	Farber et al., 2004	Stream
2000	Summer	47	-2.80	35.5252	32.0225	Farber et al., 2004	Stream
2000	Summer	48	4.70	35.5048	31.9329	Farber et al., 2004	Stream
1999	Wnt/Spr	54	-2.90	35.5453	31.8013	Farber et al., 2004	Stream
2009	Wnt/Spr	unnamed	-6.96	35.6528	33.2381	Waterisotopes Database 2017	Ground
2009	Wnt/Spr	unnamed	-5.04	35.3833	31.4500	Waterisotopes Database 2017	Stream
2023	Spring	JW9	-5.26	35.6395	32.1927	Fall and Ridder unpublished	Stream
2023	Spring	JW12	-5.36	35.7704	31.5561	Fall and Ridder unpublished	Stream
2023	Spring	JW14	-4.50	35.5686	31.6020	Fall and Ridder unpublished	Stream
2023	Spring	JW15	-5.95	35.5731	31.4670	Fall and Ridder unpublished	Stream
2023	Spring	JW17	-5.68	35.5619	31.2594	Fall and Ridder unpublished	Stream
2023	Spring	JW18	-6.57	35.5799	31.2415	Fall and Ridder unpublished	Stream
2023	Spring	JW19	-6.19	35.4978	30.3242	Fall and Ridder unpublished	Stream
2023	Spring	JW22	-5.03	35.8840	32.2154	Fall and Ridder unpublished	Stream
2023	Spring	JW26	-5.21	35.6781	32.6833	Fall and Ridder unpublished	Stream
2023	Spring	JW27	-5.23	35.6800	32.7058	Fall and Ridder unpublished	Stream
2023	Spring	JW28	-5.70	35.7979	31.8373	Fall and Ridder unpublished	Stream
2023	Spring	JW30	-4.07	35.7395	31.7762	Fall and Ridder unpublished	Stream
2023	Spring	JW33	-6.48	35.8396	32.3173	Fall and Ridder unpublished	Stream
-	Wnt/Spr	Ni‘aj	-5.68	35.5683	32.4144	-	Shell
-	Wnt/Spr	Hayyat	-5.95	35.5790	32.4227	-	Shell

APPENDIX I: CARBONIZED SEED STABLE ISOTOPES FROM TELL ABU EN-NI‘AJ

Table A6. Stable isotope values of carbon and nitrogen for seed samples from Tell Abu en-Ni‘aj, Jordan. *Estimated from radiocarbon calibrated phase endpoints. **Value was a statistical outlier and omitted from analysis.

Context (Area.Locus.Bag)	Phase	AMS age (cal BCE)	Taxa	$\Delta^{13}C$ (‰)	$\delta^{15}N$ (‰)
GG.100.289	5	2437	*Ficus carica*	19.59	9.1
GG.105.331	7	2505.5	*Ficus carica*	20.21	8.31
GG.96.302	6	2471.5	*Ficus carica*	18.16	3.72
AA.17.193	2	2312*	*Hordeum vulgare*	16.16	5.79
AA.19.122	3	2353*	*Hordeum vulgare*	15.18	9.32
AA.19.176	3	2352*	*Hordeum vulgare*	16.68	2.79
AA.24.196	4	2394*	*Hordeum vulgare*	17.34	5.10
AA.34.237	4	2396.5*	*Hordeum vulgare*	16.69	3.88
AA.67.407	6	2471.5*	*Hordeum vulgare*	19.39	5.42
AA.69.413	7	2505.5*	*Hordeum vulgare*	19.01	4.97
AA.70.414	6	2471.5*	*Hordeum vulgare*	17.91	6.21
C.111.548	6	2410	*Hordeum vulgare*	16.70	7.74
C.24.60	2	2312*	*Hordeum vulgare*	17.25	5.75
C.27.96	2	2312.5*	*Hordeum vulgare*	17.00	12.51**
C.40.141	3	2352*	*Hordeum vulgare*	17.01	5.64
C.44.156	3	2352*	*Hordeum vulgare*	16.76	7.41
C.49.175	2	2312*	*Hordeum vulgare*	17.29	5.87
C.71.254	4	2396.5*	*Hordeum vulgare*	19.10	3.31
C.73.284	4	2349	*Hordeum vulgare*	16.22	9.88
C.75.279	5	2433.5*	*Hordeum vulgare*	15.72	6.55
C.86.367	6	2542	*Hordeum vulgare*	18.25	5.16
C.93.429	6	2467.5*	*Hordeum vulgare*	16.89	8.45
C.93.430	6	2467.5*	*Hordeum vulgare*	17.27	7.37
D.54.216	7	2500.5*	*Hordeum vulgare*	14.64	5.36
G.20.74	2	2312.5*	*Hordeum vulgare*	16.93	7.04
GG.100.289	5	2397	*Hordeum vulgare*	18.22	8.72
GG.11.36	2	2312*	*Hordeum vulgare*	18.97	7.50
GG.30.94	4	2394*	*Hordeum vulgare*	16.94	7.21
GG.39.123	5	2433.5*	*Hordeum vulgare*	16.07	11.02
GG.42.127	5	2433.5*	*Hordeum vulgare*	16.86	5.99
GG.69.191	5	2433.5*	*Hordeum vulgare*	18.36	5.01
GG.70.195	5	2433.5*	*Hordeum vulgare*	16.78	6.49
GG.72.213	6	2467.5*	*Hordeum vulgare*	17.16	8.53
GG.89.269	7	2500.5*	*Hordeum vulgare*	16.21	4.92
GG.96.302	6	2467.5*	*Hordeum vulgare*	16.90	4.63
GG.99.298	6	2467.5*	*Hordeum vulgare*	15.42	8.45

H.18.61	2	2312.5*	*Hordeum vulgare*	17.51	10.20
H.22.105	2	2312.5*	*Hordeum vulgare*	18.59	6.50
I.39.146	3	2353*	*Hordeum vulgare*	18.10	7.67
II.17.84	3	2353*	*Hordeum vulgare*	16.12	5.76
K.102.346	7	2500.5*	*Hordeum vulgare*	18.32	6.67
K.105.356	7	2500.5*	*Hordeum vulgare*	17.93	2.60
K.105.363	7	2500.5*	*Hordeum vulgare*	20.08	8.63
K.18.30	3	2416	*Hordeum vulgare*	17.49	-
K.35.85	3	2352*	*Hordeum vulgare*	19.37	6.74
K.37.113	3	2352*	*Hordeum vulgare*	18.45	5.21
K.38.142	3	2352*	*Hordeum vulgare*	18.60	5.86
K.55.192	4	2394*	*Hordeum vulgare*	17.64	3.17
K.56.201	4	2396.5*	*Hordeum vulgare*	16.89	7.00
K.76.261	5	2433.5*	*Hordeum vulgare*	17.54	8.46
K.76.261	5	2437*	*Hordeum vulgare*	18.36	11.96**
K.89.303	6	2471.5*	*Hordeum vulgare*	16.94	5.28
K.91.310	7	2505.5*	*Hordeum vulgare*	19.12	5.48
K.91.313	7	2500.5*	*Hordeum vulgare*	16.46	6.61
K.99.338	7	2500.5*	*Hordeum vulgare*	17.05	9.45
L.20.74	2	2312.5*	*Hordeum vulgare*	16.98	5.22
L.21.84	2	2312.5*	*Hordeum vulgare*	17.45	4.05
M.42.187	4	2396.5*	*Hordeum vulgare*	17.04	5.76
M.44.203	4	2394*	*Hordeum vulgare*	18.41	6.82
N.41.142	3	2353*	*Hordeum vulgare*	18.93	5.67
N.8.8	2	2312.5*	*Hordeum vulgare*	16.75	6.82
Z.26.115	4	2396.5*	*Hordeum vulgare*	14.81	10.48
Z.26.115	4	2396.5*	*Hordeum vulgare*	17.10	-
AA.70.414	6	2471.5*	*Hordeum vulgare* var. *nudum*	18.54	7.41
C.106.494	6	2684	*Hordeum vulgare* var. *nudum*	18.01	5.06
C.65.225-227	3	2353*	*Hordeum vulgare* var. *nudum*	18.31	5.63
C.71.256	4	2396.5*	*Hordeum vulgare* var. *nudum*	17.68	6.57
C.75.279	5	2437*	*Hordeum vulgare* var. *nudum*	17.88	6.35
C.93.429	6	2471.5*	*Hordeum vulgare* var. *nudum*	18.83	2.75
G.20.74	2	2312.5*	*Hordeum vulgare* var. *nudum*	15.38**	7.52
GG.39.123	5	2437*	*Hordeum vulgare* var. *nudum*	18.60	3.69
GG.89.269	7	2505.5*	*Hordeum vulgare* var. *nudum*	18.40	5.50
II.17.84	3	2353*	*Hordeum vulgare* var. *nudum*	19.42	-
K.105.363	7	2505.5*	*Hordeum vulgare* var. *nudum*	18.91	11.04**
K.94.323	7	2505.5*	*Hordeum vulgare* var. *nudum*	18.43	5.76
L.20.74	2	2312.5*	*Hordeum vulgare* var. *nudum*	18.00	6.07
N.8.8	2	2312.5*	*Hordeum vulgare* var. *nudum*	15.45**	8.43
GG.100.289	5	2397	*Lathyrus sativus*	16.54	2.80
AA.12.181	3	2352*	*Lens culinaris*	17.20	3.84

AA.70.414	6	2467.5*	*Lens culinaris*	17.72	4.69
C.24.60	2	2312*	*Lens culinaris*	18.50	4.46
C.37.126	2	2250	*Lens culinaris*	16.64	1.82
C.71.256	4	2394*	*Lens culinaris*	17.56	0.03
GG.96.302	6	2467.5*	*Lens culinaris*	17.43	-1.03
K.105.363	7	2505.5*	*Lens culinaris*	18.87	1.96
K.89.303	6	2467.5*	*Lens culinaris*	19.82	3.21
L.20.74	2	2312.5*	*Lens culinaris*	14.71	-
N.8.8	2	2312.5*	*Lens culinaris*	15.21	-
N.8.8	2	2312.5*	*Lens culinaris*	15.91	2.78
C.65.225-227	3	2352*	*Olea europaea*	15.61	5.51
C.65.225-227	3	2353*	*Olea europaea*	16.31	6.03
C.71.254	4	2394*	*Olea europaea*	15.06	3.21
GG.96.302	6	2467.5*	*Olea europaea*	16.80	3.28
AA.16.113	3	2352*	*Pisum sativum*	17.08	2.63
AA.24.196	4	2396.5*	*Pisum sativum*	19.69	1.77
AA.70.414	6	2471.5*	*Pisum sativum*	21.03	5.24
C.111.548	6	2410	*Pisum sativum*	19.27	-
C.26.77	2	2312.5*	*Pisum sativum*	19.24	2.09
C.65.225-227	3	2353*	*Pisum sativum*	19.06	1.33
C.71.236	4	2378	*Pisum sativum*	19.08	-
GG.70.195	5	2437*	*Pisum sativum*	17.65	-
GG.89.269	7	2500.5*	*Pisum sativum*	15.33	1.70
H.22.105	2	2312*	*Pisum sativum*	16.76	9.43
D.16.51	1	2241	*Prosopis farcta*	-	6.04
G.21.75	2	2312*	*Prosopis farcta*	16.62	8.65
GG.100.289	5	2397	*Prosopis farcta*	17.59	-
GG.15.49	3	2280	*Prosopis farcta*	18.53	-
GG.98.295	6	2425	*Prosopis farcta*	17.47	5.87
H.42.181	4	2394*	*Prosopis farcta*	18.36	-0.21
II.13.70	3	2353*	*Prosopis farcta*	14.97	-
II.13.70	3	2353*	*Prosopis farcta*	16.90	1.90
K.94.323	7	2500.5*	*Prosopis farcta*	18.48	4.13
L.11.43	2	2312.5*	*Prosopis farcta*	17.24	-
L.11.43	2	2312.5*	*Prosopis farcta*	17.94	3.66
G.21.75	2	2312.5*	*Triticum aestivum*	18.42	5.96
GG.89.269	7	2500.5*	*Triticum aestivum*	16.62	6.30
K.89.303	6	2471.5*	*Triticum aestivum*	18.68	6.35
AA.16.113	3	2352*	*Triticum dicoccum*	16.67	-
AA.16.153	3	2352*	*Triticum dicoccum*	15.10	-
AA.19.122	3	2352*	*Triticum dicoccum*	14.05**	8.28
AA.64.390	6	2467.5*	*Triticum dicoccum*	17.16	-
AA.67.407	6	2467.5*	*Triticum dicoccum*	16.03	6.63

AA.69.413	7	2500.5*	*Triticum dicoccum*	17.75	-
AA.70.414	6	2467.5*	*Triticum dicoccum*	14.79	11.18
C.106.494	6	2684	*Triticum dicoccum*	15.67	5.06
C.107.501	7	2500.5*	*Triticum dicoccum*	17.18	5.68
C.111.548	6	2410	*Triticum dicoccum*	17.50	-
C.24.60	2	2312*	*Triticum dicoccum*	17.65	-
C.49.175	2	2312.5*	*Triticum dicoccum*	16.48	6.18
C.71.236	4	2378	*Triticum dicoccum*	36.75**	2.40
C.71.254	4	2394*	*Triticum dicoccum*	17.68	-
C.71.256	4	2394*	*Triticum dicoccum*	17.94	-
C.75.279	5	2394*	*Triticum dicoccum*	17.62	-
C.82.353	5	2433.5*	*Triticum dicoccum*	16.93	4.25
C.93.429	6	2467.5*	*Triticum dicoccum*	15.95	5.21
D.54.216	7	2505.5*	*Triticum dicoccum*	17.19	3.86
G.20.70	2	2312*	*Triticum dicoccum*	17.17	8.54
G.20.74	2	2312*	*Triticum dicoccum*	17.06	7.25
G.21.75	2	2312*	*Triticum dicoccum*	16.79	7.69
GG.11.36	2	2312*	*Triticum dicoccum*	13.17**	6.21
GG.30.94	4	2394*	*Triticum dicoccum*	16.91	7.20
GG.30.95	4	2394*	*Triticum dicoccum*	18.57	-
GG.39.123	5	2433.5*	*Triticum dicoccum*	16.98	-
GG.42.127	5	2433.5*	*Triticum dicoccum*	15.60	6.40
GG.69.191	5	2433.5*	*Triticum dicoccum*	16.70	4.92
GG.70.195	5	2433.5*	*Triticum dicoccum*	20.17**	7.81
GG.89.269	7	2500.5*	*Triticum dicoccum*	15.28	-
GG.96.302	6	2471.5*	*Triticum dicoccum*	17.82	6.00
GG.99.298	6	2467.5*	*Triticum dicoccum*	17.13	8.21
H.18.61	2	2312*	*Triticum dicoccum*	17.51	7.93
H.22.105	2	2312*	*Triticum dicoccum*	16.49	9.29
H.40.163	4	2396.5*	*Triticum dicoccum*	16.12	9.25
H.42.181	4	2394*	*Triticum dicoccum*	16.57	6.18
I.33.115	3	2353*	*Triticum dicoccum*	17.54	11.60
I.39.146	3	2353*	*Triticum dicoccum*	17.78	6.09
II.13.70	3	2353*	*Triticum dicoccum*	16.58	6.52
II.17.84	3	2353*	*Triticum dicoccum*	17.72	5.56
K.105.356	7	2500.5*	*Triticum dicoccum*	17.10	4.01
K.105.363	7	2500.5*	*Triticum dicoccum*	18.39	10.05
K.35.85	3	2352*	*Triticum dicoccum*	17.50	8.08
K.37.113	3	2352*	*Triticum dicoccum*	18.32	6.89
K.55.192	4	2396.5*	*Triticum dicoccum*	17.92	6.38
K.76.261	5	2433.5*	*Triticum dicoccum*	18.33	8.68
K.85.277	6	2471.5*	*Triticum dicoccum*	17.23	6.32
K.89.303	6	2467.5*	*Triticum dicoccum*	14.75	7.85

K.91.310	7	2500.5*	*Triticum dicoccum*	17.22	6.23
K.91.313	7	2500.5*	*Triticum dicoccum*	16.17	5.58
K.94.323	7	2500.5*	*Triticum dicoccum*	18.00	7.71
M.36.164	4	2394*	*Triticum dicoccum*	18.22	6.38
M.42.187	4	2394*	*Triticum dicoccum*	17.41	5.62
N.41.142	3	2353*	*Triticum dicoccum*	18.32	5.61
N.8.8	2	2312.5*	*Triticum dicoccum*	18.32	5.77
AA.16.113	3	2353*	*Triticum monococcum*	17.15	-
C.107.501	7	2505.5*	*Triticum monococcum*	15.23	7.17
C.71.256	4	2396.5*	*Triticum monococcum*	17.57	-
C.71.256	4	2396.5*	*Triticum monococcum*	19.34	5.87
C.93.429	6	2471.5*	*Triticum monococcum*	17.52	-
G.20.74	2	2312.5*	*Triticum monococcum*	17.32	-
GG.69.191	5	2433.5*	*Triticum monococcum*	16.51	5.75
GG.70.196	5	2433.5*	*Triticum monococcum*	15.95	8.40
GG.89.269	7	2500.5*	*Triticum monococcum*	14.98	6.85
I.39.146	3	2353*	*Triticum monococcum*	17.83	4.29
L.21.95	2	2312.5*	*Triticum monococcum*	19.63	7.31
C.89.386	5	2395	*Vitis vinifera*	17.35**	2.47
C.93.429	6	2471.5*	*Vitis vinifera*	22.27	-
G.20.74	2	2312.5*	*Vitis vinifera*	21.39	-
GG.30.94	4	2396.5*	*Vitis vinifera*	20.12	-
I.33.115	3	2353*	*Vitis vinifera*	22.87	10.93
K.37.113	3	2352*	*Vitis vinifera*	21.02	10.14
K.37.113	3	2353*	*Vitis vinifera*	21.66	-

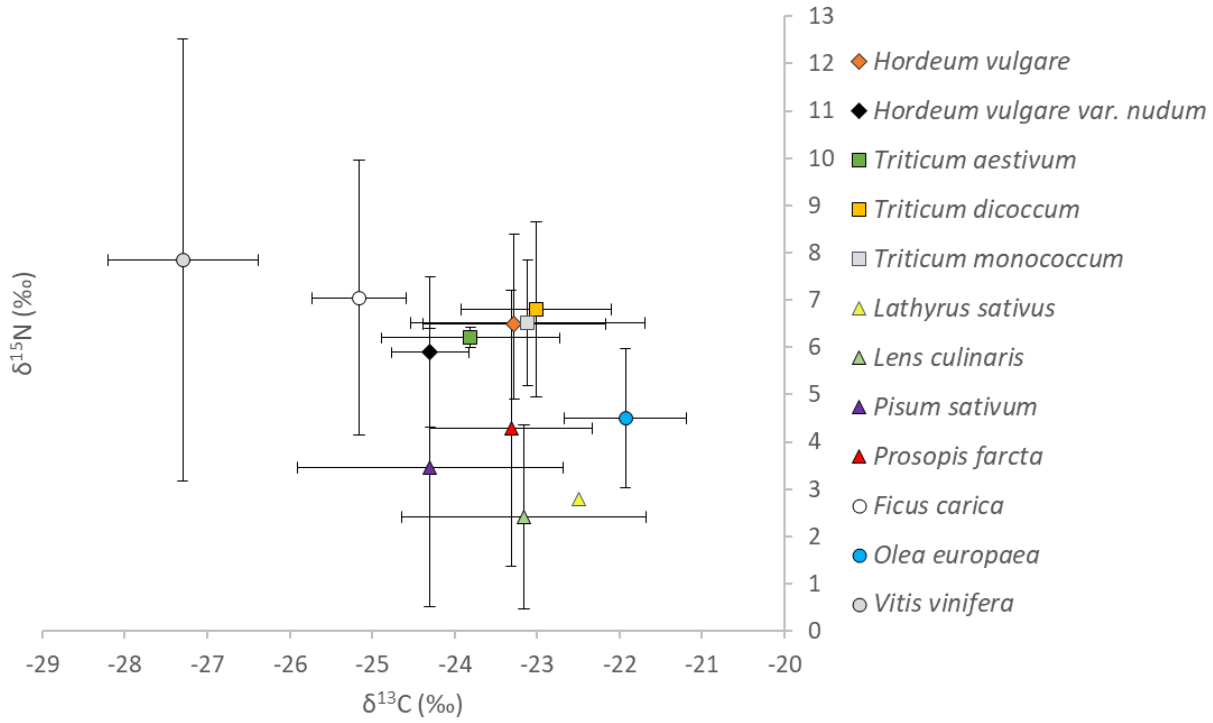

Figure A16. Plot of $\delta^{13}C$ versus $\delta^{15}N$ for carbonized seeds of common cultigens at Tell Abu en-Ni‘aj, Jordan..

APPENDIX J: CARBONIZED SEED STABLE ISOTOPES FROM TELL EL-HAYYAT

Table A7. Stable isotope values of carbon and nitrogen for seed samples from Tell el-Hayyat, Jordan. *Estimated from radiocarbon calibrated phase endpoints. **Value was a statistical outlier and omitted from analysis.

Context (Area.Locus.Bag)	Phase	AMS age (cal BCE)	Taxa	$\Delta^{13}C$ (‰)	$\delta^{15}N$ (‰)
A.26.13	2	1745	*Ficus carica*	18.59	8.36
D.60.293	5	1860.5	*Ficus carica*	18.80	3.61
P.118.182	3	1788.5	*Ficus carica*	18.46	10.64
Q.44.142	3	1788.5	*Ficus carica*	18.21	9.37
S.47.123	3	1788.5	*Ficus carica*	18.85	5.99
S.79.318	5	1860.5	*Ficus carica*	20.09	9.12
T.72.312	5	1860.5	*Ficus carica*	18.74	7.88
A.26.13	2	1745*	*Hordeum vulgare*	16.56	7.30
A.42.16	4	1816*	*Hordeum vulgare*	18.21	7.74
A.43.19	4	1816*	*Hordeum vulgare*	17.88	5.39
A.50.223	5	1860.5*	*Hordeum vulgare*	17.02	4.93
A.83.117	3	1788.5*	*Hordeum vulgare*	17.96	4.33
A.86.127	3	1788.5*	*Hordeum vulgare*	17.10	4.46
A.88.166	4	1816*	*Hordeum vulgare*	17.17	6.15
C.72.2	5	1860.5*	*Hordeum vulgare*	18.54	8.24
D.42.12	4	1816*	*Hordeum vulgare*	16.87	9.91
D.56.265	5	1788.5*	*Hordeum vulgare*	16.76	5.58
E.92.457	4	1816*	*Hordeum vulgare*	18.72	3.66
F.30.139	4	1816*	*Hordeum vulgare*	15.16	2.79
F.46.264	5	1860.5*	*Hordeum vulgare*	15.34	4.62
F.48.307	5	1860.5*	*Hordeum vulgare*	17.19	5.92
H.31.144	2	1745*	*Hordeum vulgare*	16.64	7.19
I.57.217	3	1788.5*	*Hordeum vulgare*	18.46	6.83
J.74.281	4	1816*	*Hordeum vulgare*	18.44	5.56
J.81.322	5	1860.5*	*Hordeum vulgare*	16.00	5.66
K.28.119	2	1745*	*Hordeum vulgare*	18.26	8.52
K.44.155	3	1788.5*	*Hordeum vulgare*	18.57	6.62
K.64.262	4	1816*	*Hordeum vulgare*	16.07	5.95
K.66.272	5	1860.5*	*Hordeum vulgare*	17.82	6.03
L.12.35	2	1745*	*Hordeum vulgare*	15.63	5.77
L.19.56	2	1745*	*Hordeum vulgare*	14.51	6.52
M.66.228	4	1816*	*Hordeum vulgare*	16.31	5.91
M.67.252	5	1860.5*	*Hordeum vulgare*	19.20	9.87
P.107.155	3	1788.5*	*Hordeum vulgare*	17.47	4.92
P.107.155	3	1788.5*	*Hordeum vulgare*	17.48	5.25
P.111.169	3	1788.5*	*Hordeum vulgare*	17.46	7.84

P.141.273	4	1816*	*Hordeum vulgare*	16.25	4.33
P.184.414	5	1860.5*	*Hordeum vulgare*	17.20	3.23
Q.42.141	3	1788.5*	*Hordeum vulgare*	18.45	14.36**
Q.47.163	3	1788.5*	*Hordeum vulgare*	16.35	5.84
S.61.208	3	1788.5*	*Hordeum vulgare*	18.41	5.24
S.79.318	5	1860.5*	*Hordeum vulgare*	15.77	7.49
T.14.12-13	2	1745*	*Hordeum vulgare*	18.58	6.24
T.46.207	4	1816*	*Hordeum vulgare*	17.32	8.36
T.72.312	5	1860.5*	*Hordeum vulgare*	18.35	4.05
U.19.66-69	2	1745*	*Hordeum vulgare*	17.25	-
A.26.13	2	1745	*Hordeum vulgare hexastichum*	18.33	5.39
C.72.2	5	1860.5	*Hordeum vulgare hexastichum*	15.83	5.43
H.67.392	5	1860.5	*Hordeum vulgare hexastichum*	17.48	6.19
J.81.322	5	1860.5	*Hordeum vulgare hexastichum*	16.74	4.62
K.64.262	4	1816	*Hordeum vulgare hexastichum*	17.10	5.6
T.46.207	4	1816	*Hordeum vulgare hexastichum*	18.51	10.69
T.75.327	5	1860.5	*Hordeum vulgare hexastichum*	17.60	7.63
A.36.14	3	1788.5*	*Hordeum vulgare* var. *nudum*	15.89	3.16
A.47.211	4	1816*	*Hordeum vulgare* var. *nudum*	17.90	7.30
A.83.117	3	1788.5*	*Hordeum vulgare* var. *nudum*	18.57	5.39
A.86.127	3	1788.5*	*Hordeum vulgare* var. *nudum*	17.45	6.05
A.90.259	4	1816*	*Hordeum vulgare* var. *nudum*	17.38	6.27
D.56.265	5	1860.5*	*Hordeum vulgare* var. *nudum*	16.62	8.53
D.65.311	5	1816*	*Hordeum vulgare* var. *nudum*	15.35	6.76
I.57.217	3	1788.5*	*Hordeum vulgare* var. *nudum*	17.94	8.95
K.64.262	4	1816*	*Hordeum vulgare* var. *nudum*	19.45	5.66
L.6.79	1	1685.5*	*Hordeum vulgare* var. *nudum*	15.55	7.80
P.195.397	5	1860.5*	*Hordeum vulgare* var. *nudum*	17.75	3.32
A.42.16	4	1816	*Lathyrus sativus*	15.94	4.12
A.47.21	4	1816	*Lathyrus sativus*	15.11	2.59
C.78.3	5	1860.5	*Lathyrus sativus*	17.29	2.92
H.67.392	5	1860.5	*Lathyrus sativus*	15.87	3.65
J.43.142	2	1745	*Lathyrus sativus*	17.11	1.63
J.74.281	4	1816	*Lathyrus sativus*	17.23	2.23
J.81.322	5	1860.5	*Lathyrus sativus*	15.46	6.26
L.19.56	2	1745*	*Lathyrus sativus*	14.90	2.98
T.40.162	3	1788.5*	*Lathyrus sativus*	15.45	5.73
T.64.279	5	1860.5	*Lathyrus sativus*	16.71	2.23
T.67.292	5	1860.5	*Lathyrus sativus*	16.87	2.33
T.72.312	5	1860.5*	*Lathyrus sativus*	15.18	2.63
T.72.312	5	1860.5	*Lathyrus sativus*	16.42	2.27
T.75.327	5	1860.5	*Lathyrus sativus*	15.69	3.77
A.26.13	2	1745*	*Lens culinaris*	16.11	2.02

C.70.1	4	1960	*Lens culinaris*	17.24	-
D.33.8	3	1835	*Lens culinaris*	17.41	4.11
F.49.288	5	1775	*Lens culinaris*	24.65**	-
I.29.89	2	1745*	*Lens culinaris*	16.71	3.56
I.50.200	3	1874	*Lens culinaris*	14.90	1.73
J.71.256	6	1904*	*Lens culinaris*	19.41	2.61
M.66.228	4	1816*	*Lens culinaris*	17.64	3.95
M.67.252	5	1860.5*	*Lens culinaris*	16.30	2.34
N.30.178	5	1860.5*	*Lens culinaris*	17.51	3.53
P.118.182	3	1788.5*	*Lens culinaris*	15.57	3.86
P.192.407	5	1860.5*	*Lens culinaris*	17.85	1.09
Q.67.265(2)	4	1816*	*Lens culinaris*	16.24	1.86
S.47.123	3	1824	*Lens culinaris*	16.34	4.10
S.65.235	4	1816*	*Lens culinaris*	18.35	1.70
T.51.217	4	1816*	*Lens culinaris*	15.44	5.15
T.72.312	5	1860.5*	*Lens culinaris*	17.15	3.40
T.75.327	5	1860.5*	*Lens culinaris*	14.77	3.10
A.26.13	2	1745*	*Olea europaea*	19.99	13.39
A.36.14	3	1788.5*	*Olea europaea*	16.68	-
A.42.16	4	1816*	*Olea europaea*	19.97	9.84
C.22.9	3	1804	*Olea europaea*	16.88	-
E.92	4	1821	*Olea europaea*	15.34	-
E.92	4	1816	*Olea europaea*	17.52	-
F.40.235	4	1565	*Olea europaea*	20.19	-
G.25.60-64	2	1811	*Olea europaea*	19.90	8.88
J.74	4	1838	*Olea europaea*	15.34	-
J.74	4	1819	*Olea europaea*	18.15	-
S.61.208	3	1788.5*	*Olea europaea*	16.06	-
S.65.235	4	1816*	*Olea europaea*	19.20	6.10
T.30.100	3	1824	*Olea europaea*	14.97	8.68
T.40.162	3	1788.5*	*Olea europaea*	16.94	-
T.40.162	3	1788.5*	*Olea europaea*	18.26	11.58
T.49.213	4	1816*	*Olea europaea*	17.59	10.72
T.59.253	4	1816*	*Olea europaea*	17.12	9.96
T.59.253	4	1816*	*Olea europaea*	18.18	-
T.65.304	5	1860.5*	*Olea europaea*	16.57	7.05
T.65.304	5	1860.5*	*Olea europaea*	17.24	-
T.75.327	5	1860.5*	*Olea europaea*	16.71	-
T.75.327	5	1860.5*	*Olea europaea*	17.05	3.65
T.75.331	5	1860.5*	*Olea europaea*	17.34	6.68
A.36.14	3	1788.5*	*Pistacia terebinthus*	20.42	5.66
A.86.127	3	1788.5*	*Pistacia terebinthus*	17.70	4.45
R.50.154	3	1788.5*	*Pistacia terebinthus*	20.06	5.83

A.47.21	4	1816*	*Pisum sativum*	16.41	3.71
D.65.311	5	1860.5*	*Pisum sativum*	16.09	3.21
G.25.60-64	2	1811	*Pisum sativum*	17.98	3.61
G.45.152	2	1745*	*Pisum sativum*	17.82	2.26
I.29.89	2	1745*	*Pisum sativum*	17.03	2.67
I.57.217	3	1788.5*	*Pisum sativum*	17.03	2.75
Q.74.288	5	1860.5*	*Pisum sativum*	18.54	5.71
S.65.235	4	1816*	*Pisum sativum*	17.18	2.87
T.33.111	3	1788.5*	*Pisum sativum*	16.59	1.71
T.64.279	5	1860.5*	*Pisum sativum*	17.52	2.49
T.72.312	5	1860.5*	*Pisum sativum*	14.29	3.84
T.75.331	5	1860.5*	*Pisum sativum*	15.68	2.45
A.36.14	3	1788.5*	*Prosopis farcta*	16.93	-
A.42.16	4	1816*	*Prosopis farcta*	17.71	4.96
A.47.21	4	1816*	*Prosopis farcta*	14.96	7.66
A.47.21	4	1816*	*Prosopis farcta*	17.18	8.96
A.47.211	4	1816*	*Prosopis farcta*	18.19	2.53
A.83.117	3	1788.5*	*Prosopis farcta*	17.14	4.56
C.70.1	4	1960	*Prosopis farcta*	18.30	2.32
C.70.1	4	1960	*Prosopis farcta*	18.70	-
I.57.217	3	1788.5*	*Prosopis farcta*	17.14	4.99
J.74.281	4	1816*	*Prosopis farcta*	18.00	3.16
M.67.252	5	1860.5*	*Prosopis farcta*	17.96	5.87
N.30.178	5	1860.5*	*Prosopis farcta*	16.42	5.95
N.30.178	5	1860.5*	*Prosopis farcta*	17.55	-
P.135.258	4	1816*	*Prosopis farcta*	31.71**	6.47
R.50.154	3	1788.5*	*Prosopis farcta*	16.31	-
R.50.154	3	1788.5*	*Prosopis farcta*	17.01	6.78
S.24.51	2	1709	*Prosopis farcta*	15.95	2.64
T.64.279	5	1860.5*	*Prosopis farcta*	17.32	3.20
A.26.13	2	1814	*Triticum aestivum*	17.53	2.67
A.36.14	3	1788.5*	*Triticum aestivum*	16.75	5.61
A.39.15	3	1788.5*	*Triticum aestivum*	16.02	7.65
A.47.211	4	1816*	*Triticum aestivum*	16.14	4.25
A.86.127	3	1788.5*	*Triticum aestivum*	16.19	6.35
C.72.2	5	1860.5*	*Triticum aestivum*	18.16	8.58
D.65.311	5	1860.5*	*Triticum aestivum*	16.70	6.62
E.102	5	1900	*Triticum aestivum*	15.14	-
E.102	5	1797	*Triticum aestivum*	16.48	-
G.45.152	2	1777	*Triticum aestivum*	18.65	6.50
H.67	5	1856	*Triticum aestivum*	15.97	-
H.67	5	1915	*Triticum aestivum*	16.60	-
H.67	5	1817	*Triticum aestivum*	17.00	-

I.29.89	2	1745*	*Triticum aestivum*	17.30	7.90
I.57.217	3	1788.5*	*Triticum aestivum*	16.55	5.32
K.44.155	3	1788.5*	*Triticum aestivum*	16.79	6.02
K.66.272	5	1860.5*	*Triticum aestivum*	17.12	11.77
P.107.155	3	1788.5*	*Triticum aestivum*	17.35	2.69
S.47.123	3	1824	*Triticum aestivum*	15.21	6.11
S.61.208	3	1788.5*	*Triticum aestivum*	26.98**	8.84
S.65.235	4	1816*	*Triticum aestivum*	16.71	3.36
S.79.318	5	1860.5*	*Triticum aestivum*	18.24	3.18
T.14.12-13	2	1745*	*Triticum aestivum*	15.73	7.79
T.33.111	3	1788.5*	*Triticum aestivum*	14.78	4.95
T.33.111	3	1826	*Triticum aestivum*	15.47	5.37
T.57.238	4	1816*	*Triticum aestivum*	18.86	6.23
T.64.279	5	1860.5*	*Triticum aestivum*	16.28	5.22
T.72.312	5	1860.5*	*Triticum aestivum*	17.30	6.48
T.75.327	5	1860.5*	*Triticum aestivum*	16.48	6.20
A.36.14	3	1788.5*	*Triticum dicoccum*	16.50	5.38
A.42.16	4	1816*	*Triticum dicoccum*	15.06	6.56
A.47.21	4	1816*	*Triticum dicoccum*	16.06	6.63
A.47.211	4	1816*	*Triticum dicoccum*	17.02	4.45
A.50.223	5	1860.5*	*Triticum dicoccum*	16.90	5.24
A.83.117	3	1788.5*	*Triticum dicoccum*	17.44	5.02
A.86.127	3	1788.5*	*Triticum dicoccum*	17.99	5.43
A.90.259	4	1816*	*Triticum dicoccum*	16.60	4.73
C.70.1	4	1960	*Triticum dicoccum*	18.47	7.28
D.33.8	3	1835	*Triticum dicoccum*	17.59	8.62
D.56.265	5	1788.5*	*Triticum dicoccum*	15.65	7.76
F.48.307	5	1860.5*	*Triticum dicoccum*	15.36	3.21
G.25.60-64	2	1811	*Triticum dicoccum*	15.27	4.24
G.45.152	2	1745*	*Triticum dicoccum*	16.77	7.21
H.37.104	2	1745*	*Triticum dicoccum*	17.04	7.53
I.57.217	3	1788.5*	*Triticum dicoccum*	16.54	5.00
J.71.256	6	1904*	*Triticum dicoccum*	-	9.46
J.74.281	4	1816*	*Triticum dicoccum*	19.22	6.35
J.81.322	5	1860.5*	*Triticum dicoccum*	15.62	8.79
K.28.119	2	1745*	*Triticum dicoccum*	15.29	11.76
K.44.164	3	1788.5*	*Triticum dicoccum*	18.31	6.75
K.56.212	4	1816*	*Triticum dicoccum*	16.94	9.43
K.66.272	5	1860.5*	*Triticum dicoccum*	15.48	9.54
L.12.35	2	1745*	*Triticum dicoccum*	14.22	6.25
L.19.56	2	1745*	*Triticum dicoccum*	17.99	7.00
L.6.79	1	1685.5*	*Triticum dicoccum*	-	8.07
M.52.164+167	4	1816*	*Triticum dicoccum*	14.80	7.47

N.9.27	2	1745*	*Triticum dicoccum*	18.32	7.64
P.107.155	3	1788.5*	*Triticum dicoccum*	17.03	4.84
P.141.273	4	1816*	*Triticum dicoccum*	17.75	8.89
P.155.301	4	1816*	*Triticum dicoccum*	16.99	6.30
P.184.414	5	1860.5*	*Triticum dicoccum*	16.16	5.21
Q.44.142	3	1788.5*	*Triticum dicoccum*	17.89	7.71
Q.75.309+310	5	1860.5*	*Triticum dicoccum*	16.10	4.31
S.24.51	2	1709	*Triticum dicoccum*	17.30	7.20
S.47.123	3	1824	*Triticum dicoccum*	17.56	6.67
S.65.235	4	1816*	*Triticum dicoccum*	16.17	7.89
S.79.318	5	1860.5*	*Triticum dicoccum*	14.76	6.41
T.22.55	2	615	*Triticum dicoccum*	14.82	7.05
T.25.68	2	1722	*Triticum dicoccum*	17.93	8.32
T.30.100	3	1824	*Triticum dicoccum*	15.39	6.54
T.57.238	4	1816*	*Triticum dicoccum*	14.60	4.38
T.67.292	5	1860.5*	*Triticum dicoccum*	16.97	5.56
T.75.327	5	1860.5*	*Triticum dicoccum*	18.40	3.42
A.86.127	3	1788.5*	*Triticum monococcum*	16.49	6.47
D.56.265	5	1788.5*	*Triticum monococcum*	16.98	6.83
J.43.142	2	1757	*Triticum monococcum*	15.70	9.08
K.44.164	3	1788.5*	*Triticum monococcum*	16.49	8.58
T.22.55	2	615	*Triticum monococcum*	15.28	7.85
A.36.14	3	1788.5	*Vicia ervilia*	16.44	5.52
A.47.21	4	1816	*Vicia ervilia*	16.52	2.26
A.50.223	5	1860.5	*Vicia ervilia*	14.82	2.86
A.83.117	3	1788.5	*Vicia ervilia*	16.43	4.36
T.57.238	4	1816	*Vicia ervilia*	16.84	3.08
A.26.13	2	1745	*Vicia faba*	15.57	1.34
A.36.14	3	1788.5	*Vicia faba*	15.77	2.99
A.86.127	3	1788.5	*Vicia faba*	17.08	1.78
F.30.139	4	1816	*Vicia faba*	20.21	-
H.37.104	2	1745	*Vicia faba*	19.83	0.55
I.29.89	2	1745	*Vicia faba*	16.24	2.43
M.52.164+167	4	1816	*Vicia faba*	18.04	1.43
P.107.155	3	1788.5	*Vicia faba*	15.85	0.85
T.37.135	3	1788.5	*Vicia faba*	16.25	1.88
T.57.238	4	1816	*Vicia faba*	15.71	2.7
T.65.304	5	1860.5	*Vicia faba*	17.06	2.84
G.25.60-64	2	1811	*Vitis vinifera*	19.31	6.89
K.44.155	3	1788.5*	*Vitis vinifera*	21.53	6.59
P.136.334	4	1816*	*Vitis vinifera*	18.51	11.16
P.192.407	5	1860.5*	*Vitis vinifera*	21.22	-2.06**
P.89.107	3	1788.5*	*Vitis vinifera*	22.71	-

P.90.121	3	1788.5*	*Vitis vinifera*	22.30	-
S.47.123	3	1824	*Vitis vinifera*	18.94	6.11
U.19.66-69	2	1745*	*Vitis vinifera*	21.05	-

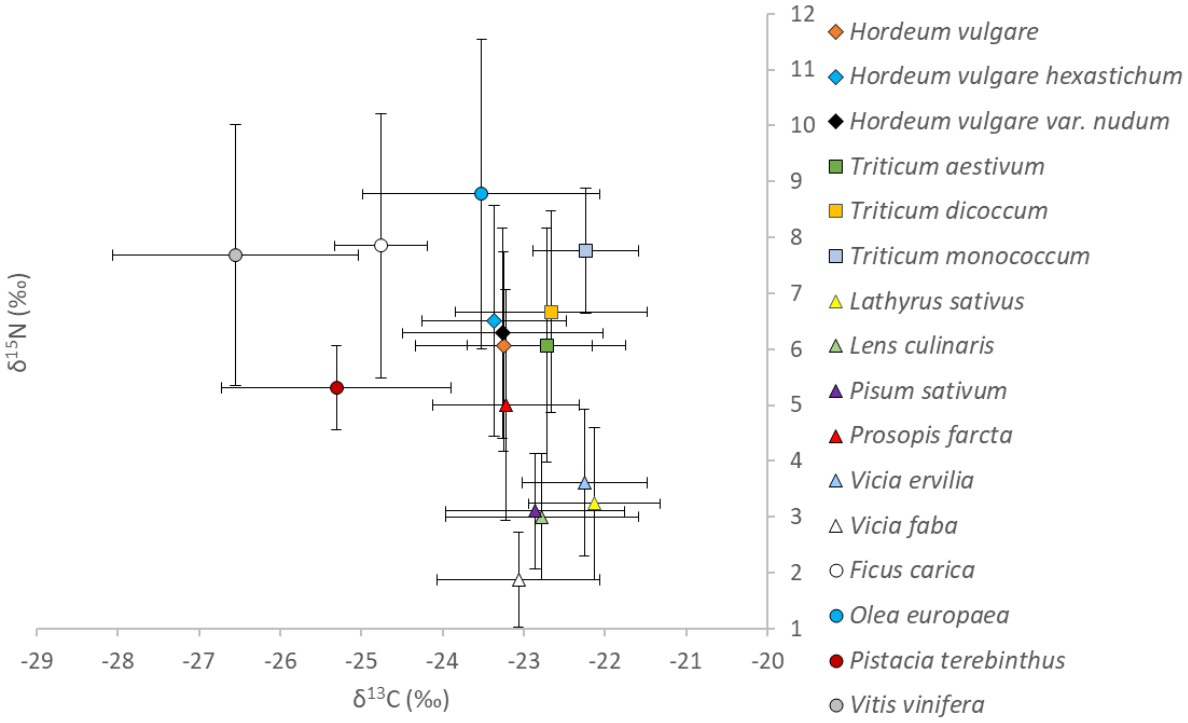

Figure A17. Plot of $\delta^{13}C$ versus $\delta^{15}N$ for carbonized seeds of common cultigens at Tell el-Hayyat, Jordan.

APPENDIX K: CARBONIZED SEED STABLE ISOTOPES FROM KHIRBAT ISKANDAR

Table A8. Stable isotope values of carbon and nitrogen for seed samples from Khirbat Iskandar, Jordan. *Estimated from radiocarbon calibrated phase endpoints. **Value was a statistical outlier and omitted from analysis.

Context (Area. Locus.Bag.Pail)	Phase	AMS age (cal BCE)	Taxa	$\Delta^{13}C$ (‰)	$\delta^{15}N$ (‰)
C.08S.201S.099S	pre-phase 1B	2483*	*Cicer arietinum*	16.21	1.91
C.6.115.75	pre-phase 1B	2604	*Cicer arietinum*	15.39	2.21
C.6.116.77	pre-phase 1B	2483*	*Cicer arietinum*	17.65	-
C.08N.167N.162N	phase 3A	2408	*Hordeum vulgare*	14.86	3.68
C.08N.168N.163N	phase 3A	2483*	*Hordeum vulgare*	17.45	2.23
C.08N.169N.064N	phase 3A	2483*	*Hordeum vulgare*	18.75	5.69
C.08N.169N.064N	phase 3A	2483*	*Hordeum vulgare*	17.76	2.51
C.08N.169N.064N	phase 3A	2483*	*Hordeum vulgare*	16.51	4.16
C.08S.161S.074S	phase 1	2483*	*Hordeum vulgare*	16.84	3.73
C.08S.177S.084S	pre-phase 1A	2483*	*Hordeum vulgare*	17.51	2.23
C.08S.177S.084S	pre-phase 1A	2483*	*Hordeum vulgare*	17.64	5.14
C.08S.178S.092S	pre-phase 1A	2586	*Hordeum vulgare*	16.98	2.80
C.08S.182S.093S	pre-phase 1A	2483*	*Hordeum vulgare*	18.18	2.78
C.08S.201S.099S	pre-phase 1B	2483*	*Hordeum vulgare*	16.83	5.85
C.6.?.47	pre-phase 1A	2483*	*Hordeum vulgare*	17.76	3.71
C.6.101.61	pre-phase 1A	2483*	*Hordeum vulgare*	17.14	3.32
C.6.106.65	pre-phase 1B	2483*	*Hordeum vulgare*	15.29	4.38
C.6.118.073/4	pre-phase 1B	2529	*Hordeum vulgare*	17.67	2.37
C.6.97.58	pre-phase 1A	2483*	*Hordeum vulgare*	17.47	4.46
C.6.97.58	pre-phase 1A	2483*	*Hordeum vulgare*	17.17	1.87
C.6.98.60	pre-phase 1A	2483*	*Hordeum vulgare*	17.97	2.36
C.6.99.61	pre-phase 1A	2483*	*Hordeum vulgare*	15.89	0.56
C.08N.163N.054N	phase 3A	2483*	*Lens culinaris*	14.77	2.48
C.08N.165N.059N	phase 3A	2483*	*Lens culinaris*	14.82	3.78
C.08N.168N.163N	phase 3A	2483*	*Lens culinaris*	15.49	1.82
C.08N.169N.064N	phase 3A	2483*	*Lens culinaris*	16.55	1.62
C.08N.169N.064N	phase 3A	2483*	*Lens culinaris*	14.49	2.77
C.08S.161S.074S	phase 1	2483*	*Lens culinaris*	16.61	2.37
C.08S.177S.084S	pre-phase 1A	2483*	*Lens culinaris*	19.20**	2.08
C.08S.201S.099S	pre-phase 1B	2483*	*Lens culinaris*	15.04	1.97
C.6.104.65	pre-phase 1B	2483*	*Lens culinaris*	15.72	2.68
C.6.115.75	pre-phase 1B	2604	*Lens culinaris*	14.59	2.37
C.6.118.073/4	pre-phase 1B	2529	*Lens culinaris*	16.40	2.47
C.6.119.79	pre-phase 1B	2483*	*Lens culinaris*	14.86	3.28
C.6.93.54	pre-phase 1A	2483*	*Lens culinaris*	15.82	1.98
C.6.97.58	pre-phase 1A	2483*	*Lens culinaris*	15.88	1.45

C.6.99.61	pre-phase 1A	2483*	*Lens culinaris*	17.18	0.97
C.08N.159N.052N	phase 3B	2480	*Pisum sativum*	14.78	5.06
C.08N.168N.163N	phase 3A	2483*	*Pisum sativum*	16.49	-0.13
C.08S.178S.092S	pre-phase 1A	2586	*Pisum sativum*	15.00	2.14
C.08S.182S.093S	pre-phase 1A	2483*	*Pisum sativum*	17.03	1.67
C.6.Bag 1.55	pre-phase 1A	2483*	*Pisum sativum*	16.60	0.03
C.08S.178S.092S	pre-phase 1A	2586	*Triticum dicoccum*	17.75	3.62
C.08S.182S.093S	pre-phase 1A	2483*	*Triticum dicoccum*	17.50	-
C.6.113.073/4	pre-phase 1B	2527	*Triticum dicoccum*	15.80	4.32
C.6.118.073/4	pre-phase 1B	2529	*Triticum dicoccum*	16.65	7.39
C.6.98.60	pre-phase 1A	2483*	*Triticum dicoccum*	17.26	-
C.6.101.61	pre-phase 1A	2483*	*Vitis vinifera*	20.75	3.63
C.6.98.60	pre-phase 1A	2483*	*Vitis vinifera*	19.33	4.73

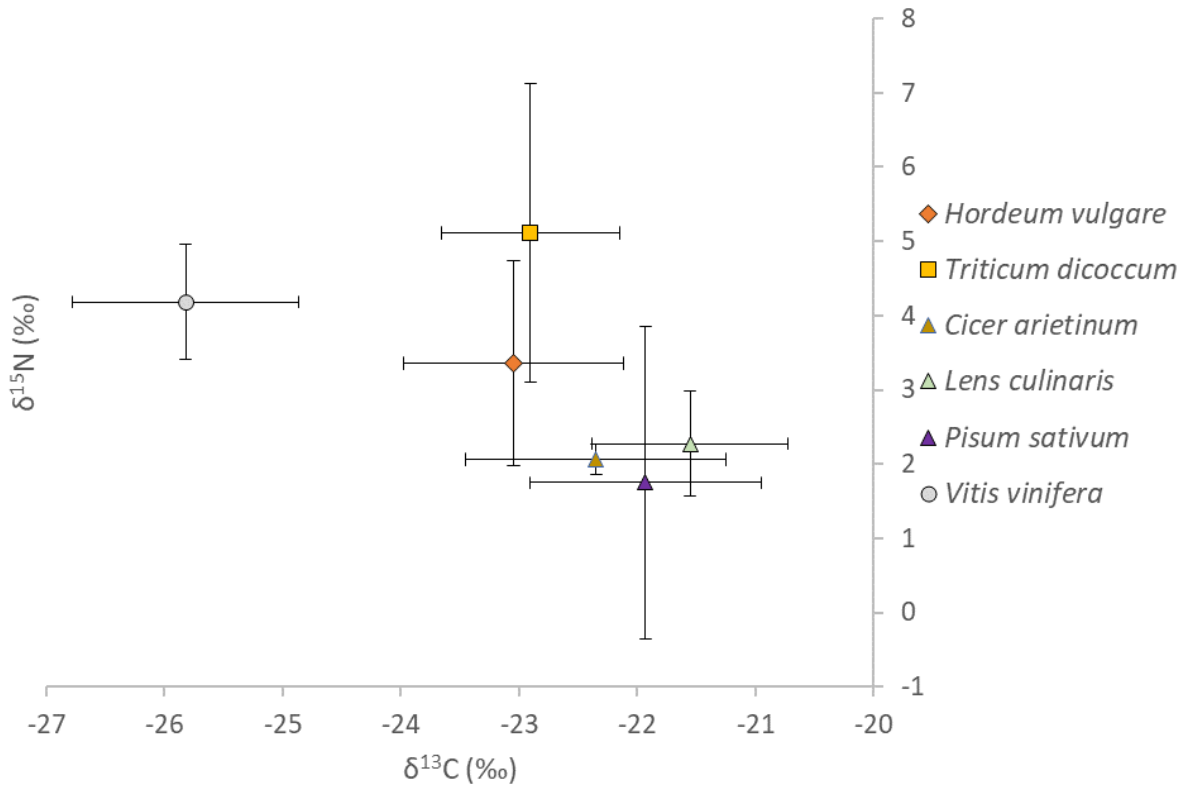

Figure A18. Plot of $\delta^{13}C$ versus $\delta^{15}N$ for carbonized seeds of common cultigens at Khirbat Iskandar, Jordan.

APPENDIX L: CARBONIZED SEED STABLE ISOTOPES FROM ZAHRAT ADH-DHRA‘ 1

Table A9. Stable isotope values of carbon and nitrogen for seed samples from Zahrat adh-Dhra‘ 1, Jordan. *Estimated from radiocarbon calibrated phase endpoints. **Value was a statistical outlier and omitted from analysis.

Context (Area.Locus.Bag)	Phase	AMS age (cal BCE)	Taxa	$\Delta^{13}C$ (‰)	$\delta^{15}N$ (‰)
K.14.62	2	1781.5	*Ficus carica*	19.06	11.55
E.10.51	4	1989.5*	*Hordeum vulgare*	19.86	13.10
I.11.63	3	1854	*Hordeum vulgare*	19.34	-
I.14.88	3	1854*	*Hordeum vulgare*	19.53	7.70
I.14.89	3	1854*	*Hordeum vulgare*	20.16	10.92
I.14.91	3	1854*	*Hordeum vulgare*	20.01	7.32
I.14.92	3	1854*	*Hordeum vulgare*	19.84	9.47
I.14.93	3	1854*	*Hordeum vulgare*	19.85	8.88
K.19.112	2?	1705	*Hordeum vulgare*	17.45	6.44
N.12.37	2	1781.5	*Hordeum vulgare*	17.83	8.23
E.10.46	4	2034	*Hordeum vulgare* var. *nudum*	16.57	6.69
I.14.89	2	1781.5	*Hordeum vulgare* var. *nudum*	17.37	7.54
I.14.91	3	1854*	*Hordeum vulgare* var. *nudum*	17.97	8.71
I.14.92	3	1854*	*Hordeum vulgare* var. *nudum*	20.60	8.03
I.14.93	3	1854*	*Hordeum vulgare* var. *nudum*	19.63	9.48
I.14.94	3	1854*	*Hordeum vulgare* var. *nudum*	18.42	6.60
I.14.97	3	1854	*Hordeum vulgare* var. *nudum*	19.24	5.84
I.14.99	3	1854*	*Hordeum vulgare* var. *nudum*	18.84	6.97
K.19.117	2?	1705	*Hordeum vulgare* var. *nudum*	18.93	12.47
K.19.120	2	1781.5	*Hordeum vulgare* var. *nudum*	18.43	11.44
K.20.126	3	1854*	*Hordeum vulgare* var. *nudum*	17.81	11.23
L.12.23	4	1989.5	*Hordeum vulgare* var. *nudum*	16.27	14.09
I.12.72	4	1989.5	*Pisum sativum*	16.12	1.96
I.14.91	2	1781.5	*Pisum sativum*	16.04	2.15
I.14.94	3	1854*	*Pisum sativum*	16.26	2.71
I.14.95	3	1854	*Pisum sativum*	17.42	2.79
I.14.96	3	1854*	*Pisum sativum*	15.72	3.17
I.14.98	3	1762	*Pisum sativum*	15.90	3.54
K.14.177	2	1781.5	*Pisum sativum*	17.30	4.93
L.19.54	3	1854*	*Pisum sativum*	15.95	2.48
I.14.86	3	1818	*Triticum aestivum*	18.94	5.44
I.14.88	3	1854*	*Triticum aestivum*	19.38	8.47
I.14.89	3	1854*	*Triticum aestivum*	19.02	6.26
I.14.91	3	1854*	*Triticum aestivum*	17.35	7.41
I.14.92	3	1854*	*Triticum aestivum*	17.47	7.10
I.14.93	3	1854*	*Triticum aestivum*	18.65	4.41

I.14.94	3	1854*	*Triticum aestivum*	17.45	7.39
K.14.62	2	1781.5	*Triticum aestivum*	15.41	7.38
K.19.117	2	1781.5	*Triticum aestivum*	17.24	12.06
A.10.41	2	1781.5	*Triticum dicoccum*	17.14	11.92
I.14.86	3	1818	*Triticum dicoccum*	18.48	9.07
I.14.88	3	1854*	*Triticum dicoccum*	17.51	6.02
I.14.92	2	1781.5	*Triticum dicoccum*	18.20	3.95
K.19.117	2	1781.5	*Triticum dicoccum*	18.95	11.53
L.06.35	2	1781.5	*Triticum dicoccum*	17.72	9.70
L.12.24	4	1989.5	*Triticum dicoccum*	17.62	7.96
I.14.93	3	1854	*Vicia ervilia*	15.70	2.25
E.03.62	2	1812.5	*Vicia faba*	15.19	4.19
M.13.73	3	1854	*Vicia faba*	16.98	5.19
I.12.72	4	1989.5	*Vitis vinifera*	22.24	6.07
I.14.92	3	1854*	*Vitis vinifera*	20.52	10.30
I.14.93	3	1854*	*Vitis vinifera*	21.93	4.58
I.14.94	3	1854*	*Vitis vinifera*	21.19	5.94
I.14.95	3	1854	*Vitis vinifera*	22.12	4.09
I.14.96	3	1854	*Vitis vinifera*	21.14	4.14
I.14.97	3	1854*	*Vitis vinifera*	20.02	7.08
I.14.98	3	1762	*Vitis vinifera*	21.39	-
J.14.30	2	1805	*Vitis vinifera*	21.71	-
J.30.107	3	1813	*Vitis vinifera*	19.04	8.83
K.14.177	2	1781.5	*Vitis vinifera*	17.95	6.19
K.20.126	3	1854	*Vitis vinifera*	17.54	12.86
L.23.118	3	1854	*Vitis vinifera*	18.31	9.94
M.13.73	3	1854*	*Vitis vinifera*	18.34	16.316**

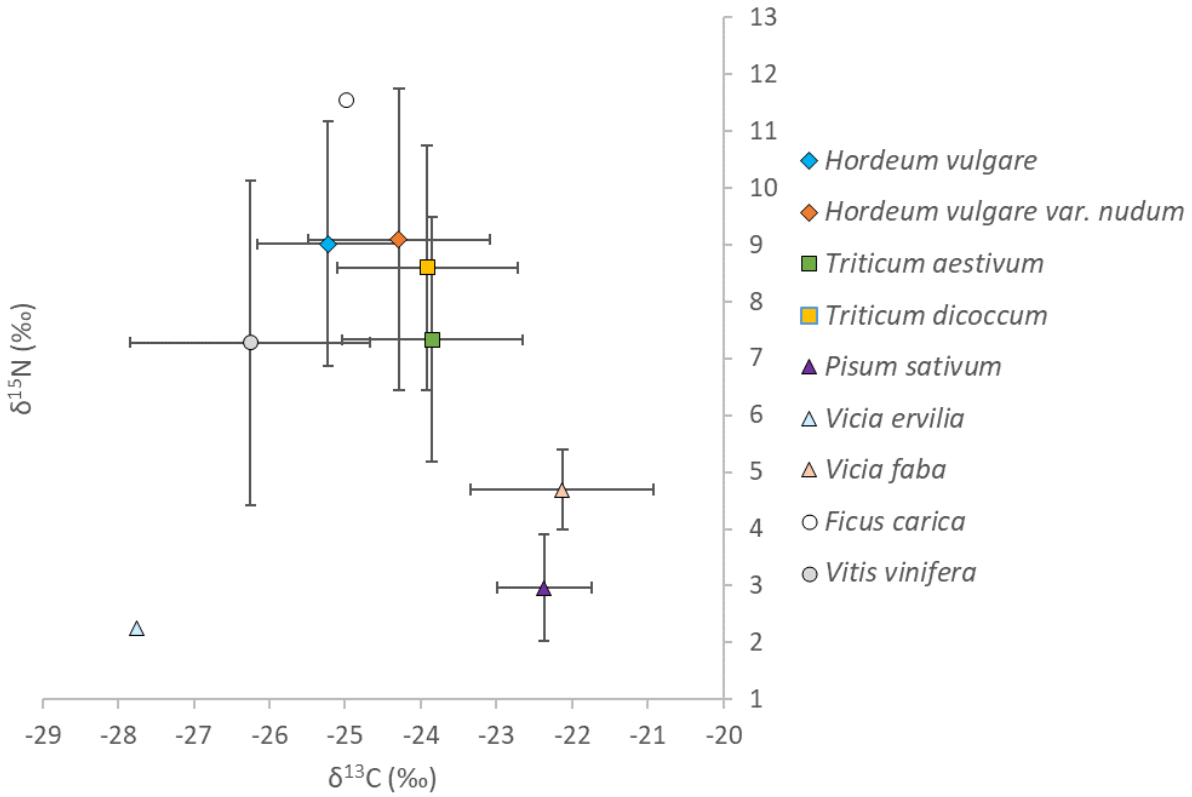

Figure A19. Plot of $\delta^{13}C$ versus $\delta^{15}N$ for carbonized seeds of common cultigens at Zahrat adh-Dhra‘ 1, Jordan.

APPENDIX M: CEREAL RATIOS ACROSS EASTERN MEDITERRANEAN ARCHAEOLOGICAL SITES

Table A10. Hordeum to Hordeum + Triticum ratios in Levantine Early to Middle Bronze Age sites shown in Figure 10.5. Median Age in years cal BCE is based on the estimated midpoint of the age or age range. The three focal sites Tell Abu en-Ni'aj, Tell el-Hayyat, Zahrat adh-Dhra' 1 are plotted based on the midpoint of radiocarbon dated phases from which seeds were recovered.

Site	Median Age (yrs cal BCE)	*Hordeum* : *Triticum* Ratio	Reference
Bab edh-Dhra'	3250	60.66	McCreery, 2003b
Beth-Shean	3250	99.29	Simchoni and Kislev, 2012
Megiddo	3250	40	ADEMNES
Ras an-Numayra	3250	91.46	White et al., 2014
Tell Nebi Mend (Qadesh)	3000	82.25	Mathias and Parr, 1989
Bab edh-Dhra'	2950	75.53	McCreery, 2003b
Tell Kabri	2950	5.66	Nicoli et al., 2023
Tel Yarmouth	2950	50	Salavert, 2008
Tell Abu al-Kharaz	2950	29.31	Fischer and Holden, 2006
Arad	2900	61.46	Hopf, 1978
Jericho	2750	9.99	Hopf, 1983
Khirbet ez-Zeraqon	2750	56.77	Riehl, 2004
Sidon	2750	100	de Moulins, 2009
Bab edh-Dhra'	2700	69.19	McCreery, 2003b
Beth-Shean	2700	50	Simchoni et al., 2007
Megiddo	2700	33.33	ADEMNES
Numeira	2700	90.25	McCreery, 1981
Tel Yarmouth	2700	58.06	Salavert, 2008
Tell Mishrifeh (Qatna)	2700	94.08	Peña-Chocarro and Rottoli, 2007
Tel Yarmouth	2600	45	Salavert, 2008
Tell Abu en-Niʻaj	2400	78.3	This Dissertation
Bab edh-Dhra'	2250	88.89	McCreery, 2003b
Jericho	2250	99.09	Hopf, 1983
Tell Mishrifeh (Qatna)	2250	85.02	Peña-Chocarro and Rottoli, 2007
Tell Nebi Mend (Qadesh)	2250	84.24	Mathias and Parr, 1989
Tell el-Hayyat	1860	67.72	This Dissertation
Zahrat adh-Dhraʻ 1	1850	72.32	This Dissertation
Jericho	1800	95.44	Hopf, 1983
Sidon	1800	53.01	de Moulins and Marsh 2012
Tell Kabri	1800	11.11	Nicoli et al., 2023
'Afula	1775	66.67	Melamed, 1996
Megiddo	1775	4.35	ADEMNES

Tell el Ifshar	1775	0	Chernoff and Paley, 1998
Shiloh	1775	82.14	Kislev, 1993
Tell Mishrifeh (Qatna)	1750	92.31	Pena-Chocarro and Rottoli, 2007
Tell el-Hayyat	1729	39.92	This Dissertation
Beth-Shean	1650	28.34	Simchoni et al., 2007
Manahat	1650	85.25	Kislev, 1998
Tell Abu al-Kharaz	1650	68.46	Fischer and Holden, 2006

APPENDIX N: CARBONIZED SEED STABLE ISOTOPES ACROSS EASTERN MEDITERRANEAN ARCHAEOLOGICAL SITES

Table A11. Values of $\Delta^{13}C$ from select *Hordeum* and *Triticum* species in the Near Eastern Neolithic to Late Bronze Age in sites shown in Figure 10.5.

Site	Age	$\Delta^{13}C$ (‰)	Taxa	Reference
Abu Hamid	NL	17.20	*Hordeum* sp.	Riehl et al., 2014
Abu Hureyra	NL	16.42	*Hordeum vulgare*	Wallace et al., 2015; Styring et al., 2016
Ain Ghazal	NL	17.08	*Hordeum vulgare*	Wallace et al., 2015; Styring et al., 2016
Ain Rahub	NL	17.17	*Hordeum* sp.	Riehl et al., 2014
Ebla	EB IV	18.95	*Triticum aestivum/durum*	Fiorentino et al., 2008
Ebla	EB IV	20.10	*Triticum* sp.	Fiorentino et al., 2008
Ebla	MBA	16.90	*Hordeum vulgare*	Fiorentino et al., 2008, Fiorentino et al., 2011
Ebla	MBA	16.13	*Triticum aestivum/durum*	Fiorentino et al., 2008
Emar	EB I-III	16.15	*Hordeum* sp.	Riehl et al., 2008; 2014
Emar	MBA	15.71	*Hordeum* sp.	Riehl et al., 2008; 2014
Emar	LBA	16.03	*Hordeum* sp.	Riehl et al., 2008; 2014
Hamoukar	CL	18.14	*Hordeum* sp.	Styring et al., 2017
Hamoukar	CL	17.87	*Hordeum vulgare*	Styring et al., 2017
Hamoukar	CL	18.03	*Triticum dicoccum*	Styring et al., 2017
Hamoukar	CL	17.20	*Triticum monococcum*	Styring et al., 2017
Jericho	EB I-III	17.10	*Triticum dicoccum*	Bruins and van der Plicht, 1998
Jericho	EB I-III	16.78	*Triticum* sp.	Bruins and van der Plicht, 1998
Jericho	MBA	17.48	*Hordeum vulgare*	Bruins and van der Plicht, 1995
Jericho	MBA	17.51	*Triticum* sp.	Bruins and van der Plicht, 1995
Khirbat Iskandar	EB IV	17.14	*Hordeum vulgare*	This Dissertation
Khirbat Iskandar	EB IV	16.99	*Triticum dicoccum*	This Dissertation
Khirbet ez-Zeraqon	EB I-III	16.80	*Hordeum* sp.	Riehl, 2004; Riehl et al., 2008; 2014
Khirbet ez-Zeraqon	EB I-III	16.20	*Triticum dicoccum*	Riehl, 2004; Riehl et al., 2008; 2014
Khirbet ez-Zeraqon	EB I-III	15.50	*Triticum monococcum*	Riehl, 2004; Riehl et al., 2008; 2014
Mezraa Teleilat Hoyuk	NL	17.09	*Hordeum* sp.	Riehl et al., 2014

Qatna (Tell Mishrifeh)	EB I-III	16.90	*Triticum dicoccum*	Riehl et al., 2008; 2014
Qatna (Tell Mishrifeh)	EB I-III	16.58	*Hordeum* sp.	Riehl et al., 2008; 2014
Qatna (Tell Mishrifeh)	MBA	16.69	*Hordeum* sp.	Riehl et al., 2008; 2014
Qatna (Tell Mishrifeh)	LBA	15.98	*Hordeum* sp.	Riehl et al., 2008; 2014
Shir	NL	16.00	*Hordeum* sp.	Riehl et al., 2014
Tell Abu en-Ni‘aj	EB IV	17.36	*Hordeum* sp.	Porson et al., 2021
Tell Abu en-Ni‘aj	EB IV	17.36	*Hordeum vulgare*	This Dissertation
Tell Abu en-Ni‘aj	EB IV	18.42	*Hordeum vulgare var nudum*	This Dissertation
Tell Abu en-Ni‘aj	EB IV	17.90	*Triticum aestivum/durum*	This Dissertation
Tell Abu en-Ni‘aj	EB IV	17.07	*Triticum dicoccum*	Porson et al., 2021; This Dissertation
Tell Abu en-Ni‘aj	EB IV	17.19	*Triticum monococcum*	This Dissertation
Tell Abu en-Ni‘aj	EB IV	17.39	*Triticum* sp.	This Dissertation
Tell al-Raqa'i	EB I-III	16.75	*Hordeum* sp.	Riehl et al., 2014
Tell Atchana	LBA	17.15	*Hordeum* sp.	Riehl et al., 2008; 2014
Tell Atchana	LBA	16.50	*Triticum aestivum/durum*	Riehl et al., 2008; 2014
Tell Atij	EB I-III	16.40	*Hordeum* sp.	Riehl et al., 2014
Tell Beydar III	CL	16.97	*Hordeum* sp.	Riehl et al., 2014
Tell Brak	CL	17.69	*Hordeum vulgare*	Styring et al., 2017
Tell Brak	CL	17.79	*Triticum aestivum/durum*	Styring et al., 2017
Tell Brak	CL	17.54	*Triticum dicoccum*	Styring et al., 2017
Tell Brak	CL	16.34	*Triticum monococcum*	Styring et al., 2017
Tell Brak	EB I-III	16.92	*Hordeum vulgare*	Styring et al., 2017
Tell Brak	EB I-III	17.48	*Triticum dicoccum*	Styring et al., 2017
Tell Brak	EB IV	17.68	*Hordeum vulgare*	Styring et al., 2017
Tell Brak	EB IV	17.18	*Triticum dicoccum*	Styring et al., 2017
Tell el'Abd	EB I-III	17.56	*Hordeum* sp.	Riehl et al., 2008; 2014
Tell el'Abd	EB IV	14.90	*Triticum dicoccum*	Riehl et al., 2008; 2014
Tell el-Hayyat	MBA	17.68	*Hordeum* sp.	Falconer and Fall, 2017
Tell el-Hayyat	MBA	17.25	*Hordeum vulgare*	This Dissertation
Tell el-Hayyat	MBA	17.26	*Hordeum vulgare var nudum*	This Dissertation
Tell el-Hayyat	MBA	16.70	*Triticum aestivum/durum*	This Dissertation
Tell el-Hayyat	MBA	16.62	*Triticum dicoccum*	This Dissertation

Tell el-Hayyat	MBA	16.19	*Triticum monococcum*	This Dissertation
Tell Esh-Shuna (Tell Nimrin)	CL	16.21	*Hordeum* sp.	Bronk Ramsey et al., 2002
Tell Esh-Shuna (Tell Nimrin)	CL	17.92	*Hordeum vulgare*	Bronk Ramsey et al., 2002
Tell Esh-Shuna (Tell Nimrin)	CL	17.04	*Triticum dicoccum*	Bronk Ramsey et al., 2002
Tell Esh-Shuna (Tell Nimrin)	EB I-III	15.97	*Hordeum* sp.	Holden, 1999; Bronk Ramsey et al., 2002, Riehl et al., 2014
Tell Esh-Shuna (Tell Nimrin)	EB I-III	13.82	*Hordeum vulgare*	Holden, 1999; Bronk Ramsey et al., 2002, Riehl et al., 2014
Tell Esh-Shuna (Tell Nimrin)	EB I-III	16.15	*Triticum dicoccum*	Holden, 1999; Bronk Ramsey et al., 2002, Riehl et al., 2014
Tell Fadous-Kfarabida	EB I-III	18.08	*Hordeum* sp.	Riehl et al., 2008; 2014
Tell Fadous-Kfarabida	EB I-III	21.20	*Triticum dicoccum*	Riehl et al., 2008; 2014
Tell Halula	NL	17.18	*Triticum aestivum/durum*	Araus, 1999; 2007
Tell Kerma	EB I-III	15.88	*Hordeum* sp.	Riehl et al., 2014
Tell Kuran	NL	16.94	*Hordeum* sp.	Riehl et al., 2014
Tell Leilan	EB I-III	18.06	*Hordeum vulgare*	Styring et al., 2017
Tell Leilan	EB IV	17.98	*Hordeum vulgare*	Styring et al., 2017
Tell Leilan	EB IV	17.81	*Triticum aestivum/durum*	Styring et al., 2017
Tell Leilan	EB IV	18.29	*Triticum dicoccum*	Styring et al., 2017
Tell Leilan	EB IV	16.99	*Triticum monococcum*	Styring et al., 2017
Tell Leilan	EB IV	18.33	*Triticum* sp.	Styring et al., 2017
Tell Mozan	EB I-III	17.61	*Hordeum* sp.	Riehl et al., 2008; 2014
Tell Mozan	EB I-III	16.60	*Triticum aestivum/durum*	Riehl et al., 2008; 2014
Tell Mozan	EB I-III	17.70	*Triticum dicoccum*	Riehl et al., 2008; 2014
Tell Mozan	EB IV	17.75	*Hordeum* sp.	Riehl et al., 2008; 2014
Tell Mozan	EB IV	16.30	*Triticum aestivum/durum*	Riehl et al., 2008; 2014
Tell Mozan	EB IV	16.80	*Triticum dicoccum*	Riehl et al., 2008; 2014
Tell Mozan	MBA	16.30	*Hordeum* sp.	Riehl et al., 2008; 2014
Tell Mozan	MBA	16.00	*Triticum aestivum/durum*	Riehl et al., 2008; 2014
Tell Mozan	MBA	17.60	*Triticum dicoccum*	Riehl et al., 2008; 2014

Tell Mozan	MBA	16.20	*Triticum monococcum*	Riehl et al., 2008; 2014
Tell Nebi Mend	EB I-III	17.06	*Hordeum vulgare*	Wallace et al., 2015
Tell Nebi Mend	EB IV	16.97	*Hordeum vulgare*	Wallace et al., 2015
Tell Nebi Mend	EB IV	15.30	*Triticum aestivum/durum*	Wallace et al., 2015
Tell Nebi Mend	LBA	16.83	*Hordeum vulgare*	Wallace et al., 2015
Tell Nebi Mend	LBA	16.45	*Triticum aestivum/durum*	Styring et al., 2017
Tell Sabi Abyad	NL	17.52	*Hordeum vulgare*	Styring et al., 2017
Tell Sabi Abyad	NL	17.59	*Triticum aestivum/durum*	Styring et al., 2017
Tell Sabi Abyad	NL	17.98	*Triticum dicoccum*	Styring et al., 2017
Tell Sabi Abyad	NL	17.78	*Triticum monococcum*	Styring et al., 2017
Tell Shioukh Faouqani	EB I-III	15.70	*Hordeum* sp.	Riehl et al., 2014
Tell Shioukh Faouqani	MBA	16.48	*Hordeum* sp.	Riehl et al., 2014
Tell Shioukh Faouqani	LBA	16.96	*Hordeum* sp.	Riehl et al., 2014
Tell Tawila	NL	16.76	*Hordeum* sp.	Riehl et al., 2014
Tell Tweini	EB IV	16.91	*Hordeum* sp.	Riehl et al., 2014
Tell Tweini	MBA	16.94	*Hordeum* sp.	Riehl et al., 2014
Tell Tweini	LBA	17.09	*Hordeum* sp.	Riehl et al., 2014
Tell Zeidan	CL	17.94	*Hordeum vulgare*	Styring et al., 2017
Tell Zeidan	CL	18.38	*Triticum aestivum/durum*	Styring et al., 2017
Tell Zeidan	CL	18.54	*Triticum dicoccum*	Styring et al., 2017
Tell Zeidan	CL	18.42	*Triticum* sp.	Styring et al., 2017
Umm Qseir	NL	16.59	*Hordeum* sp.	Riehl et al., 2014
Zahrat adh-Dhra‘ 1	MBA	17.51	*Hordeum* sp.	Fall et al., 2019; This Dissertation
Zahrat adh-Dhra‘ 1	MBA	19.53	*Hordeum vulgare*	This Dissertation
Zahrat adh-Dhra‘ 1	MBA	18.60	*Hordeum vulgare var nudum*	This Dissertation
Zahrat adh-Dhra‘ 1	MBA	18.33	*Triticum aestivum/durum*	This Dissertation
Zahrat adh-Dhra‘ 1	MBA	18.00	*Triticum dicoccum*	This Dissertation
Zahrat adh-Dhra‘ 1	MBA	16.47	*Triticum* sp.	Fall et al., 2019; This Dissertation
Ziyade	CL	16.38	*Hordeum* sp.	Riehl et al., 2014